

(19) World Intellectual Property Organization
International Bureau(43) International Publication Date
23 August 2001 (23.08.2001)

PCT

(10) International Publication Number
WO 01/60408 A2

(51) International Patent Classification⁷: A61K 45/00 (81) Designated States (national): AE, AG, AL, AM, AT, AU, AZ, BA, BB, BG, BR, BY, BZ, CA, CH, CN, CR, CU, CZ, DE, DK, DM, DZ, EE, ES, FI, GB, GD, GE, GH, GM, HR, HU, ID, IL, IN, IS, JP, KE, KG, KP, KR, KZ, LC, LK, LR, LS, LT, LU, LV, MA, MD, MG, MK, MN, MW, MX, MZ, NO, NZ, PL, PT, RO, RU, SD, SE, SG, SI, SK, SL, TJ, TM, TR, TT, TZ, UA, UG, UZ, VN, YU, ZA, ZW.

(21) International Application Number: PCT/US01/05314

(22) International Filing Date: 16 February 2001 (16.02.2001)

(25) Filing Language: English

(26) Publication Language: English

(30) Priority Data:
60/183,184 17 February 2000 (17.02.2000) US
09/732,360 7 December 2000 (07.12.2000) US

(84) Designated States (regional): ARIPO patent (GH, GM, KE, LS, MW, MZ, SD, SL, SZ, TZ, UG, ZW), Burasian patent (AM, AZ, BY, KG, KZ, MD, RU, TJ, TM), European patent (AT, BE, CH, CY, DE, DK, ES, FI, FR, GB, GR, IE, IT, LU, MC, NL, PT, SE, TR), OAPI patent (BF, BJ, CF, CG, CI, CM, GA, GN, GW, ML, MR, NE, SN, TD, TG).

(71) Applicant: SCI PHARMACEUTICALS, INC. [US/US];
3159 South Winton Road, Suite 203, Rochester, NY 14623
(US).

Published:
— without international search report and to be republished upon receipt of that report

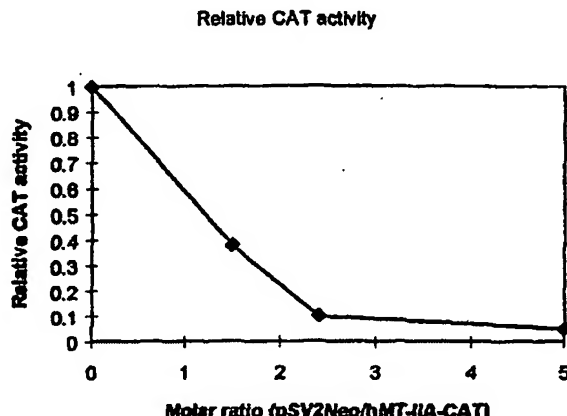
(71) Applicant and
(72) Inventor: POLANSKY, Hanan [US/US]; 294 Avalon Court, Rochester, NY 14618 (US).

(74) Agents: MICHAELS, Christopher et al.; Brown, Pinnisi & Michaels, P.C., 118 N. Tioga St., Suite 400, Ithaca, NY 14850 (US).

For two-letter codes and other abbreviations, refer to the "Guidance Notes on Codes and Abbreviations" appearing at the beginning of each regular issue of the PCT Gazette.

(54) Title: MICROCOMPETITION AND HUMAN DISEASE

WO 01/60408 A2



(57) Abstract: Cellular microcompetition for the transcription factor human GA binding protein (GABP) is a risk factor associated with obesity and obesity-related diseases such as osteoarthritis, atherosclerosis, obstructive sleep apnea, various cancers, and periodontitis. The invention uses this novel discovery to develop assays which determine the level of microcompetition in a cell. Other assays developed from the knowledge that microcompetition is occurring in cells are also disclosed. This novel discovery led to the development of assays which can determine the level of microcompetition in a cell and to select compounds to target this microcompetition syndrome. In addition, methods to treat a patient for microcompetition based disease are taught.

MICROCOMPETITION AND HUMAN DISEASE

BACKGROUND OF THE INVENTION

FIELD OF THE INVENTION

The invention pertains to the field of human diseases. More particularly, the
5 invention pertains to how microcompetition for transcription factors contributes to obesity,
cancer, atherosclerosis, osteoarthritis, hypertension and diabetes.

DESCRIPTION OF RELATED ART

The cause of many cases of obesity, cancer, atherosclerosis, osteoarthritis, and
10 diabetes is unknown. Therefore, treatment is focused on symptomolgy and effects of the
diseases and has limited effectiveness. In many cases, known treatments are associated
with serious negative side effects.

Recently, the National Cancer Institute (NIH Guide 2000) announced a program
aimed to "reorganize the 'front-end' or gateway to drug discovery." The new approach
promotes a three stage discovery process. The first stage is discovery of the molecular
15 mechanisms that underlie neoplastic transformations, cancer growth and metastasis. Next
stage is selection of a novel molecular target within the discovered biochemical pathway
known to have a unique difference between a healthy and a cancerous cell. The final stage
is design of new drugs that modify the selected target. The program encourages moving
away from screening agents by their clinical effects, such as shrinking tumor cells, *in vivo*
20 or *in vitro*, to screening agents or designing drugs by their effects on a specific molecular
mechanism. According to the NCI, screening by clinical effects identified drugs that
demonstrated clear limitations in clinical efficacy, while screening by desired molecular
effects should produce more efficaious and specific drugs.

The best drugs are those that are specifically designed to reverse the molecular
25 events that cause disease. However, it is critical that the molecular mechanisms that
underlie obesity, atherosclerosis, osteoarthritis, hypertension and diabetes be understood
before drugs can be effectively designed to treat the disease.

SUMMARY OF THE INVENTION

For the first time, this invention teaches the novel concept of microcompetition for GABP. There is a limited amount of GABP•p300 transcription complex available in the cell. The present invention teaches that cellular microcompetition for the transcription factor human GA binding protein (GABP) results in diseases such as include cancer, atherosclerosis, osteoarthritis and obesity. Moreover, other disruptions of the GABP pathway from microcompetition, diets, mutations, toxins, or drugs have a similar effect to microcompetition. This new understanding of the biochemical pathway surrounding GABP can be used to identify or design drugs to treat these diseases.

The invention includes methods of treating adverse affects associated with disruptions of the GABP pathway by microcompetition, diets, mutations, toxins, or drugs. Specifically, administering to a patient an effective amount of an agent that overcomes the disruption of the GABP pathway. The diseases that can be treated include cancer, atherosclerosis, osteoarthritis and obesity. The specific treatments can be accomplished in a variety of ways.

To most directly remove microcompetition, an agent that decreases foreign DNA N-boxes in cells can be used to eliminate the competitive binding sites. Examples of such agents are: Ganciclovir, ddI, ddC, and garlic and others described in the description. The present invention includes a method of identifying other compounds to treat the effects of microcompetition by assaying for compounds that eliminate competitive binding sites.

Other treatments of the effects of microcompetition or other disruptions of the GABP pathway are agents that stimulate phosphorylation of a GABP kinase, increases concentration of a GABP kinase, and increases affinity between GABP and GABP kinase. Examples of such agents are: dietary fiber (via sodium butyrate), sodium butyrate, acarbose, vanadate, vectors to knockout PTP1B, and others described in the description. The present invention includes a method of identifying other compounds to treat disruptions of the GABP pathway by assaying for compounds that have and affect on a GABP kinase.

Another treatment option is to use an agent that decreases the oxidative effect on GABP. Examples of such agents are: garlic and other anti-oxidants described in the description. The present invention includes a method of identifying other compounds to treat disruptions of the GABP pathway by assaying for compounds that decrease oxidative effect on GABP.

Agents that increase the concentration or effectiveness of a GABP stimulator can also be used to more effectively utilize GABP. In the converse, agents that decrease the concentration or effectiveness of a GABP suppressor can also be administered. In addition, treatment can employ an agent that increases concentration of GABP α , increases concentration of GABP β , decreases concentration of GABP γ , increases phosphorylation of GABP, increases affinity between GABP and p300/CBP, or increases concentration of p300/CBP. Such agents would largely overlap with the agents above. However, they produce more specific effects. The present invention includes a method of identifying other compounds to treat disruptions of the GABP pathway by assaying for compounds that have these specific effects.

BRIEF DESCRIPTION OF THE DRAWINGS

Figure 1 shows the relation between molar ratio of pSV2Neo/hMT-IIA-CAT and relative CAT activity.

Figure 2 shows the relation between molar ratio of bgal/CAT and relative CAT activity.

Figure 3 shows the amount of COL1A2 RNA measured in cells grown at temperature permissive (T) or nonpermissive (N) for transformation.

Figure 4 shows the effect of infection with HIV-1, heat inactivated HIV-1 and mock-infection on CD18 expression over time.

Figure 5 shows a schematic illustration of the extracellular signaling cascade and its effect on GABP.

Figure 6 shows a schematic illustration of the activation of MAPK by MEK-1, and deactivation of MAPK by either PP2A, PTP1B, or MKP-1.

Figure 7 shows a schematic illustration of the relationship between ERK signaling and microcompetition for available GABP.

5 Figure 8 shows a schematic illustration of how phosphorylated GABP stimulates the transcription of the sensitized receptor and how the new receptors increase the sensitivity of the pathway to changes in concentration of GABP kinase agent.

Figure 9 shows a schematic illustration of feedback inhibition involving GABP.

10 Figure 10 shows a schematic illustration of the effect of a downstream control relative to a sensitized receptor.

Figure 11 shows the effect of HSV-1 and LPS exposure on TF procoagulant activity (PCA) of human umbilical vein endothelial cells.

15 Figure 12 shows a schematic illustration of the effects of LPS, RSVL and RA on NF- κ B and ETS sites of the TF gene.

Figure 13 shows an schematic illustration of the P450 mediated oxidation of arachidonic acid.

Figure 14 shows the relation between MAPK activity and arachidonic acid metabolites.

20 Figure 15 shows the number of viable cells following transfection with pBARB and the "empty vector" pSV-neo.

Figure 16 shows accumulation of triglyceride, assayed by oil red staining in untreated F442A cells, or following transfection with the WT, and the "empty vector" pZIPNeo.

25 Figure 17 shows the percent reverse transmigration of peripheral blood monocellular cells as a function of time.

Figure 18 shows the effect of LPS or Cu+2 exposure on TF mRNA levels.

Figure 19 shows the GSH content in human promyelocytic leukemia cells U937 following treatment with 7-ketcholesterol.

5 Figure 20 is a photomicrograph of atheroma (type IV lesion) in proximal left anterior descending coronary artery from a 23-year old man who died of a homicide.

Figure 21 is a photomicrograph of thick part of atheroma (type IV lesion) in proximal left anterior descending coronary artery from a 19-year-old man who committed suicide.

10 Figure 22 shows TF activity over time following treatment with herpes simplex virus-1 (HSV-1), LPS or platelet-derived growth factor (PDGF).

Figure 23 shows a graphic illustration of the change in TF activity over time for a control cell and a cell harboring a GABP viral genome.

Figure 24 shows a graphic illustration of the microcompetition effect on the relation between catecholamines and lipolysis.

15 Figure 25-28 shows the measure effects norepinephrine, isoprenaline, forskolin, and dibutyryl cyclic AMP on glycerol release in adipocytes from subjects with a family trait of obesity and controls.

Figure 29 shows the measured relationship between epinephrine infusion and glycerol release in obesity versus lean.

20 Figure 30-31 shows the measured percent change and total glycerol release as a function of plasma epinephrine concentration in obese and lean women.

Figure 32 shows the percent Rb-null preadipocytes in S phase following five different treatments

25 Figure 33 shows a graphic illustration of how microcompetition reduces Rb transcription.

Figure 34 shows some of the molecules on the surface of DC and T cells participating in their binding.

Figure 35 shows a graphic illustration of how a increase in either [B7] or [Ag], increases the probability of Th1 vs. Th2 differentiation.

5 Figure 36 shows a graphic illustration of the relation between time and TF expression for cells migrating through regions of low, moderate, and high antigen concentrations.

Figure 37 shows a graphic illustration of the relation between trigger apoptosis, T-cell induced apoptosis and tissue cell damage.

10 Figure 38 shows a graphic illustration of the two peak dynamics.

Figure 39 shows a graphic illustration of the effect of an excessively slow DC on the two peaks.

Figure 40 shows the percent change in \square cell apoptosis and percent of islet area following five low-dose streptozotocin injections.

15 Figure 41 shows the effect on \square cell apoptosis of a single injection of cyclophosphamide to 3 and 12 week old NOD mice and an injection of nicotinamide and cyclophosphamide to 12 week old mice.

Figure 42 shows a graphic illustration of the effect of thioredoxin (TRX) overexpression on the two peaks.

20 Figure 43 shows a graphic illustration of the effect of DC maturation on the number of cells expressing certain concentrations of tissue factor, antigens and costimulation on their surface.

Figure 44 shows a graphic illustration of the Barratt-Boyces 2000 experimental configuration.

25 Figure 45 shows the effect of treatment on the microcompetition equilibrium.

Figure 46 shows a schematic illustration of how aberrant GABP expression can be restored.

Figure 47 shows the effect of sodium butyrate treatment on MT mRNA.

5 Figure 48 shows the effect of acarbose treatment on change in body weight over time.

Figure 49 shows the effect of vanadate treatment on PFK-2 mRNA over time.

Figure 50 shows the change in HIV-1 DNA and RNA load relative to baseline in 42 antiretroviral naive HIV-1 infected persons treated with either AZT monotherapy, a combination of AZT + ddC or a combination of AZT + ddI over a period of 80 weeks.

10 Figure 51 graphically shows the result of a regression analysis with viral DNA level as dependent variable and number of years since seroconversion as independent variable.

DETAILED DESCRIPTION OF THE INVENTION

15 The present invention starts from the discovery that microcompetition is involved in a variety of human diseases. It is only by looking through the lens of the present invention that a discernable pattern of disease progression and symptomology is understood. From this understanding the inventor was able to develop new assays, screening regiments and treatments.

20 Once microcompetition was discovered to play a role in human disease, the present inventor looked back at previous work to see if it was possible to find published observations consistent with microcompetition. Having made the original discovery, the inventor has been able to piece together and relate a mosaic of individual studies and information that heretofore seemed entirely unrelated.

25 The present invention started as a new theory of human disease and testing the hypothesis was also performed in a novel way. Once the theory was developed, a novel mechanism of action and relationship between biochemical agents was proposed, followed by a set of predictions of the effect of modification of one or more of those biochemical

agents. However, it was unnecessary to perform thousands of experiments to test the hypothesis, because others had studied the biochemical agents and recorded the effects of modifying those agents. By looking at the results of thousands of studies on dozens of biochemical agents, the set of predictions was tested and supported. Close to 600 papers 5 are referenced in this disclosure, each providing a piece of information that forms the totality of this invention.

Much of this disclosure is similar to a mosaic. In the same way, ceramic plates or colored glass are shattered and rearranged by the mosaic artist to form a new piece of art, the applicant has similarly used pieces of information evidence gleaned from work of 10 other researchers to understand the mechanism of human disease in an entirely new way.

The present invention teaches the relationship between microcompetition and human disease and this detailed description starts with a detailed explanation of microcompetition. It then progresses through the affected pathways and teaches the pieced together evidence supporting the microcompetition model. Based upon this model, 15 a series of new assays, screening regiments and treatments are described. The full citation for each reference is provided at the end of the detailed disclosure and is cited in an abbreviated fashion within the text to make the disclosure more readable.

I. Discovery 1: Microcompetition

1. Definition

20 The situation where DNA sequences compete for the same transcription complex will be called microcompetition. If we assume first that the cellular availability of at least one of the proteins constructing the transcription complex is limited, second that the complex binds DNA of two genes and third that binding stimulates the transcription of one of these genes, then microcompetition for the transcription complex reduces binding of the 25 complex to the gene, resulting in reduced transcription.

2. Molecular effect

The following studies demonstrate the effect of microcompetition on the expression of various cellular genes.

a) Human metallothionein-II_A (hMT-II_A)

CV-1 cells were cotransfected with a constant amount of plasmid containing the hMT-II_A promoter (-286 nt relative to the start of transcription to +75 nt) fused to the bacterial gene coding chloramphenicol acetyltransferase (hMT-II_A-CAT) and increasing amounts of plasmid containing the viral SV40 early promoter and enhancer fused to the bacterial gene coding for aminoglycoside resistance (pSV2Neo). Figure 1 illustrates the results of microcompetition between the two plasmids in terms of the relative CAT activity (relative CAT activity = CAT activity in the presence of pSV2Neo/CAT activity in the absence of pSV2Neo).

10 A 2.4-fold molar excess of the plasmid containing the viral enhancer reduced 90% of CAT activity. No microcompetition was observed with the viral plasmid after deletion of the SV40 enhancer.

15 The efficient inhibition of hMT-II_A promoter activity by the SV40 enhancer suggests that the enhancer has a high affinity for a limiting transcription complex that also binds the hMT-II_A promoter. Moreover, although both the hMT-II_A promoter and the SV40 enhancer bind the Sp1 transcription factor, further studies ruled out the idea that the two plasmids compete for Sp1 or factors which bind the TATA box (Scholer 1986¹)

b) Platelet derived growth factor-B (PDGF-B)

20 JEG-3 choriocarcinoma cells were transiently cotransfected with a constant amount of PDGF-B promoter/enhancer-driven CAT reporter gene (PDGF-B-CAT) and increasing amounts of a plasmid containing either the human cytomegalovirus promoter/enhancer fused to the β -galactosidase (β gal) reporter gene (CMV- β gal) or the viral SV40 early promoter and enhancer elements fused to β gal (SV40- β gal).

25 Figure 2 presents the results of microcompetition between these plasmids in terms of relative CAT activity.

Both CMV- β gal and SV40- β gal repressed the activity of PDGF-B-CAT in a concentration-dependent manner. Mutational studies of the SV40 promoter/enhancer element showed that the sequence in SV40- β gal which competes with PDGF-B is located

within the SV40 enhancer region (Adam 1996²). However, neither a specific DNA box nor responsible transcription factors were identified.

c) *Collagen type I α 2 chain (COL1A2)*

5 Skin fibroblasts were infected with temperature sensitive Rous Sarcoma Virus (ts-RSV). The amount of COL1A2 RNA was measured in cells grown at temperatures permissive (T) or nonpermissive (N) for transformation. Figure 3 presents the effect of microcompetition between the virus and the cellular gene on the concentration of RNA encoded by that gene.

10 In skin fibroblasts the amount of COL1A2 RNA was decreased 5-fold. A similar experiment showed a reduction of 3.3-fold in the amount of COL1A1 RNA (Allebach 1985³).

15 WI-38 human lung fibroblasts were transformed by a clone of SV40. The mRNA of the α 2(I) chain was absent in the SV40 transformed WI-38 fibroblasts, whereas the mRNA of the α 1(I) chain was detected on the same blot. The study eliminated a few possible reasons for the reduced expression of the α 2(I) chain in the infected cells. The chromosomes which normally carry the α 2(I) and α 1(I) genes appeared to be perfectly normal. Restriction mapping of the α 2(I) gene in the transformed cells did not show any gross insertion of the viral genome within the gene or its promoter. Methylation analysis of the promoter and 3' regions of the gene did not reveal any detectable hypermethylation 20 (Parker 1989⁴).

Normal cells synthesize the standard form of collagen type I consisting of two α 1(I) chains and one α 2(I) chain. Tumors caused by the polyomavirus, on the other hand, mainly synthesize a α 1(I) trimer (Moro 1977⁵). A high concentration of trimer was also found in SV40 transformed WI-38 human lung fibroblasts (Parker 1992⁶).
25 Microcompetition mainly decreases the expression of the α 2(I) chain (see Allebach 1985 and Parker 1989 above). Consequently, the relative shortage of the α 2(I) chain in infected cells stimulates formation of the α 1(I) trimers.

d) *Integrin (β₂ leukocyte, CD18)*

Human monocytes were infected with human immunodeficiency virus type 1 (HIV-1). The surface expression of CD18, CD11a, CD11b, CD11c, CD58, CD62L, CD54, and CD44 was measured in HIV-1 infected cells and mock-infected cells. The 5 extent and kinetics of CD11a, CD11b, CD11c, CD58 and CD62L expression were similar in HIV-1 infected cells and mock-infected cells. CD18, CD54 and CD44 showed a significant decrease in expression in the HIV-1 infected cells. When monocytes were treated with a heat-inactivated HIV-1 virus, the expression of CD54 and CD44 was similar to the expression in mock-infected cells, however, the expression of CD18 was reduced.

10 Consider the results in figure 4.

According to Le Naour, *et al.*, (1997)⁷ "treatment with heat-inactivated virus shown that regulation of CD18 expression is dependent on early HIV-related regulatory mechanisms whereas regulation of CD44 and CD54 requires viral events taking place after retrotranscription of viral RNA."

15 Adult T-cell leukemia (ATL) is etiologically associated with the human T-cell leukemia virus type 1 (HTLV-1). The mRNA of CD18 was measured in three human T-cell acute-lymphoblastic-leukemia cell lines, MOLT-4, Jurkat and CEM negative for HTLV-1, four T-cell lines, MT-2, TCL-Kan, C91/PL and C8166, which were established by transformation with HTLV-1, one T-cell line, TOM-1, derived from an HTLV-1 carrier 20 and positive for HTLV-1, and four cell lines, MT-1, TL-Om1, H582 and HuT102, which are ATL derived T-cell lines positive for HTLV-1. Overall, non ATL derived, HTLV-1 negative cell lines showed high levels of CD18 mRNA. The non ATL derived, HTLV-1 positive cell lines showed moderate levels of CD18 mRNA. The ATL derived, HTLV-1 positive cell lines showed low levels of CD18 mRNA (*Ibid*, Fig. 7, Tanaka 1995⁸).

25 Southern-blotting analysis did not reveal any gross structural changes in the CD18 gene. To test CD18 promoter activity in the ATL derived, HTLV-1 positive cell lines, TL-Om1, H582 and HuT102 were transfected with a CD18 promoter-driven CAT reporter gene. The same construct was transfected into the non ATL derived, HTLV-1 negative Jurkat cells. The results showed high CAT expression in the Jurkat cells and low CAT 30 expression in the 3 ATL derived, HTLV-1 positive cell lines. Tanaka, *et al.*, (1995)

conclude that "the down regulation of the CD18 gene in these ATL cell lines was due to lack of transcription factor(s) necessary for CD18 gene expression." The paper does not identify the transcription factor, neither does it provide an explanation for the reduced availability of the unknown factor(s).

5 The Epstein-Barr virus (EBV) selectively infects human B cells causing infectious mononucleosis (IM). Lymphoblastoid cell lines (LCLs) were derived from EBV-infected B cells obtained from normal individuals, IM patients, or by *in vitro* EBV transformation of normal B cells. LCLs grow as large cell clusters. In contrast, Burkitt lymphoma (BL) cells grow mostly as single cells or loose clusters. The CD18 surface expression was
10 measured in 10 LCLs and 10 BL cell lines. Approximately one-third of the cell population in each LCL was CD18-negative. In comparison, the majority of the malignant cells in each BL cell were CD-18 negative (Patarroyo 1988⁹).

In all these studies, competition between viral and cellular DNA for limiting regulatory factors reduces transcription of the CD18 gene.

15 3. **GABP transcription factor**

a) N-box and GABP

20 The DNA motif (A/C)GGA(A/T)(G/A) (N-box) is the core binding sequence of the transcription factor known as Growth Associated (GA) Binding Protein (GABP), Nuclear Respiratory Factor 2 (NRF-2)¹⁰, E4 Transcription factor 1 (E4TF1)¹¹ and Enhancer Factor 1A (EF-1A)¹². In this report, for simplicity, we refer to the transcription factor as GABP and to the motif as the N-box.

b) Cellular GABP genes

25 GABP binds promoters and enhancers of many cellular genes, for instance, β_2 leukocyte integrin (CD18) (nt -48 to nt -43, or -48/-43) (Rosmarin 1998¹³), interleukin 16 (IL-16) (-39/-34, -22/-17, +14/+19) (Bannert 1999¹⁴), interleukin 2 (IL-2) (-438/-434) (Avots 1997¹⁵), interleukin 2 receptor β -chain (IL-2R β) (-56/-34) (Lin 1993¹⁶), IL-2 receptor γ -chain (yc) (two sites in-69/-49) (Markiewicz 1996¹⁷), human secretory interleukin-1 receptor antagonist (secretory IL-1ra) (-93/-79) (Smith 1998¹⁸),

retinoblastoma (RB) (-200/-192) (Sowa 1997¹⁹), human thrombopoietin (TPO) (-69/-63) (Kamura 1997²⁰), aldose reductase (two sites in -186/-146) (Wang 1993²¹), neutrophil elastase (NE) (Nuchprayoon 1999²², Nuchprayoon 1997²³), folate binding protein (FBP) (two sites in -220/-194) (Sadasivan 1994²⁴), cytochrome c oxidase subunit Vb (COXVb) (two sites in +16/+26) (Basu 1993²⁵, Sucharov 1995²⁶), cytochrome c oxidase subunit IV (COXIV) (two sites immediately downstream of the major loci of transcriptional initiation) (Carter 1994²⁷, Carter 1992²⁸), mitochondrial transcription factor A (mtTFA) (Virbasius 1994²⁹), β subunit of the FoF1 ATP synthase (ATPsyn β) (-302/-298) (Villena 1998³⁰), prolactin (prl) (-101/-92) (Ouyang 1996³¹), oxytocin receptor (OTR) (-85/-65) (Hoare 1999³²).

In some of these gene GABP binds to the promoter - a site proximal to the transcription initiation site. See, for instance, CD18, COXVb, COXIV. In other genes, GABP binds an enhancer - a site distal to the transcription initiation site. See, for instance, IL-2 and ATPsyn β (see more on these genes below).

15 c) *GABP α , β and γ (GABP as activator, repressor)*

Five subunits of GABP are known. GABP α , GABP β 1, GABP β 2 (together called GABP β), GABP γ 1 and GABP γ 2 (together called GABP γ). None of the GABP subunits can stimulate transcription alone, either *in vivo* or *in vitro*. GABP α is an *ets*-related DNA-binding protein. GABP α binds the N-box.

20 GABP α forms a heterocomplex with GABP β . GABP β has an amino acid sequence in the amino-terminal which includes a four tandem repeat which is responsible for heterodimerization. GABP β also contains a leucine zipper-like motif in the carboxyl terminal which allows it to homodimerize. Through heterodimerization and homodimerization domains, GABP α and GABP β form a $\alpha_2\beta_2$ heterotetrameric complex which stimulates transcription efficiently *in vitro* and *in vivo*.

25 GABP α also forms a heterocomplex with GABP γ . An identical four tandem repeat in GABP γ is responsible for heterodimerization between GABP α and GABP γ .

However, GABP γ is lacking the leucine zipper-like motif and, therefore, does not homodimerize. The heterodimer does not stimulate transcriptional transactivation.

The degree of transactivation by GABP appears to be a result of the relative intracellular concentrations of GABP β and GABP γ (Suzuki 1998³³). An increase in 5 GABP β relative to GABP γ increases transcription, while an increase of GABP γ relative to GABP β represses transcription. A log regression on the results of Suzuki, *et al.* produced the following formula for the fold increase in transcription as a function of relative concentrations of GABP β and GABP γ (brackets indicate concentration).

$$\text{Fold increase in transcription} = 2.785 \times ([\text{GABP}\beta]/[\text{GABP}\gamma])^{0.06}$$

10 The degree of transactivation by GABP is a function of the ratio between GABP β and GABP γ . By controlling this ratio the cell regulates transcription of genes with binding sites for GABP (Suzuki 1998).

d) GABP binds p300

15 GABP binds the p300 acetyltransferase, a member of the p300/CBP family of proteins. GABP α binds directly to the C-terminal of p300 and much more weakly to the N-terminal. GABP β does not bind directly to p300 (Bannert 1999³⁴).

e) Cellular availability of p300 is limited

20 Although p300/CBP is widely expressed, its cellular availability is limited. A few studies demonstrated that competitive binding of cellular proteins to p300/CBP had an inhibitory effect on activation by certain transcription factors. Competitive binding of p300 or CBP to the glucocorticoid receptor (GR) or retinoic acid receptor (RAR) inhibited activation of a promoter dependent on the AP-1 transcription factor (Kamei 1996³⁵). Competitive binding of CBP to STAT1 α inhibited activation of a promoter dependent on both the AP-1 and *ets* transcription factors (Horvai 1997³⁶). Competitive binding of p300 to STAT2 inhibited activation of a promoter dependent on the NF- κ B RelA transcription factor (Hottiger 1998³⁷).

f) Viral GABP enhancers

The (A/C)GGA(A/T)(G/A) motif is the core binding sequence of many viral enhancers. Examples include the Polyomavirus Enhancer Area 3 (PEA3) (5108/5113, and 5202/5207) (Asano 1990³⁸), E1A enhancer (-300/-295, -200/-195) (Higashino 1993³⁹),

5 (GABP binds to the promoter of the adenovirus early-region 4, or E4, hence the name E4TF1), Rous Sarcoma Virus (RSV) enhancer (189/194) (Laimins 1984⁴⁰), Herpes Simplex Virus 1 (HSV-1) (in the promoter of the immediate early gene ICP4) (LaMarco 1989⁴¹), (Douville 1995⁴²), Cytomegalovirus (CMV) (IE-1 enhancer/promoter region) (Boshart 1985⁴³), Moloney Murine Leukemia Virus (Mo-MuLV) enhancer (8024/8048)

10 (Gunther 1994⁴⁴), Human Immunodeficiency Virus (HIV) (the two NF-κB binding motifs in the HIV LTR) (Flory 1996⁴⁵), Epstein-Barr virus (EBV) (20 copies in the +7421/+8042 oriP/enhancer) (Rawlins 1985⁴⁶) and Human T-cell lymphotropic virus (HTLV) (8 sites in the enhancer (Mauclere 1995⁴⁷) and one site in the LTR (Kornfeld 1987⁴⁸)). Moreover, some viral enhancers, for example SV40, lack a precise N-box, but still bind the GABP

15 transcription factor (Bannert 1999⁴⁹).

Some papers present evidence supporting the binding of GABP to the N-boxes of these viral enhancers. Flory, *et al.*, 1996⁵⁰ show binding of GABP to the HIV LTR, Douville, *et al.*, 1995⁵¹ show binding of GABP to the promoter of ICP4 of HSV-1. Bruder, *et al.*, 1991⁵² and Bruder, *et al.*, 1989⁵³ show binding of GABP to the adenovirus E1A enhancer element I. Ostapchuk, *et al.*, 1986⁵⁴ show binding of GABP (called EF-1A in this paper) to the polyomavirus enhancer. Gunther, *et al.*, 1994⁵⁵ show binding of GABP to Mo-MuLV.

Other papers show competition between these viral enhancers and enhancers of other viruses. Scholer and Gruss, 1984⁵⁶ show competition between the Moloney Sarcoma Virus (MSV) enhancer and SV40 enhancer and also competition between the RSV enhancer and the BK virus enhancer.

4. Microcompetition for GABP•p300.

GABP α binds p300 (Bannert 1999⁵⁷). Therefore, microcompetition for GABP is also microcompetition for GABP•p300. Since cellular availability of p300 is limited, cellular availability of GABP•p300 is also limited.

5 A virus which binds the GABP complex will be called a GABP virus.

Microcompetition for GABP•p300 between a GABP virus and a cellular GABP gene reduces cellular availability of the GABP•p300 complex to the cellular gene. Under these conditions, if the cellular gene is stimulated by the complex, the cellular gene shows reduced transcription. If the cellular gene is repressed by the complex, the cellular gene shows increased transcription.

10

II. Discovery 2: GABP•p300 binding regulation

1. ERK pathway

Extracellular signals are transmitted to the nucleus in many ways. Often signal transduction occurs through activation of a kinase found in the cytoplasm. Once activated, 15 the kinase translocates to the nucleus where it phosphorylates target transcription factors thereby modifying their capacity to regulate gene expression. For MAP kinase cascades, the signal is propagated through sequential activation of multiple kinases. These kinases amplify small input signals into large changes in output. All MAP kinases are activated by dual phosphorylation on a Thr-Xaa-Tyr motif, after which they function as proline-directed Ser/Thr kinases with minimal target sequence of Ser/Thr-Pro (Hipskind, 1998⁵⁸).

20

Growth factors and other extracellular agents that support proliferation activate the ERK (Extracellular signal-regulated kinase, previously called the MAP kinase) signaling cascade, see figure 5.

25 The kinases which make up the core of this cascade are Raf, which phosphorylates MEK, which in turn phosphorylates ERK. Raf (MAPKKK) is activated by an unclear mechanism usually dependent upon Ras. By interacting with Ras, Raf is relocalized to the membrane, which appears to be an important step for its activation. The Raf family has three known members, c-Raf (or Raf-1), B-Raf and A-Raf, and each of these proteins can

function as a MAPKKK depending upon cell type. c-Raf has been generally described as the major activator. Other kinases can also function in this capacity (i.e.- MEKKs 1 and 3) and the possibility remains open for other specific activators of the ERK cascade.

5 Raf activates the MAPKK MEK (MEK1 and MEK2), a kinase that phosphorylates both Thr and Tyr residues in the activation motif in ERK. There are five members of the ERK family identified to date, p44ERK1, p42ERK2, ERK3, ERK4, and ERK5/BMK1 (for Big MAP Kinase). Activation results in translocation of ERK to the nucleus, where it targets transcription factors and the basal transcription complex.

10 Dephosphorylation at either Thy or Tyr residue inactivates ERK. There are three classes of ERK inactivators: Type 1/2 serine/threonine phosphatases, such as PP2A, tyrosine-specific phosphatases (also called protein-tyrosine phosphatase, denoted PTP), such as PTP1B, and dual specificity phosphatases, such as MKP-1. For recent reviews of the role of these classes of phosphatases in the regulation MAP kinase activity, see Camps 2000⁵⁹, Saxena 2000⁶⁰ and Keyse 1998⁶¹. Herein the term "ERK phosphatase" denotes 15 any phosphatase which inactivates ERK. The class of all ERK phosphatases is a super class of the above three classes of ERK inactivators.

20 Figure 6 illustrates the activation of MAPK by MEK-1, a MAPKK, and deactivation of MAPK by either PP2A, a serine/threonine phosphatase, PTP1B, a tyrosine-specific phosphatase, or MKP-1, a dual specificity phosphatase. A diamond represents a kinase, an ellipse, a phosphatase, an arrow, phosphorylation, and a T-headed line, dephosphorylation.

For a discussion of the JNK/SAPK pathway see below.

2. ERK agents

25 A molecule which stimulates the phosphorylation of ERK will be called an "ERK agent." Some ERK agents include sodium butyrate (SB), trichostatin A (TSA), trapoxin, phorbol ester (phorbol 12-myristate 13-acetate, PMA, TPA), retinoic acid (RA, vitamin A), zinc and copper, interferon- γ (IFN γ), new differentiation factor (NDF or heregulin), estron, etradiol (E2), interleukin 1 β (IL-1 β), interleukin 6 (IL-6), tumor necrosis factor α

(TNF α), transforming growth factor β (TGF β) and oxytocin (OT). Consider the following evidence.

a) *Sodium butyrate (SB), trichostatin A (TSA) and trapoxin*

The ERK agents sodium butyrate (SB), trichostatin A (TSA) and trapoxin were 5 tested for their effects on the major promoter (M) of human choline acetyltransferase (ChAT). The human choline acetyltransferase gene was activated by sodium butyrate, trichostatin A, and trapoxin A in transient and stable transfection studies (Espinosa 1999⁶²). These agents also stimulated ERK1 and ERK2 phosphorylation. If the MAP kinase 10 cascade is blocked with the MAP kinase kinase (MEK) inhibitor PD98059 or by overexpression of dominant-negative mutants of Ras and ERK2, activation of ChAT promoter by sodium butyrate is suppressed (Espinosa 1999).

Transcriptional activation of cellular and transfected genes by histone deacetylase (HDAC) inhibitors is blocked by H7, an inhibitor of serine/threonine protein kinases. In 15 transient transfections with the human ChAT gene, cells were treated for 1 hour with H7, and then sodium butyrate or trapoxin were added in the continued presence of H7. Under these conditions, H7 inhibited the activation by both trapoxin and sodium butyrate (Espinosa 1999). Similar experiments were performed using the RSV LTR and the SV40 enhancer. Activation of these enhancer regions by sodium butyrate or trapoxin was suppressed by H7. In addition, activation of the RSV LTR by sodium butyrate was 20 blocked by the MEK inhibitor PD98059 while activation of the SV40 promoter was similarly depressed about three-fold (Espinosa 1999).

Transcription of the nicotinic acetylcholine receptor (AChR) in adult muscle is 25 restricted to the nuclei located at the neuromuscular junction. The N-box, a promoter element, contributes to this specialized synaptic expression of the AChR δ - and ϵ -subunits. GABP binds to the N-box *in vitro*. GABP subunits contain phosphorylation sites which serves as targets for MAP kinases and these kinases also mediate the heregulin-elicited stimulation of transcription of AChR genes in cultured chick myotubes. Phosphorylation studies in chick primary myotubes showed that heregulin stimulated GABP α and GABP β phosphorylation. Both subunits of GABP are phosphorylated *in vivo* by MAP kinases and 30 heregulin enhances their phosphorylation (Schaeffer 1998⁶³).

b) *Phorbol ester (phorbol 12-myristate 13-acetate, PMA, TPA), thapsigargin*

The murine macrophage cell line RAW 264.7 was stimulated with thapsigargin, an endomembrane Ca(2+)-ATPase inhibitor, and TPA, the protein kinase C activator. Both thapsigargin (30 nM) and TPA (30 nM) induced phosphorylation of p44/p42 MAP kinase and production of histamine in a time- and concentration-dependent manner. The specific MEK1 inhibitor PD98059 strongly suppressed both the thapsigargin and TPA induced histamine production. Another MEK1 inhibitor, U-0126, also inhibited both the thapsigargin and TPA-induced histamine production in a concentration-dependent manner (Shiraishi 2000⁶⁴).

TPA induces *in vitro* differentiation of the pluripotent K562 human leukemia cell line. Treatment of K562 cells with TPA resulted in growth arrest, polyploidy, morphological changes, and increased cell-cell and cell-substrate adhesion. These PMA-induced changes were preceded by a rapid rise in the MEK1 activity that resulted in the sustained ERK2 activation. The MEK1 inhibitor, PD098059, reversed both the growth arrest and the morphological changes induced by TPA treatment. These results demonstrate that the TPA-induced signaling cascade initiated by protein kinase C activation requires activity of MEK/ERK signaling complex in regulating cell cycle arrest (Herrera 1998⁶⁵).

TPA was used to inhibit apoptosis in HL-60 cells stimulated with the JNK/SAPK activator anisomycin. An increase in ERK activity was associated with the anti-apoptotic effect. The MEK1 inhibitor, PD98059, inhibited TPA-mediated ERK activity and abrogated the anti-apoptotic effects of TPA. Moreover, inhibition of apoptosis was attenuated by pretreatment with PKC inhibitors (Stadheim 1998⁶⁶).

c) *Retinoic acid (RA, vitamin A)*

Yen, et al., 1999⁶⁷ stated "Among the three major mitogen-activated protein kinase (MAPK) cascades—the extracellular signal regulated kinase (ERK) pathway, the c-JUN N-terminal/stress-activated protein kinase (JNK/SAPK) pathway, and the reactivating kinase (p38) pathway—retinoic acid selectively utilizes ERK but not JNK/SAPK or p38 when inducing myeloid differentiation of HL-60 human myeloblastic leukemia cells. Retinoic

acid is known to activate ERK2. The present data show that this activation is selective for the MAPK pathway. JNK/SAPK or p38 are not activated by retinoic acid.”

5 *d) Interferon- γ (IFN γ)*

IFN γ activates both ERK and PKC in human peripheral blood monocytes (Liu 1994⁶⁸). IFN γ also induced ERK activation in rat C6 glioma cells. In C6 glioma cells, transient expression of the dominant-negative form of c-Ha-Ras (Asn-17) abrogated IFN γ -induced ERK1 and ERK2 activation. Furthermore, the MEK1 specific inhibitor, PD98059, blocked this activation. These results indicate that p21ras and MEK1 are required for IFN γ -induced ERK1 and ERK2 activation (Nishiya 1997⁶⁹).

10 *e) Heregulin (HRG, or New differentiation factor, NDF)*

15 Heregulin β 1 (HRG β 1) induced ERK activation and cell differentiation in AU565 breast carcinoma cells. ERK activation remained elevated for 2 h following high doses of HRG. The MEK specific inhibitor, PD98059, inhibited activation of ERK and completely blocked HRG-induced differentiation reversing cell growth arrest. A transient transfection of a mutant constitutively active MEK1 construct into AU565 cells induced differentiation in the absence of HRG. Treatment with HRG potentiated this response. This study indicates that HRG induces the sustained activation of the MEK/ERK pathway and that this activation is essential for inducing differentiation of AU565 cells (Lessor 1998⁷⁰).

20 HRG activated the MAP kinase isoforms p44ERK1 and p42ERK2 and the p70/p85 S6 kinase in AU565, T47D and HC11 cells. HRG stimulation caused growth arrest of the AU565 cells and proliferation of the T47D or HC11 cells. HRG also stimulated tyrosine phosphorylation and *in vitro* kinase activity of ErbB-2. When PKC was activated by TPA, another ERK agent, HRG was no longer able to activate ErbB-2 in T47D cells, blocking cell proliferation. Activation of ErbB-2 by point mutation or monoclonal antibodies, also 25 stimulated MAPK and p70/p85 S6 kinase pathways. The same monoclonal antibodies also induced AU565 cell differentiation (Marte 1995⁷¹).

HRG β 2 stimulation of MDA MB-453 cells resulted in tyrosine phosphorylation of p185c-erbB2 and p180erbB4 receptors in a time- and dose-dependent fashion. Activation

of ERK (> 30-fold over untreated controls) was observed upon receptor(s) activation, as was the induction of the immediate early gene c-fos (> 200-fold) (Sepp-Lorenzino 1996⁷²). In another study, HRG β 2, the ligand for erbB3 and erbB4 caused ERK activation and mitogenesis of growth arrested T-47D human breast cancer cells. The MEK1 specific inhibitor, PD98059, completely blocked HRG-induced entry into S-phase (Fiddes 1998⁷³).

5 *f) Zinc (Zn) and copper (Cu)*

Egr1, an immediate early transcription factor, is induced after brain insults by an unknown mechanism. Short exposure to zinc led to sustained ERK activation (Park 1999⁷⁴). The MEK1 inhibitor, PD098059, inhibited ERK1/2 activation, Egr1 induction, 10 and neuronal death by zinc. That study concluded that zinc activates ERK1/2 (Park 1999). In another study, zinc enhanced ERK activity in serum-starved Swiss 3T3 cells treated with insulin and phosphocholine (Kiss 1997⁷⁵).

15 The human bronchial epithelial cell line BEAS was exposed to noncytotoxic levels of metals including Cu and Zn. Kinase activity assays and Western blots (with phospho-specific MEK1 antibody) showed that MEK1 is activated by Cu or Zn treatment. Additional Western blots using phospho-specific ERK1/2 antibody showed that PD98059, the selective MEK1 inhibitor, blocked the metal induced phosphorylation of ERK1/2 (Wu 1999⁷⁶). Activity assays of another study showed a dramatic activation of ERK, JNK and p38 in BEAS cells exposed to Zn, while Cu exposure led to a relatively small activation of 20 ERK (Samet 1998⁷⁷).

g) Estron, estradiol

Treatment of human mammary cancer MCF-7 cells with estradiol stimulates rapid and transient activation of ERK1/2. Estradiol activates the tyrosine kinase/p21ras/ERK pathway in MCF-7 cells (Migliaccio 1996⁷⁸).

25 Uterine smooth muscle from rats pretreated with estradiol-17 β alone or with estradiol-17 β and progesterone were tested for ERK expression and activity by immunoblotting with ERK1/2 antibodies and phosphorylation assays. Estrogen and progesterone both enhanced ERK activity (Ruzicka 1996⁷⁹).

In another study, immunoblot analyses and phosphorylation assays showed that estradiol-17 β (E2) stimulated ERK1/2 in rat cardiomyocytes. Specifically, the activation of ERK1/2 was rapid and transient, while a rapid but sustained increase of JNK phosphorylation was observed (Nuedling 1999⁸⁰).

5 *h) Interleukin 1 β (IL-1 β)*

Treatment with IL-1 β in cultured human airway smooth muscle cells increased levels of phosphorylated ERK (p42 and p44) 8.3- and 13-fold, respectively. Pretreatment of the cells with the MEK1 inhibitor PD98059 decreased ERK phosphorylation (Laporte 1999⁸¹).

10 IL-1 β treatment of HepG2 cells activated three ERK cascades, p46/54(JNK), p38, and ERK1/2. There was maximal induction of 20-, 25-, and 3-fold, respectively, in these three cascades (Kumar 1998⁸²). In another study, Western blotting and kinase assays showed that IL-1 β activates ERK1/2 and p38 in islets and rat insulinoma cells (Larsen 1998⁸³).

15 *i) Interleukin 6 (IL-6)*

The cytokine IL-6 utilizes its 80-kDa ligand-binding and 130-kDa signal-transducing subunits to trigger cellular responses. Treatment of the human B cell line, AF-10, with rIL-6 activated ERK. Activation of ERK in AF-10 cells occurred at the same time as the appearance of 42- and 44-kDa tyrosine phosphoproteins (p42 and p44) (Daeipoou 1993⁸⁴). When AF-10 cells were induced with rIL-6 in the presence of the tyrosine kinase inhibitors, genistein and geldanomycin, ERK activation decreased. These results indicate that IL-6 activates ERK1/2.

j) Tumor necrosis factor α (TNF α)

TNF α stimulates IL-6 production in renal cells in culture. Human primary mesangial cells (HMCs) and human proximal tubular (HPT) cells were treated for 24 hours with TNF α in the presence and absence of the specific p38 and ERK1/2 inhibitors SB203580 and PD98059, respectively, either alone or in combination. TNF α normally

activates p38 and ERK1/2. The inhibitors SB203580 and PD98059 inhibited basal and TNF α -stimulated IL-6 production in both cell types (Leonard 1999⁸⁵).

k) Transforming growth factor β (TGF β)

5 TGF β inhibits many epithelial cell types. Both TGF β 1 and TGF β 2 trigger rapid activation of p44MAPK in two proliferating epithelial cell lines, IEC4-1 and CCL64. Results for a third TGF β resistant cell line, IEC4-6 showed no activation of p44MAPK after TGF β stimulation. Resting cultures of IEC4-1 cells treated with TGF β 2 led to no significant change in either DNA synthesis or p44MAPK activity. However, addition of 10 the growth-stimulatory combination of factors (epidermal growth factor, insulin, and transferrin (EIT)) to quiescent and proliferating IEC4-1 cells stimulated DNA synthesis and led to activation of p44MAPK. The specificity for the cellular effects of growth factors may not actually occur at the level of MAPK activation, but instead at downstream events including phosphorylation of transcriptional complexes and gene activation (Hartsough 1995⁸⁶).

15 TGF β 1 also stimulates articular chondrocyte cell growth and the formation of the extracellular matrix. *In vitro* kinase assays showed a rapid activation of ERK induced by TGF β 1 (Yonekura 1999⁸⁷). The stimulation peaked at 5 min, and dropped back to basal levels within 240 min after TGF β 1 stimulation. After 240 minutes of stimulation, the c-jun N-terminal kinase activity increased only about 2.5-fold, while there was no 20 significant change in p38MAPK activity. PD98059 decreased TGF β 1 induced Elk1 phosphorylation in a dose-dependent manner (Yonekura 1999).

l) Oxytocin (OT)

25 Oxytocin (OT) treatment triggers the rapid phosphorylation of ERK2 in Chinese hamster ovary (CHO) cells (Strakova 1998⁸⁸). The MEK1 specific inhibitor, PD98059, significantly reduced OT-stimulated prostaglandin (PGE) synthesis (Strakova 1998). Oxytocin receptors (OTRs) are found in a number of human breast tumors and tumor cells. In a study of breast cancer cells (Hs578T cells), OT stimulated ERK2 phosphorylation and PGE2 synthesis in Hs578T cells (Copland 1999⁸⁹).

The rat oxytocin receptor was transfected into Chinese hamster ovary cells. Oxytocin stimulated ERK2 phosphorylation and PGE synthesis through protein kinase C activity (Hoare 1999⁹⁰). Deletion of 51 amino acid residues from the carboxyl terminus of the oxytocin receptor resulted in decreased affinity for oxytocin. Cells expressing the 5 truncated receptor showed no oxytocin-stimulated ERK2 phosphorylation or PGE synthesis (Hoare 1999).

3. Phosphorylation of GABP

ERK phosphorylates GABP α and GABP β but phosphorylation does not change the binding of GABP to DNA (Flory, 1996⁹¹, Avots, 1997⁹², Hoffmeyer, 1998⁹³, Tomaras, 10 1999⁹⁴).

Phosphorylation is known to increase binding or stabilize the complex of p300 and other transcription factors, such as NF- κ B unit p65 and Bbf (Zhong 1998⁹⁵, Bevilacqua 1997⁹⁶). The following sections present evidence consistent with the discovery that ERK phosphorylation of GABP leads to increased binding of p300 to GABP to stabilize the 15 GABP•p300 complex.

a) *ERK phosphorylation of GABP increases N-Box DNase-I hypersensitivity*

Histone acetylation occurs post-translationally, and reversibly, on the ϵ -NH₃⁺ groups of lysine residues embedded in the N-terminal tails of core histones. Histone acetyltransferases (HATs) transfer the acetyl moiety from acetyl coenzyme A to the ϵ -NH₃⁺ groups of internal lysine residues. Introduction of the acetyl group to lysine 20 neutralizes the positive charge, increases hydrophobicity and leads to unfolding of chromatin (Kuo 1998⁹⁷). Histone hyperacetylation correlates with sensitivity to digestion by deoxyribonuclease I (DNase-I) (Hebbes 1994⁹⁸). Moreover, binding of a transcription complex with HAT activity to DNA enhances DNase-I hypersensitivity around the DNA 25 binding site. p300 has HAT enzymatic activity so that binding the GABP•p300 complex enhances DNase-I hypersensitivity around the N-box.

Porcine peripheral blood mononuclear cells (PBMC) were stimulated with the ERK agent TPA. The treatment consistently enhanced DNase-I hypersensitivity of the

third intron enhancer of the TNF α gene (Kuhnert 1992⁹⁹). The major transcription factor that binds the enhancer site in the third intron of TNF α gene is GABP (Tomaras 1999¹⁰⁰). TPA treatment phosphorylated ERK which in turn phosphorylated GABP. Phosphorylation of GABP increased binding of p300. It is therefore likely that the HAT activity of p300 acetylated the histones and enhanced DNase-I hypersensitivity of the third intron enhancer.

5 **b) *ERK phosphorylation of GABP synergizes with p300 stimulation***

Human neuroepithelioma CHP126 cells were transfected with a construct containing the promoter of human choline acetyltransferase (ChAT) gene fused to the 10 luciferase reporter gene (ChAT-luciferase). These cell were stimulated with the ERK agent trapoxin which increased luciferase expression 8-fold. In a second experiment the cells were transfected with an expression vector carrying full-length p300. p300 expression increased luciferase expression 5- to 10-fold. In a third experiment the cells were transfected with p300 and stimulated with trapoxin. The combined treatment 15 increased luciferase expression 94-fold (Espinosa 1999¹⁰¹). Trapoxin phosphorylated ERK which in turn phosphorylated GABP. The combined effect of GABP phosphorylation and p300 transfection on transcription was more than additive.

20 This greater than additive increase in transcription demonstrates that two stimulators act in the same pathway, or in pathways that merge, to increase transcription from a single promoter. If the stimulators were acting independently, the largest possible level of transcription from the two together would be the sum of the two pathways, with each stimulator increasing transcription as if the other were not present (Herschlag 1993¹⁰²). A compelling interpretation of the "more than additive" results above is that phosphorylation of GABP increased binding of p300.

25 **c) *Inhibition of ERK phosphorylation blocks p300 stimulation***

H7 is an inhibitor of serine/threonine protein kinases. ERK, a serine/threonine protein kinase is therefore inhibited by H7. Activation of the ChAT promoter by either the ERK agent trapoxin or the ERK agent sodium butyrate was inhibited by 40 μ M of H7. Activation of the ChAT promoter by p300 was also inhibited by H7 in a dose-dependent

manner. H7 also suppressed the synergistic activation of the ChAT promoter triggered by trapoxin and p300 (Espinosa 1999¹⁰³). Inhibition of GABP phosphorylation decreased binding of p300, which reduced transcription.

d) Inhibition of p300 binding blocks stimulation by ERK phosphorylation

5 GABP binds p300 in between amino acids 1572 and 2370 (Bannert 1999¹⁰⁴) while the adenovirus E1A protein binds p300 between amino acids 1572 and 1818 (Eckner 1994¹⁰⁵). E1A and GABP, therefore, share an overlapping binding site on p300. By displacing GABP from p300, E1A reduces the effectiveness of GABP phosphorylation. Activation of the SV40 minimal promoter and the ChAT promoter by the ERK agent 10 sodium butyrate and by p300 was suppressed by adenovirus E1A protein (Espinosa 1999).

ERK phosphorylation of GABP increases transcription. Raf-1, a kinase involved in the ERK pathway, works with GABP to stimulate HIV-1 promoter activity (Flory 1996¹⁰⁶). These results support the idea that Raf-1 activates GABP α -and GABP β -mediated gene expression. Further tests showed that GABP is phosphorylated *in vivo* by 15 Raf-1 kinase activators (e.g. serum and TPA) and constitutive versions of Raf-1 kinase. The basal phosphorylation level of GABP α and GABP β increased 2- to 4-fold after stimulation with serum and TPA (Flory 1996).

20 To identify kinases of GABP α and β , bacterially expressed GABP α and β proteins were tested as substrates in *in vitro* kinase assays. Raf-1 did not phosphorylate GABP subunits *in vitro*, but phosphorylation of both GABP α and GABP β was detected in the reaction mixture containing MEK1, ERK2, GABP α , and GABP β . ERK1 yielded similar results. A kinase-inactive ERK1 did not phosphorylate GABP α and β (Flory 1996). These results suggest that ERK1 directly phosphorylates both GABP α and GABP β .

25 A DNA segment in the upstream region of the human IL-2 gene contains a transcription enhancer (-502 to -413). Which binds the transcription factor GABP α and GABP β at -462 nt to -446 nt (designated ERE-B) and -440 to -424 nt (designated ERE-A) (Avots 1997¹⁰⁷) respectively.

GABP is a target of the MAP signal transduction pathway in T cells. c-Raf enhances IL-2 induction through GABP factors. Co-transfection of a CAT reporter gene controlled by the distal enhancer with GABP α and β expression vectors into cells showed an increase in CAT activity. Mutation of one or both ERE motifs abrogated the induction, 5 underscoring the important functional role of GABP binding for induction of the distal enhancer. These data indicate that the c-Raf mediated increase of IL-2 induction is, at least partially, mediated by the GABP factors binding to the two ERE motifs (Avots 1997). According to Avots, *et al.*, there appears to be an important role for the MAP pathway in induction of GABP factors binding to and controlling the distal IL-2 ERE 10 enhancer motifs in T cells (Avots 1997).

4. ERK agents and microcompetition

The relationship between ERK singaling and microcompetition is summerized in figure 7.

15 Microcompetition between a GABP virus and cellular DNA reduces the availability of GABP to cellular genes. Let $[N\text{-box}_v]$ denote the cellular concentration of viral N-boxes. Let $[GABP_c]$ and $[GABP_v]$ denote the concentration of GABP bound to cellular genes and viral DNA, respectively. $[GABP_v]$ is a function of $[N\text{-box}_v]$. For every $[N\text{-box}_v] > 0$, microcompetition reduces $[GABP_c]$. An ERK agent phosphorylates GABP and stimulates p300 binding. If $[N\text{-box}_v]$ is fixed, the ERK agent stimulates the 20 transcription of GABP stimulated genes and suppresses the transcription of GABP inhibited genes.

25 Fixed $[N\text{-box}_v]$ seems to hold in cases of latent infection. In such cases, ERK phosphorylation of GABP $_v$ stimulates the formation of $N\text{-box}_v \bullet GABP_v \bullet p300$ complexes. However, there is no increase in viral replication, which might have further reduced the availability of p300 to cellular genes and diminished or even canceled the ERK effect.

5. JNK/SAPK pathway

a) *Phosphorylation of GABP*

Another signaling pathway which phosphorylates GABP is JNK/SAPK (see a figure of pathway in ERK pathway section above). Consider the following study.

5 To study the effects of JNK/SAPK on GABP, *in vivo*, HEK-293, human embryonic kidney cells were transfected with GABP α and GABP β expression vectors alone, or in combination with SAPK β expression vector and metabolically labeled with [32 P]orthophosphate. The cells were treated with anisomycin to strongly activate SAPK without affecting ERK activity. The results showed increased phosphorylation of both 10 GABP α and GABP β . The phosphorylation was further increased with SAPK β overexpression (Hoffmeyer 1998¹⁰⁸, Fig 5A and B). The study next tested the ability of these kinases to phosphorylate GABP *in vitro*, using ERK as a positive control. *In vivo* activated and immunopurified GST-tagged SAPK β , but not Flag-tagged p38, phosphorylated both subunits of GABP (Ibid, Fig. 6B). Bacterially expressed, purified, 15 and preactivated GST-SAPK α I also phosphorylated both GABP subunits *in vitro* like GST-c-Jun (Ibid, Fig. 6C). Both activated SEK and 3pK did not phosphorylate GABP. Next, the study tested another JNK/SAPK isozyme, JNK1/SAPK γ . In addition to ERK, untreated or TPA/ionomycin-stimulated A3.01 cells (a human T lymphoma cell line) 20 phosphorylated both GABP α and GABP β *in vitro* (Ibid, Fig. 6A). Based on these results, Hoffmeyer, *et al.*, concluded that “the ability of three different isoforms of JNK/SAPK (SAPK α , SAPK β , and JNK1) to phosphorylate GABP *in vitro*, in combination with the *in vivo* phosphorylation of GABP upon SAPK activation by anisomycin, suggests that GABP is targeted by JNK/SAPK-activating pathways.”

III. Discovery 3: N-box•GABP binding regulation

25 1. Redox regulation of GABP N-box binding

Oxidative stress decreases binding of GABP to the N-box, reduces transcription of GABP stimulated genes and increases transcription of GABP suppressed genes. Consider the following study.

Mouse 3T3 cells were treated for 2 h with diethyl maleate (DEM), a glutathione (GSH)-depleting agent, in the presence or absence of N-acetylcysteine (NAC), an antioxidant and a precursor of GSH synthesis. Following treatment, the cells were harvested, and nuclear extracts were prepared in the absence of a reducing agent. GABP 5 DNA binding activity was measured by EMSA analysis using oligonucleotide probes containing a single N-box (AGGAAG) or two tandem N-boxes (AGGAAGAGGAAG). Treatment of 3T3 cells with DEM resulted in a dramatic decrease in formation of the GABP heterodimer (GABP α GABP β), (Martin 1996¹⁰⁹, Fig. 2A, lane 2) and heterotetramer (GABP α_2 GABP β_2), (Ibid, Fig. 2A, lane 6) complexes on the single and double N-box. 10 Inhibition of GABP DNA binding activity by DEM treatment was prevented by simultaneous addition of NAC (Ibid, Fig. 2A, lanes 4 and 8). The reduction of GABP DNA binding activity was not due to loss of GABP protein since the amount of GABP α and GABP β 1 was unaffected by DEM or NAC treatment. Treatment of nuclear extracts prepared from DEM-treated 3T3 cells with dithiothreitol (DTT), an antioxidant restored 15 GABP binding activity. Treatment of 3T3 nuclear extracts with 5 mM GSSG nearly abolished GABP DNA binding. Based on these observations Martin *et al.*, concluded that GABP DNA binding activity is inhibited by oxidative stress, i.e. GSH depletion. The study also measured the effect of DEM treatment on expression of transiently transfected luciferase reporter constructs containing a TATA box with either upstream double N-box 20 or C/EBP binding site (Ibid, Fig. 4). DEM treatment had no effect on luciferase expression from C/EBP-TA-Luc after 6 or 8 h treatment (Ibid, Fig. 4). However, DEM treatment of cells transfected with double N-box-TATA-Luc, resulted in a 28% decrease in luciferase expression after 6 h and a 62% decrease after 8 h (Ibid, Fig. 4). Based on 25 these results, Martin *et al.*, concluded that glutathione depletion inhibits GABP DNA binding activity resulting in reduced expression of GABP-regulated genes.

These results demonstrate that oxidative stress decreases GABP binding to the N-box which in turn decreases transcription of a GABP stimulated gene and increases transcription of a GABP repressed gene.

2. Microcompetition as “excess oxidative stress”

Microcompetition for GABP also decreases binding of GABP to the N-box. Take a GABP gene sensitive to oxidative stress through GABP only¹. The effect of microcompetition on the transcription of this gene is similar to the effect of oxidative stress. In other words, for this gene, microcompetition can be viewed as “excess oxidative stress.”

IV. Discovery 4: Molecular effects of microcompetition**1. Signaling**

Let a GABP kinase be any enzyme which phosphorylates GABP. Since GABP is a new concept, we sometimes revert to ERK instead of GABP kinase. However, in such cases, unless specified, ERK actually means GABP kinase.

a) *Sensitization by GABP*

The statement “A stimulates B” means that A stimulates the expression of B either directly or indirectly. Let “AGENT” be a GABP kinase agent which activates the transcription factor GABP. Let GABP stimulate the expression of a protein P. Let [AGENT]₁ and [AGENT]₂ be two concentrations of AGENT with corresponding concentrations [P]₁ and [P]₂. The intensity of signal [AGENT]₁ relative to [AGENT]₂ is equal to [AGENT]₁/[AGENT]₂ = [P]₁/[P]₂. The intensity of an ERK signal is measured by its effect on transcription of the protein P.

Let AGENT be a GABP kinase agent which activates the transcription factor GABP. Let (AGENT, GABP) denote the signaling pathway that leads from AGENT to GABP. Every protein R, such that R is an element of the signalling cascade (AGENT, GABP) will be called an “ERK receptor for AGENT.” In other words, AGENT activates the R protein, which in turn activates GABP. For example, the leptin long receptor is an ERK receptor for leptin, and metallothionein is an ERK receptor for zinc.

¹ Oxidative stress also modifies binding of other transcription factors, such as AP1, and NF- κ B.

Let AGENT be a GABP kinase agent. If there is a protein R in the signalling cascade (AGENT, GABP), such that AGENT stimulates the expression of R, the (AGENT, GABP) pathway will be called "sensitized" and R will be called the "sensitized receptor," denoted R. Sensitization increases the intensity of a given signal by increasing 5 the number of receptors available to be activated by a given amount of GABP kinase agent..

Let R be a sensitized receptor in (AGENT, GABP). If the expression of R is stimulated by GABP, R will be called an "internally sensitized receptor." Consider figure 8.

10 An increase in AGENT stimulates the phosphorylation of GABP (step 1 and 2 in the figure). The phosphorylated GABP stimulates the transcription of R₁, the sensitized receptor (step 3). The new R₁ receptors increase the sensitivity of the pathway to a change in the concentration of the GABP kinase agent, that is, increase the probability of binding 15 between the GABP kinase agent and R₁. The increased binding further increases the number of phosphorylated GABP molecules (step 4) in a positive feedback mechanism.

In the pathway (OT, OTR, GABP), the receptor OTR is stimulated by GABP (Hoare 1999¹¹⁰). In (zinc or copper, hMT-IIA, GABP), hMT-IIA is a receptor stimulated by GABP (see discussion above). In the pathway (LPS, CD18, GABP), CD18 is a receptor stimulated by GABP (Rosmarin 1998¹¹¹). In the pathway, (IL-2, IL-2R β , γ _C, 20 GABP), IL-2R β and γ _C are two receptors stimulated by GABP (Lin 1993¹¹², Markiewicz 1996¹¹³).

According to the definition of an ERK receptor, GABP is also an ERK receptor. In addition, some GABP kinase agents increase the expression of GABP turning GABP from an ERK receptor into a sensitized receptor. Consider the following examples.

25 GABP β and γ are similar proteins which differ only by homodimerization section in the C-terminal region. Antibodies which are not specific to the C-terminus bind both proteins. Such antibodies are not sensitive enough to identify a relative change in their expression. However, since GABP β and GABP γ are almost always bound to GABP α , and since GABP β is an activator and GABP γ is a suppresser (Suzuki 1998¹¹⁴), an increase in

GABP α with an increase in gene expression indicates an increase in the GABP β concentration relative to γ .

IFN γ

Evidence suggests that interferon- γ (IFN γ) regulates GABP DNA binding by increasing the amount of the GABP proteins present in bone marrow-derived macrophages (BMDM) nuclei. IFN γ treatment of BMDM leads to induction of the binding activity (Tomaras, 1999¹¹⁵). Since the GABP β and GABP γ are almost always bound to GABP α , (Suzuki 1998), an increase in β most likely corresponds to an increase in GABP α .

The increase in DNA binding activity correlates with an increase in immunodetectable GABP α (Tomaras 1999). The essential sites for activity of GABP within the third intron of TNF α map to a highly conserved tandem repeat of *ets*-transcription factor binding sites. Mutations in the *ets* site within the intron inhibited this activity. A dominant-negative *ets* plasmid also completely negated this cooperativity. It was determined that a GGAA sequence repeat is a transcriptionally active site which interacts with an *ets* transcription factor. Specifically, GABP binds to this region. GABP binding activity is increased by treatment with IFN γ in BMDM (Tomaras 1999).

Heregulin

Heregulin increases GABP α expression specifically (Schaffer 1998). Western blot analysis of heregulin treated and non-treated cells showed that heregulin treatment leads to a 2-fold increase in the protein level of GABP α , while the GABP β protein level was unaffected (Schaffer 1998).

PMA

Bottinger, *et al.*, 1994¹¹⁶ defined the minimal defined promoter for CD18 ($\beta 2$ integrin) expression in myeloid and lymphoid cells by generating 5' and 3' deletion constructs of a segment ranging 785 bp upstream and 19 bp downstream of a major transcription start site. The region extending from nucleotides -302 to +19 supported cell-restricted and phorbol ester-inducible expression. Two adjacent promoter regions, from nt

-81 to -68 (box A) and -55 to -41 (box B), were revealed by DNase-I footprinting of this region. DNA-binding proteins that interact with box A and box B were identified through electrophoretic mobility shift assays. Using box A as a probe yielded a major complex, designated BA-1 which increased in intensity after phorbol ester-induced differentiation of the cells. The complex was also detected using the radiolabeled box B element. The complex is homologous to GABP. Antiserum specific to GABP α or GABP β abrogated binding of BA-1, while antisera to other *ets*-transcription factors had no effect (Bottinger 1994) thereby demonstrating the specificity of this interaction.

10 Expression of CD18 corresponds to the DNase-I protection profiles observed *in vitro*, suggesting that the complexes that bind to the protected elements mediate tissue specific expression of the CD18 gene. In T cells, the BA-1 complex forms over the box A and box B elements and is apparently responsible for the DNase-I protection profiles seen. Despite the formation of the same complex in the HeLa CD18 negative cell line, there is no observed DNase-I protection (Bottinger 1994).

15 In T cells the expression of GABP α and GABP β increase. Since GABP $\alpha\beta$ is an activator, Bottinger observed increased expression of CD18 and DNase-I protection on the CD18 promoter. In HeLa cells GABP α and GABP γ increase. Since GABP γ is a suppresser, Bottinger observes no expression of CD18 and little DNase-I protection on the CD18 promoter.

20 b) *Resistance*

(1) *Hypothesis*

(a) *Resistance*

Traditionally, there are two definitions of resistance, cellular level resistance and patient level resistance.

25 **Cellular level resistance:** Let L denote a ligand and O a cell. Let L produce the effect Y in O. The cell O will be called "L resistant" if a given concentration of L produces a smaller Y effect in O relative to control.

Patient level resistance: Let L denote a ligand. A patient will be called "L resistant" if the patient shows elevated levels of L relative to controls. Patient level resistance is sometimes called hyper-L-emia. Example: Insulin resistance as observed in late onset (type II) diabetes and hyperinsulinemia.

5

(b) Control

Let AGENT be a GABP kinase agent and let C be a protein. If the expression of AGENT depends on the expression of C, C will be called a "control" for AGENT. If an increase in C represses the expression of AGENT, or increases its degradation, C will be called a "negative control" and the effect on AGENT termed "feedback inhibition."

10

Let AGENT be an GABP kinase agent with the (AGENT, GABP) pathway. If GABP stimulates C, C will be called a "GABP stimulated" control. Consider figure 9.

AGENT phosphorylates GABP (step 1 and 2). GABP increases the transcription of C (step 3). C decreases the expression of the GABP kinase agent (step 4).

15

(c) Microcompetition causes resistance

Cellular level resistance

Let AGENT be a GABP kinase agent with the (AGENT, GABP) pathway. Let AGENT produce the effect Y in the cell O. Let the Y effect be dependent on transcription of a GABP gene X in O. Under microcompetition in O, a given concentration of AGENT produces a smaller concentration of X and a smaller Y effect.

20

Patient level resistance

25

Let AGENT be a GABP kinase agent with the (AGENT, GABP) pathway. Let C be a negative control for AGENT which is also GABP stimulated. Microcompetition for GABP elevates the concentration of AGENT. As a GABP kinase agent, AGENT phosphorylates the pool of GABP molecules. Phosphorylation of GABP increases C which in turn represses AGENT. However, microcompetition reduces the size of the GABP pool, or the amount of GABP available to stimulate C. Therefore, microcompetition diminishes the increase in the control C, which lessens the repression

effect on A. In the above figure, the size of the arrow in step 2 would be smaller, hence the size of the arrow in step 3 would be smaller as would be that of the arrow in step 4.

5 Note that the control C in the above figure is down stream from GABP. What if the control is positioned between the GABP kinase agent and GABP? Would microcompetition cause patient level resistance in such a pathway?

Let R be an internally sensitized receptor in (AGENT, GABP) with C as a negative control for AGENT. If R stimulates C (C is downstream from R), microcompetition for GABP elevates the concentration of AGENT. This is illustrated by figure 10.

10 AGENT phosphorylaes GABP (step 1 and 2). GABP increases the transcription of R₁ (step 3). R₁ increases the effect on GABP (step 4A) and increases the expression of the control C (step 4B), which then decreases the expression of the GABP kinase agent (step 5). Microcompetition decreases the size of the arrows in step 2, 3, 4A, 4B and 5.

If the control is down stream from the sensitized receptor, microcompetition causes patient level resistance.

15 Consider the following two pathways (OT, OTR, GABP), (zinc or copper, hMT-IIA, GABP) as examples. In these pathways, the sensitized receptor directly binds the GABP kinase agent. Therefore, the control must be down stream from the sensitized receptor, and the pathways must show patient level resistance under microcompetition. This conclusion can be reached independent of any information about the control. The 20 pathway (LPS, CD18, GABP) is similar. Elicitation of a bioequivalent reaction requires a higher concentration of LPS in a cell infected by a GABP virus compared to a non infected cell. The pathway (IL-2, IL-2R β , γ C, GABP) is different (see below).

25 Let the set $\{(AGENT_i, GABP, C_i)\}$ include all pathways with a GABP kinase agent AGENT_i and control C_i downstream from GABP. For all AGENT_i, microcompetition for GABP reduces the expression of C_i, which, in steady state, increases the concentration of AGENT_i. Using the resistance terminology, it can be said that microcompetition for GABP causes cells infected with a GABP virus to show AGENT_i patient level resistance.

2. Oxidative stress

Microcompetition intensifies the effects of oxidative stress (see chapter on atherosclerosis).

3. Transcription**5 a) *Retinoblastoma susceptibility gene (Rb)*****(1) GABP is an activator of Rb**

Notations:

Rb represents the retinoblastoma susceptibility gene

pRb represents the retinoblastoma susceptibility e protein

10 The Rb promoter includes a N-box at (-198,-193). Several experiments were performed in which plasmids were produced. pXRP1 included the normal (-686,-4) segment of the Rb promoter. pXRP3 included the same segment with a mutated N-box and RBF-1x4 included 4 copies of the Rb N-box as promoter. All promoters controled expression of the luciferase (luc) reporter gene. Cotransfection of hGABP α and hGABP β 1 expression plasmids with pXRP1 into SL2 *Drosophila* cells showed a 10-fold increase in reporter gene activity. Cotransfection with RBF-1x4 showed a 13-fold increase. Cotransfection with pXRP3, the mutated N-box, showed no increase (Sowa 1997¹¹⁷). Based on these observations, and other results, Sowa, *et al.*, concluded that hGABP has a strong transactivating effect on the Rb gene promoter, suggesting that hGABP is the main transactivator for the core promoter element of the Rb gene.

(2) Rb is a microcompetition-repressed gene

GABP viruses microcompete with the Rb promoter for GABP. Therefore, viral infection of cells decreases Rb expression. Moreover, the higher the concentration of viral DNA, the greater the decrease in Rb expression.

b) Breast cancer type 1 gene (BRCA1)

(1) GABP is an activator of BRCA1

The BRCA1 promoter includes three N-boxes at (-200,-178). Plasmids with point mutations in the central N-box, alone or in combination with mutations in the other N-boxes, were transfected in MCF-7, a human breast cell line. The mutated plasmids showed a 3-fold reduction in promoter activity (Atlas 2000¹¹⁸, Fig 2). Nuclear extracts from MCF-7 formed a specific complex with the N-boxes region. Through crosslinking, supershift assays and binding to recombinant GABP $\alpha\beta$ (Ibid, Fig 4, 5), GABP $\alpha\beta$ was identified as the main transcription factor interacting with the N-boxes. An artificial promoter containing the multimerized N-boxes region was transactivated by cotransfection with GABP α and GABP $\beta 1$ in both MCF-7 and T47D, another human breast cell line (Ibid, Fig 6). These observations indicate that BRCA1 is a GABP stimulated gene.

(2) BRCA1 is a microcompetition-repressed gene

GABP viruses microcompete with the BRCA1 promoter for GABP. Therefore, viral infection of cells will decrease BRCA1 expression. Moreover, higher concentrations of viral DNA, lead to greater decreases in BRCA1 expression.

c) Fas gene (Fas, APO-1, CD95)

(1) GABP is an activator of Fas

The Fas promoter includes two N-boxes at (-857,-852) and (-833,-828). Jurkat cells, a T cell line, were transiently transfected with a luciferase reporter gene driven by different lengths of the Fas promoter. The cells were stimulated for 10 h with anti-CD3 mAb, PMA and PMA/ionomycin. Deletion of the two N-boxes reduced activation by 50-75% (Li 1999¹¹⁹, Fig 1). Mutation of the N-boxes also reduced stimulated luciferase activity (Ibid, Fig 7). Cell stimulation resulted in formation of specific complexes on the N-boxes region. Mutation of the N-boxes reduced formation of these complexes (Ibid, Fig 4). Antibodies against GABP α and β inhibited formation of these complexes (Ibid, Fig 6A). Two or four copies of the Fas/GABP site (-863,-820) were inserted into a reporter plasmid carrying the pGL3/promoter. Anti-CD3 mAb, PMA and PMA/ionomycin stimulated luciferase activity 8-20 fold in Jurkat transfected cells (Ibid, Fig 9). Mutation

of the N-boxes significantly reduced induction of luciferase activity in response to stimulation. These observations indicate that Fas is a GABP stimulated gene.

(2) Fas is a microcompetition-repressed gene

5 GABP viruses microcompete with the Fas promoter for GABP. Therefore, viral infection of cells decreases Fas expression. Moreover, the higher the concentration of viral DNA, the greater the decrease in Fas expression.

d) *Tissue factor (TF) gene*

(1) Transcription

(a) *ETS related factor(s) repress TF transcription*

10 (i) ETS related factor(s) bind (-363 to -343) and (-191 to -172)

A study used DNase I footprinting to map the sites of protein-DNA interaction on the (-383 to +8) fragment of the TF promoter. That study used nuclear extracts prepared from uninduced and lipopolysaccharide-induced THP-1 monocytic cells. Six regions were identified. Region number 7 (-363 to -343) and region number 2 (-191 to -172) contain an N-box. THP-1 extracts formed two complexes on a consensus N-box. Both complexes were competed with excess unlabeled N-box and 200-fold excess of a (-363 to -343) probe. The (-191 to -172) probe, although not as effective as the (-363 to -343) probe, showed approximately 30% reduction in N-box complex formation (Donovan-Peluso 20 1994¹²⁰, Fig. 9).

Another study used the (-231 to -145) fragment of the TF promoter as probe. Nuclear extracts prepared from uninduced and lipopolysaccharide-induced THP-1 monocytic cells formed two complexes on the (-231 to -145) probe. To characterize the proteins that interact with the DNA sequence, the study used the sc-112x antibody from 25 Santa Cruz Biotechnology. According to the manufacturer's literature, the antibody has broad cross-reactivity with members of the ETS family. Incubation of the antibody with the nuclear extracts abrogated the formation of the upper complex on the (-231 to -145) probe (Groupp 1996¹²¹, Fig. 5).

(ii) (-191 to -172) also binds NF- κ B

Monocytic THP-1 cells were stimulated with LPS for various times up to 24 h. TF mRNA increased by 30 min and reached a peak at 1 h. Levels dropped considerably by 2 h returning, eventually, to preinduction levels (Hall 1999¹²², Fig. 1). The same study 5 conducted EMSA studies using the (-213 to -172) fragment of the TF promoter. The results showed that two complexes, indicated as III and IV, appear at 30 min, with binding reaching a peak at 1-2 h. At 4 h and later, the complexes are no longer detected. A 100-fold molar excess of a (-213 to -172) probe, or a NF- κ B consensus oligonucleotide, compete with complexes III and IV (Ibid, Fig. 2B). An antibody against p65 and to a 10 lesser extent, anti-c-Rel, supershifted complex III. These data demonstrate a transient binding of two NF- κ B complexes to the (-213 to -172) fragment between 30 min and 2 h. However, the affinity of complexes for the NF- κ B site was much lower than the affinity of 15 the complexes on the adjacent proximal AP1 site.

This study also provides evidence indicating that LPS induces proteolysis of I κ B 15 and translocation of p65 and c-Rel from the cytoplasm to the nucleus. Western blot analyses showed that very little p65 was present in the nucleus in unstimulated cells. After 10 min of LPS induction, nuclear p65 begins to appear and peak at 1 h, declining again by 2 h. A concomitant decrease in cytoplasmic p65 corresponds to the observed 20 increase in nuclear p65 (Ibid, Fig. 4).

20 (iii) The (-363 to -343) factor(s) repress TF transcription

Holzmuller, *et al.*, (1999¹²³) call the (-363 to -343) fragment of the TF promoter the Py-box. Deletion of the 5'-half of the Py-box increased expression of a luciferase reporter gene (Ibid, Fig. 3A and B). The relative increase was similar for LPS induced or 25 nontreated cells and was independent of the existence of NF- κ B site (Ibid, Fig. 3C). Mutation of the N-box part of the Py-box resulted in complete loss of binding activity to the Py-box.

30 (iv) Competition between ETS related factor(s) and NF- κ B for (-191 to -172)

Donovan-Peluso, *et al.*, (1994¹²⁴, see above) showed that the (-191 to -172) probe was less effective in competing with the consensus N-box compared to the (-363 to -343)

probe. According to the authors, the data suggest that there might be competition for binding to the (-191 to -172) fragment by NF- κ B and ETS related factors. In such a case, NF- κ B binding to a (-191 to -172) probe reduces the concentration of the probe available to for ETS binding. This competition can explain the reduced ability of (-191 to -172) to compete for ETS binding relative to (-363 to -343). Moreover, the NF- κ B site and the N-box in the (-191 to -172) fragment overlap. The presence of overlapping sites also suggests competition where occupancy by either factor might preclude binding by the other.

10

(v) Microcompetition stimulates TF transcription

Microcompetition between a GABP virus and the TF promoter decreases the availability of the ETS related complexes in the nucleus.

15 NF- κ B binding to (-191 to -172) increases transcription. Competition between NF- κ B and ETS related factors for (-191 to -172) suggests that the decrease in availability of the ETS related factors in the nucleus increases the binding of NF- κ B to the (-191 to -172) fragment and increases TF expression.

20 Binding of ETS related factor(s) to the (-363 to -343) fragment represses transcription. The repression is similar in extracts from untreated, or LPS- or TNF- α -induced cells. Moreover, the repression is independent of NF- κ B binding. This observation suggests that the ETS related factor(s) suppress transcription in quiescent cells and maintain the rates in activated cells at a moderate level (Holzmuller 1999¹²⁵). The decrease in availability of the ETS related factor(s) in the nucleus reduces the (-363 to -343) repression and increases TF expression.

25 The GABP virus microcompetes with the TF promoter for the ETS related factor(s), therefore, viral infection of monocytes/macrophages increases TF expression. Moreover, the higher the concentration of viral DNA, the greater the increase in TF expression.

(b) *GABP viruses increase TF expression*

(i) Transfection

A few studies measured the expression of TF relative to an internal control. Those studies used two controls, CMV β gal (Moll 1995¹²⁶, Nathwani 1994¹²⁷) and pRSVCAT (Mackman 1990¹²⁸). Although the studies used different transfection protocols; Moll, *et al.*, (1995) used psoralen- and UV-inactivated biotinylated adenovirus and streptavidine-poly-L-lysine as vectors for DNA delivery, Nathwani, *et al.*, (1994) used electroporation and Mackman, *et al.*, (1990) used DEAT-dextran, they all report an increase in TF expression relative to a promoterless plasmid. According to Moll, *et al.*, (1995), the cells "are being already partially activated following the transfection procedure." The level of activation was similar in unstimulated and LPS stimulated cells. The internal controls include promoters of GABP viruses. The control promoters microcompete with the TF promoter for ETS related factor(s). The reduced availability of ETS related factor(s) increases the transcription of the reporter gene fused to the TF promoter.

(ii) Infection

Confluent monolayers of human umbilical vein endothelial cells (HUVEC) were exposed to 0.1 μ g/ml LPS for 4 hours and HSV-1. At appropriate time intervals, TF procoagulant activity (PCA) was assessed by clotting assays. Figure 11 presents the results.

Maximal TF PCA activity was observable 4 hours after infection and was still detectable 20 hours post infection. Both the HSV infection and LPS exposure show a similar activity profile over time. However, the maximal activity induced by HSV is about a 1/2 of LPS. Further studies with specific blocking antibodies to human TF support the notion that the PCA is indeed due to TF.

HUVEC were also infected with HSV-1 inactivated by either ultra-violet-irradiation or heat. The cellular TF PCA was measured in lysates of control, LPS stimulated (0.1 mg/ml for 4 hours), or infected cells. Virally infected cells were maintained in culture for up to 48 hours and visually inspected for cytopathic effects as evidence for lytic infection. Obvious morphologic changes were evident in cells infected with competent virus after 18 to 24 hours. In comparison, no signs of infection were visible in cells infected with heat or UV-treated virus even after 48 hours. The TF PCA of

the different treatments measured 4 hours post infection is summarized in the following table.

	TF PCA (U/ml)
Control	74
LPS	1753
HSV-1	773
Heated HSV-1 (80° × 30 min)	691
UV irradiated HSV-1	384

5 Virus inactivated by UV or heat is still capable of inducing TF activity (Key 1993¹²⁹).

This study measures the effect of infection with an inactivated GABP virus on TF transcription. The reduced TF transcription is consistent with microcompetition between the viral DNA and the TF promoter for the ETS related factor(s) despite the fact that the infecting viruses were not viable.

10 (c) *The effect of ERK agents on TF transcription*
 Many papers report the effects of c-Fos/c-Jun, c-Rel/p65, Sp1 and Egr-1 binding on TF transcription. LPS and PMA are ERK agents and, therefore, phosphorylate the ETS related factors. However, LPS and PMA also stimulate the binding of NF-κB and Egr-1, respectively, to the TF promoter. In figure 12, the effect of LPS on NF-κB is presented by dotted lines, and on ERK by solid lines. As such, LPS and PMA are not useful in isolating the effect of ETS phosphorylation on TF transcription. The next section presents two ERK agents, *all-trans* retinoic acid (ATRA) and resveratrol, which have no effect on NF-κB, Ap1 and Sp1. As ERK agents, ATRA and resveratrol phosphorylate the ETS related factor(s), stimulate the binding of p300, and, therefore, should repress TF transcription.

15 20 (i) *All-trans* retinoic acid (ATRA)

Monocytes were incubated for 30 minutes with various doses of ATRA before LPS stimulation. ATRA inhibited LPS induction of TF expression in a dose-dependent manner (Oeth 1998¹³⁰, Fig. 1A). The LPS induction of TF activity was also inhibited by ATRA in THP-1 monocytic cells (Ibid, Fig. 2A). Specifically ATRA reduced the basal levels of TF mRNA in unstimulated cells and abolished the LPS induction of TF mRNA (Ibid, Fig. 3A). However, ATRA did not affect DNA binding of the c-Fos/c-Jun, c-Rel/p65 or Sp1 transcription factors to the AP1, NF- κ B and Sp1 sites.

5 (ii) Resveratrol (RSVL)

Confluent monolayers of human umbilical vein endothelial cells (HUVEC) were 10 treated with resveratrol (100 μ mol/L) for 2 hours. Following resveratrol treatment, the cells were stimulated for 6 hours with either LPS, TNF α , IL-1 β , or PMA. The results showed that resveratrol markedly suppressed LPS-, TNF α -, IL-1 β -, and PMA-induced TF activity (Pendurthi 1999¹³¹, Fig. 1A). The inhibition varied from 60% to more than 90%. HUVEC monolayers were also treated with different concentrations of resveratrol (0 to 15 200 μ mol/L) for 2 hours. Following resveratrol treatment, the cells were stimulated with TNF α , IL-1 β , or PMA. The data showed that resveratrol inhibited the induction of TF expression in a dose-dependent manner. To test the effect of resveratrol in monocytes, mononuclear cell fractions were treated with various concentrations of resveratrol (0 to 100 μ mol/L) for 2 hours and then stimulated with LPS (100 ng/mL) for 5 hours. The 20 results showed that resveratrol inhibited LPS-induced TF expression in monocytes in a dose-dependent manner (Ibid, Fig. 2). To test the effect of resveratrol on TF mRNA, HUVEC monolayers were treated with various concentrations of resveratrol (0, 5, 20, 100, and 200 μ mol/L) for 2 hours, and then stimulated with LPS, TNF α , IL-1 β , or PMA for 2 hours. Resveratrol treatment reduced TF transcription in a dose-dependent manner. 25 However, the reduced transcription was not due to diminished binding of c-Fos/c-Jun or c-Rel/p65 to the TF promoter. Resveratrol did not significantly change the binding of c-Fos/c-Jun to the AP-1 sites. Resveratrol treatment had no significant effect on binding activity to the AP-1 site in either unstimulated or LPS-, TNF α -, IL-1 β -, or PMA- 30 stimulated endothelial cells (Ibid, Fig. 7). Resveratrol also did not significantly change the binding of NF- κ B to the TF promoter. Unstimulated cells showed little binding of NF- κ B, whereas LPS, TNF α , IL-1 β , or PMA induced formation of a prominent DNA-protein

complex on the NF- κ B site. Preincubation of cells with resveratrol (100 μ mol/L) for 2 hours had no effect on formation of the NF- κ B DNA-protein complex (Ibid, Fig. 8).

Both ATRA and resveratrol are ERK agents and, therefore, phosphorylate the ETS related factor(s). In general, phosphorylation of ETS related factor(s) stimulates binding 5 of p300. The ETS•p300 complex, when bound to the TF promoter, represses TF transcription. The repression is independent of NF- κ B, Ap1 or Sp1.

(2) Deactivation ("encryption") as a function of membrane concentration

(a) *TF surface dimers are inactive*

According to Bach, *et al.*, (1997¹³²), surface TF exists in two forms, monomers and 10 dimers. Both monomers and dimers bind FVIIa. However, only monomers are active. Self-association of TF monomers prevents access to an essential macromolecular substrate binding site. The concept of inactive (cryptic) dimers is consistent with the crystal 15 structures of the extracellular domain of TF. The structure suggest that TF dimerization does not block FVIIa binding but covers the macromolecular substrate binding site on the opposite face of TF.

Bach, *et al.*, (1997) provide ample evidence consistent with this model. Consider 20 the following experiments. HL-60 cells were exposed to 10⁻⁶ mol/L PMA for various times. The intact cells were assayed for TF procoagulant activity (PCA) either before or following a brief exposure to 10 μ mol/L ionomycin. In comparison to PMA treatment alone, a combined ionomycin and PMA testament resulted in a dramatic increase in 25 expression of TF PCA (Ibid, Fig. 1). The rapid appearance of the activity suggests that *de novo* protein synthesis was not involved (Ibid, Fig. 2). The calcium influx activated the latent TF PCA. Also, the inhibition by calmidzaolium (CMZ) implicates calmodulin (CaM) as an essential link in the process (Ibid; Fig. 3, 4). Moreover, FVIIa bound to TF 30 on untreated cells as well as ionophore-treated cells (Ibid, Fig. 5, experiment 1 and 2). Thus, restricted formation of TF-FVIIa does not account for inactive (cryptic) TF PCA. The TF-FVIIa complex readily bound the pseudosubstrate tissue factor pathway inhibitor-activated factor X (TFPI-FXa) on ionophore-treated cells, but was resistant to TFPI-FXA inhibition on untreated cells. Similar inhibition on ionophore-treated cells was

demonstrated with XK1, another pseudosubstrate of TF-FVIIa. These results suggest that calcium influx exposes a TFPI-FXa/XK1 binding site on TF. Lastly, HL-60 cells were treated with DTSSP, a monobifunctional amino-reactive protein shown to cross-link cell surface TF. Following the treatment, TF was immunopurified and visualized by Western blotting. The products of DTSSP cross-linking were TF dimers (Ibid, Fig. 7, lane 1, 2). When the cells were treated with ionomycin before cross-linking, almost no cross-linking was observed (Ibid, Fig. 7, lane 3). The decreased cross-linking suggests that TF does not self-associate on ionophore treated cells. Both the TF cross-linking and the encrypted TF PCA were preserved by treating the cells with CMZ before the addition of ionophore (Ibid, Fig. 7, lane 4).

(b) *Increase in surface concentration induces dimers, reduces activity*

Nemerson, *et al.*, (1998¹³³) link the surface concentration of TF with its rate of catalytic activity. To establish such a link, Nemerson and Giesen incorporated a recombinant TF (TF₁₋₂₄₃), which contained the transmembrane, but not the cytoplasmic domain, into appropriate phospholipid vesicles and measured their catalytic activity (k_{cat}). The results showed that the k_{cat} , or catalytic rate constant, which reflects the catalytic activity of each TF-FVIIa molecule, fell monotonically as a function of TF surface density. Moreover, following exposure of vesicles with high surface-density of TF (about 50 molecules of TF on the surface of a 100 nm vesicle) to a cross-linking reagent, Nemerson and Giesen were able to detect dimers and higher n-mers. Nemerson and Giesen suggested that these results are consistent with a model where clustered TF molecules have lower maximal catalytic activity compared to dispersed molecules.

To test the significance of the cytoplasmic domain in activation, Wolberg, *et al.*, (2000¹³⁴) transfected cells with either full length TF, or TF lacking its cytoplasmic domain. The results showed that TF activation by a calcium ionophore was independent of the cytoplasmic domain.

(c) *TF self regulation through dimers*

Schecter, *et al.*, (1997¹³⁵) show the effect of agonist stimulation on TF surface concentration and activity over time. TF mRNA was barely detectable in quiescent aortic

smooth muscle cells (SMC) (Ibid, Fig. 1). FCS induced a marked rise in TF mRNA levels, beginning at ~ 1 h and persisting for ~ 8 h. Accumulation of TF mRNA in response to PDGF BB and α -thrombin was similar to that seen with 10% FCS (Ibid, Fig. 1). To test the effect of the rise in TF mRNA on protein synthesis over time, quiescent SMC were treated with growth agonist and examined by immunostaining every hour for the first 4 h, and every 2 h for additional 20 h. Untreated quiescent SMC showed minimal TF antigen. Cells stimulated with 10% FCS, PDGF AA, or BB, or thrombin receptor peptide, produced a pronounced perinuclear staining of TF antigen beginning at ~ 2 h and peaking at 4-6 h. At 4-6 hours, TF antigen was also detected diffusely on the ruffled edges of the plasma membrane. Perinuclear staining persisted for ~ 8-10 h after stimulation, and then gradually dissipated. At 16-24 h, a patchy distribution of antigen staining near or on the membrane was noted with diminished perinuclear staining. Schechter, *et al.*, (1997)¹³⁶ measured the intensity of immunofluorescent staining along a line which traverses the nucleus and connects opposite sides of the cell membrane, and displayed the results graphically. At 4 h, the graph shows a bimodal distribution with two peaks, around the nucleus and along the membrane (Ibid, Fig. 5a, insert). At 16 h, the graph shows a much smaller peak around the nucleus and a much larger peak along the membrane (Ibid, Fig. 5b, insert).

Schechter, *et al.*, (1997)¹³⁷ also measured the effect of PDGF simulation on TF activity. PDGF induced an approximately fivefold increase in surface TF activity (Ibid, Fig. 7) 4-6 h after treatment, with a return to baseline by 20 h.

The temporal events reported in this study show that the initial increase in TF membrane staining (4 h post stimulation) is associated with an increase in TF activity, while the subsequent increase in membrane staining (16 h post stimulation) is associated with a decrease in TF activity. The patches of TF staining on the cell surface are most prominent at a time (10-12 h after agonist stimulation) when surface TF activity is minimal. The study finds this relationship intriguing and proposes that the patches may represent inactive TF multimers.

e) *P-selectin gene*

P-selectin (CD62P, GMP140, LECCAM-3, PADGEM) is expressed in megakaryocytes and endothelial cells. In endothelial cells P-selectin is stored in specialized granules known as Weibel-Palade (WP) bodies. After activation with inflammatory mediators, such as histamine, thrombin, or complement proteins, WP bodies fuse with the plasma membrane, resulting in increased P-selectin expression on the endothelial apical surface. One function of P-selectin is to mediate leukocyte adherence to activated endothelium.

(1) Transcription

(a) *GABP is a repressor of P-selectin*

Two conserved N-boxes were identified in the mouse and human P-selectin genes. The mouse distal N-box is positioned at (-327,-322) and the proximal at (-104,-99). The human distal N-box is positioned at (-314,-309) and the proximal at (-103,-108). A labeled probe encoding the murine proximal N-box formed two DNA-protein complexes with nuclear extracts from BAEC (Pan 1998¹³⁸, Fig. 6B), bEnd.3, HEL and CHRF288 cells. Complex formation varied with different batches of nuclear extracts, characteristic of GABP binding. Competition with a HSV-1 Immediate Early (IE) N-box probe, which binds GABP, prevented complex formation with BAEC nuclear extracts (Ibid, Fig. 6D). Based on these observations, Pan, *et al.*, concluded that the proximal N-box most likely binds the ubiquitously expressed GABP.

Mutation of the AGGAAG proximal N-box to AGCTAAG eliminated DNA-protein complex formation (Pan 1998, Fig. 6C). BAEC transfected with a reporter gene directed by the murine P-selectin promoter with the mutated N-box showed 2-10-fold increased expression compared to the wild-type promoter (Ibid, Fig. 6F). The increased transcription indicates that binding of the Ets related factor to the proximal N-box represses the P-selectin gene. Deletion of the distal N-box had no effect on reporter gene expression. The increased transcription of the mutated gene indicates that GABP is a repressor of P-selectin.

(b) *Microcompetition stimulates P-selectin transcription*

GABP viruses microcompete with the P-selectin promoter for GABP. Therefore, viral infection of endothelial cells increases P-selectin expression. Moreover, the higher 5 the concentration of viral DNA, the greater the increase in P-selectin expression.

f) *β_2 integrin gene*

(1) Transcription

(a) *GABP is an activator of β_2 integrin*

β_2 integrin (CD18) is a leukocyte-specific adhesion molecule. GABP binds three 10 N-boxes in the CD18 promoter and transactivates the gene (Rosmarin 1995¹³⁹, Rosmarin 1998¹⁴⁰).

(b) *Microcompetition represses β_2 transcription*

Latent infection by a GABP virus results in microcompetition between viral DNA and CD18 promoter which decreases the expression of CD18 (see Le Naour 1997¹⁴¹, 15 Tanaka 1995¹⁴², Patarroyo 1988¹⁴³ above). Moreover, the higher the concentration of viral DNA, the greater the decrease in CD18 expression.

g) *α_4 integrin gene*

α_4 integrin (CD49d) is expressed in B cells, thymocytes, monocytes/macrophages, 20 granulocytes and dendritic cells. α_4 binds β_1 integrin to form $\alpha_4\beta_1$ (CD49d/CD29, VLA-4). $\alpha_4\beta_1$ binds vascular cell adhesion molecule-1 (VCAM-1), which appears on the surface of activated endothelial cells, and fibronectin (Fn), a major component of the extra-cellular matrix (ECM).

(1) Transcription

(a) *GABP is an activator of α_4 integrin*

25 Rosen, *et al.*, (1994¹⁴⁴) show that GABP binds the (-51,-46) N-box in the α_4 promoter. The binding of GABP activated transcription of the α_4 integrin gene in Jurkat cells, a T-cell line.

(b) *Microcompetition represses α_4 transcription*

Rosen, *et al.*, (1994) show that microcompetition with an Ets binding site from the Moloney sarcoma virus long terminal repeat inhibited binding of GABP to the α_4 integrin promoter. GABP viruses microcompete with the α_4 promoter for GABP. Therefore, viral 5 infection of macrophages decreases α_4 expression. Moreover, the higher the concentration of viral DNA, the greater the decrease in α_4 expression.

h) *Hormone sensitive lipase (HSL) gene*

Hormone sensitive lipase (HSL, Lipe, EC 3.1.1.3) is an intracellular neutral lipase highly expressed in adipose tissue. HSL is the rate limiting enzyme in triacylglycerol and 10 diacylglycerol hydrolysis. HSL also mediates cholesterol esters hydrolysis generating free cholesterol in steroidogenic tissues and macrophages.

(1) HSL is a microcompetition-suppressed gene

(a) *N-box*

The region -780 bp 5' of exon B to the start of exon 1 was suggested to include 15 potential regulatory sites of the human HSL gene in adipocytes (Talmud 1998¹⁴⁵, Grober 1997¹⁴⁶). This region includes 15 N-boxes. Moreover, three pairs are located within short distances of each other. The distance between the pair at (+268,+272), (+279,+285) is 5 bp or 1.0 helical turn (HT), at (+936,+942), (+964,+970) is 22 bp or 2.5 HT, and at (+1,253,+1259), (+1270,+1276) is 11 bp or 1.5 HT.

20 Of the dozens of known ETS factors, only GABP, as a tetrameric complex, binds two N-boxes. Typically, the N-boxes are separated by multiples of 0.5 helical turns (HT). There are 10 bp per HT. Consider the following table (based on Yu 1997¹⁴⁷, Fig 1)

Gene	Sequence	Dist.*
Murine Laminin B2	<u>CTTCCTCCTGGCGCGCTCTCGAGTGCGCGCTCGGAAG</u>	26 bp 3.0 HT
Human type IV collagenase	<u>TTTCCGCTGCATCCAGACTTCCT</u>	11 bp 1.5 HT

Human CD4	<u>AGGAGCCTGCCATCGGGCTTCCT</u>	12 bp 1.5 HT
Murine CD4	<u>AGGAGCCTCACGACCAGGCTTCCT</u>	12 bp 1.5 HT
Murine COX Vb	<u>CGGAAGTCCCGCCCATCTTGCTCAGCCTGTTCCCGGAAG</u>	27 bp 3.0
Murine COX IV	<u>CTTCCGGTTGCAGGGCCCCGTTCTTCG</u>	15 bp 2.0 HT
Ad2-ML	<u>CGTCCTCACTCTCTTCG</u>	6 bp 1.0 HT
Helical turns	0 0.5 1.0 1.5 2.0 2.5 3.0	

* Distance measure in bp (base pair) or HT (helical turns).

The 1.0, 2.5 and 1.5 helical turns separating the HSL N-boxes pairs is consistent with characteristic GABP heterotetramer binding.

It is interesting to note that the HSL testis-specific promoter also includes two N-boxes separated by 11 bp or 1.5 helical turns (Blaise 1999¹⁴⁸). Many "TATA-less" promoters bind GABP to an N-box in their initiator element. Specifically, HSL is a TATA-less gene. Three N-boxes on the HSL gene, (+35,+41) in exon B and (+964,+970), (+1110,+1116) in intron B are conserved in the mouse HSL gene (see sequence U69543 in Talmud 1998¹⁴⁹).

10

(b) *Transfection*

The Swiss mouse embryo 3T3-L1 fibroblasts can differentiate into adipocyte-like cells. The undifferentiated cells contain a very low level of HSL activity. While differentiated adipocyte-like cells show a 19-fold increase in HSL activity (Kawamura 1981¹⁵⁰).

15

3T3-L1 preadipocytes were induced to differentiate by incubation with insulin (10 μ g/ml), dexamethasone (10 nM), and iBuMeXan (0.5 mM) for 8 consecutive days following cell confluence. HSL mRNA was measured in undifferentiated confluent controls and differentiated 3T3-L1 cells transfected with the ZIPNeo vector. Although differentiated 3T3-L1 cells usually show significant HSL activity, the 3T3-L1 differentiated cells transfected with ZIPNeo showed decreased HSL mRNA (Gordeladze

20

1997¹⁵¹, Fig 11 left). ZIPNeo carries the Moloney murine leukemia virus LTR which binds GABP. Microcompetition between the viral LTR and the HSL promoter leads to reduced expression of the HSL gene.

The following section presents the clinical effect of microcompetition.

5 **V. Discovery 5: Clinical effects of microcompetition**

A. Cancer

1. Effect of microcompetition on cell proliferation and differentiation

The current paradigm holds that, *in vivo*, viral proteins are the mediators of host cell manipulation. Consider, as examples, the extensive research published on the SV40 large T antigen, Epstein-Barr virus BRLF1 protein, papillomavirus type 16 E6 or E7 oncoproteins or adenovirus E1A. The possibility of host cell manipulation independent of viral protein is ignored.² This paradigm is so ingrained that even when protein-independent manipulation presents itself in the lab, the investigators disregard its significance. Consider the following studies as examples, each uses two types of plasmids. One plasmid includes a gene of interest, cellular Rb or viral T antigen. The other plasmid includes the neomycin-resistance (Neo) gene only under the control of a viral promoter. This plasmid is regarded as "empty," and is, therefore, used as control. All three studies report results showing a significant effect of the "empty" plasmid on cell cycle progression, increased proliferation and reduced differentiation. However, none of these studies includes any reference to these results. The results are completely ignored.

² A possible exception might be integration of viral DNA into cellular genome. Such integration may result in mutations, deletions or methylation of host cell DNA. However, even this manipulation of cellular function is mediated, in many cases, by viral proteins. Consider, as examples, the HIV-1 IN protein or the retrovirus integrase which mediate viral integration.

a) Microcompetition stimulates proliferation

HuH-7 human hepatoma cells were transfected with pBARB, a plasmid in which the β -actin promoter regulates the expression of the Rb gene and the simian virus (SV40) promoter regulates the expression of the neomycin-resistance (neo) gene. The cells were 5 also transfected with the pSV-neo plasmid, which only includes the SV40 promoter on the neo gene. Since pSV-neo does not include the β -actin promoter and the Rb gene, it was regarded as "empty" and was used as control. The cells were incubated in the chemically defined medium IS-RPMI with 5% FBS or serum free IS-RPMI. The number of viable 10 cells were counted at the indicated times. The results are summarized in figure 15 (Awazu 1998¹⁵², Fig 2A). Wild means non transfected cells. The SD is about the size of the triangular and circular symbols.

Rb transfection resulted in reduced cell proliferation at day 6 relative to non transfected "wild" type HuH-7 cells. Transfection of the "empty" vector resulted in increased proliferation. The "empty" vector includes the SV40 promoter which binds 15 GABP. Microcompetition between the viral promoter and cellular genes leads to increased proliferation (for the identity of the cellular genes, see below).

b) Microcompetition inhibits differentiation

HSV-neo is a plasmid that expresses the neomycin-resistance gene under the control of murine Harvey sarcoma virus long terminal repeat (LTR) (Armelin 1984¹⁵³). 20 pZIPNeo expresses the neomycin-resistant gene under the control of the Moloney murine leukemia virus long terminal repeat (Cepko 1984¹⁵⁴). PVU0 carries an intact early region of the SV40 genome which expresses the SV40 large tumor antigen and SV40 small tumor antigen (Higgins 1996¹⁵⁵). The murine 3T3-L1 preadipocytes were transfected with PVU0. The cells were also transfected with HSV-neo and pZIPNeo as "empty" controls. 25 Following transfection, the cells were cultured under differentiation inducing conditions. Glycerophosphate dehydrogenase (GPD) activity was measured as a marker of differentiation. The results are presented in the following table (Higgins 1996¹⁵⁶, Table 1, first four lines).

Vector	Cell line	GPD activity (U/mg of protein)
None	L1	2,063 1,599
HSV-neo	L1-HNeo	1,519 1,133
ZIPNeo	L1-ZNeo	1,155 1,123
PVU0	L1-PVU0	47,25

Transfection of PVU0 and expression of the large and small T antigens resulted in a statistically significant decrease in GPD activity. However, transfection of the "empty" vectors, HSV-neo and ZIPNeo, although less than PVU0, also reduced GPD activity. In a 5 t-test, assuming unequal variances, the p-value for the difference between the HSV-neo vector and no vector is 0.118, and the p-value for the difference between ZIPNeo and no vector is 0.103. Given that the sample includes only two observations, a p-value around 10% for vectors carrying two different LTRs indicates a trend. Both the murine Harvey sarcoma virus LTR and the Moloney murine leukemia virus LTR bind GABP.

10 Microcompetition between the viral LTR and the 3T3-L1 preadipocyte GABP genes regulating cell cycle leads to the reduced differentiation, indicated by the reduced GPD activity.

The wild-type early region of SV40 was inserted into the "empty" pZIPNeo plasmid (same plasmid as in Higgins 1996, see above). The new plasmid is called the 15 "wild-type" (WT) and expresses the SV40 large T antigen. 3T3-F442A preadipocytes were transfected with either WT or pZIPNeo. Accumulation of triglyceride, assayed by oil red staining, was used as a marker of differentiation. Seven days postconfluence, the number of staining of cells was recorded. Consider figure 16. Darker staining indicates increased differentiation. (A) marks untreated F442A cells, (B) marks cells transfected 20 with ZIPNeo, (C) marks cells transfected with WT (Cherington 1988¹⁵⁷, Fig 4 A, B and C).

Transfection with WT, the vector expressing SV40 large T antigen, reduced differentiation, see triglyceride staining in (C) and (A). However, transfection with the 25 "empty" vector, although less than WT, also reduced differentiation, see triglyceride staining in (B) relative to (A) and (C).

pZIPNeo utilizes the Moloney murine leukemia virus long terminal (LTR), a region which binds GABP. Microcompetition between the viral LTR and the cellular genes regulating cell cycle progression leads to reduced differentiation, indicated by reduced accumulation of triglyceride.

5 2. **Pathogenesis**

a) **Rb**

(1) **Hypophosphorylated form of pRb and cell cycle**

The cell cycle starts with a growth period (G1). Prior to a time in late G1, called R-point, the cell "decides" whether to divide or exit the cell cycle. An exit results in growth arrest, differentiation, senescence or apoptosis. A decision to divide leads to a series of orderly processes starting with DNA synthesis (S), a second growth period (G2), mitosis and cell division (M), and a return to G1. As cells progress through the cell cycle, pRb undergoes a series of phosphorylation events. In G0 and early G1, pRb is primarily unphosphorylated. As cells approach the G1/S boundary, pRb becomes phosphorylated by cyclin D/CDK4 and cyclin D/CDK6 kinases as seen by a higher-molecular-weight species of pRb. Further phosphorylation by cyclin E/CDK2 kinase occurs in late G1. Phosphorylation is progressive and continuous throughout the S phase and into G2/M. Phosphopeptide analysis demonstrated that pRb is phosphorylated on more than a dozen distinct serine or threonine residues throughout the cell cycle (Sellers 1997¹⁵⁸).

20 Let un-pRb denote the unphosphorylated form of pRb, hypo-pRb, the hypo or under phosphorylated form of pRb and hyper-pRb, the hyperphosphorylated form of pRb. Un/hypo-pRb denotes the set of all pRb either un or hypophosphorylated.

25 Accumulation of un/hypo-pRb leads to G1 arrest. This hypothesis is supported by many observations. For instance, E2F is a transcription factor associated with cell proliferation. Un/hypo-, but not hyper-pRb, binds and inactivates E2F. The cellular introduction of viral oncogenes such as HPV16 E7, adenovirus E1A, and simian virus 40 (SV40) large T antigen result in cell proliferation. These viral oncogenes bind un/hypo-, but not hyper-pRb and disable its suppressive capacity. The human osteogenic sarcoma cell line SAOS-2 lacks full length nuclear pRb protein. Transfection of the Rb gene in

these cells result in G0/G1 growth arrest. Co-transfection of cyclin D2, E or A resulted in pRb phosphorylation and a release from G0/G1 arrest (Dou 1998¹⁵⁹)

(2) Rb transcription increases in arrest and differentiation

5 The following studies show increased Rb transcription in arrested or differentiated cells.

(a) mRNA measurements

10 Murine erythroleukemia (MEL) cells are virus-transformed erythroid precursor cells which can be induced to differentiate by a variety of chemicals. MEL cells were induced to differentiate with dimethyl sulfoxide (DMSO) or hexamethylene bisacetamide (HMBA). Expression of globin was used as a marker of differentiation. The cells showed a 11- and 7-fold increase in Rb mRNA following DMSO and HMBA treatment, respectively, with maximum expression on day three of induction (Coppola 1990¹⁶⁰, Fig 1). This increase preceded the accumulation of globin mRNA, the marker of differentiation. The peak in Rb mRNA occurred simultaneously with growth arrest and terminal differentiation. Another cell line, S2 myoblasts derived from C3H10T1/2 mouse embryonic by 5-azacytidine treatment, was induced to differentiate by depletion of mitogens from the medium. Expression of α -actin, a muscle specific gene, was used as a marker of differentiation. Seven to twelve hours following feeding with 2% horse serum (low mitogen conditions), the cells showed an increase in pRb mRNA. The increase continued over the next 48 hours (Ibid, Fig 2). The study estimates a 10-fold Rb mRNA induction, an increase which was accompanied by an increase in α -actin expression. In a B cell line, A20 and a pre-B cell line 300-18, the Rb gene is expressed at very low levels compared to actin. In three plasmacytoma lines, representing very late stages of B cell differentiation, Rb mRNA was 8-fold higher. These results are consistent with those of MEL and S2 cells. All cell lines showed an increase in steady-state Rb mRNA in late stages of differentiation, which is maintained in dividing cells. Based on these observations, Coppola, *et al.*, concluded that in all three lineages (erythroid, muscle, and B-cell) differentiation is associated with increased Rb mRNA.

An enriched epithelial cell population from 20-day fetal rat lungs was immortalized with a replication-defective retrovirus encoding a temperature-sensitive SV40 T antigen (T Ag). One cell line, designated 20-3, maintained a tight epithelial-like morphology. At the permissive temperature (33°C), 20-3 cells grow with a doubling time of 21 h. At the non-permissive temperature (40°C), doubling time increased to more than 80 h (Levine 1998¹⁶¹, Fig 4a). 20-3 cells, incubated at the permissive temperature (33°C) show almost no Rb mRNA while at the non-permissive temperature (40°C) the cells show a more than 100-fold increase in Rb mRNA (Ibid, Fig 6b). The increase is significant at 24 h after temperature shift-up and peaks at 48-72 h (Ibid, Fig 7a). Terminally differentiated and growth arrested alveolar type 1 cells are first observed at day 20-21 of gestation. Prior to this time the lung shows active growth and cell proliferation. Total RNA was isolated from 17- and day fetal lungs and assayed for Rb mRNA. The results show a 2.5-fold increase in Rb mRNA during this period relative to control gene EFTu.

P19 embryonal carcinoma cells were induced to differentiate into neuroectoderm with retinoic acid (RA). Undifferentiated cells show very low levels of Rb mRNA and protein. Twenty four hours following RA exposure, the cells showed a marked increase in Rb expression with mRNA levels increasing 15-fold by 4-6 days (Slack 1993¹⁶², Fig 2). RAC65 is a mutant clone of P19 cells that fails to differentiate. The cells contain a truncated RAR α receptor. Following RA exposure, the cells showed no increase in Rb mRNA (Ibid, Fig 3). P19 cells transfected with RB-CAT, a reporter gene driven by the Rb promoter, expressed CAT with kinetics similar to the Rb gene (Ibid, Fig 5b, 6). The post-mitotic neurons developed in RA-treated cultures contained only the hypophosphorylated form of pRb (Ibid, Fig 7, 8). Based on these observations, Slack, *et al.*, concluded that the increased Rb expression associated with cell differentiation appears to result from enhanced transcription.

DS19/Sc9 is a MEL cell line which when treated with in G1, prolonged the next G1 (Richon 1992¹⁶³, Fig 2A). The cells which emerged from the prolonged G1, progressed through cell cycle for at least another two to five generations (cycle time of 10 to 12 h), and permanently arrested in G1/G0 expressing characteristic of terminal erythroid differentiation. Over 90% of the DS19/Sc9 cells became irreversibly committed to differentiate by 48 h of culture with HMBA. Protein extracts prepared from asynchronous

cultures induced with HMBA demonstrated a 2-to 3-fold increase in total amount of pRb. There was no change in proportions of hypo- or hyper-pRb (Ibid, Fig 4A). An increase in the level of total pRb was detected as early as 24 h after onset of culture with HMBA, and pRb increased as the number of cells recruited to terminal differentiation increased

5 through 100 h of cultured (Ibid, Fig. 4A). HMBA-induced an increase in pRb in all phases of the cell cycle while no change in pRb protein level was detected in DS19/Sc9 cultured without HMBA. The increase in pRb in cells cultured with HMBA was accompanied by an increase in the level of Rb mRNA. A 3.6-fold increase in Rb transcription was observed with no change in mRNA stability. DS19/VCR-C is a vincristine-resistant

10 variant of the parental DS19/Sc9 with an accelerated rate of differentiation. HMBA treatment of DS19/VCR-C showed a more prolonged G1 arrest and a higher percentage of cell committed to terminal differentiation compared to DS19/Sc9. During G1 arrest, DS19/VCR-C also showed more hypo-pRb compared to DS19/Sc9. In HMBA-induced MEL cells, every cell division increased the absolute amount of pRb protein, whereas the

15 degree of phosphorylation continues to fluctuate through cell cycle progression. This increase was accompanied by an increase in mRNA resulting from an increased rate of transcription. Based on these observations, Richon, *et al.*, proposes the following model. An inducer increases Rb transcription resulting in higher hypo- and total-pRb concentration. The increase in hypo-pRb prolongs G1 however, the initial increase in

20 hypo-pRb is most likely not sufficient for permanent G1 arrest. Therefore, cells reenter the cell cycle for a few more generations. While cells continue to divide, the increased rate of transcription results in hypo-pRb accumulation. When a critical hypo-pRb concentration is reached, the cells irreversibly commit to terminal differentiation. This model describes the determination of the commitment to differentiate as a stochastic

25 process with progressive increases in the probability of G1/G0 arrest and differentiation established through successive cell divisions.

Many studies report a relationship between Rb phosphorylation, cell cycle arrest and differentiation. These studies use the different gel mobility of hyper-pRb relative to un/hypo-pRb to show protein phosphorylation or dephosphorylation. Since these studies are interested in the transition between the two states, they do not report changes in total concentration of each form of pRb. Specifically, they do not quantify protein levels with densitometry. However, in some cases, visual inspection of the blots can provide valuable

information. Consider the following study. Actively growing LS174T colon cancer cells, which constitutively express pRb, were induced to differentiate with sodium butyrate. Three days following exposure, a lower molecular weight, or unphosphorylated pRb molecule became visible. After the fourth day of treatment, when significant growth inhibition was observed, the unphosphorylated species were predominant (Schwartz 5 1998¹⁶⁴, Fig 5). A careful inspection of the blots in Fig 5 suggests that the concentration of hypo-pRb at day 4 (lane 6) is higher than the initial concentration of hyper-pRb (lane 1 and 2). Even if we assume that dephosphorylation of hyper-pRb produces a hypo-pRb 10 species associated with growth arrest (and not protein degradation), the differences in total concentration at day 0 and day 4 indicate a potential need for increased transcription (an increase in mRNA stability, or rate of translation is also possible).

Summary: The transcription of the Rb gene increases with growth arrest and differentiation.

15 (3) Microcompetition increases probability of developing cancer

Rb is a GABP stimulated gene. Microcompetition decreases Rb transcription which in turn increases the probability of developing cancer.

b) ***BRCA1***

(1) BRCA1 and cell proliferation

20 Transcriptional or translational inactivation of the BRCA1 gene increases cell proliferation.

Normal mammary epithelial cells and MCF-7 breast cancer cells were treated with unmodified 18 base deoxyribonucleotides complementary to the BRCA1 translational initiation site. The anti-BRCA1 oligonucleotides decreased BRCA1 mRNA by 70-90% 25 compared to control oligonucleotides (Thompson 1995¹⁶⁵, Fig 6) and the anti-BRCA1 treated cells showed accelerated proliferation rate (*Ibid*, Fig 4a,c).

NIH3T3 cells were transfected with a vector expressing BRCA1 antisense RNA resulting in reduced expression of endogenous BRCA1 protein. The transfected cells,

unlike parental and sense transfectants, showed accelerated growth rate, anchorage independent growth and tumorigenicity in nude mice (Rao 1996¹⁶⁶, Fig 4).

Retroviral transfer of wild-type BRCA1 gene to breast and ovarian cancer cell lines inhibited growth *in vitro*. Transfection of wild-type BRCA1 also inhibited 5 development of MCF-7 tumors in nude mice. Peritoneal treatment with retroviral vector expressing wild-type BRCA1 inhibited tumor growth and increased survival among mice with established MCF-7 tumors (Hold 1996¹⁶⁷). A phase I clinical study employing gene transfer of BRCA1 into 12 patients with extensive metastatic cancer showed stable disease for 4-16 weeks in eight patients, tumor reduction in three patients and radiographic 10 shrinkage of measurable disease in one patient (Tait 1997¹⁶⁸).

Reduced expression of BRCA1 resulted in increased cell proliferation while increased expression of BRCA1 resulted in reduced tumor development.

(2) BRCA1 in cancer

(a) *Germline mutations*

15 The majority of familial breast cancer and ovarian cancer cases result from germline mutations in the BRCA1 gene.

(b) *Sporadic breast cancer*

Many studies showed decreased BRCA1 transcription in sporadic breast tumors (Russel 2000¹⁶⁹, Rio 1999¹⁷⁰, Rice 1998¹⁷¹, Magdinier 1998¹⁷², Ozcelik 1998¹⁷³, 20 Thompson 1995¹⁷⁴). The decrease intensifies with tumor progression yet the cause of the decreased transcription is unknown. Two possible causes, somatic mutations and promoter methylation, do not seem to provide an explanation. Somatic mutations of the BRCA1 gene are rare in sporadic breast and ovarian tumors (Russel 2000¹⁷⁵, Rio 1999¹⁷⁶, Furtreal 1994¹⁷⁷, Merajver 1995¹⁷⁸), and methylation of the BRCA1 promoter was 25 demonstrated in only a small percentage of sporadic breast cancer samples (Cattaneo 1999¹⁷⁹, Magdinier 1998¹⁸⁰, Rice 1998¹⁸¹, Dobrovic 1997¹⁸²). The majority of breast and ovarian tumors show neither somatic mutations nor promoter methylation.

(3) Microcompetition increases probability of developing cancer

BRCA1 is a GABP stimulated gene. Microcompetition decreases BRCA1 transcription which increases the probability of developing breast and ovarian cancer.

5 c) *Fas*

(1) *Fas and cancer*

Cell population density is determined by balancing between cell growth and cell death. Programmed cell death, or apoptosis, is the final step in a series of morphological and biochemical events. Fas antigen is a 48-kDa cell surface receptor homologous to the 10 tumor necrosis factor (TNF) family of transmembrane proteins. Fas binding by the Fas ligand, or by antibodies, triggers rapid cell apoptosis.

15 Fas induced apoptosis was initially identified in the immune system. Ligation of Fas induced apoptosis in activated T cells, B cells, and natural killer cells. In addition, Fas was identified in many epithelial cells. Although the role of Fas in non-lymphoid tissues is not completely understood, maintenance of normal cell turnover and removal of potentially oncogenic cells have been suggested. Consider, as example, the epithelial layer of colonic mucosa. These cells show a rapid rate of cell turnover and high expression of Fas. It is conceivable that the high rate of colonocyte removal is Fas induced.

20 (a) *Germline mutations*

Germline mutations in Fas gene is associated with spontaneous development of plasmacytoid tumors in lpr mice (Davidson 1998¹⁸³) and neoplasms in two autoimmune lymphoproliferative syndrome (ALPS) patients (Drappa 1996¹⁸⁴).

(b) *Sporadic cancers*

25 Many studies showed progressive reduction in Fas expression in many cancers. Consider, Keane, *et al.*, (1996¹⁸⁵) results in breast carcinomas, Gratas, *et al.*, (1998¹⁸⁶) results in esophageal carcinomas, Strand, *et al.*, (1996¹⁸⁷) results in hepatocellular carcinomas, Moller, *et al.*, (1994¹⁸⁸) results in colon carcinomas and Leithauser, *et al.*, (1993¹⁸⁹) results in lung carcinomas. The reduced Fas expression results from reduced

transcription of the Fas gene. Consider the observations in Das, *et al.*, (2000¹⁹⁰) showing reduced Fas transcription in ovarian, cervical and endometrial carcinoma tissues and four ovarian and three cervical carcinoma cell lines. Also consider the results in Butler, *et al.*, (1998¹⁹¹) demonstrating reduced Fas transcription in colon tumors, and in Keane, *et al.*, (1996¹⁹²) showing reduced Fas mRNA levels in six out of seven breast cancer cell lines. As in the case of the BRCA1 gene, the cause of decreased transcription is unknown. The same two possible causes, somatic mutations and promoter methylation, also fail to explain the observed reduction in Fas transcription. Allelic loss or somatic mutations of the Fas gene are rare (Bertoni 2000¹⁹³, Lee 1999A¹⁹⁴, Lee 1999B¹⁹⁵, Shin 1999¹⁹⁶, Butler 1998¹⁹⁷), and no methylation was found in the Fas promoter (Butler 2000¹⁹⁸). The majority of carcinomas show no somatic mutations or promoter methylation in the Fas gene.

15 (2) Microcompetition increased probability of developing cancer

Fas is a GABP stimulated gene. Microcompetition decreases Fas transcription leading to an increased probability of developing cancer.

3. Signaling

a) *ERK agents inhibit proliferation, stimulate differentiation*

ERK agents phosphorylate GABP, increase Rb, BRAC1 and Fas transcription and induce cell cycle arrest and differentiation.

20 (1) Constitutive active MAP kinase kinase 1 (MEK1)

AU565 breast carcinoma cells were transiently transfected with a constitutively active MEK1 mutant or a control vector. Expression of the constitutively active MEK1 resulted in a significant increase in ERK activity as determined by the use of an antibody against phosphorylated ERK (Lessor 1998¹⁹⁹, Fig. 6A, B). Oil Red O staining was used as a measure of cell differentiation. 53.6% of cells transfected with the constitutively activated MEK1 vector were Oil Red O positive. In contrast, only 20.8% of the cells transfected with the control vector were positive. Based on these observations, Lessor, *et*

et al., concluded that constitutive activation of the MEK/ERK pathway in AU565 cells is sufficient to mediate differentiation.

5 (2) Heregulin β 1 (HRG β 1)

AU565 breast carcinoma cells were treated with 10 ng/ml HRG β 1 for 7 days. The treatment increased ERK activity 4-fold after 10 min. The initial increase dropped to control levels by 15 min. Following the drop, a second sustained increase in activity was observed for 105 min (Lessor 1998²⁰⁰, Fig 1). HRG β 1 treatment decreased cell number by 56% as compared to non treated controls (Ibid, Fig 4). Addition of 0-10 μ M PD98059, a specific MEK inhibitor (see above) resulted in a dose-dependent reversal of HRG β 1-induced cell growth arrest (Ibid, Fig 4). Pretreatment with PD98059 also inhibited HRG β 1-induced differentiation in a dose-dependent manner (Ibid, Fig 5), with 10 μ M PD98059 completely blocking the HRG β 1-induced differentiation. Based on these observations Lessor, *et al.*, concluded that sustained³ activation of the MEK/ERK pathway is both essential and sufficient for HRG β 1-induced differentiation of AU565 cells.

15 (3) Phorbol ester (TPA)

ML-1, human myeloblastic leukemic cells, were treated with 0.3 ng/ml TPA. As a result, ERK2 activity increased with a 6- and 4-fold induction at 1 and 3 h, respectively. Thereafter, the activity decreased to below basal levels (He 1999²⁰¹, Fig 1A). The time-dependent ERK2 activation was further illustrated by a shift to a slower-migrating form of ERK2, representing the phosphorylated ERK2 (Ibid, Fig 1B). ML-1 cells treated with 0.3 ng/ml TPA for 3 days, followed by an additional 3 days in culture after removal of TPA, ceased to proliferate and displayed morphological features typical of monocytes/macrophages (Ibid, Fig. 6c). Exposure to PD98059, the MEK inhibitor, led to a 2- and 10-fold reduction in TPA-activated ERK2 activity at 1 and 3 h, respectively (Ibid, Fig 3). Cells treated simultaneously with 10 μ M PD98059 and 0.3 ng/ml TPA continued to proliferate and exhibited morphology of undifferentiated cells (Ibid, Fig 6A, D). Based

³ Exposure to low doses of HRG β 1 (0.01 ng/ml) induced a 7-fold transient 5 min peak in ERK activation which dropped to control levels by 90 min. This dose showed no sustained activation (Ibid, Fig 1). The 0.01 ng/ml HRG β 1 treatment results in cell proliferation.

on these observations, He, *et al.*, concluded that activation of the MEK/ERK signaling pathway is necessary for TPA-induced mononuclear cell differentiation.

(4) Transforming growth factor- β 1 (TGF β 1)

An enriched epithelial cell population from 20-day fetal rat lungs was immortalized with a replication-defective retrovirus encoding a temperature-sensitive SV40 T antigen (T Ag). One cell line, designated 20-3, maintained a tight epithelial-like morphology. At the permissive temperature (33°C), 20-3 cells grow with a doubling time of 21 h. At the non-permissive temperature (40°C) doubling time increased to more than 80 h (Levine 1998²⁰², Fig 4a). The labeling index is a function of [³H]thymidine incorporation in DNA, and therefore correlates with cell replication. Treatment of 20-3 cells with 5 ng/ml TGF β 1 for 72 h decreased the labeling index to 80% at the permissive temperature (33°C) and to less than 5% at the non-permissive temperature (40°C) (*Ibid*, Fig 5c). Treated cells cultured at the non-permissive temperature for 72 h and then shifted to the permissive temperature for additional 24 h showed an index below 10%. The low labeling index reveals that extensive terminal growth arrest occurred during the non-permissive temperature period. Treatment with the ERK agent TGF β 1 resulted in reduced replication of the epithelial cells in both permissive and non-permissive temperatures.

4. Carcinogens

a) *Oxidative stress increases the probability of developing cancer*

Oxidative stress decreases binding of GABP to the N-box, reduces transcription of GABP stimulated genes, and increases transcription of GABP suppressed genes (see microcompetition chapter above). Microcompetition for GABP also decreases binding of GABP to the N-box, which increases the probability of developing cancer (see above). Therefore, oxidative stress also increases the probability of developing cancer. Moreover, oxidative stress increases replication of some GABP viruses, see, for instance, the stimulating effect of oxidative stress on cytomegalovirus (CMV) (Vossen 1997²⁰³, Scholz 1996²⁰⁴), Ebstein-Barr virus (EBV) (Ranjan 1998²⁰⁵, Nakamura 1999²⁰⁶), and HIV (Allard 1998A²⁰⁷, Allard 1998B²⁰⁸). If the cell harbors such a GABP virus, the probability of developing cancer as a result of oxidative stress is even higher.

b) *Carcinogens induce oxidative stress*

Many carcinogens, genetic and epigenetic, induce oxidative stress, see, for instance, nicotine (Helen 2000²⁰⁹, Yildiz 1999²¹⁰, Yildiz 1998²¹¹) and asbestos (Afaq 2000²¹², Abidi 1999²¹³, Liu 2000²¹⁴, Marczynski 2000A²¹⁵, Marczynski 2000B²¹⁶, Fisher 2000²¹⁷, Brown 2000²¹⁸). By increasing oxidative stress, these carcinogens reduce GABP binding, decrease expression of Rb, fas and BRCA1, and increase the probability of developing cancer. The effect of these carcinogens on GABP binding might be the main reason for their carcinogenic capacity.

5. Viruses in cancer

Many studies report detection of viral genomes in human tumors. The following table summarizes some of these reports.

Virus	Cancer
Epstein-Bar virus (EBV)	Burkitt's lymphoma (BL)
	Nasopharyngeal carcinoma (NPC)
	Hodgkin's disease
	Some T-cell lymphomas
	Polymorphic B cell lymphomas
	B-cell lymphoproliferation in immunosuppressed individuals
	Breast cancer
SV40	Brain tumors
	Osteosacromas
	Mesotheliomas
HIV	Breast cancer
Human T cell lymphotropic virus - I (HTLV-I)	Adult T-cell leukemia
Human papilloma virus (HPV)	Anogenital cancers
	Skin cancers
	Oral cancers
Hepatitis B virus (HBV)	Hepatocellular carcinoma
Hepatitis C virus (HCV)	Hepatocellular carcinoma
Human herpes virus 8 (HHV8, KSHV)	Kaposi's sarcoma,
	Body cavity lymphoma

See also recent reviews on human tumor viruses, Butel 2000²¹⁹, zur Hausen 1999²²⁰, Hoppe-Seyler 1999²²¹. On EBV and breast cancer see Bonnet 1999²²², Labrecque 1995²²³, and the editorial by Magrath and Bhatia 1999²²⁴. On HIV and breast cancer see 5 Rakowicz-Szulczynska 1998²²⁵.

EBV, SV40, HIV and HTLV-I are GABP viruses. Microcompetition between a GABP virus and cellular genes causes cancer. An interesting aspect of microcompetition is its ability to explain how viral infection can cause cancer independent of proto-oncogene expression or viral integration into host DNA.

10 **B. Atherosclerosis**

1. **Motility**

a) Introduction

b) ECM-cell and cell-cell adhesion

15 The extracellular matrix (ECM) is comprised of several proteins, including collagens, fibronectin, laminins and proteoglycans assembled into a network structure. Cells bind to ECM proteins through transmembrane-surface receptors. The receptors include integrins, cadherins, immunoglobulins, selectins and proteoglycans. The cadherins and selectins are mostly involved in cell-cell adhesion. The integrins and 20 proteoglycans are mostly involved in cell-ECM binding. Cell-adhesion molecules connect external ligands and the cytoskeleton and participate in signal-transduction.

c) Motility

25 A cell is said to show motility if it changes position over time. A change of position of the entire cell is called migration. A change in position of any part of the cell periphery is called projection. The two processes share common features, such as polarization, cytoskeletal reorganization and formation of new cell-ECM adhesion points.

d) Morphology

The first phase in cell migration is polarization. During polarization the cell creates clear "front-back" asymmetry in which actin and cell-surface receptors accumulate at the leading edge of the cell. The second phase of migration is protrusion of the plasma membrane from the front of the cell in the form of fine, tubular structures called filopodia, or a broad, flat membrane sheet called lamellipodium. The third phase is establishing new ECM-cell points of contact. This binding prevents retraction of the newly extended membrane and provides "grip" for the tractional force required for cell movement. The two final stages of cell migration are flux of intracellular organelles into the newly extended sections of the cell, and retraction of, or breaking off, the trailing edge. The result of this process is directional movement of the cell body (Sanserson 1999²²⁶)

e) Direction

A simple characterization of direction of movement is a change in distance relative to a reference point in space. Let circulating blood define such a reference point.

Movement of cells out, or away from circulation, will be called forward motility. Diapedesis of monocytes to enter the intima (also called migration, emigration or transmigration) is an example of forward motility. Movement of macrophages deeper into the intima is another example of forward motility. Movement of cells toward, or into circulation, will be called backward motility. Reverse transendothelial migration is an example of backward motility.

2. P-selectin-, β_2 integrin-, α_4 -integrin-propelled forward motility

The first section discusses the relationship between p-selectin, β_2 integrin and α_4 -integrin and motility without reference to direction. The direction issue is covered in the second section.

25 *a) Motility*

(1) Transendothelial migration

Leukocyte migration from blood into tissue starts with crossing the endothelium. This phase is called transendothelial migration, transmigration or emigration.

Transmigration involves multiple steps, including rolling of leukocytes along the endothelium, firm adhesion of leukocytes to endothelium called margination, and movement of leukocytes through endothelial intercellular junctions. In this process P-selectin mediates rolling of leukocytes on the endothelium (Dore 1993²²⁷). An increase in endothelial surface expression of P-selectin increases leukocyte rolling and transmigration.

Many studies demonstrated the role of the surface receptors CD18 (CD11a/CD18, CD11b/CD18, CD11c/CD18) and VLA-4 ($\alpha_4\beta_1$, CD49d/CD29) in this process of transendothelial migration (Shang 1998A²²⁸, Shang 1998B²²⁹, Meerschaert 1995²³⁰, Meerschaert 1994²³¹, Chulyan 1993²³², Kavanaugh 1991²³³). The two studies by Shang, *et al.*, (1998A, 1998B) also showed that these molecules participate in forward motility through a barrier of human synovial fibroblasts (HSF).

(2) Intimal motility

CD18 and α_4 also participate in motility inside the intima. Consider the following studies.

To test the effect of α_4 expression on cell motility, α_4 was expressed in a Chinese hamster ovary (CHO) cell line deficient in $\alpha_5\beta_1$ integrin (CHO B2). The parental α_5 deficient CHO B2 cells were unable to adhere, spread or migrate on a surface coated with 10 μ g/ml mouse cellular fibronectin. Expression of $\alpha_4\beta_1$ integrin in the CHO B2 cells enabled the cells to adhere, spread and migrate on the fibronectin coated surface (Wu 1995²³⁴).

To test the effect of CD18 on cell motility, neutrophils were stimulated with 0.5×10^{-8} M fMLP. The stimulation increased random motility through a three-dimensional collagen type I gel (0.1 to 1.0 mg/mL). In a 0.4 mg/mL collagen gel, antibodies against CD18 (anti-CD18) decreased motility of stimulated neutrophils by 70% (Saltzman 1999²³⁵). Based on these observations Saltzman, *et al.*, concluded that under conditions of high hydration, or when fiber density is relatively low, neutrophil migration through collagen gels is CD18-dependent.

To test the effect of CD18 on cell motility, another study stimulated neutrophils with 10^{-8} M fMLP for 10 min. On unstimulated cells, CD18 was randomly distributed on

the nonvillous planar cell body. Stimulation of the round, smooth neutrophils induced a front-tail polarity, i.e., a ruffled frontal pole and contracted rear pole with a distinct tail knob at the posterior pole. Moreover, immunogold-labeling and backscattered electron images detected a 4-fold increase in CD18 surface membrane concentration compared to 5 unstimulated cells. The immunogold-labeled CD18 accumulated mainly on ruffled plasma membrane at the frontal pole of polar neutrophils. The contracted rear end showed few colloidal gold particles (Fernandez-Segura 1996²³⁶). Based on these observations, Fernandez-Segura, *et al.*, concluded that CD18 may participate in the locomotion of neutrophils.

10 A third study stimulated rat mesentery with platelet-activating factor (PAF; 10⁻⁷ M). After 30-40 min of the chemotactic stimulation, numerous polymorphonuclear leukocytes (PMNs), predominantly neutrophils and monocytes/macrophages, were observed migrating further into the extravascular tissue. Immunofluorescence flow cytometry revealed a 3-fold increase in CD18 expression on extravasated PMNs compared 15 with blood PMNs. Intravital time-lapse videomicroscopy was used to analyze migration velocity of activated PMNs. Median migration velocity in response to PAF stimulation was $15.5 \pm 4.5 \mu\text{m}/\text{min}$ (mean \pm SD). Treatment with two different antibodies against CD18 significantly reduced migration velocity by 17% (mAb CL26) and 22% (mAb WT.3) (Werr 1998²³⁷). Based on these *in vivo* observations Werr, *et al.*, concluded that 20 CD18 participates in extravascular PMN locomotion.

25 Since the extracellular matrix (ECM) contains fibronectin and collagen, the observations of Wu (1995²³⁸) and Saltzman (1999²³⁹) above are consistent with intimal α_4 integrin- and CD18-propelled leukocyte motility. Moreover, the morphological changes reported by Fernandez-Segura (1996) and the extravascular CD18-propelled leukocyte motility reported by Werr (1998) support such a mechanism.

b) Direction

30 The first segment of leukocyte forward motility, transendothelial transmigration, is α_4 integrin- and CD18-propelled. From the basal side of the endothelium, leukocytes continue their forward motility into the intima until they reach a certain depth. Werr, *et al.*, (1998) showed that forward motility in the extravascular space is CD18-propelled.

Since the intima is sandwiched between the endothelium and the extravascular space, forward motility in the intimal segment is, most likely, CD18-propelled.

(See more on direction control, or "cell turning," below)

3. TF-propelled backward motility

5 As above, the first section discussed the relation between TF and motility without reference to direction. The direction is covered in the second section.

a) Motility

TF expression induces cell spreading. Consider the following studies.

10 The human breast cancer cell line MCF-7 constitutively expresses TF on the cell surface. aMCF-7 is a subline of MCF-7. Muller, *et al.*, (1999²⁴⁰) show that adhesion of aMCF-7 cells to surfaces coated with FVIIa or inactivated FVIIa (DEGR-FVIIa) was significantly accelerated during the first 2 h after seeding compared to surfaces coated with BSA. In addition, the number of cells adhering to anti-TF IgG was significantly higher than the number of cells adhering to anti-FVII or a control IgG (*Ibid*, Fig. 6A).

15 Accelerated adhesion and spreading of cells on surfaces coated with anti-TF mAb VIC7 was blocked by recombinant TF variants (sTF₁₋₂₁₉, sTF₉₇₋₂₁₉) covering the epitope of anti-TF mAb VIC7 (residues 181-214). No effect was seen with sTF₁₋₁₂₂. However, if anti-TF IID8 (epitope area 1-25) was used for coating, sTF₁₋₁₂₂ blocked accelerated adhesion and spreading of cells. To conclude, the Muller, *et al.*, results demonstrate that *in vitro*-cultured cells, that constitutively express TF on the cell surface, adhere and spread on surfaces coated with both catalytically active and inactive immobilized ligands for TF.

20 Ott, *et al.*, (1998²⁴¹) showed that J82 bladder carcinoma cells that constitutively express high levels of TF adhere and spread on surfaces coated with monoclonal antibodies specific for the extracellular domain of TF. The spontaneously transformed endothelial cell line ECV304 or human HUVEC-C endothelial cells also adhered and spread on TF ligand when stimulated with TNF α to induce TF expression.

25

In malignant and nonmalignant spreading epithelial cells, TF is localized at the cell surface in close proximity to, or in association with, both actin and actin-binding proteins

in lamellipodes and microspikes, at ruffled membrane areas and at leading edges. Cellular TF expression at highly dynamic membrane areas suggest an association between TF and elements of the cytoskeleton (Muller 1999²⁴²). Cunningham, *et al.*, (1992²⁴³) showed that cells deficient in actin binding protein 280 (ABP-280) have impaired cell motility.

5 Transfection of ABP-280 into these cells restored translocational motility. Ott, *et al.*, (1998²⁴⁴) identified ABP-280 as a ligand for the TF cytoplasmic domain and showed that ligation of the TF extracellular domain by either FVIIa or anti-TF resulted in ligation of the TF cytoplasmic domain by ABP-280, reorganization of the subcortical actin network, and expression of specific adhesion contacts different from integrin mediated focal

10 adhesions.

b) Direction

(1) Reverse transendothelial migration.

Randolph, *et al.*, (1998²⁴⁵) used an *in vitro* model consisting of HUVEC grown on reconstituted bovine type I collagen. The reverse transmigration assays used freshly isolated or precultured peripheral blood monocellular cells (PBMC) incubated with endothelium for 1 or 2 hours to allow accumulation of monocytes in the subendothelial collagen. Following initial incubation, the nonmigrated cells were removed by rinsing the cultures. At given intervals a few cultures were processed to enable counting of the cells underneath the endothelium. The remaining cultures were rinsed to remove cells that may have accumulated in the apical compartment by reverse transmigration, and incubation was continued. Let percent reverse transmigration represent the percentage decrease in the number of cells beneath the endothelium relative to the number of subendothelial cells at 2 hours. Figure 17 shows the percent reverse transmigration as a function of time.

25 The results showed that mononuclear phagocytes (MP) that enter the subendothelial collagen later exit the cultures by retraversing the endothelium with a t1/2 of 48 hours. The endothelial monolayer remained intact throughout the experiments.

(2) Role of tissue factor in reverse transendothelial migration

Two MoAbs against TF, VIC7 and HTF-K108, strongly inhibited reverse transmigration for at least 48 hours (*Ibid*, Fig. 2A). In comparison, 55 other isotype-

matched MoAbs tested had little or no effect, specifically, anti-factor VIIa, -IVE4 or -IIH2 did not inhibit reverse transmigration (Ibid, Fig. 2C). A direct comparison of the effect of VIC7 relative to IB4, a MoAb against $\beta 2$ integrin, revealed $78 \pm 15\%$ inhibition of reverse transendothelial migration by VIC7 relative to no inhibition by IB4 in the same three 5 experiments (Ibid, Fig. 2B). None of the MoAbs affected the total number of live cells in the cultures.

10 (3) TF amino acids 181-214 essential for reverse transmigration.

Studies of epitope mapping showed that the epitope for VIC7 included recognition of at least some amino acids between residues 181-214. Soluble TF inhibited reverse transmigration by $69 \pm 2\%$ in eight independent experiments (Ibid, Fig. 4). Only fragments containing amino acid residues carboxyl to residue 202 blocked reverse transmigration effectively (Ibid, Fig. 4). This result agrees well with the location of the epitope for VIC7.

15 (4) TF and endothelium adhesion

Experiments were conducted to explore the existence of a ligand to TF on the endothelium. Unstimulated HUVEC were added to wells coated with TF or control proteins in the presence or absence of anti-TF MoAb. After 2 hours incubation, 20 endothelial cell adhesion to TF fragments containing amino acid residues 202-219 was greater than their binding to control surfaces or to TF fragments lacking these residues (Ibid, Fig. 8A). Spreading of HUVEC during the first 2 hours was observed on surfaces coated with TF fragments carrying residues 97-219 or 1-219. Surfaces coated with a TF fragment spanning amino acids 1-122 showed much less spreading. These results show that endothelial cells express binding sites for TF, and that the TF residues 202-219 25 participate in this adhesion.

(5) Reverse transmigration and TF self association

30 LPS stimulation increases cell surface TF activity through increased concentration of cell surface TF molecules and increased conversion of TF dimers to monomers. Monocytes and HUVEC were stimulated with LPS. VIC7 recognized a single band of 47 kD in the LPS-stimulated cells, but not in the unstimulated cell extracts (Ibid, Fig. 3). In

unstimulated cells TF is self-associated, most likely in the 181-219 region, and, therefore, unavailable for VIC7 binding. LPS stimulation converts the dimers to monomers and exposes the VIC7 binding site. The same region participates in binding to endothelial cells. Since VIC7 inhibits reverse transmigration by competitive binding to the 181-219 region, self-association also inhibits reverse transmigration.

4. Cell turning

Let CD18, α_4 integrin and TF be called propulsion genes. Since leukocyte forward motility is α_4 integrin- and CD18-propelled, and backward motility is TF-propelled, a signaling system should exist that coordinates expression of the propulsion genes. This system should determine the direction of cell motility. The following sections describe such a system.

a) *Two propulsion systems*

Forward and backward motility are propelled through mostly different molecules.

Antibodies against many molecules participating in forward motility do not inhibit reverse transmigration. Randolph, *et al.*, (1998²⁴⁶) tested a variety of MoAbs against a list of molecules known to mediate binding between leukocytes and endothelium during apical-to-basal transmigration. Even though MoAbs were shown to access subendothelial antigens, neutralizing MoAbs to E-selectin, vascular cell adhesion molecule-1 (VCAM-1), and platelet/endothelial cell adhesion molecule-1 (PECAM-1) showed no effect on reverse transmigration. Ott, *et al.*, (1998²⁴⁷) showed that a RGD peptide known to block several matrix-binding integrins does not abolish spreading on coagulation protease factor VIIa (*Ibid*, Fig. 2A).

On the other hand, antibodies against TF, which participates in backward motility, do not inhibit forward motility. Resting monocytes do not express TF, however LPS stimulates their expression of TF. Randolph, *et al.*, (1998) showed that the TF MoAb VIC7 inhibits adhesion of LPS-stimulated, but not resting, monocytes to unstimulated or TNF-activated HUVEC by $35 \pm 7\%$. However, VIC7 did not inhibit migration of LPS-stimulated monocytes already bound to the apical side of the endothelium. Since

circulating monocytes do not express TF, it is reasonable to conclude that TF does not participate in adhesion to the endothelium during forward motility (TF adhesion to the apical side of the endothelium is probably important in backward motility, see below). Since TF also does not participate in the subsequent steps in apical-to-basal

5 transendothelial migration, TF has no role in forward motility.

Ott, *et al.*, (1998²⁴⁸) also noted that J82 cells spreading on TF ligand have a different morphology compared to cells adherent to fibronectin through integrins (*Ibid*, Figs. 2A and 2B), thereby suggesting a qualitative difference in the two adhesive events.

b) *Signaling*

10 (1) Extracellular effects on forward motility
Extracellular signal-regulated kinase (ERK) agents are extracellular molecules which transmit a signal resulting in the phosphorylation of ERK. See chapter on ERK for examples. ERK agents stimulate GABP•p300 binding. In leukocytes, this binding stimulates transcription of CD18 and α_4 , which, in turn, stimulates forward motility.

15 Moreover, the stimulated binding of GABP•p300 represses TF, and therefore, represses backward motility.

A molecules is regarded a chemoattractant if it stimulates leukocytes forward motility. Considering chemoattraction in the framework of propulsion yields an interesting insight. In leukocytes, chemoattraction is the result of ERK phosphorylation.

20 In other words, if a molecule leads to the phosphorylation of ERK, it should show chemoattraction. fMLP is an example for such a molecule. fMLP is a syntactic compound found in bacterial products. Several studies demonstrated that fMLP binding to its receptor results in phosphorylation of ERK1 and ERK2 (Chang 1999²⁴⁹ in rat neutrophils, Yagisawa 1999²⁵⁰ in human monocytes, Coffer 1998²⁵¹ in human neutrophils). As an ERK agent, fMLP should demonstrate chemoattraction. As expected, Yamada, *et al.*, (1992²⁵²) showed that fMLP is a chemoattractant for blood mononuclear cells.

Mildly oxidized LDL (also termed "minimally modified" LDL, and therefore denoted mmLDL) and oxidized LDL (oxLDL) are also ERK agents. Consider the following studies.

Rat vascular smooth muscle cells (VSMC) were exposed to 25 μ g/ml of Cu^{+2} - oxidized LDL (oxLDL). The results showed a rapid stimulation of both ERK1 and ERK2 with peak activity at 5 min and a return to near baseline by 60 min (Kusuhara 1997²⁵³, Fig. 1). 25 μ g/mL of minimally oxidized LDL (mmLDL) caused a smaller increase in ERK activity with a similar time course (Kusuhara *et al.*, call this type of LDL "native LDL.") However, they propose that this type of LDL is actually minimally oxidized. Therefore, we call it mmLDL). The increase in ERK activity relative to 200 nmol/L PMA treatment, was 54.3% for oxLDL and 35.2% for mmLDL. Both oxLDL and mmLDL stimulated ERK activity in a concentration-dependent manner (Ibid, Fig. 3). Human monocytes showed minimal ERK stimulation by either oxLDL or mmLDL (Ibid, Fig. 7A). In contrast, human monocyte-derived macrophages cultured for 7 days showed significant ERK activity in response to oxLDL (Ibid, Fig. 7B) but no response to mmLDL (Ibid, Fig. 7B). Bovine aortic endothelial cells showed no response to either oxLDL or mmLDL (Ibid, Fig. 7C). Based on these observations Kusuhara, *et al.*, concluded ERK activation is cell type dependent, degree of oxidation dependent, LDL receptor dependent and that the rapidity of the ERK response to LDL indicates that ERK activation is LDL internalization independent.

Deigner, *et al.*, (1996²⁵⁴) reported similar effects of mmLDL and oxLDL on ERK in U-937 macrophage-like cells, Balagopalakrishna, *et al.*, (1997²⁵⁵) in aortic smooth muscle cell, Kamarna, *et al.*, (1999²⁵⁶) and Bassa, *et al.*, (1998²⁵⁷) in mesangial cells.

Both mmLDL and oxLDL are ERK agents, and therefore, chemoattractants. Quinn, *et al.*, (1987²⁵⁸) demonstrated that oxLDL is a chemoattractant when bound to macrophages in the subendothelial space. However, in contrast to stimulated macrophages, circulating monocytes are not chemoattracted by oxLDL binding. To chemoattract monocytes, oxLDL uses an indirect approach. Subendothelial oxLDL stimulates endothelial cells to produce monocytes chemoattractant (chemotactic) protein - 1 (MCP-1, also called RANTES) which is an ERK agent. MCP-1 is released into

circulation and binds monocytes. Monocyte bound MCP-1 stimulates CD18 and α_4 integrin, resulting in adhesion to endothelium and transmigration.

Another special example is bacterial LPS, a known chemoattractant which is an ERK agent. LPS is a direct chemoattractant when bound to its receptor (before 5 internalization), and an indirect chemoattractant through stimulation of MCP-1 which is a strong ERK agent.

(2) Intracellular effects on forward and backward motility

(a) Redox regulation of GABP N-box binding

Oxidative stress decreases the binding of GABP to the N-box, reduces 10 transcription of GABP stimulated genes and increases transcription of GABP suppressed genes. Consider the following study.

Mouse 3T3 cells were treated for 2 h with diethyl maleate (DEM), a glutathione (GSH)-depleting agent, in the presence or absence of N-acetylcysteine (NAC), an 15 antioxidant and a precursor of GSH synthesis. Following treatment, the cells were harvested, and nuclear extracts were prepared in the absence of a reducing agent. GABP DNA binding activity was measured by EMSA analysis using oligonucleotide probes containing a single N-box (AGGAAG) or two tandem N-boxes (AGGAAGAGGAAG). Treatment of 3T3 cells with DEM resulted in a dramatic decrease in the formation of 20 GABP heterodimer (GABP α GABP β), (Martin 1996²⁵⁹, Fig. 2A, lane 2) and heterotetramer (GABP α ₂GABP β ₂), (I β 1 δ , I γ 2A, lane 6) complexes on the single and double N-box. Inhibition of GABP DNA binding activity by DEM treatment was prevented by 25 simultaneous addition of NAC (Ibid, Fig. 2A, lanes 4 and 8). The reduction of GABP DNA binding activity was not due to loss of GABP protein since the amount of GABP α and GABP β 1 was unaffected by DEM or NAC treatment. Dithiothreitol (DTT) is an antioxidant. DTT treatment of nuclear extracts prepared from DEM-treated 3T3 cells restored GABP binding activity. Treatment of 3T3 nuclear extracts with 5 mM GSSG nearly abolished GABP DNA binding. Based on these observations Martin *et al.*, concluded that GABP DNA binding activity is inhibited by oxidative stress, i.e. GSH depletion. The study also measured the effect of DEM treatment on the expression of

transiently transfected luciferase reporter constructs containing a TATA box with either an upstream double N-box or C/EBP binding site (Ibid, Fig. 4). DEM treatment had no effect on luciferase expression from C/EBP-TA-Luc after 6 or 8 h treatment (Ibid, Fig. 4). However, DEM treatment of cells transfected with double N-box-TATA-Luc, resulted in a 5 28% decrease in luciferase expression after 6 h and a 62% decrease after 8 h (Ibid, Fig. 4). Based on these results, Martin *et al.*, concluded that glutathione depletion inhibits GABP DNA binding activity resulting in reduced expression of GABP-regulated genes.

10 Oxidative stress decreases GABP binding to the N-box, which in turn decreases transcription of a GABP stimulated gene and increases transcription of a GABP repressed gene.

15 Microcompetition for GABP also decreases binding of GABP to the N-box. Take a GABP gene sensitive to oxidative stress through GABP only⁴. The effect of microcompetition on the transcription of this gene is similar to the effect of oxidative stress. In other words, for this gene, microcompetition can be viewed as leading to "excess oxidative stress."

(b) *Redox regulation of propulsion genes*

20 Oxidative stress reduces the binding of GABP α to the N-box. Assume the propulsion genes, TF, CD18 and α_4 integrin, are responsive to oxidative stress exclusively through GABP. GABP stimulates CD18 and α_4 integrin transcription. Reduced binding of GABP α to DNA decreased CD18 and α_4 integrin transcription resulting in diminished forward motility. On the other hand, GABP represses TF transcription, oxidative stress increases TF transcription, stimulating backward motility.

(i) TF

oxLDL effect on TF transcription

25 oxLDL increases TF transcription. Consider the following studies.

⁴ Oxidative stress also modifies binding of other transcription factors, such as AP1, and NF- κ B.

Exposure of human monocytic THP-1 cells for 10 hours to concentrationd of up to 20 $\mu\text{mol/L}$ Cu^{+2} had no effect on procoagulant activity. However, in the presence of 1 $\mu\text{mol/L}$ 8-hydroxyquinoline, Cu^{+2} produced a dose dependent expression of procoagulant activity (Crutchley 1995²⁶⁰, Table 1). The effect of Cu^{+2} was replicated with the copper transporting protein ceruloplasmin. Cu^{+2} is known to produce lipid peroxidation and free radical generation. Therefore, the study tested the possibility that the procoagulant activity resulted from oxidative stress. Several lipophilic antioxidants, including probucol (20 $\mu\text{mol/L}$), vitamin E (50 $\mu\text{mol/L}$), BHT (50 $\mu\text{mol/L}$), and a 21-aminosteroid antioxidant U74389G (20 $\mu\text{mol/L}$), inhibited the Cu^{+2} induced procoagulant activity (Ibid, Fig. 4). The increased procoagulant activity was due to TF. Cu^{+2} induced intracellular oxidative stress which increased TF transcription. The kinetics of the induction of Cu^{+2} was compared to LPS. Exposure to LPS or Cu^{+2} resulted in an increase TF mRNA levels. Relative to basal levels, LPS increased mRNA 2.5-fold after 2 hours of exposure, declining to basal levels by 6 hours. In contrast, at 2 hours, Cu^{+2} reduced mRNA levels to 50% followed by a 3.5-fold increase at 6 hours (see figure 18). The Cu^{+2} and LPS induced TF expression also differed in the response to antioxidants. While all four antioxidants inhibited Cu^{+2} induced TF expression, only vitamin E inhibited LPS induced expression.

The LPS effect on TF transcription is mostly mediated through the NF- κ B site. Crutchley, *et al.*, (1995) results indicate that oxidative stress increased TF transcription through a different site. This conclusion is also supported by the negative effect of oxLDL on NF- κ B binding to its site as demonstrated in human T-lymphocytes (Caspar 1999²⁶¹), Raw 264.7, a mouse macrophage cell line (Matsumura 1999²⁶²), peritoneal macrophages (Hamilton 1998²⁶³), macrophages (Schackelford 1995²⁶⁴), and human monocyte derived macrophage (Ohlsson 1996²⁶⁵). The results of these studies are consistent with reduced binding of GABP to the N-box in the (-363 to -343) region of the TF gene (see above).

Another study tested the effect of oxLDL on TF transcription. The binding of advanced glycation end products (AGE) with their receptor (RAGE) result in intracellular oxidative stress indicated by reduced glutathione (GSH) levels (Yan 1994²⁶⁶). Monocytes incubated with AGE-albumin (AGE-alb) for 24 hours showed an increase in TF mRNA expression (Khechai 1997²⁶⁷, Fig. 1B). Presence of the translational inhibitor

cycloheximide completely suppressed the AGE-alb induced TF mRNA accumulation (Ibid, Fig. 1B). The antioxidant N-Acetylcysteine (NAC) increases the levels GSH and NAC is easily transported into the cell. Incubation of cells with AGE-alb in the presence of 30 mmol/L NAC resulted in a concentration dependent inhibition of TF activity (Ibid, 5 Fig. 2A) and TF antigen expression. Moreover, TF mRNA expression was almost completely suppressed (Ibid, Fig. 2C). Based on these results Khechai, *et al.*, concluded that oxidative stress is responsible for TF gene expression.

Crutchley, *et al.*, (1995²⁶⁸) showed that although reduced oxidative stress decreases TF mRNA, the LPS induced increase in TF mRNA is insensitive to certain antioxidant. 10 Brisseau, *et al.*, (1995²⁶⁹) showed a similar insensitivity of the LPS induced increase in TF mRNA to the antioxidant NAC. Since Khechai, *et al.*, (1997) reported that NAC increases TF mRNA, the combined results of Brisseau, *et al.*, (1995) and Khechai, *et al.*, (1997) are also consistent with reduced GABP binding to the N-box in the (-363 to -343) region resulting from oxidative stress.

15 See also Ichikawa, *et al.*, (1998²⁷⁰) which reported simliar results in human macrophage-like U937 cells treated with the oxidant AGE and the antioxidants catalase and probucol.

oxLDL effect on TF antigen localization

20 The induced TF is localized to regions important in cell motility. Consider the following studies.

25 Endotoxin treatment of human glioblastoma cells (U87MG) resulted in preferential localization of TF antigen in membrane ruffles and peripheral pseudopods. Most prominent TF staining was observed along thin cytoplasmic extensions at the periphery of the cells. Moreover, membrane blebs, associated with cell migration, were also heavily stained (Carson 1993²⁷¹). Endotoxin treatment of macrophages also resulted in a high concentration of TF antigen in membrane ruffles and microvilli relative to smooth areas of the plasma membrane or endocytosis pits (Lewis 1995²⁷², Fig. 2). The membrane ruffles and microvilli contained a delicate, three dimensional network of short fibrin fibers and fibrin protofibrils decorated in a linear fashion with anti-fibrin(ogen) antibodies. oxLDL

treatment of macrophages resulted in similar preferential localization of TF antigen in membrane ruffles and microvilli.

5 Although the two studies use different terms, "cytoplasmic extensions" and "blebbed" (Carson 1993), vs "microvilli" and "membrane ruffles" (Lewis 1995), the terms, most likely, describe the same phenomenon.

oxLDL effect on TF activity

oxLDL increases TF activity. Consider the following study.

10 Lewis, *et al.*, (1995²⁷³) demonstrate the effect of oxLDL treatment on TF activity. In culture, monocytes, and monocyte-derived macrophages expressed little or no procoagulant activity. Endotoxin treatment induced TF activity, peaking at 4 to 6 hours and decreasing over the following 18 hours (*Ibid*, Fig. 1). Cells exposed to minimally oxidized LDL (oxLDL) showed similar TF activation. The endotoxin and oxLDL treatments resulted in 115- and 58-fold increase in TF activity, respectively (*Ibid*, Table 1).

15 **oxLDL effect in non-monocytic cells**

oxLDL also increases TF mRNA in smooth muscle cells (SMC) and endothelial cells. Consider the following two studies.

20 Quiescent rat SMC contained low levels of TF mRNA. Treatment of SMC with LDL or oxLDL significantly increased TF mRNA (Cui 1999²⁷⁴, Fig. 1). Densitometric analysis showed that oxLDL increases TF mRNA 38% more than does LDL. The accumulation of TF mRNA induced by LDL or oxLDL was transient. Maximum level of TF mRNA was observed 1.5-2 hours following LDL or oxLDL stimulation (*Ibid*, Fig. 2), declining significantly over the following 5 hours. TF mRNA response to stimulation in human aortic SMC was similar. Nuclear run-on assays and mRNA stability experiments indicated that the increase in TF mRNA resulted mainly from increased transcription.

25 Another study exposed human endothelial cells to minimally oxidized LDL (oxLDL) or endotoxin for varying times. Northern blot analysis of total RNA showed a sharp increase in TF mRNA at 1 hour, a peak at 2 to 3 hours, and a decline to basal levels

at 6 to 8 hours after treatment. The half-life of TF mRNA in oxLDL and endotoxin exposed endothelial cells was approximately 45 and 40 minutes, respectively. The rate of TF mRNA degradation was similar at 1 and 4 hours post treatment. Nuclear runoff assays showed a significant increase in TF transcription rate following exposure of the cells to 5 oxLDL or LPS (Fei 1993²⁷⁵).

In monocytes/macrophages, oxLDL treatment reduces the binding of NF- κ B to its site (see above). Since NF- κ B stimulates TF transcription, the decreased binding diminishes the positive oxLDL effect on TF transcription mediated through the GABP site. In endothelial cells (Li 2000²⁷⁶) and smooth muscle cells (Maziere 1996²⁷⁷), oxLDL 10 treatment increases the binding of NF- κ B. This increase adds to the positive GABP mediated effect.

(ii) CD18

Oxidative stress reduces CD18 transcription. Consider the following study.

ICAM-1 is a ligand for CD18. Human polymorphonuclear leukocytes (PMN) 15 were exposed to hypoxic condition. As a result, the adhesion of PMN to recombinant ICAM-1, but not BSA coated surfaces, increased (Montoya 1997²⁷⁸, table 1). Anti-CD18 mAb abolished the increased adhesion (Ibid, Fig. 1). The antioxidant pyrrolidine dithiocarbamate (PDTC) reduced PMN intracellular oxidative stress (Ibid, Fig. 2). PDTC treatment of PMN increased PMN adhesion to tumor necrosis factor- α (TNF α) stimulated 20 HUVEC monolayers (Ibid, Fig. 4). Pyrrolidine, which lacks antioxidant activity, failed to increase adhesion. Anti-CD18 abrogated the PDTC enhanced adhesion (Ibid, Fig. 5). Under flow conditions, a significant number of PMN were rolling at low velocities on the apical surface of the HUVEC monolayer. PDTC treatment reduced rolling distance and 25 rolling velocities (Ibid, Fig. 10), increasing the number of stably adhered PMN. These observations indicate that reduced oxidative stress stimulates CD18 expression.

Hypoxia results in reduced oxidative stress, and therefore, stimulates GABP binding (Martin 1996²⁷⁹). Increased GABP binding stimulates CD18 transcription (Rosmarin 1998²⁸⁰), and therefore, CD18 adhesion. The observations in Montoya (1997, above) are consistent with such a mechanism.

(c) *Special oxidative stress inducers*(i) *Oxidized LDL*

Oxidative stress inducers of special importance (see below) are mmLDL and oxLDL.

5 **Oxidized LDL depletes GSH**

mmLDL and oxLDL deplete intracellular GSH, and therefore induce oxidative stress. Consider the following studies.

10 GSH content was determined in cultured human endothelial cells after 24 h incubation with native LDL or oxLDL at 30, 40 or 50 µg of protein/ml. The results showed that at 30 µg/mg, GSH content slightly but significantly increased (10%). In contrast, at 40 and 50 µg/ml, the GSH content decreased by 15 and 32%, respectively, (only significant at 50 µg/ml, $P < 0.05$) (Therond 2000²⁸¹, Fig. 2B). Moreover, the results also showed that all oxLDL lipid fractions induced depletion of intracellular GSH (Ibid, Fig. 3B).

15 Another study tested the effect of a specific oxLDL fraction on intracellular GSH. Human promyelocytic leukemia cells U937 were treated with 7-ketocholesterol. U937 cells were used since they respond to oxysterols in concentrations similar to those observed in endothelial and smooth muscle cells, and since U937 are frequently used to model the response of macrophages to oxysterols in humans. The GSH content was 20 measured by flow cytometry with monochlorobimane. The results are summarized in figure 19 (Lizard 1998²⁸², Fig 5A).

At all time points, GSH content in the 7-ketocholesterol treated cells was lower compared to controls ($P < 0.05$).

Oxidized LDL cell loading reduces CD18 expression

25 According to Gray and Shankar (1995²⁸³) "AthMø (Atherosclerotic Macrophages) showed a substantial reduction in CD11b and CD18 cell surface expression. NMø (Normal rabbit peripheral blood Monocytes), on the other hand, had strong surface expression of both CD11b and CD18. In comparison to NMø that have been in cell

culture for a short time, cell surface expression of the CD11b/CD18 integrin on AthM ϕ is strongly down-regulated. Furthermore, these immunohistochemical studies provided evidence that the loss of CD11b/CD18 integrins is a function of the extent of lipid loading and perhaps the stage of the foam cell formation. It is our observation from looking at 5. these cytologic preparations, that when stained for adhesion molecules, the smaller more normal appearing cells with very little lipid in them actually have the majority of staining, whereas the larger, more lipid laden cells have absolutely no staining in them."

Oxidized LDL cell loading reduces forward motility

10 Mouse peritoneal macrophages were loaded with lipids by precircubation with acetylated LDL (acLDL) for various periods (100 μ g/ml). The macrophages turned foam cells were used to fill the upper wells of a modified Boyden chamber. The lower wells contained Zymosan A activated mouse serum (ZAMS). Zymosan A is a cell-wall extract of *Saccharomyces cerevisiae*. ZAMS is a chemoattractant for macrophages. After 3 h, the membrane in the Boyden chamber was removed and the cells which did not migrate to the 15 lower surface were wiped off. The migrated cells were fixed and counted. The results showed decreased macrophage migration with increased preincubation time with acLDL. Since, preincubation time correlated positively with lipid content, higher lipid content resulted in reduced migration (Trach 1996²⁸⁴, Fig. 4a,b). (Similar results are reported in Pataki, *et al.*, (1992²⁸⁵), an earlier study with H. Robenek as principle investigator.) 20 Quinn, *et al.*, (1985²⁸⁶) also reports reduced motility of resident macrophages with modified LDL as chemoattractant.

25 Bacterial particles are macrophage chemoattractants (for LPS, see above, for fMLP, see Yamada, *et al.*, (1992²⁸⁷)). However, it seems likely that macrophage loading with one type of toxic substance (oxLDL, bacterial particles) reduces chemoattractance of the other. The results in the above studies are consistent with such a concept. In these studies, the zamosan chemoattractance was reduced with the increase in cell loading of modified LDL.

(ii) Bacterial particles

Bacterial particles, such as LPS or fMLP (a syntactic particle that represents bacterial products), are another important type of oxidative stress inducers (see below).

The products of the respiratory burst have low molecular weight, and therefore, diffuse out of the phagolysosome into cytoplasm and nucleus. The resulting oxidative stress effects TF transcription through the N-box and not the NF- κ B site (see above). On the other hand, the bacterial particles, such as LPS, also increase TF transcription through the NF- κ B site. These two effect act synergistic. Such a synergy is probably needed for quick removal of the relatively highly toxic bacterial particles (compared to oxLDL toxicity) by faster clearance of bacterially loaded macrophages from infected tissues.

10 c) *Net propulsion*

Consider a tissue resident molecule which is both an oxidant and an ERK agent. As an ERK agent the molecule chemoattracts circulating or resident leukocytes by increasing their expression of CD18 and α_4 integrin, inducing forward motility. The leukocyte migrate toward the molecule and phagocytize it. Once internalized, the molecule induces oxidative stress, i.e., depletes GSH, which, in turn, reduces binding of GABP to the N-boxes on TF, CD18 and α_4 integrin, resulting in increased expression of TF and reduced expression of CD18 and α_4 integrin. These changes reduces forward propulsion and increase backward propulsion, until backward propulsion is greater. Since net force is the vector sum of all forces acting upon an object, the new net propulsion turns the leukocyte back toward circulation. The final step of this process is reentry into circulation.

C. Atherosclerosis- fibrous cap atheroma formation

The first major class of atherosclerotic lesions is the fibrous cap atheroma. The fibrous cap is a distinct layer of connective tissue completely covering a lipid core. The fibrous cap consists of smooth muscle cells in a collagen-proteoglycan matrix with a variable number of macrophages and lymphocytes (Virmani 2000²⁸⁸). The following sections describe the mechanism of fibrous cap atheroma formation.

1. LDL pollution

Plasma LDLs passively cross the endothelium (see below) by diffusion through the plasma membrane. Higher concentration of plasma LDL result in increased influx of LDL. Unlike other tissues, the intima lacks lymphatic vessels. Therefore, to reach the nearest lymphatic vessels, located in the medial layer, the LDL should pass through the intima. However, this passage is partly blocked by an elastic layer situated between the intima and the media (Pentikainen 2000²⁸⁹). According to Nordestgaard, *et al.*, (1990²⁹⁰) "less than 15% of the LDL cholestryl ester that entered the arterial intima penetrated beyond the internal elastic lamina." A fraction of the influxed LDL is passively effluxed through the endothelium. Another fraction is hydrolyzed. The remaining intimal LDLs bind the extracellular matrix (ECM). The ECM is composed of a tight negatively charged proteoglycan network. Certain sequences in the LDL apoB-100 contain clusters of the positively charged amino acids lysine and arginine. These sequences, called heparin-binding domains, interact with the negatively charged sulphate groups of the glycosaminoglycan chains of the proteoglycans (Boren 1998²⁹¹, Pentikainen 2000²⁹²). Subendothelial agents modify (oxidize) the matrix bound LDL.

Passive influx

Nordestgaard 1992²⁹³ reports a linear correlation between plasma concentration of cholesterol in LDL, IDL, VLDL and arterial influx. Moreover, in cholesterol-fed rabbits, pigs and humans, arterial influx of lipoproteins depended on lipoprotein particle size. Other studies report that arterial influx of LDL in normal rabbits did not depend on endothelial LDL receptors. According to Nordestgaard, *et al.*, these results indicate that the transfer of lipoprotein across endothelial cells and into the intima is a "nonspecific molecular sieving mechanism." Schwenke (1997²⁹⁴) measured the intima-media permeability to LDL in different arterial regions in normal rabbits on a cholesterol-free chow diet. The results showed that the aortic arch is 2.5-fold more permeable to LDL compared to descending thoracic aorta (*Ibid*, Table 2). The concentration of undegraded LDL in the aortic arch was almost twice as great compared to the descending thoracic aorta (*Ibid*, Table 3). In cholesterol-fed rabbits, as a result of hypercholesterolemia, the mass transport of LDL cholesterol into all arterial regions was greatly increased. However, hypercholesterolemia did not influence intima-media permeability of any

arterial region (Ibid, Table 2). Kao, *et al.*, (1994²⁹⁵), Kao, *et al.*, (1995²⁹⁶) showed that open junctions with gap widths of 30-450 nm between adjacent endothelial cells were only observed in the branched regions of the aortic arch, and not in the unbranched regions of the thoracic aorta. Moreover, LDL labeled with colloidal gold were present within most 5 of these open junctions, while no gold particles were found in the normal intercellular channels (i.e., 25 nm and less) of both regions. These results are consistent with a nonspecific molecular sieving mechanism.

Passive efflux

10 Rabbits of the St Thomas's Hospital strain show elevated plasma levels of VLDL, IDL, and LDL. In both lesioned and nonlesioned aortic arches of these rabbits, the logarithms of the fractional loss of VLDL, IDL, LDL, HDL, were inversely and linearly correlated with the diameter of these macromolecules (Nordestgaard 1995²⁹⁷). This observation suggests that, similar to influx, the efflux of LDL through the endothelium can 20 also be described as a "nonspecific molecular sieving mechanism."

15 2. LDL clearance

a) *Model*

Modified LDL is chemotactic to circulating monocytes (see above). As a result, 20 endothelial cells increase the surface expression of P-selectin and circulating monocytes increase CD18 and α_4 integrin expression (other surface molecules also change their expression). The increased expression of forward propulsion genes increases adhesion of circulating monocytes to the endothelium (margination) and emigration (see forward motility above). Once in the intima, monocytes differentiate into macrophages and start to accumulate modified LDL thereby turning into foam cells. The intracellular oxidative stress induced by the modified LDL particles decreases CD18 and α_4 integrin transcription 25 and stimulates TF transcription. The decreased CD18 and α_4 integrin expression reduces forward propulsion. The transient increase in TF activity on the surface of foam cells induces backward propulsion. When backward propulsion surpasses forward propulsion the cell turns back. When the foam cells reach the endothelium, they first bind the basal

surface and then the apical surface of the endothelium. When TF adhesion activity returns to its basal level, the apical bound foam cells are released into circulation.

b) Observations

(1) Enhanced forward motility

5 There is extensive research showing more adhesion and emigration of monocytes in atherosclerosis.

(2) Enhanced backward motility

(a) *Foam cell clearance*

The results of the following studies are consistent with clearance of foam cells.

10 Twenty-two Yorkshire pigs were fed a high fat diet. The animals were killed 12, 15 and 30 weeks after diet initiation, and tissue samples were examined by light and electron microscopy. At 15 weeks, lesions were visible as raised ridges even at low magnification (Gerrity 1981²⁹⁸, Fig. 1). Large numbers of monocytes were adherent to the endothelium over lesions, generally in groups (Ibid, Fig. 5), unlike the diffused adhesion observed at prelesion areas. Foam cells overlaid lesions at all three stages, although more frequently at 12 and 15 weeks. The foam cells had numerous flaplike lamellipodia and globular substructure (Ibid, Fig. 6). Some foam cells were fixed while passing through the endothelium, trapped in endothelial junctions alone (Ibid, Fig. 8) or in pairs (Ibid, Fig. 9). In all cases, the attenuated endothelial cells were pushed luminally (Ibid, Fig. 14). The luminal portion of the trapped foam cells had an irregular shape, with numerous cytoplasmic flaps (lamellipodia and veil structures), empty vacuoles and reduced lipid content compared to the intimal part of the cell (Ibid, Fig. 8 and 9). Foam cells were also infrequently found in buffy coat preparations from arterial blood samples (Ibid, Fig. 7), and rarely in venous blood. According to Gerrity, these findings are consistent with backward migration of foam cells and suggest that such a migration indicates the existence of a foam cell mediated lipid clearance system.

25 Another study fed 10 male pigtail monkeys an atherogenic diet and 4 monkeys a control diet. Twelve days after diet initiation, and at monthly intervals up to 13 months,

5 animals were killed and tissue samples were examined by light and electron microscopy. The endothelial surface of the aorta in control animals was covered with a smooth, structurally intact endothelium (Faggiotto 1984-I²⁹⁹, Fig. 4A). Occasionally, the surface showed small focal areas protruding into the lumen (Ibid, Fig. 4B). Cross sectional examination of the protrusions revealed foam cells underlying the intact endothelium (Ibid, Fig. 3A). During the first 3 months, the endothelium remained intact. However, on larger protrusions the endothelium was extremely thin and highly deformed. At 3 months, the arterial surface contained focal sites of endothelial separation with a foam cell filling the gap (Ibid, Fig. 10A). The luminal section of the foam cell showed numerous lamellipodia. In addition, thin sections of endothelial cells bridged over the exposed foam cell, deforming the surface of the foam cell (Ibid, Fig. 10B). Moreover, rare occasional foam cells were observed in blood smears of some controls. During the first 3 months, when the endothelium was intact, the number of circulating foam cells increased (Faggiotto 1984-II³⁰⁰, Fig. 10). Based on these observations Faggiotto, *et al.*, concluded 10 that foam cells egress from the artery wall into the blood stream, confirming the 15 conclusions of Gerrity (1981).

20 A third study feed 36 male New Zealand White rabbits a cholesterol-enriched diet and 37 rabbits a control diet. Both groups were exposed to electrical stimulation (ES) known to induce arteriosclerotic lesions. The stimulation program lasted 1, 2, 3, 7, 14, or 28 days. At these intervals, tissue samples were collected, processed, and examined by transmission electron microscopy (TEM). After 1 day of ES, intimal macrophages of hypercholesterolemic rabbits showed loading of lipids (Kling 1993³⁰¹, Fig. 3b). These cells were often responsible for markedly stretching the overlying endothelial cells. After 2 days, foam cells were fixed while passing through endothelial junctions (Ibid, Fig. 8a). 25 Neighboring endothelial cells were often pushed luminally, indicating outward movement of the macrophage (Ibid, Fig. 8a). The outward movement of the cells was also supported by the finding that the intimal portion of the foam cells transmigrating the endothelium was intact, while the lumina portion was often ruptured and associated with platelets. (Ibid, Fig. 8b,c). Under the prolonged influence of the atherogenic diet, emerging foam cells 30 became more frequent. In all cases, the emerging foam cells migrated through endothelial junctions without damaging the endothelium. Based on these observations, Kling, *et al.*, concluded that "similar to observations of Gerrity and Faggiotto, *et al.*, we have electro

microscopic evidence that the macrophages, loaded with lipid droplets, were capable of migrating back from the intima into the blood stream ... thus ferrying lipid out of the vessel wall."

5 (b) *Increased TF expression on foam cell*

The following studies show increased TF expression on foam cells.

Seven White Carneau pigeons were fed an atherogenic diet and three animals received a control diet. The diet regimen lasted 8-10 months and was shown to be sufficient to induce lesions in the thoracic aorta. The concentrations of tissue factor (TF) antigen in circulating monocytes, cultured macrophages, and macrophages from 10 atherosclerotic lesions were ultrastructurally analyzed using immunogold labeling. The plasma cholesterol of the cholesterol-fed animals was elevated compared to controls. Upon dissection, all cholesterol-fed animals revealed fatty streaks and atherosclerotic plaque at the celiac bifurcation of the thoracic aorta. Monocytes isolated from normocholesterolemic and hypercholesterolemic animals had approximately 1 15 immunogold particle per 2 μm of plasma membrane (Landers 1994³⁰², Fig. 2). The low level of TF antigen in the plasma membrane is consistent with the lack of TF procoagulant activity in freshly-isolated monocytes or monocyte-derived macrophages maintained in culture. Monocytes newly adherent to lesion surface also showed low levels of TF antigen (0.3 particles/ μm of plasma membrane). In contrast, the lumenally exposed surface of 20 foam cells projecting into the arterial lumen from subendothelial intima showed high levels of TF antigen (7.3 particles/ μm of plasma membrane). The distribution of TF concentrations on the surface of macrophages was bimodal. Circulating and newly adherent macrophages had low levels of TF antigen. Projecting foam cells had high level of TF antigen. (The immunogold labeling of endothelial cells either underlying the 25 adherent macrophages or flanking intimal foam cells protruding into the lumen was minimal.) According to Landers, *et al.*, these observations are consistent with the egressing foam cells reported by Gerrity. Another unpublished observation reported in Landers, *et al.*, (1994) is the association between short term lesion regression and the transient increase in clot formation on lesions.

5 Faggiotto 1984-I³⁰³ showed the existence of foam cells in peripheral blood smears from hyperlipidemic monkeys. Most of these cells showed no adherence to plastic cell culture dishes, however, TF induces such adherence. Since egressing foam cells show high concentrations of TF antigen, either TF is removed from the cell surface while in circulation or, more likely, TF adhesion activity is reduced by encryption (see below).

10 Lander, *et al.*, (1994) and Faggiotto, *et al.*, (1984) observations are consistent with the following model. Modified LDL increases TF transcription. The initial increase in TF concentration on the surface of foam cells results in backward motility. The cells pass through gap junctions by first binding the basal and then the apical side of the endothelium. Concurrently, the concentration of surface TF continues to increase. The additional surface TF deactivates many surface TF molecules through the formation of TF dimers (encryption). The encrypted foam cells are consequently released from the endothelium surface and join circulation.

3. Atherogenesis

15 a) Model

Let $\text{Trapped}_{\text{FC}}$, $\text{Egress}_{\text{FC}}$ and Total_{FC} denote the number foam cells trapped in the intima, the number of foam cells in the process of egressing from the subendothelial space and the total number of intimal foam cells, respectively. $\text{Trapped}_{\text{FC}} + \text{Egress}_{\text{FC}} = \text{Total}_{\text{FC}}$. Denote the fraction of foam cells trapped in the intima with $\%_{\text{Trapped}}$. Assume that 20 inefficiencies in foam cell backward motility, denoted I , increase $\%_{\text{Trapped}}$, which is the percentage of trapped foam cells. Also assume that $\%_{\text{Trapped}}$ is independent of Total_{FC} , the total number of intimal foam cells.

$$(1) \text{Trapped}_{\text{FC}} = \%_{\text{Trapped}}(I) \times \text{Total}_{\text{FC}}$$

Let $\text{Rate}_{\text{lesions}}$ denote the rate of atherosclerotic lesion formation.

$$25 (2) \text{Rate}_{\text{lesions}} = f(\text{Trapped}_{\text{FC}}) = f(\%_{\text{Trapped}}(I) \times \text{Total}_{\text{FC}})$$

The following derivatives summarize the relationship between changes in Total_{FC} or I and $\text{Rate}_{\text{lesions}}$.

$$(3) \frac{\partial \text{Rate}_{\text{lesions}}}{\partial \text{Total}_{\text{FC}}} = \frac{\partial \text{Rate}_{\text{lesions}}}{\partial \text{Trapped}_{\text{FC}}} \cdot \%_{\text{Trapped}}$$

$$(4) \frac{\partial \text{Rate}_{\text{lesions}}}{\partial I} = \frac{\partial \text{Rate}_{\text{lesions}}}{\partial \text{Trapped}_{\text{FC}}} \cdot \text{Total}_{\text{FC}} \cdot \frac{\partial \%_{\text{Trapped}}}{\partial I}$$

Consider equation 3. $\frac{\partial \text{Rate}_{\text{lesions}}}{\partial \text{Trapped}_{\text{FC}}} > 0$. $\%_{\text{Trapped}}$ is fixed. Therefore,

5 $\frac{\partial \%_{\text{Trapped}}}{\partial \text{Total}_{\text{FC}}} > 0$, an increase in total number of intimal foam cells increases the rate of lesions formation. An increase in LDL pollution increases the entry of monocytes which increases the total number of intimal foam cells thereby resulting in increased rate of lesion formation.

Consider equation 4. $\frac{\partial \text{Rate}_{\text{lesions}}}{\partial \text{Trapped}_{\text{FC}}} > 0$. $\text{Total}_{\text{FC}} > 0$. $\frac{\partial \%_{\text{Trapped}}}{\partial I} > 0$. Therefore,

10 $\frac{\partial \text{Rate}_{\text{lesions}}}{\partial I} > 0$, an increase in backward motility inefficiencies increases the rate of lesion formation.

b) *Observations*

There are numerous observations consistent with such a model of atherogenesis. Most of these observations relate to the effect of the total number of intimal foam cells on rate of lesion formation (equation 3). For instance, diet or genetically induced 15 hypercholesterolemia increase plasma concentrations of LDL, resulting in increased LDL pollution. The increased oxLDL bound to the ECM chemoattracts monocytes. As expected in equation 3, the increase in Total_{FC} results in an increased rate of lesion formation. Another example is LDL pollution of the edges of blood vessel bifurcations resulting from low shear stress (Malek 1999³⁰⁴). As expected, these areas show a higher 20 propensity to develop atherosclerotic lesions.

The opposite direction also holds. A reduction in LDL pollution reduces the rate of atherosclerotic formation. For instance, studies showed that in an animal, several months of a lipid-reduced diet resulted in a decreased number of foam cells and regression

of fatty streaks (Trach 1996³⁰⁵, Pataki 1992³⁰⁶, Wissler 1990³⁰⁷, Dudrick 1987³⁰⁸, Tucker 1971³⁰⁹). Other studies showed that a genetic deficiency in ICAM-1, P-selectin or E-selectin (Collins 2000³¹⁰), a genetic double deficiency in P-selectin and E-selectin (Dong 1998³¹¹) or treatment with monoclonal antibodies against VAL4 or ICAM-1 (Patel 1997³¹²) reduced monocyte recruitment resulting in a diminished rate of atherosclerotic lesions formation. More studies showed that a mutation in all basic amino acids in the proteoglycan-binding region of apoB-100, which prevents binding of the heparin proteoglycans in ECM, resulted in only mild atherosclerosis despite strong hypercholesterolemia (Pentikainen 2000³¹³). The diminished concentration of ECM bound oxLDL attracted fewer monocytes resulting in reduced Total_{FC}.

For a review of the different theories of atherosclerosis, see Stary, *et al.*, (1994³¹⁴).

c) *Microcompetition*

(1) *Endothelial layer*

15 (a) *Microcompetition increased monocyte recruitment*

Latent infection of endothelial cells increases P-selectin expression thereby inducing increased transmigration of monocytes. According to equation (3) above, the increased number of foam cells increases the rate of lesion formation.

(2) *Subendothelial space*

20 (a) *Subendothelial environment stimulates virus replication intensifying microcompetition*

The subendothelial environment transactivates latent viral infection in monocytes turned macrophages. Consider the following studies.

25 Cytomegalovirus (CMV) is a GABP virus. Circulating monocytes are nonpermissive for CMV replication, they show no expression of viral gene products even when cells harbor a viral genome (Taylor-Wiedeman 1994³¹⁵). In monocytes the virus is in a latent state. Viral replication is dependent on expression of viral immediate-early (IE) gene products controlled by the major immediate-early promoter (MIEP). HL-60, promyelocytic leukemia cells that can differentiate into macrophages, were transfected

with MIEP-CAT, a reporter-plasmid construct controlled by the CMV MIEP. Coculture of MIEP-CAT-transfected cells with endothelial cells (ECs) increased MIEP-CAT activity 1.7 fold over baseline activity in noncocultured HL-60 cells (Guetta 1997³¹⁶, Fig. 1A). Coculture of MIEP-CAT-transfected cells with smooth muscle cells (SMCs) increased 5 MIEP-CAT activity 4.5-fold over baseline (Ibid, Fig. 1B). Treatment with 50 to 200 µg/mL oxLDL activated MIEP in a concentration dependent manner (Ibid, Fig. 2.). A 2.0-fold increase was the largest observed effect of oxLDL (Ibid, Fig. 1C). Coculture with ECs plus oxLDL led to a 7.1-fold increase over baseline, larger than the two separate effects. Based on these results Guetta, *et al.*, concluded that exposure of monocytes turned 10 macrophages to ECs, SMCs, and oxLDL in the subendothelial space favors transactivation of latent CMV.

Moreover, when cerulenin, an inhibitor of fatty acid biosynthesis, was added to mouse fibroblasts infected with Moloney murine leukemia virus (MMuLV), virus 15 production was drastically reduced (Ikuta 1986B³¹⁷, Katoh 1986³¹⁸). Cerulenin also inhibited Rous sarcoma virus (RSV) production in chick embryo fibroblasts (Goldfine 1978³¹⁹).

Following entry to the subendothelial space, monocytes differentiate into 20 macrophages. Monocyte differentiation transactivated the human CMV IE gene (Taylor-Wiedeman 1994³²⁰), and, in some cases, produced productive HCMV infection (Ibanez 1991³²¹, Lathey 1991³²²). Similarly, differentiation of THP-1 premonocytes (Weinshenker 1988³²³) and T2 teratocarcinoma cells (Gonczol 1984³²⁴) also produced HCMV replication.

Subendothelial monocyte-derived macrophages are exposed to ECs, SMCs and 25 oxLDL. If a macrophage harbors a GABP viral genome, the subendothelial environment stimulates viral replication and the increase in viral DNA intensifies microcompetition.

(b) *Microcompetition reduces intimal forward motility (macrophage superficial stop)*

Increased viral replication in the subendothelial space intensifies microcompetition leading to reduced expression of CD18 and $\alpha 4$ integrin which stops the macrophage at a 30 reduced intimal depth. The oxLDL deep in the intima is not cleared and remains ECM

bound. While trapped foam cells form fatty streaks, the ECM bound oxLDLs form the lipid core of the atherosclerotic plaque. The following observations are consistent with such a mechanism.

5 The core of an atherosclerotic plaque actually forms concurrently with fatty streaks. The core has a tendency to extend from a position initially deep in the intima toward the lumen of the artery with increasing age. The lipid in the core region seems to originate directly from plasma lipoproteins and not from foam cell necrosis. Foam cells are usually seen in superficial intima in the region between the core and the endothelial surface (Guyton 1995³²⁵). Consider the following two photomicrographs, figures 20 and
10 21, as examples (Stary 1995³²⁶, Fig. 1 and Fig. 2).

Figure 20 is a photomicrograph of atheroma (type IV lesion) in proximal left anterior descending coronary artery from a 23-year old man who died of a homicide. Extracellular lipids form a confluent core in the musculoelastic layer of eccentric adaptive thickening. The region between the core and the endothelial surface contains 15 macrophages and foam cells (FC). There is no increase in smooth muscle cells or collagenous fibers. "A" indicates adventitia, "M," media. Fixation by pressure-perfusion with glutaraldehyde and maraglas embedding. One-micron thick section. About 55x magnification.

20 Figure 21 is a photomicrograph of thick part of atheroma (type IV lesion) in proximal left anterior descending coronary artery from a 19-year-old man who committed suicide. Core of extracellular lipid includes the formation of cholesterol crystals. Foam cells (FC) overlie core on the aspect toward lumen. Macrophages that are not foam cells (arrows) occupy the proteoglycan layer (pgc) adjacent to endothelium (E) at lesion 25 surface. "A" indicates adventitia, "M," media. Fixation by pressure-perfusion with glutaraldehyde and maraglas embedding. One-micron thick section. About 220x magnification.

(c) *Microcompetition reduces backward motility (reduced foam cell clearance)*

30 The studies by Randolph, *et al.*, (1996³²⁷) and Randolph, *et al.*, (1998³²⁸) (see above) have a similar experimental setting. However, Randolph, *et al.*, (1996) tested the

effect of mAb against ICAM-1 and mAb against CD18 on reverse transmigration. The results showed that Fab fragments of mAb against ICAM-1 (R6.5) completely blocked egression of mononuclear phagocytes (MP) from IL-1-treated HUVEC/amnion cultures for a total of 5 h (Ibid, Fig. 9A). When incubation of MP-HUVEC cocultures (IL-1-
5 pretreated HUVEC) was extended to 12 h, anti-ICAM-1 Fab fragments inhibited reverse transmigration of monocytes by 53% (Ibid, Fig. 9b). Anti CD18 Fab fragments (TS1/18) suppressed reverse transmigration by an average of 71% at 5 h of incubation (Ibid, Fig. 9a). Based on these observations Randolph, *et al.*, concluded that one role of CD18 and ICAM-1 in reverse transmigration is to accelerate initial kinetics.

10 These results indicate the existence of an intial delay in the activation of TF propelled backward motility. This delay might be necessary to allow other cell changes required for TF propelled motility such as cell skeleton modifications. During this delay other molecules, such as CD18, propel backward motility.

15 Many studies measured the effect of certain agents on TF activity over the first few hours following treatment. For instance, Key, *et al.*, (1993³²⁹) infected HUVEC with herpes simplex virus-1 (HSV-1) or exposed the cells to LPS and measured TF PCA activity. Schecter, *et al.*, (1997³³⁰) measured the effect of platelet-derived growth factor (PDGF) stimulation on TF activity on surface of human aortic smooth muscle cell (SMC). The results reported in these studies are presented in figure 22. HSV-1 and LPS lines
20 represent PCA activity in U/ml (Key 1993, Fig. 1). PDGF line represents TF activity relative to untreated cells (Schecter 1997, Fig. 7)

Lewis, *et al.*, (1995³³¹) reported stimulated monocytes, and monocyte-derived macrophages with oxLDL or LPS (see above) and measured TF activity. The results showed that both agents had similar effects.

25 Combining the observations in Randolph, *et al.*, (1996³³²) with these observations suggests that TF driven backward motility starts around the time when TF activity is maximized. Moreover, TF propelled reverse transmigration occurs while TF activity is declining. We call this observation a "soft landing." We propose that a soft landing might reduce the probability of an undesired coagulation reaction on the surface of egressed

foam cells or might increase the probability of foam cell release from the apical surface of endothelium.

In general, a_{TF} denotes TF activity and c_{TF} denotes TF surface concentration on cell surface. Let $a_{TF_{stop}}$ denote TF activity that cannot support reverse transmigration. If 5 $a_{TF_{stop}}$ is reached before a foam cell has reached the apical surface of the endothelium, the cell is trapped. Let $\Delta_c TF_{oxLDL}$, $\Delta_c TF_v$ denote an increase in TF membrane concentration resulting from stimulation with oxLDL and from microcompetition with a GABP virus, respectively. Let $a_{TF_{basal}}$ denote basal TF activity prior to stimulation.

Consider a control cell, denoted "cc," and a cell harboring a GABP viral genome, 10 denoted "vc." Microcompetition between the TF promoter and the GABP virus stimulates TF transcription (see the section on TF gene, above). Let $t = 0$ mark the time of monocyte completed differentiation into a macrophage following entry into subendothelial space. For every $t > 0$, microcompetition results in $\Delta_c TF_v(t) > 0$.

In both cells, for every $t > 0$, $c_{TF}(t) = c_{TF_{basal}} + \Delta_c TF(t)$. However, for viral cell 15 $\Delta_c TF(t) = \Delta_c TF_{oxLDL}(t) + \Delta_c TF_v(t)$ (we assume an additive effect for the oxLDL and virus combination). Since $\Delta_c TF_v(t) > 0$ for viral cells, at any time t , TF concentration on surface of a viral cell is greater than TF concentration on surface of control cell. Consider figure 23.

"cc, c_{TF} " and "vc, c_{TF} " lines represent the increase in TF surface concentration as 20 a function of time for a control cell and viral harboring cell, respectively. The "cc, a_{TF} " and "vc, a_{TF} " curves represent the change in TF activity as a function of time for these cells. The vertical distance between "vc, c_{TF} " and "cc, c_{TF} " represents the effect of microcompetition on the surface concentration of TF. The increase in surface TF concentration shifts the "vc, a_{TF} " curve to the left. As a rule, in both cells the same TF 25 surface concentration generates the same TF activity. For instance, points 7 and 8 represent the same surface concentration and therefore produce the same activity, represented by points 5 and 9, the points of maximum activity. Points 1 and 3 also represent the same surface concentration. These points produce activity 2 and 4, the activity associated with cells at rest, or "stopped" cells.

For every delay ≥ 0 , $t_{stop,cc} - t_{start} > t_{stop,vc} - t_{start}$ (see figure). The time during which the viral cell is actually moving towards circulation is shorter compared to control. Assume the probability of reaching the endothelial apical surface increases with movement time. Since the viral cell movement time is shorter, its probability of being trapped is higher.

Another observation relates to cell velocity. Assume the delay is the same for both cells, i.e. $cc = vc$. The shift of the “ vc, t ” curve results in lower TF activity on the viral cell for every t of actual movement (every $t > t_{start}$ in the figure). Assume that cell velocity depends on TF activity. Then, at any time, the viral cell is slower than the control cell.

10 The reduced velocity also increases the probability of being trapped.

Microcompetition between a GABP virus and TF increases the probability of being trapped in the subendothelial space. Denote the number of viral N-boxes with V_{Nbox} . Higher V_{Nbox} increases the inefficiencies in foam cell backward motility, denoted I in the above clearance model.

15 Modify equation (2).

$$(5) Rate_{lesions} = f(\%_{trapped}(I(V_{Nbox}))) \times Total_{FC}$$

The following derivative represents the effect of V_{Nbox} on $Rate_{lesions}$, the rate of lesion formation.

$$(6) \frac{\partial Rate_{lesions}}{\partial V_{Nbox}} = \frac{\partial Rate_{lesions}}{\partial Trapped_{fc}} \cdot Total_{FC} \cdot \frac{\partial \%_{trapped}}{\partial I} \cdot \frac{\partial I}{\partial V_{Nbox}}$$

20 Consider equation (6). $\frac{\partial Rate_{lesions}}{\partial Trapped_{fc}} > 0$, $Total_{FC} > 0$, $\frac{\partial \%_{trapped}}{\partial I} > 0$ (see above).

$\frac{\partial \%_{trapped}}{\partial V_{Nbox}} > 0$. Therefore, $\frac{\partial Rate_{lesions}}{\partial V_{Nbox}} > 0$. Microcompetition increases the rate of lesion formation. Moreover, the larger the number of viral N-boxes in the infected cells, the higher the rate of lesion formation.

25 In addition, CD18 is also a GABP stimulated gene (see above). Therefore, microcompetition between the GABP virus and CD18 gene results in reduced expression

of the cellular gene. According to Randolph, *et al.*, (1996), the role of CD18 is to accelerate the initial kinetics of reverse transmigration (see above). A decrease in CD18 expression might further reduce foam cell velocity, increasing the probability of being trapped in the subendothelial space. Microcompetition therefore has a double impact on reverse transmigration.

5 D. Atherosclerosis-intimal thickening

A second major class of atherosclerotic lesions is pathological intimal thickening. Intimal thickening consists mainly of smooth muscle cells in a proteoglycan-rich matrix. Pathological intimal thickening should be considered as a class independent of fibrous cap 10 atheroma since the majority of lesion erosion occurs over areas of intimal thickening with minimal or no evidence of a lipid core (Virmani 2000³³³). Smooth muscle cell (SMC) proliferation, which results in neointima formation and intimal thickening, accounts for a significant rate of restenosis after percutaneous transluminal coronary angioplasty, a widespread treatment for coronary artery disease. The following sections identify the 15 cause of SMC proliferation, neointima formation and intimal thickening in atherosclerosis.

1. Microcompetition reduces Rb transcription in SMC

SMCs are permissive to HCMV (Zhou 1996³³⁴) and HSV (Benditt 1983³³⁵). Rb is a GABP stimulated gene. Microcompetition with viral DNA decreases Rb transcription in SMCs (see the section on cancer).

20 2. Reduced Rb expression in atherosclerotic plaque

Rb mRNA is reduced in atherosclerotic plaque. Consider the following study.

Rabbits were fed a high cholesterol diet for six months. The results showed that the atherosclerotic plaques, covering 91% of the intimal aortic surface of aorta thoracalis, contained less Rb mRNA ($P < 0.05$) compared to normal aortic arteries (Wang 1996³³⁶). 25 Based on this result, Wang, *et al.*, suggested that "the abnormal expression of ... Rb antioncogene may play an important role in arterial SMC proliferation and pathogenesis of atherosclerosis."

3. Increased pRb expression reduces neointima formation

Rb is important in SMC arrest and differentiation. Increased Rb transcription (Claudio 1999³³⁷, Schwartz 1999³³⁸, Smith 1997³³⁹), or reduced pRb phosphorylation (Gallo 1999³⁴⁰), decreased SMC proliferation and neointima formation. Since 5 microcompetition reduces Rb transcription, an infection with a GABP virus result in SMC proliferation, neointima formation and pathological intimal thickening.

E. Thrombosis

Plaque rupture may lead to in situ formation of a thrombus. The rupture exposes the TF excessively expressed on surface of foam cells. The exposed TF triggers the 10 coagulation event.

F. Viruses in atherosclerosis

The idea of infection as a risk factor for atherosclerosis and related cardiovascular diseases is more than 100 years old. However, it was not until the 1970s that experimental data was published supporting the role of viruses in atherosclerosis. The mounting 15 evidence linking infectious agents and atherosclerosis prompted the scientific community to organize the International Symposium of Infection and Atherosclerosis, held in Annecy, France, December 6-9, 1998. The main objective of the symposium was to evaluate the role of infection in the induction/promotion of atherosclerosis on the basis of evidence from recent data on pathogenesis, epidemiologic and experimental studies, to define 20 prevention strategies and promote further research. Consider the following studies presented at the symposium. The studies were published in a special issue of the *American Heart Journal* (see *American Heart Journal*, November 1999).

Chiu presented a study which found positive immunostainings for C pneumoniae (63.6%), cytomegalovirus (CMV) (42%), herpes simplex virus-1 (HSV-1) (9%), P 25 gingivalis (42%), and S sanguis (12%) in carotid plaques. The study found 1 to 4 organisms in the same specimen (30%, 24%, 21%, and 6%, respectively) and the micro-organisms were immunolocalized mostly in macrophages (Chiu 1999³⁴¹).

In a critical review of the epidemiologic evidence, Nieto suggested that "most epidemiologic studies to date (Nieto 1999³⁴², Table I and II) have used serum antibodies as

surrogate indicators of chronic viral infection. However, there is evidence suggesting that serum antibodies may not be a valid or reliable indicator of chronic or latent infections by certain viruses. In a pathological study of patients undergoing vascular surgery for atherosclerosis serology, for example, for the presence of serum cytomegalovirus antibodies was not related to the presence of cytomegalovirus DNA in atheroma specimens." However, according to Nieto, four studies, Adam, *et al.*, (1987³⁴³), Li, *et al.*, (1996³⁴⁴), Liuzzo, *et al.*, (1997³⁴⁵) and Blum, *et al.*, (1998³⁴⁶) showed strong positive associations between CMV infection and clinical atherosclerosis. A strong association was also found in a 1974 survey of the participants in the Atherosclerosis Risk in 5 Communities (ARIC) study between levels of cytomegalovirus antibodies and the presence of subclinical atherosclerosis, namely carotid intimal-medial thickness measured by B-mode ultrasound (Nieto 1999³⁴⁷).

Nieto also reported results of a prospective study of clinical incident coronary heart disease (CHD). The study was a nested case-control study from the Cardiovascular Health 10 Study (CHS) conducted in an elderly cohort. Preliminary results from this study found no association between cytomegalovirus antibodies at baseline and incident CHD over a 5 year period. However, HSV-1 was strongly associated with incident CHD, particularly among smokers (odds ratio [OR] 4.2). It should be noted that a more recent prospective study of CMV, HSV-1 in CHD found that participants in the Atherosclerosis Risk in 15 Communities Study (ARIC) study with highest CMV antibody levels at base line (approximately in the upper 20%) showed increased relative risk (RR, 1.76, 95% confidence interval, 1.00-3.11) of CHD incidence over a 5 year period, adjusted for age, sex and race. After adjustment for additional covariates of hypertension, diabetes, years of education, cigarette smoking, low-density lipoprotein and high-density lipoprotein 20 cholesterol levels, and fibrinogen level, the RR increased slightly. (The study found no association between CHD and the highest HSV-1 antibody levels (adjusted RR, 0.77; 95% confidence interval, 0.36-1.62) (Sorlie 2000³⁴⁸)).

Nieto (1999) also mentioned some recent studies which documented increased risk 25 of restenosis after angioplasty in patients with serologic evidence of cytomegalovirus infection. For instance, Nieto reported a study by Zhou and colleagues which included 75 consecutive patients undergoing directional coronary atherectomy for symptomatic

coronary artery disease. Six months after atherectomy, the cytomegalovirus-seropositive patients showed significantly greater reduction in luminal diameter and significantly higher rate of restenosis compared to controls (43% vs 8% OR 8.7). These results were independent of known cardiovascular disease (CVD) risk factors.

5 Finally, Nieto mentioned that cytomegalovirus infection has been associated with another form of atherosclerotic disease: accelerated atherosclerosis in the coronaries after heart transplantation. In the first study showing this association, cytomegalovirus serology after transplantation seemed to be one of the most significant predictors of graft atherosclerosis and survival in general. This difference was independent of serologic 10 status before transplantation and the presence of symptomatic infection. Similar results have been replicated in subsequent studies.

Based on these studies Nieto concludes that "despite its limitations, the epidemiologic evidence reviewed above is consistent with a broad range of experimental and laboratory evidence linking viral (and other) infections and atherosclerosis disease."

15 In a review of animal studies, Fabricant, *et al.*, (1999³⁴⁹) described their experiments with Marek's disease herpesvirus (MDV). The initial experiment used 4 groups of specific pathogen-free (SPF) white leghorn chickens, P-line cockerels of the same hatch, genetically selected for susceptibility to MDV infection. Groups 1 and 2 were inoculated intratracheally at 2 days of age with 100 plaque forming units of clone-purified, 20 cell free, CU-2 strain of low-virulence MDV. Groups 3 and 4 were controls. For the first 15 weeks, all birds in the 4 groups were fed the same commercial low cholesterol diet (LCD). Beginning with the 16th and ending with the 30th week, MDV-infected group 2 and uninfected group 4 were placed on a high cholesterol diet (HCD). The other two groups remained on LCD. Atherosclerotic lesions visible at gross inspection were only 25 observed in MDV-infected birds of groups 1 (LCD) and 2 (HCD). These arterial lesions were found in coronary arteries, aortas, and major arterial branches. In some instances, the marked atherosclerotic changes involved entire segments of the major arteries practically occluding the arterial lumen. Other arterial lesions visible at gross inspection were observed as discrete plaques of 1 to 2 mm. These arterial lesions were not found in 30 any of the uninfected birds of group 3 (LCD) or the uninfected hypercholesterolemic birds

of group 4. Many proliferative arterial lesions with intimal and medial foam cells, cholesterol clefts, and extracellular lipid and calcium deposits had marked resemblance to chronic human atherosclerotic lesions. Moreover, immunization against MDV prevented the MDV-induced atherosclerotic lesions.

5 The main conclusion of the symposium was that “although studies are accumulating that indicate a possible relation between infection and atherosclerosis, none of them has yet provided definite evidence of a causal relationship. ... Moreover, the demonstration of a causative role of infectious agents in atherosclerosis would have an enormous impact on public health” (Dodet 1999³⁵⁰) (A similar view is expressed in a
10 review published recently, see Fong 2000³⁵¹).

What is “definitive evidence?” What evidence will convince Dodet, and others, that viruses are not merely associated with atherosclerosis but actually cause the disease?

15 The research on viruses in cancer provides an answer. According to zur Hausen (1999³⁵²) “The mere presence of viral DNA within a human tumor represents a hint but clearly not proof for an aetiological relationship. The same accounts for seroepidemiological studies revealing elevated antibody titres against the respective infection.” What constitutes proof is evidence that meets the following four criteria, especially the fourth one. According to zur Hausen “the fourth point could be taken as the most stringent criterion to pinpoint a causal role of an infection.”

Table 1: zur Hausen’s criteria for defining a causal role for an infection in cancer

1. Epidemiological plausibility and evidence that a virus infection represents a risk factor for the development of a specific tumor.
2. Regular presence and persistence of the nucleic acid of the respective agent in cells of the specific tumor.
3. Stimulation of cell proliferation upon transfection of the respective genome or parts therefrom in corresponding tissue culture cells.
4. Demonstration that the induction of proliferation and the malignant phenotype of specific tumor cells depends on functions exerted by the persisting nucleic acid of the respective agent.

The fourth point requires an understanding of the "mechanisms of virus mediated cell transformation." Crawford (1986³⁵³) and Butel (2000³⁵⁴) also emphasize the significance of understanding the mechanism in attributing a causal role to infection. According to Crawford: "one alternative approach to understanding the role of the papillomaviruses in cervical carcinoma is to identify the mechanisms by which this group of viruses may induce the malignant transformation of normal cells." According to Butel: "molecular studies detected viral markers in tumors, but the mechanism of HBV involvement in liver carcinogenesis remains the subject of investigation today." When the other kind of evidence is in place, understanding the mechanism turns a mere association into a causal relation.

The discovery of microcompetition and its effect on macrophage propulsion and SMC replication provides the mechanism that produces atherosclerosis. This discovery supplies the missing "definitive evidence" for a causal relationship between viruses and atherosclerosis.

15 G. Metastasis

1. Increased TF expression promotes metastasis

The expression of TF is increased in various metastatic tumors such as non-small-cell lung cancers (Sawada 1999³⁵⁵), colorectal cancer (Shigemori 1998³⁵⁶), melanoma (Meuller 1992³⁵⁷), prostate cancer (Adamson 1993³⁵⁸), colorectal carcinoma cell lines and metastatic sublines to the liver (Kataoka 1997³⁵⁹), breast cancer (Sturm 1992³⁶⁰), and in a variety of cancer cell lines (Hu 1994³⁶¹). Moreover, TF expression directly correlates with tumor aggressiveness (see above studies and following reviews, Ruf 2000³⁶², Schwartz 1998³⁶³).

In an intervention study which generated two matched sets of cloned human melanoma lines, one expressing a high level and the other a low level of normal human TF molecule, by retroviral-mediated transfections of a nonmetastatic parental line. The tumor cells were injected into the tail vein of severe combined immunodeficiency (SCID) mice. The results showed that metastatic tumors in 86% of the mice injected with the high-TF lines and in 5% of the mice injected with the low-TF lines (Bromberg 1995³⁶⁴). Based on

these results, Bromberg, *et al.*, concluded that "high TF level promotes metastasis of human melanoma in the SCID mouse model."

2. Microcompetition increases TF transcription, and therefore, metastasis

TF is a GABP suppressed gene. Microcompetition increases TF transcription (see 5 above). Therefore, an infection with a GABP virus promotes metastasis.

3. Osteoarthritis

H. Mutation studies

1. Collagen type I α 2 chain (COL1A2)

a) *COL1A2 is a microcompetition-repressed gene*

10 See above (the study with viral plasmid).

Moreover, the COL1A2 is ERK responsive. ERK stimulates COL1A2 transcription. One study examined the influence of hypergravity on collagen synthesis in human osteoblast-like cells (hOB), as well as the involvement of the MAP kinase 15 signaling cascade. They found that hypergravity led to significantly increased phosphorylation of ERK 1/2. When the MAPK kinase pathway was inhibited by PD98059, hypergravity-induced stimulation of both collagen synthesis as well as COL1A2 mRNA expression decreased by about 50% (Gebken 1999³⁶⁵).

2. COL1A2 deficiency

a) *COL1A2 causes EDS*

20 A latent infection by a GABP virus results in microcompetition between viral DNA and the COL1A2 gene which decreases the expression of the cellular gene (see above). A heterozygous mutation of the COL1A2 gene causes the Ehlers-Danlos syndrome type-VII. EDS patients suffer from COL1A2 protein deficiency. Therefore, 25 research on EDS type-VII can be used to gain insights on the effects of a GABP viral infection on animal and human health.

(1) EDS is associated with hypermobility of certain joints

5 The COL1A2 deficiency in EDS type-VII causes hypermobility of joints (Byers 1997³⁶⁶, Giunta 1999³⁶⁷). A hypermobile joint is defined as a joint whose range of movement exceeds the norm for that individual, taking into consideration age, sex, and ethnic background. The primary cause of hypermobility is ligamentous laxity, which is determined by each person's fibrous protein genes (Grahame 1999³⁶⁸).

10 A high concentration of collagen type I, 55-65% of dry weight, is found in the matrix components of interarticular fibrocartilages (menisci) tissues. Meniscus tissues are found in the temporomandibular, sternoclavicular, acromiocalvicular, wrist and knee joints. High concentration of collagen type I is also found in connecting fibrocartilages, such as vertebrae discs. As a result of COL1A2 deficiency, these joints show a higher degree of hypermobility compared to other joints. We call the temporomandibular, sternoclavicular, acromiocalvicular, wrist, knee and lumber joints the "Vulnerable Joints."

15 (2) Hypermobility in obesity

A latent infection by a GABP virus results in microcompetition between viral DNA and the COL1A2 gene which decreases the expression of COL1A2. A COL1A2 deficiency causes hypermobility in vulnerable joints, specifically, in the lumbar joints. A 20 infection also results in decreased expression of the hMT-II_A gene and obesity (see above). Therefore, obese people should show hypermobility in their lumbar joints.

A modified Schober test was used to examine lumbar mobility. To perform the test, the subjects were first asked to stand erect. While erect, three marks were placed on the subject's skin overlaying the lumbosacral spine. The first mark was placed at the lumbosacral junction, the second mark was placed 5 cm below the first, and the third 25 mark was placed 10 cm above the junction. The subject was then asked to bend forward as far as possible, as though to touch the toes. The new distance between the second and third mark was measured. Lumbar mobility is defined as the difference between this measurement and the initial distance of 15 cm. The study group included 2,350 men and 670 women between the ages of 21 and 67 years.

Obesity (defined as weight/height) markedly affected the flexibility measurements. For every increase in obesity by one standard deviation, an increase of 0.4 cm was measured in the modified Schober measurement. The results showed that younger subjects are more mobile in their lumbar joints. Female subjects in their 20's showed an increase of 0.42 cm in the modified Schober measurement compared to female in their 60's. Men showed a 1.04 cm increase over the same age difference. The increased flexibility demonstrated by the most obese subjects (top 16%, or 1 SD of weight/height subjects) is equal to the increase in flexibility associated with 40 year age difference in female (0.4 cm compared to 0.42 cm), and is almost half the increase associated with that age difference in men (0.4 cm compared to 1.04 cm) (Batti'e 1987³⁶⁹).

(3) Hypermobility causes osteoarthritis

15 A study with EDS patients found that 16 out of 22 over the age of 40 have osteoarthritis of one or more joints (referenced in Grahame 1989³⁷⁰). In the general population, evidence is more circumstantial. However, the Leeds groups produced evidence of a likely association between joint laxity and osteoarthritis (OA). The study compared 50 women with symptomatic OA to age matched controls. The study found a direct correlation between developing OA and the degree of hypermobility (Scoott 1979³⁷¹).

20 The association between hypermobility and osteoarthritis was studied in specific joints. Sharma, *et al.*, (1999³⁷²) report that laxity is greater in the unininvolved knees of OA patients compared to knees of older controls. The authors concluded that at least some of the increased laxity of OA may predate the disease. Jonsson, *et al.*, (1996³⁷³) compared 50 female patients with clinical thumb base (first carpometacarpal joint) OA to 25 age matched controls. The results showed that hypermobility features were much more prevalent in the 50 patients compared to controls. The authors also report another study with 100 patients (including both males and females) that found a direct correlation between hypermobility and clinical severity of thumb base OA. They concluded that a causal relationship exists between articular hypermobility and thumb base OA.

(4) Osteoarthritis in obesity

Microcompetition causes hypermobility which causes osteoarthritis in vulnerable joints. Microcompetition also causes obesity. Therefore, obese people should show osteoarthritis in vulnerable joints.

A study compared the OA disease traits in different joints of female twins aged 5 48-70. The results showed that, in twins, an increase in the body weight increased the likelihood of developing osteoarthritis in the knee in both the tibiofemoral joint (TFJ) and patellofemoral joint (PFJ) and in the hand in the first carpometacarpal joint (CMC I). Specifically, after adjustment for other potential risk factors, for every 1 kg increase in body weight a twin had a 14% increased risk of developing TFJ osteophytes, a 32% 10 increased risk of developing PFJ osteophytes, and a 10% increased risk of developing CMC osteophytes compared to their co-twin. Moreover, the weight difference was also observed in asymptomatic woman, which indicates that weight gain predates OA and, therefore, is not a result of OA (Cicuttini 1996³⁷⁴).

Note that this twin study demonstrates an association between obesity and OA 15 independent of genetic factors, and is, therefore, inconsistent with the genetic mutation explanation of obesity (see above).

A longitudinal study began in 1962 with baseline examinations of clinical, biochemical, and radiologic characteristics. In 1985 follow-up examination characterized 20 osteoarthritis in 1,276 participants, 588 males and 688 females, ages 50-74. Baseline obesity was measured by an index of relative weight. The results showed that the likelihood of developing osteoarthritis of the hand over the 23 year period increased with an increase in the index measuring baseline relative weight. Higher baseline relative weight was also associated with greater subsequent severity of the disease. Moreover, during the 23 year period, most subjects gained weight. However, after adjustment for 25 baseline weight, the increase in body weight was not associated with either the likelihood of developing osteoarthritis of the hand or the severity of the disease, which indicates that OA is not a result of weight gain (Carman 1994³⁷⁵).

In obesity some joints seem to be susceptible to osteoarthritis while others are 30 protected. The knees and the thumb base, for instance, are often damaged while the hips are disease free. Since both are weight bearing joints, the difference in susceptibility to

osteoarthritis indicates a cause other than mechanical wear-and-tear. The pattern of OA in obesity also does not correspond to a general metabolic cause for the disease. A metabolically induced deterioration of cartilage should result in small differences in the severity of OA between joints, unlike the differences observed in joints of obese people. 5 van Sasse, *et al.*, call the pattern of OA in obesity "strange," and claims that "whatever the final explanation for the etiology of OA, we believe that it will have to take into account the strange pattern of the association between OA and obesity" (van Saase 1988³⁷⁶).

These studies suggest three insights. First, obesity is associated with 10 osteoarthritis in only specific joints - van Saase's "strange" list of susceptible joints. Second, obesity and osteoarthritis do not a result from of each other. Third, the association between obesity and osteoarthritis is independent of genetic factors. Obesity and OA resulting from microcompetition between viral and cellular DNA is consistent with all three insights. First, van Saase's "strange" list of susceptible joints coincides 15 with the list of vulnerable joints. Second, both obesity and OA result from microcompetition and not from each other. Last, microcompetition results from a viral infection and not from a genetic mutation.

b) *Collagen type I α 2 chain (COL1A2), obesity and obstructive sleep apnea (OSA)*

20 Obesity is associated with hypermobility of vulnerable joints. The temporomandibular joint belongs to the list of vulnerable joints. Therefore, in obesity the temporomandibular joint is hypermobile.

The mandible and tongue protrusion of obese patients was compared to controls. The subject was asked to protrude the mandible or tongue as far forward as possible 25 (MAX), and 50% was measured as the midpoint between maximum protrusion and the position were the tongue tip is resting between the incisors (50%). The difference between resting position R and MAX and between R and 50%, is denoted R-MAX and R-50%, respectively. The results showed that obese subjects differed from controls in the degree of change in cross-sectional area (CSA) in the oropharynx. The 50% mandibular protrusion (R-50%) and the maximum tongue protrusion (R-MAX) produced greater 30

relative increases in oropharyngeal cross-sectional area in obese subjects compared to controls (Ferguson 1997³⁷⁷). Increased oropharyngeal cross-sectional area indicates an increased capacity for mandibular protrusion. Such increased capacity indicates hypermobility of the temporomandibular joint.

5 During sleep, the tonic activity of the masseter decreases. In a supine position the mandible drops and the mouth opens. A hypermobile temporomandibular joint lets the mandibular drop further and the mouth open wider than a normal joint.

10 A study compared the time spent with mandibular opening in OSA patients and healthy controls. In controls, 88.9% of total sleep time was spent with narrow mandibular opening (less than 5 mm). In contrast, in OSA patients, 69.3% of the total sleep time was spent with wide mandibular opening (more than 5 mm). Moreover, in healthy adults, there was no difference in mandibular posture between the supine and lateral recumbent positions, while in OSA patients, sleep stage affects the mandibular opening during sleep in the supine position only (Miyamoto 1999³⁷⁸).

15 The abnormal low position of the hypermobile mandibular causes the upper airway disturbances during sleep. Therefore, hypermobility of the temporomandibular joint causes OSA.

Without reference to hypermobility of the temporomandibular joint, Miyamoto, *et al.*, (1999) proposes a similar description of the events leading to apnoeic episodes.

20 Microcompetition causes obesity. Microcompetition also causes hypermobility of the temporomandibular joint which causes OSA. Therefore, obesity is associated with OSA (note that the OSA patients in Ferguson, *et al.*, (1997³⁷⁹) and Miyamoto, *et al.*, (1999) studies above are obese).

I. Obesity

1. Background

2. The obesity epidemic

5 "The prevalence of obesity (defined as body mass index $\geq 30 \text{ kg/m}^2$) increased from 12.0% in 1991 to 17.9% in 1998. A steady increase was observed in all states; in both sexes; across age groups, races, education levels; and occurred regardless of smoking status" (Mokdad 1999³⁸⁰).

3. Three proposed causes for the epidemic

10 As proposed throughout the scientific community, the three "classical" causes of the obesity epidemic are increased energy intake, reduced energy expenditure, and genetic mutation.

a) *Increased energy intake ("too much food")*

15 Many large scale studies refute the idea that increased energy intake is the cause of obesity. The USDA Nationwide Food Consumption Survey 1977-1988 collected data from over 10,000 individuals. The analysis found that the average fat intake in the United States decreased from 41% to 37% of calorie intake between 1977 and 1988 and the average total energy intake decreased, by 3% in women and by 6% in men. "The reductions in average fat and energy intake were associated with a progressive increase in the prevalence of obesity in the US adult population" (Weinsier 1998³⁸¹).

20 An even larger study reported similar results based on pooled data from NHANES II and III, USDA Nationwide Food Consumption Survey, Behavioral Risk Factor Survey System, and Calorie Control Council Report (Heini 1997³⁸²). "In the adult US population the prevalence of overweight rose from 25.4% from 1976 to 1980 to 33.3% from 1988 to 1991, a 31% increase. During the same period, average fat intake, adjusted for total 25 calories, dropped from 41.0% to 36.6%, an 11% decrease. Average total daily calorie intake also tended to decrease, from 1,854 kcal to 1,785 kcal (-4%). Men and women had similar trends. Concurrently, there was a dramatic rise in the percentage of the US

5 population consuming low-calorie products, from 19% of the population in 1978 to 76% in 1991" (Ibid). The authors conclude that "reduced fat and calorie intake and frequent use of low-calorie food products have been associated with a paradoxical increase in the prevalence of obesity" (Ibid). Similar surveys conducted in Great Britain corroborate these studies.

b) Reduced energy expenditure ("too little exercise")

10 Many have turned their attention to reduced physical activity as an alternative explanation for the obesity epidemic. "The only available explanation for the paradoxical increase in body weight with a decrease in fat and energy intake is that physical activity declined" (Ibid). The data disprove this explanation as well.

15 In recent years several population surveys have shown unchanging levels of physical activity among Americans. For example, in the Behavioral Risk Factor Survey which included 30,000 to 80,000 individuals annually, the prevalence of obesity increased from 12% to 17.9% between 1991 and 1998 but physical inactivity did not change substantially (Ibid).

c) Genetic mutation

20 "The fact that the increased rates of obesity have been observed within the last two decades has been viewed as evidence that genetic factors cannot be held responsible. Indeed, systematic changes of the population-based frequencies of specific alleles predisposing to obesity cannot possibly have occurred within this short time span." (Hebebrand 2000³⁸³) A significant change in the human gene pool requires many generations. A genetic mutation explanation for the increase in obesity implies that the human gene pool has changed over a single generation. "Although research advances have highlighted the importance of molecular genetic factors in determining individual 25 susceptibility to obesity, the landmark discoveries of leptin, uncoupling proteins and neuropeptides involved in body weight regulation, cannot explain the obesity epidemic" (Hill 1998³⁸⁴). "Genes related to obesity are clearly not responsible for the epidemic of obesity because the gene pool in the United States did not change significantly between 1980 and 1994" (Koplan 1999³⁸⁵).

4. Knockout studies

a) *Human metallothionein-II_A (hMT-II_A)*(1) hMT-II_A is a microcompetition-suppressed gene

5 A latent infection by a GABP virus results in microcompetition between the viral DNA and the hMT-II_A gene which decreases the expression of the cellular gene (see above). A disruption of the metallothionein gene in transgenic mice also reduces the expression of the cellular gene. Therefore, research with MT-null mice can produce insights on the effects of a GABP viral infection on animal and human health.

(2) MT-I and MT-II null mice are obese

10 Mice with disrupted MT-I and MT-II genes are apparently phenotypically normal. The disruption shows no adverse effect on the ability to reproduce and rear offspring. However, after weaning, MT-null mice consume more food and gain more weight at a more rapid rate than control mice. The majority of the adult male mice in the MT-null colony show moderate obesity (Beattie 1998³⁸⁶).

15 b) *Integrin (β₂ leukocyte, CD18)*

Notations and terminology:

β₂ = CD18

α_L = CD11a (L for Leukocytes) expressed in all leukocytes

20 α_M = CD11b (M for Monocytes/Macrophage) expressed in monocytes/ macrophages, granulocytes, natural killer cells, a sub population of T cells

LFA-1 = Lymphocyte-Function-associated Antigens 1

MAC-1 = Macrophage 1

CR3 = Complement Receptor type 3

α_Lβ₂ = CD11a/CD18 = LFA-1 (LFA-1 binds ICAM-1 and ICAM-2)

$\alpha_M\beta_2$ = CD11b/CD18 = MAC-1 = CR3 = Mo-1 (MAC-1 binds ICAM-1, C3b, fibrinogen and factor X)

(1) CD18 is a microcompetition-suppressed gene

CD18 is a leukocyte-specific adhesion molecule. GABP binds three N-boxes in the CD18 promoter and transactivates the gene (Rosmarin 1995³⁸⁷, Rosmarin 1998³⁸⁸). Since CD18 is a GABP stimulated gene, latent infection by a GABP virus results in microcompetition between the viral DNA and the CD18 promoter thereby decreasing the expression of CD18 (see Le Naour 1997³⁸⁹, Tanaka 1995³⁹⁰, Patarroyo 1988³⁹¹ above). Moreover, the higher the concentration of viral DNA, the greater the decrease in CD18 expression.

(2) ICAM-1 or MAC-1 null mice are obese

CD18 participates in forming the CD11a/CD18 molecule which binds ICAM-1. ICAM-1 null mice (ICAM-1 --/--) gain more weight than control mice after 16 weeks of age, and eventually became obese despite no obvious increase in food intake. Under a high fat diet, ICAM-1 --/-- mice show an increased susceptibility to obesity. CD18 also participates in forming the CD11b/CD18 molecule which binds MAC-1. MAC-1 null mice (MAC-1 --/--) are also susceptible to diet-induced obesity and exhibited a strong similarity in weight gain with sex-matched ICAM-1 --/-- mice (Dong 1997³⁹²).

5. Pathogenesis

20 6. Hormone sensitive lipase (HSL) gene

a) *HSL is a microcompetition-suppressed gene*

See above.

b) *Reduced HSL mRNA in obesity*

25 HSL mRNA, protein expression, and enzyme activity were measured in abdominal subcutaneous adipocytes from 34 obese drug-free and otherwise healthy males and females and 14 non-obese control subjects. The results showed reduced HSL mRNA,

protein expression and enzyme activity (Large 1999³⁹³, Table 3). The findings were age and gender independent. Based on these results Large, *et al.*, conclude that "a decreased synthesis of the HSL protein at the transcriptional level is a likely factor behind the findings of decreased HSL expression in adipocytes from obese subjects. ... Decreased 5 HSL expression may at least in part explain the well-documented resistance to the lipolytic effect of catecholamines in obesity."

In line with these results, a subsequent study by the same laboratory showed a 73% reduction in HSL protein levels in obesity (Elizalde 2000³⁹⁴, Fig 4C and Table 1).

c) *Catecholamines resistance in obesity*

10 (1) *HSL regulation*

Catecholamines bind β_1 -, β_2 - and β_3 -adrenergic receptors (β_1 AR, β_2 AR and β_3 AR, respectively) and α_2 adrenergic receptors (α_2 AR).

(a) *Transcription*

Activation of β_2 AR (Maudsley 2000³⁹⁵, Pierce 2000³⁹⁶, Elorza 2000³⁹⁷, Luttrell 15 1999³⁹⁸, Daaka 1998³⁹⁹) or β_3 AR (Cao 2000⁴⁰⁰, Gerhardt 1999⁴⁰¹, Soeder 1999⁴⁰²) activates ERK which phosphorylates GABP which in turn binds p300, resulting in increased HSL transcription.

(b) *Post-translation*

Activation of β_1 AR, β_2 AR, β_3 AR activates a cAMP dependent protein kinase A. 20 The protein kinase phosphorylates HSL, resulting in increased hydrolytic activity against triacylglycerol and cholestryl ester substrates. Insulin deactivates HSL via protein phosphatases or inhibition of protein kinase.

(2) *Reduced response to stimulation*

(a) *Hypothesis*

25 Microcompetition reduces HSL expression. Since HSL is rate limiting in triacylglycerol and diacylglycerol hydrolysis, microcompetition reduces steady state lipolysis. Moreover, as ERK agents, β_2 AR and β_3 AR agonists, specifically

catecholamines, stimulate HSL transcription. Microcompetition also lessens the increase in HSL transcription, resulting in impaired stimulated lipolysis. Consider figure 24.

At steady state, microcompetition reduces lipolysis per adipocyte.

Microcompetition also reduces the slope of the lipolysis line. That is, with increased 5 stimulation, the relative lipolysis deficiency (the vertical difference between the two lines) increases.

A number of *in vivo* and *in vitro* studies demonstrated the reduced ability of catecholamines to stimulate lipid mobilization from subcutaneous adipose tissue.

(b) *In vitro* studies

10 Hellstrom, *et al.*, (1996)⁴⁰³ treated abdominal subcutaneous adipocytes from 13 non-obese subjects with at least one first-degree relative with body mass index of 27 kg/m² or more (Hob) and 14 controls (Hnorm) with norepinephrine, a major endogenous lipolytic agent, isoprenaline, a non-selective beta-adrenoceptor agonist, forskolin, a direct activator of adenylyl cyclase, and dibutyryl cyclic AMP, an activator of protein kinase and thereby HSL. Figures 25, 26, 27 and 28 represent the effect of these treatments on the 15 glycerol release (pmol•cell•2h⁻¹) from adipocytes.

The average rate of lipolysis induced by all four treatments was reduced by about 50% (p from 0.001 to 0.01) in subjects with a family trait of obesity compared to controls.

20 Isoprenaline (Shimizu 1997⁴⁰⁴), dibutyryl cAMP (Shimizu 1997) and forskolin (Yarwood 1996⁴⁰⁵) activated ERK in adipocytes. Isoprenaline also activated ERK in CHO/K1 cells expressing the human β_3 AR (Gerhardt 1999⁴⁰⁶). As ERK agents the agonists phosphorylate GABP. Microcompetition in obese adipocytes reduces the maximum number of GABP molecules available for HSL promoter binding. Hence, the observed resistance for these agonists stimulation. Moreover, as expected, an increase in 25 the agonist concentration increased the relative lipolysis deficiency.

Hellstrom, *et al.*, (1996) also measured the HSL maximum activity and HSL mRNA at steady state. The maximum activity was reduced 50% in Hob (p < 0.05).

mRNA (amol HSL/µg total nucleic acids) was reduced by 20% ($p > 0.05$, not significant). The study did not measure HSL mRNA after stimulation.

5 The following studies use the concept of maximum adipocyte lipolysis capacity in response to stimulation by various agonists by comparing glycerol release in adipocytes from obese male and female to controls. In all studies the adipocyte incubation in the presence of the agonist lasted 2 h.

10 Large, *et al.*, (1999⁴⁰⁷) treated abdominal subcutaneous adipocytes from 34 obese drug-free and otherwise healthy males or females and 14 non-obese controls, with isoprenaline, a non-selective β -adrenergic receptor agonist, or dibutyryl cAMP, a phosphodiesterase resistant cAMP analogue. The results showed reduced maximum values for isoprenaline- and dibutyryl cAMP induced glycerol release by 40-50% in the obese group, when expressed per g lipid.

15 Hellstrom, *et al.*, (2000⁴⁰⁸) treated abdominal subcutaneous adipocytes from 60 obese and 67 non obese subjects, age 19-60 y, with isoprenaline, dibutyryl cyclic AMP, and forskolin, an activator of adenylyl cyclase. The results showed reduced maximum values for isoprenaline-, dibutyryl cAMP-, and forskolin induced glycerol release by 50% in the obese group. Moreover, 42 of the 67 lean subjects had at least one obese member among first degree relatives, but not all family members, and not both parents. The non-obese subject with the family trait for obesity showed a similar reduction in maximum 20 glycerol release compared to lean subjects without the family trait.

(c) *In vivo* studies

25 Consider Bougneres 1997⁴⁰⁹. To study the effect of epinephrine on lipolysis in obesity, epinephrine was infused stepwise at fixed doses of 0.75 and then 1.50 µg/min to 9 obese children (160 \pm 5% ideal body weight) aged 12.1 \pm 0.1 yr during the dynamic phase of fat deposition, and in 6 age-matched non-obese children. As an *in vivo* lipolysis index, the study used glycerol flux. In the basal state, obese children had a 30% lower rate of glycerol release per unit fat mass than lean children. Figure 29 represents the measured relationship between epinephrine infusion and glycerol release.

Consider Horowitz (2000⁴¹⁰). Lipolytic sensitivity to epinephrine was measured in 8 lean [body mass index (BMI): $21 \pm 1 \text{ kg/m}^2$] and 10 upper body obese (UBO) women (BMI: $38 \pm 1 \text{ kg/m}^2$; waist circumference $>100 \text{ cm}$). All subjects underwent a four-stage epinephrine infusion (0.00125, 0.005, 0.0125, and 0.025 microgram·kg fat-free mass⁻¹·min⁻¹) plus pancreatic hormonal clamp. Glycerol rates of appearance (R_a) in plasma were determined by stable isotope tracer methodology. Figure 30 represents the measured percent change in glycerol release as a function of plasma epinephrine concentration.

Figure 31 represents the same results in terms of total glycerol release per fat mass (FM).

Both the Bougneres (1997) and Horowitz (2000) results are consistent with microcompetition as the underlying cause of catecholamine resistance in obesity.

d) Adipocyte hypertrophy in obesity

HSL is a GABP gene. Microcompetition reduces HSL expression which results in adipocyte hypertrophy. Consider the following study.

HSL knockout mice were generated by homologous recombination in embryonic stem cells. Cholesterol ester hydrolase (NCEH) activities were completely absent from both brown adipose tissue (BAT) and white adipose tissue (WAT) in mice homozygous for the mutant HSL allele (HSL^{-/-}). The cytoplasmic area of BAT adipocytes was increased 5-fold in HSL^{-/-} mice (Osuga 2000⁴¹¹, Fig 3a). The median cytoplasmic areas in WAT was enlarged 2-fold (Ibid, Fig 3b). The HSL knockout mice showed adipocyte hypertrophy.

Obesity is characterized by adipocyte hypertrophy. Osuga (2000) results are consistent with microcompetition as the underlying cause of adipocyte hypertrophy in obesity.

It is interesting that body weight of the HSL^{-/-} mice was not different, at least until 24 weeks of age, from wild-type. The reason was probably lack of adipocyte hyperplasia in HSL^{-/-} mice. Consider the following section.

7. Retinoblastoma susceptible gene (Rb)

a) *Rb is a microcompetition-suppressed gene*

See above.

b) *Adipocyte hyperplasia in obesity*

5 Rb-null (pRb^{-/-}) preadipocytes show a higher proliferation rate compared to wild type. A study measured the percentage of pRb^{-/-} 3T3 cells in S phase following five different treatments, cells grown in DMEM (asynchronous cells, marked A), cells grown to confluence in DMEM containing 10% calf serum and then maintained for 6 days in the same mixture (marked C), confluent cells split into subconfluent conditions (marked CR),
10 confluent cells treated for 6 days with an adipocyte differentiating mixture (marked D), and differentiated cells split into subconfluent conditions (marked DR). The results are summarized in figure 32 (Classon 2000⁴¹², Fig 3A).

Asynchronous pRb^(-/-) cells show a tendency for excessive cell replication. Moreover, pRb^(-/-) differentiated cells show a higher probability for cell cycle re-entry. It
15 should be emphasized that although pRb seems to affect the establishment of a permanent exit from cell cycle, pRb is not absolutely required since expression of C/EBP α and PPAR γ bypasses the requirement for pRb and causes pRb^(-/-) cells to differentiate into adipocytes (Classon 2000, Fig 1B).

20 Transcription of the Rb gene increases with growth arrest and differentiation (see above). The relationship between pRb concentration and adipocyte differentiation was tested in a study that compared proliferative and differentiated brown (primary) and white (3T3-F442A) adipocytes in culture. The differentiation stage of the cells was determined following detection of lipid accumulation and expression of the specific differentiation markers aP2 and UCP-1. The results showed almost undetectable pRb levels in
25 proliferative undifferentiated cells. On the other hand, pRb was clearly detected in nuclei of differentiated primary brown adipocytes (Puigserver 1998⁴¹³, Fig. 2A) with lipid accumulation in their cytoplasm and UCP-1 expression (Ibid, Fig 3) and in 3T3-F442A cells with lipid accumulation and aP2 expression. Moreover, Puigserver, *et al.*, note that "the pRb levels measured by immunoblotting clearly increased during differentiation of

3T3 F442A cells (Ibid, Fig. 2B)" and that "there was an apparent positive correlation between pRb expression and lipid accumulation, since nuclei from cells with more lipid droplets in their cytoplasm were more strongly immunostained for pRb than those of cells with less lipid droplets (Ibid, Fig. 2A)."

5 Richon, *et al.*, (1992⁴¹⁴) proposed the following model for the relationship between Rb and growth arrest and differentiation (see also above). An inducer increases Rb transcription resulting in higher hypo- and total-pRb concentration. The increase in hypo-pRb prolongs G1. However, the initial increase in hypo-pRb is most likely not sufficient for permanent G1 arrest. Therefore, cells reenter cell cycle for a few more generations.

10 While cells continue to divide, the increased rate of transcription results in hypo-pRb accumulation. When a critical hypo-pRb concentration, or threshold, is reached, the cells irreversibly commit to terminal differentiation. This model describes the determination of the commitment to differentiate as a stochastic process with progressive increases in the probability of G1/G0 arrest and differentiation established through successive cell divisions.

15 Such a model would predict an increase in the number of cell cycle generations required for producing the threshold Rb concentration, under conditions of suppressed Rb transcription. Consider figure 33.

20 Microcompetition reduces Rb transcription. Therefore, the number of generations required to reach the required Rb concentration ($[Rb]_0$) under microcompetition (N_M) is greater than the number in controls (N_C). In obesity, therefore, one should observe excessive replication *in vitro* (Roncari 1986⁴¹⁵, Roncari 1981⁴¹⁶) and hyperplasia *in vivo*.

25 Returning to the non-obese HSL^{-/-} mice (Osuga 2000, see above). Both HSL and Rb are microcompetition-suppressed genes. Therefore, both genes show reduced expression in obesity, resulting in adipocyte hypertrophy and hyperplasia. Since Rb transcription is most likely independent of HSL expression, pRb in HSL^{-/-} mice is not under expressed and adipocytes in HSL^{-/-} mice are not hyperplastic.

8. Studies in signaling

9. Resistant ERK agents in obesity

The following are ERK agents showing cellular level or patient level resistance in obesity (for definition of cellular and patient level resistance and its relationship to 5 microcompetition, see above).

a) *Oxytocin*

The oxytocin receptor (OTR) is a GABP gene (see above). Stock, *et al.*, (1989⁴¹⁷) tested whether the plasma level of oxytocin was elevated in obese subjects and if so, whether it was affected by weight reduction following gastric banding. Plasma levels of 10 oxytocin were 4-fold higher in the obese subjects than in the control subjects. After the operation, oxytocin levels dropped dramatically, but were still markedly higher than control.

Moreover, obese pregnant women need more oxytocin stimulation of labor. Johnson, *et al.*, found that, compared to a control group matched for age and parity, there 15 was a significantly increased need for oxytocin stimulation of labor in obese patients weighing at least 113.6 kg (250 pounds) during pregnancy (Johnson 1987⁴¹⁸).

b) *Zinc and Copper*

Serum zinc, copper and magnesium levels were measured in healthy and obese children using atomic absorption spectrophotometry. Serum zinc and copper levels of 20 obese children (mean value 102.40 ± 2.78 micrograms/dL mean value 132.34 ± 1.79 micrograms/dL, respectively) were markedly higher than control (mean value 80.49 ± 2.98 micrograms/dL, and mean value 107.58 ± 1.62 micrograms/dL, respectively). Serum copper concentrations were also significantly higher in obese children compared to healthy controls (Yakinci 1997⁴¹⁹).

25 Serum zinc and copper levels were also determined in 140 diabetic patients and 162 healthy controls. A sub group of patients were classified as overweight (greater than 15% relative body weight). Obese patients showed a statistically significant increase in

zinc levels while the copper level positively correlated with the zinc level (D'Ocon 1987⁴²⁰).

5 Taneja, *et al.*, (1996⁴²¹) measured the concentration of zinc in hair of obese men and women. The results showed a positive linear correlation between body weight, or body weight/height ratio, and hair zinc concentration. The correlation was stronger in men.

The following hormones and cytokines, which are all GABP kinase agents, also show resistance in obesity.

c) *Insulin*

10 Patients with non-insulin-dependent diabetes mellitus (NIDDM) and/or obesity generally suffer from insulin resistance (IR). Interestingly, most NIDDM patients are obese. Ludvik, *et al.*, studied the effect of obesity and NIDDM on insulin resistance. Both lean NIDDM subjects and obese normal subjects were significantly insulin resistant compared to lean normal subjects (Ludvik 1995⁴²²).

15 Another study observed kinetic defects in insulin action in insulin resistant nondiabetic obese subjects. Insulin-stimulated glucose disposal was slower to activate and more rapidly deactivated in obese than in normal subjects. Oral glucose tolerance tests (OGTTs) were done in five controls and five obese subjects. While each of the control subjects had normal glucose tolerance, only two obese subjects tested normal for glucose tolerance. The remaining three obese subjects had impaired glucose tolerance. 20 During the OGTT, both glucose and insulin levels were significantly higher in the obese subjects than the controls (Prager 1987⁴²³).

d) *Leptin*

25 The levels of leptin in plasma increases with body weight (body mass index, BMI kg/m²). Plasma leptin levels are higher in females compared to males (Tasaka 1997⁴²⁴).

The ob/ob mouse has a mutated ob gene. The deficiency of leptin in the ob/ob mouse produces severe obesity. Contrary to the ob/ob mouse (and the db/db mouse with the mutated leptin receptor), in most obese humans the leptin and leptin receptors genes

are normal. Moreover, except for some rare cases, the level of leptin in obese humans is elevated rather than reduced (Bjorbaek 1999⁴²⁵).

e) *Estrone, estradiol*

5 Urinary excretion of estrone (E1), estradiol (E2) and estriol (E3) was measured in obese post-menopausal women before and 6-12 months following participation in a weight loss program. Prior to the weight loss program, there was a significant correlation between estrone, weight and the Quetelet-index of obesity and between estriol and the Quetelet-index (de Waard 1982⁴²⁶).

10 Serum levels of sex hormones were studied in healthy, white postmenopausal women (mean age 58 years). Extraction, column chromatography, and radioimmunoassay were used in combination to measure the serum concentrations of estrone, estradiol, testosterone, and androstenedione. Obesity was a major predictor of estrone and estradiol levels. Obese women had estrone levels 40% higher than nonobese women (Cauley 1989⁴²⁷).

15 In a subsequent study, Cauley, *et al.*, (1994⁴²⁸) compared sex steroid hormone levels between white and black women 65 years of age or older. The researchers used the same techniques to measure the serum levels of estrone, androstenedione, and testosterone as in the 1989 study. The results showed that black women had significantly higher serum estrone concentrations and markedly lower androstenedione levels 20 compared to white women. There was a corresponding difference in the degree of obesity between the two groups.

f) *Interleukin 1 β (IL-1 β)*

25 Human coronary artery specimens from patients suffering from either coronary atherosclerosis or cardiomyopathy were studied for levels of IL-1 β (Galea 1996⁴²⁹). The presence of IL-1 β correlated with disease severity. The study discovered that IL-1 β protein is elevated in the adventitial vessel walls of atherosclerotic coronary arteries compared to coronary arteries from nonischemic cardiomyopathic hearts.

Serum IL-1 β levels were also determined in patients with ischaemic heart disease. The results showed that the mean serum IL-1 β concentrations were higher in patients with ischaemic heart disease, in particular in those with minimal coronary artery disease and angina (Hasdai 1996⁴³⁰).

5 g) *Interleukin 6 (IL-6)*

Type II diabetes mellitus (non-insulin-dependent diabetes mellitus, NIDDM) is associated with increased blood concentrations of markers of the acute-phase response, including interleukin-6. The combination of hypertriglyceridaemia, low serum HDL-cholesterol concentrations, hypertension, obesity and accelerated atherosclerosis, termed metabolic syndrome X, is often associated with NIDDM. To investigate this association, two groups of Caucasian NIDDM patients were studied. The first group, with any 4 or 5 features of syndrome X, was compared with the second group, with 0 or 1 feature of syndrome X. The groups were matched for age, sex, diabetes duration, glycaemic control and diabetes treatment. Age and sex matched healthy non-diabetic subjects were controls. The results showed a marked increase in serum IL-6 between the three groups. The lowest levels were found in non-diabetic subjects, intermediate levels in NIDDM patients with 0 or 1 feature of syndrome X and the highest levels in NIDDM patients with a 4 or 5 features (Pickup 1997⁴³¹, Pickup 1998⁴³²).

h) *Tumor necrosis factor α (TNF α)*

20 Sixty five patients were tested for TNF α levels. The majority of the patients had android obesity, elevated leptin, insulin resistant, coronarographically confirmed microvascular angina pectoris or IHD. Most of the patients suffered from a myocardial infarction with one or more significant stenoses on the epicardial coronary arteries. Fifty percent of the patients had elevated TNF α , and 28% elevated IL-6 (Hrnciar 1999⁴³³).

25 10. *Non resistant ERK agents in obesity*

Some GABP kinase agents show no resistance. Consider the following cases.

a) Interleukin 2 β (IL-2 β)

IL-2 β is an ERK agent with the receptors, interleukin 2 receptor β chain (IL-2R β) and IL-2 receptor γ -chain (γ c). Both receptors are stimulated by GABP (Markiewicz 1996, Lin 1993). Microcompetition for GABP reduces transcription of the receptors.

5 Since any control in this pathway has to be downstream from the receptors, microcompetition for GABP diminishes expression of the control. The reduced expression of the control reduces its repressive effect on IL-2 β , which elevates the concentration of IL-2 β . However, IL-2 β itself is a GABP stimulated gene (Avots 1997⁴³⁴). Therefore, microcompetition also reduces transcription of IL-2 β . The combined effect of

10 diminished repression on transcription and diminished transactivation of transcription can result in a decline, increase, or no change in the concentration of IL-2 β in obesity.

b) GM-CSF

Granulocyte-macrophage colony stimulating factor (GM-CSF) is an ERK agent. One study showed that GM-CSF (20 ng/ml) significantly inhibited neutrophil apoptosis.

15 The inhibition of apoptosis was significantly attenuated by PD98059, an MEK1 specific inhibitor (Klein 2000⁴³⁵). Another study showed that bone marrow-derived macrophages proliferate in response to GM-CSF. The MEK1 specific inhibitor, PD98059, blocked the GM-CSF stimulated cell proliferation. Moreover, this study showed the time-course of ERK activation by GM-CSF, where maximal activation occurred 5 min after stimulation

20 (Valledor 2000⁴³⁶).

As a GABP kinase agent one would expect to observe resistance in obesity and obesity related disease. However, the GM-CSF gene is transactivated by ets1 (Thomas 1997⁴³⁷). Therefore, microcompetition for ets1 can result in either a decline, increase or no change in GM-CSF concentration in obesity and obesity related diseases.

25 **11. Studies with viruses**

Until recently, the relationship between viral infection and human obesity has been completely ignored.

12. Human adenovirus 36 (Ad-36)

A recent study inoculated chickens and mice with human adenovirus Ad-36. Weight matched groups were inoculated with tissue culture media as non-infected controls. Ad-36 inoculated and uninfected control groups were housed in separate rooms under biosafety level 2 or better containment. The chicken study was repeated three times. The first chicken experiment included an additional weight matched group of chickens that was inoculated with CELO (chick embryo lethal orphan virus), an avian adenovirus. Food intake and body weight were measured weekly. At the time of sacrifice blood was drawn and visceral fat was separated and weighed. Total body fat was determined by chemical extraction of carcass fat. In experiment 1, the results showed that the visceral fat of the Ad-36 chickens was 100% greater than controls (Dhurandhar 2000⁴³⁸, Table 1), in experiment 2, visceral fat was 128% greater than controls (Ibid, Table 3), in experiment 3, visceral fat was 74% greater than control (Ibid, Table 4). In all three experiments there was no difference in food intake or body weight between Ad-36 chickens and controls. Chickens inoculated with CELO virus showed no change in visceral fat. The Ad-36 mice visceral fat was 67% greater than controls and mean body weight was 9% greater. There was no difference in food intake. Sections of the brain and hypothalamus of Ad-36 inoculated animals showed no overt histopathological changes. Ad-36 DNA could be detected in adipose tissue, but not skeletal muscles of randomly selected animals for as long as 16 weeks after Ad-36 inoculation. Based on these results Dhurandhar concluded that "the role of viral disease in the etiology of human obesity must be considered."

13. HIV

Recently, several studies documented a new syndrome associated with HIV infection termed "lipodystrophy," or "fat redistribution syndrome" (FRS). The symptoms typical of FRS, such as peripheral lipodystrophy, central adiposity, hyperlipidemia and insulin resistance (for a recent review see Behrens 2000⁴³⁹), are similar to syndrome X symptoms (Engelson 1999⁴⁴⁰) (Syndrome X is also known as "insulin resistance" or plain "obesity.") The cause of FRS is unknown. The temporal association between the recognition of FRS and the application of protease inhibitor therapy has led several investigators to conclude that FRS is a result of protease inhibitor therapy. However,

since FRS was also identified in HIV-infected patients who were not taking protease inhibitors, other researchers concluded that FRS might be a characteristic of the HIV infection, only unmasked by prolonged survival associated with protease inhibitors treatment.

5 HIV is a GABP virus. HIV infection results in microcompetition between virus and the host which leads to obesity. (Moreover, recent studies report that HIV infection is associated with a greater risk of developing atherosclerosis and diabetes mellitus. Atherosclerosis and diabetes mellitus are another two diseases caused by microcompetition.)

10 **J. Microcompetition-like obesity**

1. **Hypothesis: Genetic mutation, injury, diet or a weak ERK signal**

15 A genetic mutation, injury or diet can result in a deficiency in an ERK agent or ERK receptor. Such deficiency produces a weak ERK signal. A weak ERK signal disrupts the GABP pathway, and therefore, induces microcompetition-like clinical symptoms.

2. **Examples**

a) ***Leptin***

20 Homozygous mutations in genes encoding leptin or the leptin receptor lead to early-onset obesity and hyperphagia (Clement 1998⁴⁴¹). For instance, mutation in the ob (leptin) gene is associated with obesity in the ob/ob mouse.

Obesity in the db/db mouse is associated with mutations in the db (leptin receptor) gene. An alternatively spliced transcript of the leptin receptor encodes a form with a long intracellular domain. The db/db mouse produces this alternatively spliced transcript with a 106 nucleotide insertion that prematurely terminates the intracellular domain. Moreover, the db/db mouse also exhibits a point mutation (G→T) in the same gene. The long intracellular domain form of the receptor participates in signal transduction and the

inability to produce the long form in db/db mice contributes to their extreme obese phenotype (Chen 1996⁴⁴²).

Obesity in the Zucker fatty (fa/fa) rats is associated with mutations in the fa gene which encodes a leptin receptor. The fa mutation is a missense mutation (269 gln→pro) in the extracellular domain of the leptin receptor. This mutation causes a decrease in cell-surface expression, a decrease in leptin binding affinity, defective signaling to the JAK-STAT pathway and reduced ability to activate transcription of the egr1 promoter (de Silva 1998⁴⁴³). Yamashita, *et al.*, found that by binding to the long form of its receptor, leptin increased the tyrosine phosphorylation of STAT3 and ERK in Chinese hamster ovary (CHO) cells. In CHO cells with a fa mutated receptor, the leptin induced phosphorylation of both STAT3 and ERK was lower (Yamashita 1998⁴⁴⁴).

ERK complements

Let A and B be two ERK agents. Assume that A is not an ERK receptor for B. Administration of B can alleviate the symptoms associated with a deficiency in A or an ERK receptor for A.

If A is not an ERK receptor for B, B will be called an "ERK Complement" for A. Notice that the relationship is asymmetric. If B is downstream from A, B is an ERK complement for A, while A is not an ERK complement for B.

IL-1 β as ERK complement for leptin

A low dose injection of human recombinant IL-1 β to genetically obese ob/ob and db/db mice normalized glucose blood levels for several hours (del Rey 1989⁴⁴⁵). In another study, chronic intracerebroventricular (ICV) microinjection of IL-1 β to obese (fa/fa) Zucker rats caused a 66.1% decrease in nighttime food intake (Ilyin 1996⁴⁴⁶).

Luheshi, *et al.*, (1999⁴⁴⁷) showed that IL-1 β is an ERK receptor for leptin. However, IL-1 β can still be as ERK complement for leptin if leptin is not a receptor for IL-1 β (asymmetry of the complement condition).

TNF α as ERK complement for leptin

ICV microinjection of TNF α (50, 100 and 500 ng/rat) to obese (fa/fa) Zucker rats in triplicate decreased short-term feeding (4 hours) by 17%, 20%, and 20%, nighttime feeding (12 hours) by 13%, 14% and 13% and total daily food intake by 11%, 12% and 11%, respectively (Plata Salaman 1997⁴⁴⁸).

5 LPS as ERK complement for leptin

Administration of LPS (0.1, 1, 10, 100 μ g) to db/db mice induced a significant decrease in food intake (25%, 40%, 60%, 85%, respectively, in the first 24 hours post injection). The effect on ob/ob mice was similar (Faggioni 1997⁴⁴⁹).

b) *Insulin*

10 A mutation in the insulin receptor substrate-1 (IRS-1) is a risk factor for coronary artery disease (CAD). Insulin resistance is correlated with a higher risk of atherosclerosis. Insulin receptor substrate-1 (IRS-1) is a key component of tissue insulin sensitivity. A mutation (G972R) of the IRS-1 gene, which reduces IRS-1 function and has been connected to decreased sensitivity to insulin, was studied to see if it had any role 15 in predisposing individuals to coronary artery disease (CAD). In this study, CAD patients had a much higher incidence of the mutation than the control group (18.9% versus 6.8%, respectively). The relative risk of CAD associated with the mutation increased in the obese patients and patients with a cluster of abnormalities of insulin 20 resistance syndrome. These results indicate that the G972R mutation in the IRS-1 gene is a strong independent predictor of CAD. In addition, this mutation significantly enhanced the risk of CAD in both obese patients and in patients with clinical features of the insulin resistance syndrome (Baroni 1999⁴⁵⁰).

c) *Transforming growth factor- β (TGF β)*

25 Mutations in the TGF β receptor type II gene are associated with various cancers. Several human gastric cancer cell lines were studied for genetic abnormalities in the TGF β type II receptor gene. Deletion of the type II receptor gene in two of eight cell lines, and amplification of the gene in another two lines, was detected in Southern blots. Other abnormalities in the gastric cancer cells resistant to the growth inhibitory effect of

TGF β included expression of either truncated or undetectable TGF β type II receptor mRNAs. The one cell line not resistant to the growth inhibitory effect of TGF β showed no abnormalities in type II receptor gene (Park 1994⁴⁵¹). Mutation of the TGF β receptor type II gene is characteristic of colon cancers with microsatellite instability or replication errors (RER+). Specific mutations in a polyadenine repeat of the TGF β type II receptor gene are common in both RER+ colon cancers and RER+ gastric cancers (Myeroff 1995⁴⁵²).

Mutations in the TGF β receptor type II gene are also associated with atherosclerosis. High fidelity PCR and restriction analysis was adapted to analyze 10 deletions in an A10 microsatellite within the TGF β receptor type II gene. DNA from human atherosclerotic lesions, and cells grown from lesions, showed acquired 1 and 2 bp deletions in TGF β receptor type II gene. The mutations could be identified within specific patches of the lesion, while surrounding tissue, or unaffected arteries, exhibited the wild-type genotype. This deletion causes loss of receptor function, and thus, 15 resistance to the antiproliferative and apoptotic effects of TGF β 1 (McCaffrey 1997⁴⁵³).

A deficiency in the TGF β receptor type II gene causes osteoarthritis. An overexpressed TGF β cytoplasmically truncated type II receptor competes with the 20 cellular receptors for complex formation, thereby acting as a dominant-negative mutant receptor. Transgenic mice expressing the dominant-negative mutant receptor in skeletal tissue developed progressive skeletal degeneration. The pathology strongly resembled human osteoarthritis. This controlled experiment in mice shows that a weak TGF β signal leads to the development of degenerative joint disease similar to osteoarthritis in humans (Serra 1997⁴⁵⁴).

d) Estrone and estradiol

25 The ovaries in polycystic ovary syndrome (PCOS) produce less estradiol in response to follicle-stimulating hormone (Caruso 1993⁴⁵⁵). PCOS is associated with high blood pressure, hyperinsulimia, insulin resistance and obesity.

Ovariectomy reduces the concentration of estradiol, sometimes to undetectable levels (Wronski 1987⁴⁵⁶). Ovariectomy is also associated with obesity.

e) Zinc and Copper

Singh, *et al.*, (1998⁴⁵⁷) surveyed 3,575 subjects, aged 25 to 64 years. The results showed that the prevalence of coronary artery disease (CAD), diabetes and glucose intolerance is associated with lower intake of dietary zinc. In addition, hypertension, 5 hypertriglyceridemia and low high-density lipoprotein cholesterol levels increased as zinc intake decreased.

f) Metallothionein-null

Metallothionein is a receptor of the ERK agent zinc. After weaning, MT-null mice consumed more food and gained more weight at a more rapid rate than control 10 mice. The majority of the adult male mice in the MT-null colony showed moderate obesity (Beattie 1998⁴⁵⁸).

g) CD18-null

Chinese hamster ovary (CHO) fibroblast cell lines were engineered to express the CD11a/CD18 or CD11b/CD18 antigens. These cell lines were induced with LPS. 15 Otherwise LPS-nonresponsive fibroblasts became responsive to LPS upon heterologous expression of CD11a/CD18 and CD11b/CD18 (Flaherty 1997⁴⁵⁹). CD11c/CD18 also activated cells after binding to LPS (Ingalls 1995⁴⁶⁰). In another study, both wild type CD11b/CD18 and mutant CD11b/CD18 lacking the cytoplasmic domains still transmitted a signal in response to LPS (Ingalls 1997⁴⁶¹). Although full length CD11b/CD18 is 20 needed for productive phagocytic signals, LPS activation does not require the cytoplasmic domains. Perhaps CD11b/CD18 activates cells by presenting LPS to a downstream signal transducer (Ingalls 1997). These studies indicate that CD11a/CD18 and CD11b/CD18 are receptors of the ERK agent LPS.

CD11a/CD18 binds the intercellular adhesion molecule-1 (ICAM-1). ICAM-1 25 null mice (ICAM-1 *-/-*) gained more weight than control mice after 16 weeks of age, and eventually became obese despite no obvious increase in food intake. ICAM-1 *-/-* mice also showed an increase susceptibility to develop obesity under a high fat diet.

CD11b/CD18 binds macrophage 1 (MAC-1). MAC-1 null mice (MAC-1 $^{-/-}$) were also susceptible to diet-induced obesity, and exhibited a strong similarity in weight gain with sex-matched ICAM-1 $^{-/-}$ mice (Dong 1997⁴⁶²).

3. Stroke

5 K. Stroke

1. Introduction

10 Stroke (cerebrovascular accident, CVA) is cardiovascular disease resulting from disrupted blood flow to the brain due to occlusion of a blood vessel (ischemic stroke) or rupture of a blood vessel (hemorrhagic stroke). Interruption in blood flow deprives the brain of oxygen and nutrients, resulting in cell injury in affected vascular area of the brain. Cell injury leads to impaired or lost function of body parts controlled by the injured cells. Such impairment is usually manifested as paralysis, speech and sensory problems, memory and reasoning deficits, coma, and possibly death.

15 The two types of ischemic strokes, cerebral thrombosis and cerebral embolism, are most common, accounting for about 70-80 percent of all strokes. Cerebral thrombosis, the most common type of stroke, occurs when a blood clot (thrombus) forms blocking blood flow in an artery supplying blood to the brain. Cerebral embolism occurs when a wandering clot (an embolus) or another particle forms in a blood vessel away from the brain, usually in the heart. The clot is carried by the bloodstream until it lodges in an artery supplying 20 blood to the brain blocking the flow of blood.

2. Microcompetition and stroke

25 Microcompetition causes atherosclerosis. Like coronary artery occlusion, atherosclerosis in arteries leading blood to the brain (such as carotid artery) or in the brain may result in arterial occlusion through plaque formation or plaque rupture and in situ formation of a thrombus (see chapter on atherosclerosis above). Lammie (1999⁴⁶³) reports observations supporting similar pathogenesis in coronary artery disease (CAD) and stroke.

In general, numerous studies report the association between atherosclerosis and stroke (see, for instance, Chambliss 2000⁴⁶⁴, O'Leary 1999⁴⁶⁵).

5 In addition, microcompetition increases TF expression on circulating monocytes. Monocytes originate from CD34+ progenitor cells (Hart 1997⁴⁶⁶, Fig 3). CD34+ cells are permissive for a GABP viral infection. For instance, Zhuravskaya, *et al.*, (1997⁴⁶⁷) demonstrated that human cytomegalovirus (HCMV), a GABP virus, persisted in infected bone marrow (BM) CD34+ cells (see also, Maciejewski and St Jeor 1999⁴⁶⁸, Sindre 10 1996⁴⁶⁹). The infection of CD34+ with a GABP virus increases TF expression on circulating monocytes. Such excessive TF expression in stroke patients was documented in a few studies (see, for instance, Kappelmayer 1998⁴⁷⁰). The excessive TF expression increases the probability of coagulation and formation of an embolus.

L. Autoimmune disease

1. Conceptual building blocks

a) *T-cell deletion vs. retention and Th1 vs. Th2 differentiation*

15 Dendritic cells (DC) and macrophages are professional antigen presenting cells (professional APC). For simplicity, the text uses the symbol DC to represent both types of professional APC.

DC bind T cells. Figure 34 illustrates some of the molecules on the surface of DC and T cells participating in this binding.

20 Strength of DC and T-cell binding, denoted $[DC \bullet T]$, is a positive function of B7 concentration on surface of DC, denoted $[B7]$, a negative function of CTLA4Ig concentration on surface of T-cell, denoted $[CTLA4Ig]$, and a positive function of concentration of the major histocompatibility complex (MHC) bound to antigen on DC, denoted $[Ag]$. The following formula present these relationships.

$$25 [DC \bullet T] = f([B7], [CTLA4Ig], [Ag])$$

(+) (-) (+)

An (+) sign under [B7] means a positive relationship, that is, an increase in B7 surface concentration increases the strength of DC and T-cell binding. A (-) sign under a variable indicates a negative relationship.

5 We assume a greater than zero rate of substitution between [B7] and [Ag], that is, increase in [B7] can compensate, to a certain degree, for decrease in [Ag], and vice versa.

[DC•T] determines CD8+ retention vs. deletion and Th1 vs. Th2 differentiation.

(1) Increase in [DC•T] increases the probability of peripheral CD8+ retention vs. deletion

10 Low [DC•T] leads to peripheral CD8+ proliferation and deletion. The deletion is specific for the antigen presented on MHC. High [DC•T] results in peripheral CD8+ proliferation and retention. T-cells do not differentiate between self or foreign antigen. They respond only to [DC•T].

Define antigen specific peripheral tolerance as deletion of T-cells specific for this antigen. Using this term, it can be said that low [DC•T] induces tolerance.

15 (2) Increase in [DC•T] increases the probability of Th1 vs. Th2 differentiation

T helper lymphocytes can be divided into two subsets of effector cells based on their function and the cytokines they produce. The Th1 subset of CD4+ T cells secretes cytokines usually associated with inflammation, such as interleukin 2 (IL-2), interleukin 12 (IL-12), interferon γ (IFN γ) and Tumor necrosis factor β (TNF β), and induces cell-mediated immune responses. The Th2 subset produces cytokines such as interleukin 4 (IL-4), interleukin 5 (IL-5), interleukin 6 (IL-6), interleukin 10 (IL-10), and interleukin 13 (IL-13), which help B cells to proliferate and differentiate and is associated with humoral-type immune responses (see recent review Constant 1997⁴⁷¹).

25 In relevant physiological conditions, low [DC•T] induces CD4+ differentiation into Th2 while high [DC•T] induces Th1 differentiation. [B7] and [Ag] increase [DCT] (see formula above). Therefore, increase in either [B7] or [Ag], increases the probability of Th1 vs. Th2 differentiation. This concept is represented in figure 35.

The results in Rogers and Croft (1999⁴⁷²) support such a relationship. Naive CD4 cells were stimulated with varying doses of moth cytochrome c (MCC) presented on splenic APC and cultured for 4 or 12 days. An equivalent number of surviving T cells was restimulated with a single dose of Ag and assayed for secretion of Th1 and Th2 cytokines.

5 The results showed that the length of differentiation period (4 or 12 days) affects the cytokine profile induced by varying doses of native peptide (Rogers and Croft 1999⁴⁷³). Overall, after 12 days of differentiation, lower doses of high affinity peptides produced T-cells mostly secreting Th2 cytokines. In contrast, higher doses of high affinity peptides resulted in more T-cells secreting Th1 cytokines. These, and other results, were

10 summarized by Roger and Croft in a figure (*Ibid*, Fig 7) almost identical to the figure above. (The figure for T-cells after 4 days in culture is different. However, since autoimmune disease is a chronic condition, extended exposure to APC seem to be a better description of the CD4+ T-cells *in vivo* environment)

b) Increase in probability of antigen internalization increases [Ag] and [B7]

15 An antigen is a molecule that induces an internalization response in DC (phagocytosis, cell engulfment, etc). Cell debris, apoptotic cells, foreign proteins, etc. are antigens, that is, activate an internalization response by DC.

An increase in the concentration of internalized antigens stimulates antigen processing and presentation on DC surface, or [Ag]. The increase in the concentration of 20 internalized antigens also increases [B7], or costimulation (see, for instance, Rovere 2000⁴⁷⁴ and Rovere 1998⁴⁷⁵ for observation consistent with this concept).

Consider a stationary DC. Increase in antigen concentration in the DC environment increases the DC probability of antigen internalization. Consider a DC migrating through an environment with fixed antigen concentration. Slower DC migration increases the DC probability of antigen internalization. Therefore, both increase in antigen concentration in the cell environment, and decrease in the cell migration speed, increase [Ag] and [B7].

Assume an increase in concentration of internalized antigens decreases cell migration speed. The decrease in migration speed amplifies a small increases in antigen

concentration in the DC environment into a large increases in [Ag] and [B7]. Such amplification increases the sensitivity of DC to its environment.

c) Chemokines carry a homing signal for T-cells and circulating professional APCs

5 A source DC releases chemokines. The chemokines direct activated T-cell and more DC to the source. The steering of T-cells and new DC is most effective when the source DC is stationary (otherwise, T-cells and new DC need to chase a moving target).

10 Some of the chemokines secreted by DC are RANTES (regulated upon activation, normal T cell expressed and secreted), MIP-1 α , MIP-1 β (macrophage-inflammatory protein-1 α and 1 β). CCR5 is a receptor for these chemokines variably expressed on monocytes, activated T cells, natural killer cells, and dendritic cells.

d) Cytotoxic T lymphocytes (CTL)

15 Assume a stationary source DC releasing chemokines. Antigen specific CTL enter the tissue near the stationary DC and bind and destroy all target cells, that is, cells which present the specific antigen on their MHC. The target cells include the stationary DC and all tissue cells which present the antigen.

2. Model

20 Damaged tissue is defined as tissue showing abnormal morphology. Tolerance, activation and autoimmune disease are defined as immune dynamics which result in no tissue damage, reversible, or self correcting tissue damage, and irreversible tissue damage, respectively. Note that these definitions are different from acute vs. chronic immune activation.

The following sections present a model which describes the conditions inducing tolerance, activation and autoimmune disease.

a) Tolerance

Tolerance is defined as immune dynamics which result in no tissue damage.

Consider the following dynamics.

5 Terminology: In the atherosclerosis chapter foam cell migration back to circulation was called backward motility. Since backward motility essentially means out of tissue migration, this text uses the same term to describe DC migration from tissue to lymph vessel.

10 DC continuously enter tissues. In tissue, the cells collect, process and present antigens on MHC. Internalized antigens induce oxidative stress, which decreases binding of GABP to the tissue factor (TF) promoter, resulting in increased TF expression (see 15 effect of GABP on TF expression above in atherosclerosis chapter). TF propels DC backward motility, that is migration out of tissue and into a lymph vessel. Since backward motility takes a relatively short time, the DC entering the lymph vessel show only a small increase in [B7]. Moreover, under normal conditions, the concentration of antigens in the DC migration path is low. As a result, the DC entering the lymph vessel also show low 20 [Ag]. In the draining lymph node, DC bind naive T-cells expressing T-cell receptors (TCR) which match the presented antigens. Since [B7] and [Ag] are low, [DC•T] is low 15 (see formula above). As a result, the bound T-cells proliferate and die.

b) Immune activation

20 Activation is defined as immune dynamics which result in reversible tissue damage.

(1) The "slow DC" model

25 Consider a tissue with excessive local production of an antigen. For simplicity, let the antigen originate from a single cell, called the origin. Antigen concentration near the origin is not uniform. Some regions contain "normal," or low, concentrations, other contain moderate concentrations, yet other contain high antigen concentrations. Consider three dendritic cells DC_A, DC_B and DC_C. DC_A, DC_B and DC_C migrate through the regions of "normal," moderate, and high antigen concentrations, respectively. Higher antigen concentration results in higher rate of antigen internalization, faster increase in cellular

free radicals and faster increase in TF expression (oxidative stress reduces the binding of GABP to the TF gene and increases its transcription, see above). Consider figure 36.

TF activity, marked a_{TF} , is a function of surface TF concentration. A faster increase in TF concentration moves the a_{TF} graph to the left (the atherosclerosis chapter discusses the shape of the a_{TF} curve and the relationship between a_{TF} and TF surface concentration). Assume the speed of DC migration in tissue can be represented as a linear function of a_{TF} . Then, the distance traveled by a DC is equal to the integral of its a_{TF} function from t_0 , the time the cell starts backward motility, to the time the DC leaves the tissue and enters a lymphatic vessel. Consider DC_A . DC_A starts to migrate at time t_0 and at time t_1 (point 2) reaches the lymphatic vessel. The area under curve A from point 1 to point 2 is equal to the distance traveled by DC_A . Mark this area with $\int_{t_0}^{t_1} Adx$. Consider DC_B . Curve B represents a faster increase in TF concentration on the DC. To reach the lymphatic vessel, DC_B must travel the same distance as DC_A . However, DC_B needs a longer time to travel this distance, or $t_2 > t_1$. At time t_1 , the distance traveled by DC_B is represented by the area under curve B defined by points 3 and 5, or $\int_{t_0}^{t_1} Bdx$. This area is only part of the area under curve A defined by points 1 and 2, in symbols, $\int_{t_0}^{t_1} Bdx < \int_{t_0}^{t_1} Adx$. To increase the area, or distance travels by DC_B , t_2 must be greater than t_1 . See the area defined by points 3 and 4 in the figure. Does every DC reach the lymphatic vessel? To answer this question assume that every a_{TF} greater than $a_{TF_{stop}}$ propels migration. DC_B spends a longer time migrating, however, the cell reaches the lymphatic vessel. In comparison, to successfully reach the lymphatic vessel, DC_C must spend an even longer time on the (same) road. In the figure, this time is marked by t_3 . This extra time is prevents the cell from reaching the lymphatic vessel. According to the figure, to reach the lymphatic vessel, DC_C depends on TF activities that no longer propel migration. All a_{TF} between points 8 and 7 are bellow $a_{TF_{stop}}$. DC_C ends up trapped in tissue. Moreover, the higher the concentration of antigen in the DC environment, the less is the distance traveled by the cell, and the nearer the cell's final resting site relative to the origin.

(2) The "two peak" system

Consider insulin producing β cells as an example for tissue in the "slow DC" model above. Assume β cells are induced to increase their production of antigens, resulting in an increase in the concentration of antigens in the DC migratory path. Such an 5 increase might result from injury, infection, transgene expression, etc (see examples below). Since, in most cases, antigen production involves apoptosis, we call this initial event "trigger apoptosis." For simplicity, let trigger apoptosis is self limiting. The curve illustrating the number of apoptotic β cells over time is bell shaped (see following figure). If we assume that every β cell produces the same concentration of antigens, this curve can 10 also represent the antigen concentrations in the DC environment.

DC continuously migrate through the pancreas. As a result of the excessive production of autoantigen, some DC internalize more antigens and begin to slow down, which further increases their antigen internalization. A few slower migrating DC reach the lymph vessel (DC_B above) and than the draining lymph node where they present 15 higher [Ag] and [B7] to T-cells inducing proliferation and retention. Other slower migrating DC end up trapped in the tissue (DC_C above). These cells release chemokines which direct activated T-cells to the site of excessive antigen production. The chemokines also direct more DC to the same site which amplifies the initial reaction. Infiltrating T-cell bind trapped DC and β cells inducing a second wave of apoptosis. The T-cell induced 20 apoptosis decreases the number of trapped DC, the production of DC chemokines, the infiltration of T-cells and new DC, returning immune dynamics to tolerance. Since the T-cell induce apoptosis is self limiting, it is represented in figure 37 with a bell shape curve.

Overall, the number of viable β cells is equal the initial number of β cells minus the total number of apoptotic cells (initial number of β cells - trigger apoptosis - T-cell 25 induced apoptosis). In figure 37, the sum of apoptotic cells is represented by the curve 0,1,2,3 and the corresponding "number of viable β cells" curve is illustrated in the top half of the figure. Note that the peak of the "sum curve" corresponds to the turn in the S shape of the "number of viable β cells" curve, and the end of the "sum curve" corresponds to the minimum point on the "number of viable β cells" curve (see doted arrows). The right 30 hand side of the "number of viable β cells" curve illustrates β cell neogenesis. Note that

the final number of viable β cell is equal the initial number, and therefore, at termination tissue damage is reversed.

(3) The "two peak" dynamics

5 Assume an increase in trigger apoptosis. How does the two peak system respond to such a change? Consider figure 38.

The increase in trigger apoptosis produces more antigens. DC internalize more antigens. The excess oxidative stress increases TF surface expression. DC migration to the lymph node is slower, and therefore, T-cell activation is delayed. However, when DC eventually reach the lymph node, they present higher [Ag] and [B7], and, therefore, 10 activate more T-cells (higher probability for activation and retention rather than activation and deletion). Moreover, more DC are trapped in the tissue. These cells produce more chemokines and chemoattract more T-cell which infiltrate the tissue producing higher rate of apoptosis. Overall, the increase in trigger apoptosis shifts the second peak right and up.

c) *Autoimmune disease*

15 (1) The "excessively slow DC" model

Autoimmune disease is defined as immune dynamics which produce irreversible tissue damage, or abnormal tissue morphology.

Consider a situation where an exogenous disruption (local or systematic) slows DC backward motility. These DC will be called "excessively slow." Since TF propels 20 backward motility, a disruption which decreases or increases TF surface concentration (both directions have the similar effects because of TF encryption, see the atherosclerosis chapter above) can produce excessively slow DC. Consider figure 39.

The disruption shifts the second peak to the right. As with increased trigger apoptosis, DC migration to the lymph node is slower, which result in a shift of the second 25 peak right and up. The sum of β cell apoptosis in this case is represented by the two peak curve (0,4,5,6,7). The question is what is the shape of the corresponding "number of viable β cells" curve? Excessive β cell apoptosis induces excessive tissue damage. If tissue regeneration capacity is limited, there exist a level of β cell apoptosis which result

in permanent reduction in the number of viable β cells. Note that in the figure above, the corresponding "number of viable β cells" curve shows complete destruction of β cells. Under limited regeneration capacity, such damage is irreversible, and, therefore, describes autoimmune disease.

5 3. Predictions and evidence

The studies described in the following section use different interventions. In terms of the two peak model, these interventions decrease or increase trigger apoptosis, excessively slow DC backward motility, etc. The following sections compares the predicted effects of such interventions with the actual reported responses.

10 a) *Animal models*

The expression of cellular molecule, M, in a tissue cell C (C is not a DC) is called "excessively high" if the normal process of antigen production in C causes autoimmune disease.

15 Some transgenic animals are designed to express a foreign gene (see examples below). Since cells show variable transgene expression, it likely that some cells show high transgene expression (and others low expression). Since excessively high transgene expression produces an autoimmune disease, we call the cells with high transgene expression "immune susceptible cells." The situation of autoimmune disease in transgenic animals without further intervention is sometimes called "spontaneous" (see examples below). Using this term, it can be said that, in transgenic animals, the immune susceptible cells show a high probability for spontaneous destruction.

20 (1) *Tolerance dynamics*

25 A recent review summarizes many observation relating to issues of ignorance and tolerance (Heath 1998⁴⁷⁶). Based on these observations Heath, *et al.*, concluded that "taken together, there is compelling evidence that in order to maintain self-tolerance a specialized APC is capable of capturing tissue antigens, transporting them to the lymphoid compartment, i.e., the draining lymph nodes, and presenting them to both naive CD4+ and CD8+ T cells. ... This APC appears to be capable of processing exogenous antigens into

class I and class II pathways. ... The above data argue for the existence of a "professional" APC that constitutively induces tolerance to antigens expressed in extralymphoid tissues. ... In studies using transgenic mice expressing different levels of OVA in the pancreas, we have recently found that antigen concentration is critical in determining whether such 5 antigens are cross-presented in the draining lymph nodes. ... The level of antigen expression appears to determine whether an antigen induces cross-tolerance or is ignored by naive T cells. ... It is interesting to note that deletion of both CD4+ and CD8+ T cells is preceded by a period of proliferation, suggesting that the APC responsible for tolerance induction must be capable of activating T cells into proliferative cycles. Moreover, the 10 APC is a cell capable of trafficking from peripheral tissues to draining lymph node. Even more importantly for CD8+ T cell tolerance, this APC must be capable of capturing exogenous antigens and cross-presenting them in class I pathway. Various cell types have been shown to have the capacity to cross present exogenous antigens *in vitro*, including myeloid-derived DCs, macrophages, and B cells."

15 Unlike the factors regulating the balance between tolerance and ignorance, the factors determining the choice between tolerance and priming are not well understood. According to Heath, *et al.*, what determines the choice between tolerance and priming "is probably one of the outstanding questions at the moment." According to Sallusto and Lanzavecchia (1999⁴⁷⁷) in another recent review: "finding the factors that regulate the 20 balance between tolerance and response is now considered the holy grail of immunology."

(2) Two peaks

(a) O'Brien 1996

An intervention induces trigger apoptosis in insulin producing β cells. According to the two peak model, if the trigger apoptosis is substantial, such intervention should 25 produce two peak apoptosis and substantial decrease in the number of viable β cells.

Five to six week old male C57B1/6 mice were injected low-dose (40 mg/kg body weight) streptozotocin (stz) per day for five consecutive days. Two peaks in the incidence of β cell apoptosis occurred. The first peak at day 5, which corresponded to an increase in blood glucose concentration, and the second at day 11, when lymphocytic islet infiltration 30 (insulitis) was maximal (O'Brien 1996⁴⁷⁸, Fig. 3 and 4. See figure 40).

Insulitis did not begin until day 9, by which time treated animals had developed overt diabetes. β -cell apoptosis preceded the appearance of T-cells in the islets and continued throughout the period of insulitis. This study supports the two peak model were the first peak is trigger apoptosis and the second is T-cell induced apoptosis.

5

(b) O'Brien 2000

An intervention increases oxidative stress in β cells and dendritic cells. Pancreatic islets are especially susceptible to oxidative stress. A study showed that low gene expression of the antioxidant enzymes superoxide dimutase (SOD), catalase, and glutathione peroxidase in pancreatic islets compared with various other mouse tissues (Lenzen 1996⁴⁷⁹). Moreover, induction of cellular stress by high glucose, high oxygen, and heat shock treatment did not affect antioxidant enzyme expression in rat pancreatic islets or in RINm5F insulin-producing cells (Tiedge 1997⁴⁸⁰). Based on these results Tiedge, *et al.*, concluded that "insulin-producing cells cannot adapt the low antioxidant enzyme activity levels to typical situations of cellular stress by an upregulation of gene expression." The oxidative stress inducing intervention should, therefore, result in trigger apoptosis. According to the two peak model, if the trigger apoptosis is substantial, such intervention produces two peak apoptosis and substantial decrease in the number of viable β cells.

20

In mice, the first 3 postnatal weeks are characterized by marked changes in the activities of enzymes that protect against oxidative stress (glutathione peroxidase/reductase, catalase and superoxide dismutase), relative to older mice (Herman 1990⁴⁸¹). It should be noted that Herman, *et al.*, measured the expression of these enzymes in liver, lung and kidney tissues. However, let assume that DC in 3 week old mice are also protected against oxidative stress, and that β cell show a much lower level of protection (reasonable assumption in light of Tiedge, 1997 above). In such a case, according to the two peak model, oxidative stress in 3 week old mice should induce trigger apoptosis with a smaller shift to the right of the second peak, relative to older mice. Moreover, if the trigger apoptosis is also smaller in 3 week mice relative to older mice, it is possible that the sum of β cell apoptosis will show a single peak.

Finally, older mice treated with antioxidant and then oxidant should show attenuated two peaks.

5 Consider the results in the following study. A study administered a single intraperitoneal injection of cyclophosphamide (CY, 150 mg/kg body weight) to 3 and 12 week old male non-obese diabetic (NOD/Lt) mice. The study also administered, to another group of 12 week old mice, a single intraperitoneal injection of nicotinamide (NA, 500 mg/kg body weight) followed 15 minutes later by a single CY injection. The effect of these treatments on β cell apoptosis is presented in figure 41 (O'Brien 2000⁴⁸², Fig 3).

10 The total number of apoptotic β cells were observed within the islets of Langerhans in haematoxylin and eosin-stained sections of the pancreata in all three groups harvested from 8 h until 14 days following treatment. However, the shape of the three curves representing the sum of β cell apoptosis is different. The 3 week mice under CY treatment show a single peak, the 12 week mice under CY show a two peak curve, and the 12 week mice under NA/CY show attenuated two peaks.

15 Since CY injection induces oxidative stress and NA is an antioxidant, these results support the predictions of the two peak model.

(c) *Hotta 1998*

20 An intervention produced transgenic NOD mice (Tg) that overexpress thioredoxin (TRX), a redox-active protein, in β cells. The increased protection against oxidative stress reduces trigger apoptosis. According to the two peak model, reduced trigger apoptosis, shifts the second peak left and down. Consider figure 42.

25 Moreover, for simplicity, let assume that overt diabetes associates with destruction of a certain, fix number of β cells (in reality, it is actually a range and not fixed number). This number is represented by the sum of the areas (integrals) under the two peaks. In the figure, the added area is restricted by dashed lines marked T1 and T2. Consider areas A, B, C and D. To represent the same number of apoptotic cells, A + C should be equal to B + D. The smaller the size of area B the larger the size of area D, or the delay in onset of diabetes. Let the distance between points 1 and 2 indicate the size of area B. A small

distance indicates a small area B, and therefore, predicts a substantial delay in onset of diabetes.

Consider the results of the following study. The average insulitis score of 12-wk-old female NOD transgenic mice and their female TRX negative littermates were 5 1.63 ± 0.32 and 1.57 ± 0.26 (mean SEM), respectively (Hotta 1998⁴⁸³). Although, the difference is statistically insignificant, the TRX Tg score is a little higher than the Non Tg score, as predicted by the model. Moreover, the small difference, indicates a small area B, and therefore, a delay in onset of diabetes. As predicted, the first observed onset of diabetes was delayed from week 14 in Non Tg to week 23 in TRX Tg. Moreover, TRX 10 Tg mice showed a markedly reduced cumulative incidence of diabetes at week 32 compared to Non Tg (Ibid, Fig 4).

Similar observations are reported in Kubish 1997⁴⁸⁴.

Numerous other studies showed reduced insulitis and delayed diabetes in NOD mice following treatment with antioxidants, such as, nicotinamide (vitamin B3) (Kim 15 1997⁴⁸⁵, Reddy 1990⁴⁸⁶), vitamin E (Beales 1994), lipoic acid (Faust 1994⁴⁸⁷), U78518F (Rabinovitch 1993⁴⁸⁸).

Cyclosporin reduces TF expression, therefore, reduces DC trapping and diabetes in NOD (Mori 1986⁴⁸⁹) and BB Wistar rats (Laupacis 1983⁴⁹⁰).

(3) Autoimmune disease

20 According to the "slow DC" model of autoimmune disease, an intervention that induces high expression of autoantigen on DC, and too little or too much expression of tissue factor (TF), produces tissue damage.

25 Presentation of high autoantigen concentration can result from transfection, immunization with autoantigen, increased apoptosis, etc. Insufficient TF surface concentration can result from, for instance, inhibition of TF transcription. Excessive TF expression can result from excessive antigen endocytosis (through oxidative stress), microcompetition, CD40L treatment, LPS treatment, etc. Consider the following studies.

(a) *Studies with lymphocytic choriomeningitis virus (LCMV)*(i) *LCMV characteristics*

Let assume that LCMV is a GABP virus. This assumption is consistent with the following evidence. The glycoprotein (GP) protomer of the lymphocytic choriomeningitis virus (LCMV) has two N-boxes at positions (-44,-38) and (-3,+3). The distance between the two N-boxes is 35 bp. Of the dozens of known ETS factors, only GABP, as a tetrameric complex, binds two N-boxes. Typically, the N-boxes are separated by multiples of 0.5 helical turns (HT) (see discussion and references in the hormone sensitive lipase (HSL) gene above). There are 10 bp per HT. The 35 bp, or 3.5 helical turns separating the N-boxes in the GP promoter are consistent with characteristic GABP heterotetramer binding.

LCMV ARM 53b strain establishes a persistent infection in DC. Consider the following evidence. LCMV strains can be divided into two groups. The first group marked CTL-P+, includes viruses isolated from lymphocytes or macrophages obtained from CD4, perforin, and TNF α ko mice persistently infected for at least 7 months. These viruses failed to generate LCMV-specific CTL responses and caused a persistent infection. The second group marked CTL-P+, includes viruses isolated from CNS of TNF α ko mice. These viruses elicited a potent LCMV-specific CTL response, which cleared the virus within 2 wk and left no evidence of persistent infection. The Armstrong (ARM) 53b strain is a CTL-P+ virus (Sevilla 2000⁴⁹¹, Table I). According to Sevilla, *et al.*, "first, DCs are the primary cell infected *in vivo* by CTL-P+ LCMV variants; second, CTL-P+ viruses astoundingly infect >50% of CD11c+ (cellular marker for most DC in mouse lymphoid tissue) and DEC-205+ (antigen expressed on DC in lymphoid tissues) cells."

Expression of a gene under the control of the rat insulin promoter (RIP) in transgenic mice induces a large number of immune susceptible cells. Consider the following evidence. Six percent transgenic mice expressing the LCMV glycoprotein (GP) or nucleoprotein (NP) under control of the rat insulin promoter (RIP-GP, RIP-NP) in β cells, developed hyperglycemia. The pancreatic tissue of these mice revealed swollen islets with a group glass appearance (Oldstone 1991, Fig 4A). No other treatment was necessary to produce an immune reaction.

Other transgenic mice carrying the hemagglutinin (HA) of the A/Japan/305/57 strain of influenza virus gene, or interferon- γ (IFN γ) under the control of RIP (RIP-HA and RIP-IFN γ , respectively), developed spontaneous diabetes with lymphocytic infiltration (Roman 1990⁴⁹², Sarvetnick 1990⁴⁹³). It is interesting that transgenic mice expressing IFN γ under control of rat glucagon promoter (RGP-IFN γ), which is expressed in α cells, did not develop diabetes. The increase in IFN γ concentration induced no net β cell destruction. The observed β cells apoptosis in transgenic RGP-IFN γ mice was compensated by vigorous regeneration. Specifically, the islets showed no insulitis (Yamaoka 1999⁴⁹⁴). According to Yamaoka, *et al.*, "IFN γ alone is insufficient for the complete destruction of β cells *in vivo*." In terms of microcompetition, the microcompetition between the mouse's own insulin promoter (MIP) and the foreign rat's insulin promoter (RIP), reduces the expression of insulin, leading, eventually, to β cell destruction and trigger apoptosis. Therefore, RGP which does not microcompete with MIP does not produce diabetes.

15 (ii) Diabetes

RIP-GP transgenic mice show high GP expression in β cells (some mice spontaneously develop diabetes). However, most mice do not develop diabetes. In the resistant mice the expression of GP is not excessively high. In these mice, GP expression is not high enough to spontaneously produce autoimmune disease. According to the two peak model, although antigen production is high (high trigger apoptosis), it is not sufficiently high to result in permanent β cell destruction and diabetes. Infection with LCMV excessively slows DC shifting the second peak right and up. This shift tips the balance in some resistant mice towards diabetes.

20 Consider the following studies.

1. Transgenic mice that express the viral glycoprotein (GP) or nucleoprotein (NP) from lymphocytic choriomeningitis virus (LCMV) under control of the rat insulin promoter (RIP-GP, RIP-NP) in pancreatic β cells develop autoimmune diabetes (IDDM) after infection with LCMV ARM 53b (Ohashi 1991⁴⁹⁵, Oldstone 1991⁴⁹⁶).
2. Adoptive transfer of autoreactive CD8+ cytotoxic T-lymphocytes (CTL) that are present in the periphery of RIP-GP or RIP-NP transgenic mice that were active *in vitro*

and *in vivo* into uninfected transgenic recipients rarely resulted in hyperglycemia nor in insulitis, despite their ability to home to the islets and induce peri-insulitis (von Herrath 1997⁴⁹⁷). The weak trigger apoptosis induces peri-insulitis. However, without LCMV infection not enough DC are trapped in near the β cells to produce massive insulitis and 5 significant T-cell induced apoptosis. In terms of the two peak model, without LCMV infection which slows DC, the second peak does not show enough shift to the right and up.

3. The P14 TCR single-transgenic model express a LCMV-GP specific T-cell receptor. In P14 transgenic mice tolerance is induced with repeated intravenous administration of the LCMV GP peptide epitope GP33. Peptide administration resulted in 10 upregulation of T-cell activation markers, such as CD69(Garza 2000⁴⁹⁸, Fig. 1a). In addition, whereas transgenic T-cells from untreated mice were incapable of lysing peptide pulsed target *ex vivo*, *in vivo* peptide treatment induced T-cell cytolytic activity (*Ibid*, Fig. 1b). Finally, peptide administration induced expansion of T-cells followed by deletions (*Ibid*, Fig. 1C).

15 Tissue circulating DC internalize the administered GP33 peptide. The DC moderately slow down, increase surface Ag expression and costimulation, and eventually migrate to the lymph node where they present the moderate concentration of surface Ag and costimulation to T-cells, causing activation, proliferation and deletion. *Ex vivo* treatment with GP33 fail to activate T-cell since activation requires presentation by DC.

20 Intravenous administration of GP33 to double transgenic mice (RIP-GP/P14) expressing GP on pancreatic β cells and LCMV-GP-specific T-cell receptor on T-cells surprisingly did not induce diabetes (*Ibid*, Fig 2a).

25 In both models, administration of GP33 activates T-cells. However, since DC do not slow enough to be trapped in tissue, no homing signal is produced to chemoattract the activated T-cells to the inlets.

Immunization of the double transgenic mice intravenously with GP33 and FGK45, a rat anti-mouse-CD40 activating antibody, unlike immunization with GP33 and a rat polyclonal antiserum as iso-type-matched control, produced diabetes in all GP33 + anti-CD40 treated mice (*Ibid*, 2a). In both groups, the induction of T-cell activation markers

and cytotoxic activity were identical. However, GP33 + control Ab produced mild pancreatic infiltration, while GP33 + anti-CD40 produced sever insulitis (Ibid, Fig 2b,c,d).

CD40 ligation on monocytes/macrophages induces TF cell surface expression. Specifically, treatment of purified monocytes with a with a stimulating anti-CD40 mAb (BL-C4) strongly induced monocyte procoagulant activity (PCA) which was related to TF expression as shown by flow cytometric analysis (Pradier 1996⁴⁹⁹). Exposure of monocytes/macrophages to either cell membranes isolated from activated CD4+ T-cells (expressing CD40L) or a human rCD40L increased TF surface expression and enzymatic activity (Mach 1997⁵⁰⁰, Fig. 2A, and B, Table). Anti-CD40L mAb blocked induction of TF in response to CD40 ligation. A similar effect on TF expression was observed in vascular smooth muscle cells (SMC) (Schonbeck 2000⁵⁰¹).

CD40 ligation increases monocytes/macrophages and, most likely, dendritic cell, TF expression. TF expression on monocytes/macrophage and dendritic cells propels backward motility (see chapter on atherosclerosis above). A CD40L deficiency, therefore, should reduce dendritic cell migration to draining lymph node. A study analyzed the *in vivo* DC response to skin contact sensitization in CD40 ligand -/- mice. Immunohistochemistry of skin sections in unsensitized CD40 ligand -/- mice revealed no differences in terms of numbers and morphology of dendritic epidermal Langerhans cells (LC) compared to wild-type C57BL/6 mice. However, following hapten sensitization migration of LC out of skin was dramatically reduced and accumulation of DC in draining lymph nodes substantially diminished in CD40 ligand -/- mice compared to control (Moodycliffe 2000⁵⁰², Fig 2, 3). These observation are consistent with intact forward motility and deficient dendritic cell backward motility.

The effect of CD40 ligation on TF expression, can explain the results in Garza 2000 above. FGK45, the anti-CD40 agonist, increased TF expression on DC. The increased TF expression slowed down DC migration. As a result some DC arrived to the lymph node with increased surface GP33 concentration and costimulation. Other DC were trapped in the tissue. According to the slow DC model of autoimmune disease, the double transgenic mice treated with GP33 and FGK45 should develop diabetes. Moreover,

Garza, *et al.*, report that administration of GP33 and LPS, another inducer of TF expression, as expected, also resulted in diabetes.

(iii) Lupus

5 The H8 transgenic mice express the LCMV glycoprotein epitope (GP) 33-41 under control of a major histocompatibility complex (MHC) class I promoter. Since MHC class I is most likely expressed every cell, H8 mice express and present the GP33 epitope in every cell, specifically DC. Adoptive transfer of CD8+ T-cells from LCMV T-cell receptor transgenic mice into H8 mice led to efficient induction of peripheral tolerance after a period of transient activation and deletion (Ehl 1998⁵⁰³). In contrast, infection with 10 LCMV 1-3 days after T-cell adoptive transfer, resulted in disease. The mice showed signs of wasting 6-8 d after infection and 20-40% under specific pathogen-free conditions (up to 100% under non specific pathogen-free conditions) died within 12-15 d after infection. The remaining mice continued to lose weight and all died 3-5 mo after infection. Tissue 15 examination revealed CD8+ T-cell infiltration in various organs, such as spleen, liver, gut, and skin (Ibid, Fig. 3). Infection of control mice did not lead to detectable clinical symptoms.

20 The spleen, liver, gut and skin show significant rate of tissue renewal indicating a considerable rate of normal cell apoptosis. This normal cell apoptosis loads antigens, including GP33, on surface of surveilling DC. DC internal expression of GP33 also loads antigens on these cells. However, these loadings produces GP33 (and other antigens) surface concentration only sufficient to generate tolerance and not T-cell infiltration. Infection of H8 mice with LCMV slows DC (some to a halt) in all tissues, resulting in increased antigen surface concentration. According to the tow peak model, the increase in antigen surface concentration and DC trapping result in T-cell infiltration in many tissues.

25 Compare RIP-GP and H8 transgenic mice infected with LCMV in terms of DC surface concentration the GP33 antigen.

	RIP-GP	H8
Pancreas	•	• DC internal GP33 expression

	<ul style="list-style-type: none"> • <u>(Very) high</u> transfection apop. + • LCMV reduced backward motility 	<ul style="list-style-type: none"> + • <u>Low</u> tissue renewal + • LCMV reduced backward motility
Spleen	<ul style="list-style-type: none"> • • <u>High</u> tissue renewal + • LCMV reduced backward motility 	<ul style="list-style-type: none"> • DC internal GP33 expression + • <u>High</u> tissue renewal + • LCMV reduced backward motility
Liver	<ul style="list-style-type: none"> • • <u>High</u> tissue renewal + • LCMV reduced backward motility 	<ul style="list-style-type: none"> • DC internal GP33 expression + • <u>High</u> tissue renewal + • LCMV reduced backward motility
Gut	<ul style="list-style-type: none"> • • <u>High</u> tissue renewal + • LCMV reduced backward motility 	<ul style="list-style-type: none"> • DC internal GP33 expression + • <u>High</u> tissue renewal + • LCMV reduced backward motility
Skin	<ul style="list-style-type: none"> • • <u>High</u> tissue renewal + • LCMV reduced backward motility 	<ul style="list-style-type: none"> • DC internal GP33 expression + • <u>High</u> tissue renewal + • LCMV reduced backward motility

5 In spleen, liver, gut and skin, internal expression of GP33 tips the balance from tolerance (or delayed infiltration) in RIP-GP mice, to T-cell infiltration in H8 mice (compare cells in table above for same tissue in both mice models). In pancreas, the lack of DC internal expression of GP33 in RIP-GP mice is probably more than compensated by the increase apoptosis in pancreatic β cells induced by transfection with RIP-GP (see above).

The concepts presented in this table also predict that in H8 mice the rate of T-cell infiltration in different tissues, is correlated with the rate of tissue renewal.

10 Another prediction suggested by this table is that any other treatment of H8 mice which slows DC enough produces similar results. Ehl, *et al.*, tried a variety of infection and inflammatory stimuli. Specifically, they used 10 μ g LPS. LPS increases TF

expression on DC (see chapter on atherosclerosis above) and therefore, slows DC backward motility. LPS treatment of H8 mice induced activation (Ibid, Fig. 8 b).

5 Systematic lupus erythematosus (also called disseminated lupus erythematosus, lupus, lupus erythematosus and SLE) is a chronic inflammatory autoimmune disease that affect many organs such as skin, joints, kidney, heart, lung and nervous system. At onset, only one organ system is usually involved, however, additional organs may be affected later. A typical observation in lupus patients and animal models is spontaneous T-cell activation and organ infiltration.

10 Consider an infection with a GABP virus which result in sufficiently high viral genome number in circulating DC. Microcompetition between the viral and TF N-boxes increases TF surface expression which reduces DC backward motility. According to the two peak model, the excessively slowing of DC backward motility induces pathologies similar to the symptoms observed in lupus patients. The organs affected first are those that show temporary or typical high trigger apoptosis (injured organs or organ with high 15 tissue renewal).

20 Monocyte/macrophage infection with a GABP virus result in atherosclerosis (see chapter on atherosclerosis above). Both DC and macrophages originate from CD34+ progenitor cells (Hart 1997⁵⁰⁴, Fig 3). CD34+ cells are permissive for a GABP viral infection. For instance, Zhuravskaya, *et al.*, (1997⁵⁰⁵) demonstrated that human cytomegalovirus (HCMV), a GABP virus, persisted in infected bone marrow (BM) CD34+ cells (see also, Maciejewski and St Jeor 1999⁵⁰⁶, Sindre 1996⁵⁰⁷). According to the proposed models, infection of CD34+ cells, therefore, result in both lupus and atherosclerosis. The observed concurrence of lupus and atherosclerosis is well documented. See for instance some recent reviews on the issue of accelerated 25 atherosclerosis in systemic lupus erythematosus (Ilowite 2000⁵⁰⁸, Urowitz 2000⁵⁰⁹). Such observation are consistent with microcompetition, TF propelled backward motility, and the two peak model.

30 Another interesting observation explained by these models is hypercoagulation thrombosis in lupus. The infection of CD34+ with a GABP virus increases TF expression on circulating monocytes. Such excessive TF expression in lupus was documented in a

few studies (see, for instance, Dobado-Berrios 1999⁵¹⁰). The excessive TF expression increases the probability of coagulation. (More on thrombosis in lupus and other diseases see the chapter on stroke.

(iv) Graft versus host disease (GVHD)

5 DC from H8 mice (H8-DC) constitutively express the GP33 epitope. A single injection of 10^6 H8-DC (high dose) to RIP-GP transgenic mice resulted in no glycemic change or transient increase in blood glucose to intermediate levels (15-20 mM), eventually returning to normal levels within a few days (Ludewig 1998⁵¹¹, Fig. 1A). A single injection of 10^5 H8-DC (intermediate dose) did not result in diabetes. However, 10 repetitive H8-DC injections of intermediate doses, i.e., three doses of 10^5 DC in 6-d intervals (Ibid, Fig. 1C), or four doses of 10^4 DC in 2-d intervals (Ibid, Fig 1D), resulted in T-cell infiltration (Ibid, Fig 3) and diabetes. 50% of the repetitively immunized mice developed diabetes between day 10 and 14, while 40% developed hyperglycemia by days 18-21. Based on these observations Ludewig, *et al.*, concluded that “the duration of 15 antigenic stimulation by professional APCs, i.e., the integral of CTL activity over time, determines the disease outcome in this model of autoimmune diabetes.”

Consider a DC migrating “near” pancreatic β cells at a certain speed. During the time the DC spends “near” the β cells, it has a certain probability, denoted P, to internalize 20 a certain concentration [Ag] of β cell antigens. Now, consider two DC also migrating at this speed. Assuming independent DC migration and internalization, the probability that at least one of them internalizes [Ag] is $2P$ (the independent assumption does not hold if, for instance, the two DC co-migrate and end up internalizing a portion of [Ag] each). Under the independent assumption, an increase in the number of migrating DC, without 25 change in other conditions, increases the probability of antigen internalization. Consider, as an alternative situation, one DC migrating at half the original speed. Since the time the DC spends near the β cells is twice as long, its probability that the cell internalize [Ag] is $2P$, the same as the probability of the two DC migrating at the original speed. Increasing 30 the number of migrating DC and slowing migration of the existing pool of DC produce the same effect. Repetitive immunization with H8-DC is equivalent to slowing DC backward motility. Since the integral of T-cell induced apoptosis over time determines the outcome

of autoimmune disease in the case of slow DC migration (see two peak model above), the same integral is important in the case of repetitive DC immunization.

5 Graft-versus-host disease (GVHD) is a complication following allogeneic bone marrow (BM) transplantation (BMT). A typical observation in GVHD patients is spontaneous T-cell activation and organ infiltration. Approximately, 50% of patients undergoing allogeneic BMT with related HLA-matched donor develop GVHD.

10 A study measured the percentage of DC present in blood mononuclear cells (MNC) in patients following allogeneic and autologous stem cell transplantation and healthy controls. The mean number of DC as a percentage of MNC was 0.58%, 0.40% and 0.42%, for patients following allogeneic transplantation showing no GVH symptoms, patients following autologous transplantation, and healthy controls, respectively ($P = 0.06$ for the difference between allogeneic and autologous patients) (Fearnley 1999⁵¹², Fig 3, 6). These results indicate that allogeneic stem cell transplantation increases DC number. The higher DC number increases the probability of antigen internalization. In tissues with high 15 normal apoptosis (rapidly renewing tissues), such an increase might result in T-cell infiltration and tissue apoptosis.

(v) Vaccination with DC

20 Let the expression of TF, CD86 and level of antigen presentation on DC (denoted $[Ag]$) be correlated. Treatment with CD40L, pulsing, apoptosis of tissue of bystander cells, transfection with a gene expressing an epitope increase TF, CD86 and $[Ag]$. This increase is called maturation. Let assume that the distribution of number of DC expressing TF, CD86 and $[Ag]$ is normal. Consider figure 43.

25 Maturation in the figure is represented by a shift of the DC distribution to higher TF, CD86 and $[Ag]$ values. According to the TF propelled backward motility model there exists a certain level of TF expression which traps DC. This level is marked with a thick line in the figure. A cell with lower TF concentration is migration-borne (capable of migrating). A cell with higher TF concentration is trapped.

Consider vaccination with two kinds of cells, less mature and more mature, denoted with solid lines in the figure. This model provides the following predictions.

Vaccination with the less mature cells induces no trapping. All cells migrate out of tissue. In contrast, vaccination with more mature cells induces cell trapping. Some cells migrate out of tissue, represented by the area under the DC distribution left of the thick line), while the rest are trapped (the area right of the thick line).

5 Consider the following study. DC from CD14+ peripheral blood monocytes of rhesus macaques were cultured for 4 days in GM-CSF and IL-4. The cells show no expression of CD83, the mature DC marker, moderate expression of the costimulatory molecules CD80, CD86, and CD40, and high levels of MHC class I and class II (Barratt-Boyes 2000⁵¹³, Fig. 1). These cells were designated immature DC. Other cells were
10 cultured for additional 2 days (total of 7 days) with added CD40L, a known inducer of rapid maturation. The addition of CD40L induced uniform expression of CD83, and high expression of CD80, CD86, and CD40 (Ibid, Fig. 1). These cells were designated mature DC. To determine the relative efficiency of immature and mature DC migration, the site of injection was inspected 36 h after injection of cells. Injection of 2.7×10^6 immature DC
15 resulted in minor localized acute inflammatory response. No fluorescently labeled cells could be identified at that time. In contrast, injection of 3.7×10^6 mature DC resulted in a severe acute inflammatory infiltrate at the site of injection in two out of three animals. A large number of fluorescently labeled DC were detected in the dermis at 35 h in these animals (Ibid, Fig. 8). The experimental configuration in this study is presented in figure
20 44.

Many more mature DC are trapped following injection with mature rather than immature cells. Compare the areas right of the thick line under the mature and immature curves. According to the study the size of the area representing the trapped DC following injection of immature cells should be zero. However, according to the two peak model, to
25 produce T-cell infiltration, some DC should be trapped. This inconsistency can be resolved if we assume that the infiltration T-cells cleared most of the few trapped cells before the 36 hours inspection.

This study reports another important observation. Following injection of immature and mature DC, a portion of the injected cells (0.07 - 0.12%) reached the lymph node
30 (Ibid, Fig. 7) producing an immune reaction at the injection site. In terms of the figure

above, in both cases the area under the curves, left of the thick line, is not empty. Both injections included migration-borne DC. Similar observations are reported in Hermans 2000⁵¹⁴. However, not all injected DC migrate to the lymph node. Some enter circulation. These DC can end up in any tissue. According to the discussion above, if enough injected 5 DC enter circulation over an extended period of time, they might produce an immune reaction in tissues with abnormally high epitope expression or rapidly renewing tissues. Consider the following studies.

SM-LacZ transgenic mice widely express the β -galactosidase (β -gal) antigen in 10 cardiomyocytes of the right ventricle and in arterial smooth muscle cells. Repetitive treatment of SM-LacZ mice with DC presenting β -gal peptide resulted in vascular immunopathology with strong lymphocytic infiltration in small and medium-sized arteries and in the right ventricle (Ludewig 2000⁵¹⁵). Immunization of SM-LacZ mice with DC pulsed with an irrelevant peptide produced a mild liver infiltration and no anti- β -gal CTL activity. Immunization of nontransgenic mice with DC presenting the β -gal peptide also 15 produced a mild liver infiltration and no anti- β -gal CTL activity. Naive SM-LacZ mice showed no specific CTL reactivity (Ibid, Fig. 2B). Similar observations of autoimmune disease induce by DC immunization is reported in Roskrow (1999⁵¹⁶).

(b) *Studies with Theiler's murine encephalomyelitis virus (TMEV)*

20 (i) TMEV characteristics
TME viruses are members of the genus *Cardiovirus* in the family *Picornaviridae*. These viruses can be divided into two groups based on their neurovirulence characteristics following intracerebral (i.c.) inoculation of mice. Highly virulent strains, such as GDVII virus, cause a rapidly fatal encephalitis. The less virulent strains, such as BeAn and DA 25 show at least a 10-fold reduction in the mean 50% lethal dose (LD_{50}) compared to the virulent strains. Moreover, they can establish a persistent infection in the central nervous system (CNS).

Let assume that all three TMEV strains, GDVII, BeAn and DA are GABP viruses. This assumption is consistent with the following evidence. The 5' UTR of all three strains 30 includes 9 N-boxes. Moreover, the 5' UTR of all three strains includes a pair of N-boxes

(positions (-129,-123) and (121,-115), or positions (935,941) and (943,949) when numbered according to the BeAn sequence). It is interesting the the pair in GDVII is different than the pair in BeAn and DA. In GDVII the pair of N-boxes (underlined) is CTTCCGCTCGGAAG while the pair in BeAn and DA is CTTCCTCTCGGAAG. The 5 GDVII pair is symmetrical while the pair in BeAn and DA is not. The asymmetry in BeAn and DA might result in reduced affinity to GABP, and therefore, reduced rate of transcription initiation. This interpretation is consistent with the following evidence.

10 In a series of experiments, Lipton and co-workers attempted to identify the DNA sequence responsible to the difference in these strains virulence. In these studies they constructed recombinant TMEVs by exchanging corresponding genomic regions between GDVII and BeAn. One such recombinant virus is Chi 5L, in which the (933,1142) BeAn sequence replaces the original GDVII sequence. Inoculation of Chi 5L into mice by the i.c. route showed attenuated neurovirulence. The LD₅₀ value for Chi 5L was $\geq 7.5 \times 10^5$ in 15 comparison to 10 for GDVII (Lipton 1998⁵¹⁷, table 1). Replacing the original GDVII pair of N-boxes with the BeAn pair resulted in reduced virulence.

(ii) Demyelination (multiple sclerosis)

As with many other viruses, TMEV infection spreads from cell to cell. However, the identity of infected cells and order of viral cell-to-cell spread determines the clinical outcome. Consider an infection with a BeAn and DA virus. The first T-cells infected in the 20 nervous system are neurons. The infection results in cell apoptosis. The cell debris is internalized by surveilling macrophages, slowing the cells backward motility, trapping a few cells which induces T-cell infiltration. These events are characteristic of the acute phase, which terminates when the neuronal infection is cleared, inflammation in gray matter subsides, and neuron apoptosis returns to normal levels. However, during the acute 25 phase the virus spreads from neurons to some infiltrating macrophages, establishing a persistent infection. The infection increases surface TF expression, slows backward motility of some macrophages and traps others in the white matter. Since infection is not lytic, trapped macrophage continue to internalize schwann cell/oligodendrocyte debris or apoptotic cells produced in normal cell turnover, or as a result of myelin damage. The 30 internalized myelin is processed and presented on cell surface. The loaded macrophage release cytokines providing a homing signal to T-cells and new infiltrating macrophages.

Both trapped macrophages and schwann cells/oligodendrocytes present myelin on their surface bound to MHC. The infiltrating T-cells bind the presented myelin on trapped macrophage and schwann cells/oligodendrocytes and destroy them. The result such destruction is demyelination. The observations in the following studies support such a sequence of events.

5 Tsunoda, *et al.*, (1997⁵¹⁸) show that the first T-cells infected in the nervous system are neurons and that the initial limited inflammation in the gray matter subsides concurrently with the decline in neuronal apoptosis. Similar observations are reported by Ha-Lee, *et al.*, (1995⁵¹⁹).

10 According to Lipton, *et al.*, (1995⁵²⁰) virus antigen(s) was first detected in the white matter on day 14 post inoculation. On days 14 and 22, virus antigen(s) was occasionally seen within long stretches of axons extending from the gray matter into anterior white matter (*Ibid*, Fig 2A). MOMA-2-positive cells (MOMA-2 is a monoclonal antibody to macrophages), some of which contained virus antigen(s), were observed in 15 close proximity to infected axons (*Ibid*, Fig. 2A). This observation suggests that TMEV leaves the gray matter by axonal spread, is released from the axoplasm as motor neurons, and then secondarily infects macrophages in the white matter. The fact that motor neurons are the principle virus target in the acute gray matter phase of infection and the predominantly anterolateral location of virus antigen-positive cells in the white mater on 20 days 14, 22, and 29 support this conclusion. Increasing umber of virus antigen-positive, MOMA-2-positive cells appeared in the thoracic cord white matter between days 14 and 49 and then remained at this level of infection until day 73. However, only a small fraction of MOMA-2-positive cells contained virus antigen(s) during this period (*Ibid*, Fig. 2B). The early infiltration and apparent spread of these cells from anterior to posterior in 25 the spinal cord, with a tendency for virus antigen-positive cells to be found at the periphery of advancing edges of lesions (*Ibid*, Fig 3), also supports this conclusion. Based on these observation Lipton, *et al.*, concluded that at least some of the MOMA-2-positive cells have a hematogenous origin, and that infection occurs upon entry of these cells into the CNS.

Miller, et al., (1997⁵²¹) reports the temporal appearance of T-cell response to viral and known encephalitogenic myelin epitopes in TMEV-infected SJL/J mice. Clinical signs being approximately 30 days after infection and display chronic progression with 100% of the animals affected by 40-50 days postinfection. Ultraviolet light (UV)-
5 inactivated TMEV produced a T-cell proliferation in spleen of infected mice both at day 33 postinfection, concomitant with onset of clinical signs, and at day 87. In contrast, at 33 postinfection, the major encephalitogenic epitope on myelin proteolipid protein (PLP139-151 and PLP178-191) and myelin basic protein (MBP84-104) did not produce T-cell proliferation in spleen, cervical or pooled peripheral lymph nodes. However, a response to
10 PLP139-151 was observed in all lymphoid compartment at day 87 postinfection. Similar temporal observations are associated with the appearance of CD4+ Th1-mediated delayed-type hypersensitivity (DTH) responses. The immunodominant TMEV VP2 70-86 epitope produced DTH at all times tested. In contrast, the PLP139-151 epitope first produced DTH only at day 52, persisting through day 81 postinfection (Ibid, Fig. 1C). Assessment
15 of DTH to a larger panel of encephalitogenic myelin epitope during late chronic disease (164 days postinfection), showed persistence of peripheral T-cell reactivity to both VP2 70-86 and PLP178-151 and appearance of responses to multiple, less immunodominant myelin epitopes including PLP56-70, PLP178-191, and the immunodominant myelin oligodendrocyte glycoprotein epitope (MGO92-106) (Ibid, Fig 1d). The study calls these
20 observations "epitope spreading" and defines it as the process whereby epitopes distinct from and non-cross-reactive with an inducing epitope become major targets of an ongoing immune response. The longer macrophages are trapped in white matter, the higher the concentration of presented epitopes on cell surface. Since "rare" epitopes require longer macrophage residence time to accumulate at high enough concentrations, the reported
25 epitope spreading indicates abnormally long macrophage residence time, or abnormally high macrophage trapping.

b) Human studies

Numerous studies report similar observations in all autoimmune diseases. Consider T-cell infiltration as an example. For the sake of brevity, in every disease we
30 report observations which relate to different aspects of the above models.

(1) Diabetes

1. According to the "excessively slow" DC model, tissue cell destruction follows T-cell infiltration. T-cell infiltration, or insulitis, was extensively reported in pre-diabetic and recent-onset diabetic patients, see, for instance, Signore (1999⁵²², a review), Foulis (1991⁵²³), Foulis (1984⁵²⁴).

5

2. Coxsackie B4 virus infect pancreatic β -cells inducing limited β cell death (Roivainen 2000⁵²⁵). The limited β -cell destruction does not result in diabetes. However, according to the two peak model, the "trigger apoptosis" result in T-cell infiltration. According to the excessively slow DC model, in individual harboring a GABP virus the T-cell induced apoptosis might result in diabetes. Consistent with this prediction, some 10 recent studies found a strong association between Coxsackie B4 virus infection and onset of insulin-dependent diabetes mellitus in humans (Andreolletti 1998⁵²⁶, Andreolletti 1997⁵²⁷, Frisk 1997⁵²⁸, Clements 1995⁵²⁹). If Coxsackie B4 is a GABP virus, and can 15 infect DC, the cellular events resulting from a Coxsackie B4 viral infection resemble the events of a TMEV infection (see above).

(2) Multiple sclerosis (MS)

1. According to the "excessively slow" DC model trapped DC show high expression of B7, specifically B7.2 (also called CD86). Therefore, plaque from MS patients, and specifically trapped macrophages, should show high expression of B7.

20 Consider the following studies.

Infiltrating macrophages in brain sections from MS patients showed significant B7 immunoreactivity, in contrast to normal brains which showed no B7 immunoreactivity (De Simone 1995⁵³⁰). Another study found B7.1 staining in plaque from MS patients localized predominantly to lymphocytes in perivenular inflammatory cuffs, and B7-2 staining 25 predominantly on macrophages in inflammatory infarcts (Windhagen 1995⁵³¹).

2. According to the "excessively slow" DC model trapped DC express chemokine, such as MIP-1 α , MIP-1 β and RANTES. Therefore, plaque from MS patients, and specifically trapped macrophage, should show high expression of these chemokines. Consider the following studies.

A study measured expression of the CC chemokines MIP-1 α , MIP-1 β , and RANTES in brain tissue from MS patients using reverse transcriptase-polymerase chain reaction techniques. Both MIP-1 β and RANTES were significantly elevated in brain tissue of MS patients. In addition, MIP-1 α was also increased, although not significantly. 5 Immunohistochemistry revealed that MIP-1 α and MIP-1 β immunoreactivity was predominantly found in perivascular and parenchymal macrophages containing myelin degradation products (Boven 2000⁵³²)

(3) Psoriasis (Ps) and atopic dermatitis (AD)

1. The effectiveness of the immune system deteriorates with age (see reviews 10 Khanna 1999⁵³³, Ginaldi 1999⁵³⁴), which might explain the increased incidence of infectious diseases in the aged. Consider an individual harboring a persistent infection of a GABP virus in DC (for instance, cytomegalovirus). At every age, the balance between two forces, the virus drive to replicate, and the capacity of the immune system to control or clear the infection, determines the viral genome copy number present in infected cells. 15 A decline in immune system effectiveness, therefore, increases viral genome copy number. Consistent with that conclusion, Liedtke, et al., (1993⁵³⁵) showed an increase in the prevalence of herpes simplex virus 1 (HSV-1) neuronal latency with age.

Increase in viral genome copy number intensifies microcompetition, which slows DC and result in higher [Ag] and [B7] on surface of DC reaching the draining lymph node. 20 The increase in [Ag] and [B7] increases [DC•T], which increases the probability of Th1 vs. Th2 differentiation. This argument predicts a decline in Th2 and increase in Th1 autoimmune diseases with age. Consider the following evidence.

Atopic dermatitis (AD), is a Th2 disease, while psoriasis (Ps) is a Th1 disease. A study systematically examined patients attending a dermatology clinic for the presence of 25 AD and/or Ps. Nine hundred and eighty-three patients were studied - 224 with AD, 428 with Ps, 45 with both AD and Ps, and 286 controls. The results showed that 16.7% of the AD patients had also Ps, and 9.5% of Ps patients had AD. In consecutive occurrences, Ps generally followed AD (Beer 1992⁵³⁶). Out of the 45 patients with both AD and Ps, 26 patients had onset of AD first and Ps later in life (average age = 10 and 26, respectively), 9

subjects (all children) had simultaneous onset of AD and Ps, and 1 patient had first onset of Ps at the age of 16, followed by AD+Ps at the age of 18 and return to Ps.

2. Increase in CTLA4Ig decreases [DC•T] (see formula above). As a result, T-cell induced apoptosis decreases which decreases inflammation (DC infiltration, T-cell infiltration, etc). Consider the following studies.

Patients with psoriasis vulgaris received four intravenous infusions of the soluble chimeric protein CTLA4Ig (BMS-188667) in a 26-wk, phase I, open label dose escalation study. Clinical improvement was associated with reduced cellular activation of lesional T-cells and DC. Concurrent reductions in B7.1 (CD80), B7.2 (CD86) were detected on 10 lesional DC, which also decreased in number within lesional biopsies. Skin explant experiments suggested that these alterations in activated or mature DCs were not the result of direct toxicity of CTLA4Ig for DC (Abrams 2000⁵³⁷). Based on these observations, Abrams, *et al.*, concluded that "this study highlights the critical and proximal role of T-cell activation through the B7-CD28/CD152 costimulatory pathway in maintaining the 15 pathology of psoriasis, including the newly recognized accumulation of mature DCs in the epidermis."

3. According to the "excessively slow" DC model trapped DC show high expression of B7, specifically B7.2 (also called CD86). Therefore, lesions from AD and Ps patients, and specifically trapped DC, should show high expression of B7. Moreover, 20 since DC increase B7 expression while migrating out of tissue, in case of Langerhans cells, while migrating from epidermis to dermis and then lymph vessel, B7 expression on Langerhans cells in dermis should be higher than cells in epidermis. Consider the following studies.

A study measured the expression of co-stimulatory molecules in AD and Ps 25 patients. B7.2 and B7.1 were detected on dendritic-shaped cells not only in the epidermis but also in the dermis in the inflammatory lesions of atopic dermatitis (n = 12). B7.2 was expressed in all cases (100%), while B7.1 was expressed in only five cases (42%). These molecules were not detected in normal control subjects (n = 8) (Ohki 1997⁵³⁸). Neither B7.1 nor B7.2 was detected on keratinocytes. Stronger expression of B7.2 over B7.1 was

also observed in psoriasis vulgaris (n = 11). The expression rate of these molecules on Langerhans cells increased in the dermis.

4. A persistent infection of DC with a GABP virus increases the probability of developing an autoimmune disease. Moreover, an increase in viral load should exacerbate 5 the disease. Consider the following studies.

To detect active infection a study compared the antigen expression of cytomegalovirus (CMV), a GABP virus, in peripheral blood mononuclear cells (PBMC) from psoriatic patients (n = 30) with healthy volunteers (n = 65). The results showed higher CMV antigenaemia in psoriasis (43%) compared with healthy laboratory staff 10 (12%, P < 0.01) and blood donors (6%, P < 0.001) (Asadullah 1999⁵³⁹).

Another study reports the development of psoriasis vulgaris in Four patients suffering from immune deficiency related to HTLV III, a GABP virus. The psoriasis was extensive, exsudative, and almost refractory to therapeutical approaches. The bulk of dermal infiltrating mononuclear cells were CD8+ T lymphocytes (Steigleder 1986⁵⁴⁰).

15 HIV is a GABP virus. According to a recent review (Mallon 2000), "psoriasis occurs with at least undiminished frequency in HIV-infected individuals." Moreover, according to the paper, "It is paradoxical that, while drugs that target T lymphocytes are effective in psoriasis, the condition should be exacerbated by HIV infection." See also the review by Montazeri, *et al.*, (1996⁵⁴¹). Another study reported clinical improvement of 20 HIV-associated psoriasis in parallel with a reduction in HIV viral load induced by effective antiretroviral therapy (Fischer 1999⁵⁴²).

4. Other autoimmune diseases

There many more autoimmune diseases not discussed above. Some are asthma, rheumatoid arthritis and thyroiditis. As predicted by the excessively slow DC and the two 25 peak models, studies with patients and animal models of these diseases report observations similar to the ones already mentioned. For instance, studies in animal models of asthma showed that DC collect antigens in the airways, upregulate [Ag] and [B7], migrate to the thoracic lymph nodes where they present the antigens to T cells (Vermaelen 2000⁵⁴³).

Other studies showed that DC are essential for development of chronic eosinophilic airway inflammation in response to inhaled antigen in sensitized mice (Lambrecht 2000A⁵⁴⁴, Lambrecht 2000B⁵⁴⁵, Lambrecht 1998⁵⁴⁶). More studies showed the significant role of B7 in allergic asthma (Mathur 1999⁵⁴⁷, Haczku 1999⁵⁴⁸, Padrid 1998⁵⁴⁹, Keane-5 Myers 1998⁵⁵⁰). Similar observations were reported in rheumatoid arthritis (see, for instance, Balsa 1996⁵⁵¹, Liu 1996⁵⁵²), and thyroditis (see, for instance, Wantanabe 1999⁵⁵³, Tandon 1994⁵⁵⁴).

VI. Discovery 6: Other disruptions of GABP pathway

1. Drug induced molecular disruptions

10 Microcompetition disrupts the GABP pathway. Some drugs also disrupt this pathway. As a result these drugs induce "side effects" similar to the clinical symptoms characteristic of microcompetition. Some of these side effects are weight gain, insulin resistance, and hypertension. The following sections propose the mechanism underlying these side effects.

15 a) *Cytochrome P450*

Three distinct pathways of arachidonic acid (AA) oxidation have been described. The enzyme systems involved are regiospecific and stereospecific. Of the three pathways, the products of the cyclooxygenase and lipoxygenase pathways have been extensively researched. Research on the products of the "third pathway", the cytochrome P450-dependent monooxygenases, is less extensive. The "third pathway", mediated by CYP enzymes, uses NADPH and molecular oxygen in a 1:1 stoichiometry. Three types of oxidative reactions are known to occur. Olefin epoxidation (epoxigenases) produces 4 sets of regio-isomers, the epoxyeicosatrienoic acids (EETs), specifically, the (5,6-), (8,9-), (11,12-) and 14,15-EETs. Allylic oxidation produces hydroxyeicosatetraenoic acids (HETEs), specifically, (5-), (8-), (9-), (11-), (12-) and 15-HETEs. Omega oxidation produces the 19- and 20-HETEs. These sets are summarized in figure 13.

b) Arachidonic acid metabolites activate ERK

Rabbit VSMCs were treated with the vehicle dimethyl sulfoxide (DMSO) alone or 20 μ M PD98059 (PD) for 4 h and then exposed to 0.25 μ M 12(R)-, 12(S)-, 15, or 20-hydroxyeicosatetraenoic acid (HETE) for 10 min. Figure 14 presents MAP kinase activity in these cells (Muthalif 1998⁵⁵⁵, Fig. 3A).

The study also showed that 20-HETE specifically activated ERK1 and ERK2 (Ibid, Fig 3D). Similar activation of MAPK by 12-, and 15-HETE are reported in Wen 1996⁵⁵⁶ and Rao 1994⁵⁵⁷. Another study tested the effect of 14,15-epoxyeicosatrienoic acid (EET) on ERK activation. LLCPKc14, an established proximal tubule epithelial cell line derived from pig kidney, were treated with 14,15-EET (20 μ m) for 15 min, then tyrosine phosphorylated proteins in cell lysates were immunoprecipitated with anti-phosphotyrosine antibodies and immunoblots probed with an antibody which recognizes ERK1 and ERK2. The results showed that 14,15-EET stimulated ERK1 and ERK2 phosphorylation (Chen 1999⁵⁵⁸, Fig 2D).

To summarize, 12(S)-, 15, or 20-HETE and 14,15-EET activate ERK. In other words, these arachidonic acid metabolites are ERK agents.

c) 12(S)-, 15, or 20-HETE and 14,15-EET CYP specific enzymes

The following table lists a few cytochrome P450 enzymes which produce ERK agents metabolites. We call these enzymes CYP-ERKs. When the study is tissue specific, the tissue type is mentioned in the reference column.

Enzyme	ERK agent product	Reference*
CYP1A2	14,15-EET	Rifkind 1995 (human liver)
CYP2B4	14(R),15(S)-EET	Zeldin 1995 (lung)
CYP2C8	14,15-EET	Rifkind 1995 (human liver)
CYP2C9	15(R)-HETE	Bylund 1998, 12-HETE
		Rifkind 1995 (human liver)
CYP2C19	14,15-EET	Bylund 1998, Keeney 1998 (14S 15R, skin keratinocytes)
	12R-HETE	Keeney 1998 (skin keratinocytes)
	15R-HETE	Keeney 1998 (skin keratinocytes)

CYP2C23	14,15-EET	Imaoka 1993 (rat kidney)
CYP2C29	14,15-EET	Luo 1998
CYP2C39	14,15-EET	Luo 1998
CYP2C37	12-HETE	Luo 1998

*Bylund 1998⁵⁵⁹, Imaoka 1993⁵⁶⁰, Zeldin 1995⁵⁶¹, Rifkind 1995⁵⁶², Luo 1998⁵⁶³, Keeney 1998⁵⁶⁴

d) Drug inhibition of CYP-ERK and microcompetition-like diseases

5 Microcompetition reduces the expression of GABP stimulated genes and increases the expression of GABP suppressed genes. Inhibition of an ERK agent produces the same effect. Consider a drug which only inhibits CYP-ERK. That is, the drug has no other chemical reactions, such as inhibition of another enzyme. Call such a drug an "empty" drug. An empty drug should produce the same clinical profile as microcompetition.

10 The following table lists drugs which inhibit CYP-ERKs and their microcompetition-like side effects (mostly weight gain, some insulin resistance and atherosclerosis).

Drug	Cytochrome P450 (CYP type)	Microcompetition-like symptoms
Cytochrome P450 inhibitors		
Phenytoin	Kidd 1999 ⁵⁶⁵ (CYP2C9) Ring 1996 ⁵⁶⁶ (CYP2C9) Miners 1998 ⁵⁶⁷ (CYP2C9)	Egger 1981 ⁵⁶⁸
Glipizide	Kidd 1999 ⁵⁶⁹ (CYP2C9)	Campbell 1994 ⁵⁷⁰
Carbamazepin	Petersen 1995 ⁵⁷¹ (CYP2C9) Meyer 1996 ⁵⁷² (through drug interaction)	Hogan 2000 ⁵⁷³ Mattson 1992 ⁵⁷⁴
Valproic Acid, sodium valproate	Sadeque 1997 ⁵⁷⁵ (check) (CYP2C9)	Bruni 1979 ⁵⁷⁶ Egger 1981 ⁵⁷⁷ Zaccara 1987 ⁵⁷⁸ Mattson 1992 ⁵⁷⁹ Sharpe 1995 ⁵⁸⁰
Losartan	Song 2000 ⁵⁸¹ (CYP2C9) Meadowcroft 1999 ⁵⁸² (CYP2C9) Miners 1998 ⁵⁸³ (CYP2C9)	Camargo 1991 ⁵⁸⁴
Simvastatin	Transon 1996 ⁵⁸⁵ (CYP2C9)	Matthews 1993 ^{586,1}
Olanzapine	Ring 1996 ⁵⁸⁷ (CYP2C9)	Osser 1999 ⁵⁸⁸ Koran 2000 ⁵⁸⁹

Clozapine	Ring 1996 ⁵⁹⁰ (CYP2C9) Fang 1998 ⁵⁹¹ (CYP2C9) Prior 1999 ⁵⁹² (CYP1A2, CYP2C19)	Osser 1999 ⁵⁹³
Fluvoxamine Fluoxetine (Prozac)	Olesen 2000 ⁵⁹⁴ (CYP1A2, CYP2C19) Miners 1998 ⁵⁹⁵ (CYP2C9) Schmider 1997 ⁵⁹⁶ (CYP2C9)	Harvey 2000 ^{597,II} Sansone 2000 ⁵⁹⁸ Michelson 1999 ^{599,II} Darga 1991 ^{600,II}
Tolbutamide	Ring 1996 ⁶⁰¹ (CYP2C9) Miners 1998 ⁶⁰² (CYP2C9) Lasker 1998 ⁶⁰³ (CYP2C9, CYP2C19)	Wissler 1975 ^{604,II} Ballagi-Pordany 1991 ^{605,III}
Anastrozole	Grimm 1997 ⁶⁰⁶ (CYP1A2, CYP2C9)	Wiseman 1998 ⁶⁰⁷ Lonning 1998 ⁶⁰⁸ Buzdar 1998 ⁶⁰⁹ Jonat 1997 ⁶¹⁰ Buzdar 1997 ⁶¹¹ Hannaford 1997 ⁶¹² Buzdar 1997 ⁶¹³ Buzdar 1996 ⁶¹⁴ Jonat 1996 ⁶¹⁵
Nelfinavir (PI)	Khaliq 2000 ⁶¹⁶ (CYP2C19) Lillibridge 1998 ⁶¹⁷ (CYP2C19, CYP1A2) ^V	VI
Ritonavir (PI)	Muirhead 2000 ⁶¹⁸ (CYP2C9) Kumar 1999 ⁶¹⁹ (CYP2C9, CYP2C19) Kumar 1996 ⁶²⁰ (CYP2C9) Eagling 1997 ⁶²¹ (CYP2C9)	VI
Amprenavir (PI)	Fung 2000 ⁶²² (CYP2C9)	VI
Saquinavir (PI)	Eagling 1997 ⁶²³ (CYP2C9)	VI
Cytochrome P450 inducers		
Nifedipine	Fisslthaler 2000 ⁶²⁴ (CYP2C9)	Krakoff 1993 ⁶²⁵ Maccario ⁶²⁶ Andronico 1991 ^{627,IV}

I Increase in BMI was associated with smaller decrease in common femoral arterial stiffness.

II Fluoxetine produces a transient weigh loss leading to gain in body weight in the long term.

5

III Tolbutamide induced atherosclerosis.

IV Nifedipine reduced insulin resistance.

V Inhibition occurs at supratherapeutic concentrations.

VI Replacing, or not including a protease inhibitor in therapy was associated with attenuated fat distribution abnormalities and insulin resistance (Barreiro 2000⁶²⁸, Mulligan 2000⁶²⁹, Gervasoni 1999⁶³⁰, Carr 2000⁶³¹, Martinez 2000⁶³², see also review, Passalari 2000⁶³³).

5 Drugs are not "empty." Drugs have other chemical reactions aside from inhibition of CYP-ERK. Take a microcompetition induced clinical symptom, such as weight gain. There are three possible events. The other chemical reactions might increase, decrease or not change body weight. Take the combined effect of CYP-ERK inhibition and the other chemical reactions. The H_0 hypothesis assumes a uniform (random) distribution of these 10 events, that is, the probability of every such event is 1/3 so that the probability that a CYP-ERK inhibitor causes weight gain is 1/3. The probability that each of two CYP-ERK different inhibitors cause weight gain is $(1/3)*(1/3)$. In the table above there are 16 drugs, 15 CYP-ERK inhibitors and 1 CYP-ERK inducer. The probability that the 15 inhibitors 15 increase weight and the 1 inducer reduces weight, under the H_0 assumption, is $(1/3)^{16}$ or < 0.0001.

2. Mutation, injury, and diet induced molecular disruptions

See section on obesity.

VII. Discovery 7: Treatment

A healthy system is in stable equilibrium. Microcompetition establishes a new, 20 stable equilibrium which reflects the modified availability of transcription resources. Assume that the two equilibria are points in a measure space, that is, a space with a unit and direction. In fact, almost all molecular and clinical measurements define such a space. Assume that any point in this space indicates a disease, and that the severity of the disease increases with the distance from the healthy system equilibrium. In this space, the 25 distance between the microcompetition equilibrium and the healthy system equilibrium is small. The small distance between equilibria results in slow progression of the microcompetition diseases. Atherosclerosis or cancer, for instance, may take years to become clinically evident. Consider figure 45.

Denote difference between equilibria with Δ , and denote difference between the microcompetition equilibrium (M_E) and the healthy system equilibrium (H_E) with $\Delta(M_E - H_E)$. Most successful treatments create a new equilibrium (T_E) somewhere between M_E and H_E . The small distance between the microcompetition equilibrium and the healthy system equilibrium poses a challenge in measuring the effectiveness of such treatments.

5 Since T_E is between M_E and H_E , the distance between T_E and M_E is even smaller than the distance between H_E and M_E , $\Delta(T_E - H_E) < \Delta(M_E - H_E)$. We assumed that the rate of disease progression/regression, of the microcompetition diseases is a function of the distance between equilibria. Hence, the difference in rate of disease progression between the rate

10 of progression after treatment and during microcompetition is even smaller. Since the clinical changes induced by the move from point H_E to M_E are usually difficult to measure, the clinical changes induced by the move from point M_E to T_E are also difficult to measure (most likely even more difficult).

15 To address this issue, the following sections report results of studies which meet two conditions. One, since treatment effectiveness is reflection of the distance between two states of system equilibrium, only *in vivo* studies are included. Second, since the effect of treatment is slow to occur, only results of clinical and animal studies conducted over extended periods of time, at least a few weeks, are included. In some cases, the included studies report results which were obtained after years of treatment.

20 The studies are divided into three sections. The first section includes studies with GABP kinase agents. These agents stimulate the phosphorylation of a GABP kinase, such as ERK or JNK. The second section includes studies with antioxidation agents. These agents reduce oxidation stress in infected cells. The third section includes studies with viral N-box agents. These agents reduce the concentration of viral DNA in the host.

25 Consider figure 46. The targets of these treatments are marked with filled boxes. Microcompetition between viral N-box and cellular genes for GABP is marked with a thick arrow.

1. GABP kinase agents

5 A GABP kinase agent stimulates the phosphorylation of a GABP kinase, such as ERK or JNK. The increase in the GABP kinase phosphorylation increases transcription of GABP stimulated genes and decreases transcription of GABP suppressed genes (see above). Since, microcompetition has the opposite effect on these classes of genes, a GABP kinase agent leads to slower progression of the microcompetition diseases.

a) *Dietary fiber***(1) Effect on sodium butyrate**

10 Dietary fiber lead to the production of sodium butyrate, a short chain fatty acid (SCFA), during anaerobic fermentation in the colon.

(2) Effect on ERK

Sodium butyrate is an ERK agent (see above). As a result, sodium butyrate phosphorylates GABP, which, in turn, potentiates binding of p300.

(3) Effect on microcompeted genes**15 (a) *Metallothionein***

Microcompetition with a GABP virus decreases expression of metallothionein (see above). Treatment with sodium butyrate activated the metallothionein (MT) gene in certain carcinoma cell lines. Consider the following studies.

20 Different embryonal carcinoma cell lines show different basal levels of MT mRNA. For instance, the F9 cell line shows intermediate basal levels of MT expression, while PC13, a similar cell line, shows very high levels. Since OC15S1 stem cells usually have very low basal levels, these cell were chosen for testing the effect of sodium butyrate on MT mRNA. OC15 embryonal carcinoma (OC15 EC) cells differentiate during 4 days in culture in the presence of retinoic acid (OC15 END). OC15 EC and 25 OC15 END cells were treated with sodium butyrate and the MT mRNA levels were analyzed by Northern blots and quantified by densitometry. Figure 47 presents the results (Andrews 1987⁶³⁴, Fig 1).

The results show that sodium butyrate increases MT mRNA in both undifferentiated OC15 EC and differentiated OC15 END cells. F9 EC cells, although having higher MT basal mRNA levels, responded similarly to sodium butyrate treatment. It should be noted that the effect of sodium butyrate was specific since sodium propionate and sodium acetate, the other two products of bacterial fermentation in the colon, had no effect on MT mRNA levels.

Another study used ROS 17/2.8, a cloned rat osteosarcoma cell line. In this study, sodium butyrate induced MT synthesis in a dose-dependent manner (Thomas 1991⁶³⁵).

A third study used rat primary, non-transformed hepatocytes. Sodium butyrate treatment of these cells produced a 2-4 fold increase in MT mRNA (Liu 1992⁶³⁶, Fig 6).

It is interesting that in the non-transformed cells sodium butyrate increased MT mRNA 2-4 fold, while in some carcinoma cell lines the increase was 20 fold (see, for instance, the increase in MT mRNA in OC15 embryonal carcinoma cells above). A compelling explanation is that the relatively low basal MT mRNA in OC15 cells result from microcompetition with viral DNA present in these cells. In such a case, sodium butyrate should show a larger effect in OC15 relative to the non-transformed cells.

(4) Effect on clinical symptoms

(a) *Obesity, insulin resistance, hypertension*

The Coronary Artery Risk Development in Young Adults (CARDIA) Study, a multicenter population-based cohort study, tested the change in cardiovascular disease (CVD) risk factors over a 10 year period (1985-1986 to 1995-1996) in Birmingham, AL; Chicago, IL; Minneapolis, MN; and Oakland, CA. A total of 2,909 healthy black and white adults, age 18 to 30 years at enrollment, were included in the study. The results showed that dietary fiber consumption was inversely associated with body weight in both blacks and whites. At all levels of fat intake, subjects consuming the most fiber gained less weight than those consuming the least fiber. Moreover, fiber consumption was also inversely associated with fasting insulin levels and systolic and diastolic blood pressure in both black and white subjects. (Ludwig 1999⁶³⁷).

Fifty-two overweight patients, mean body mass index (BMI) = 29.3, participated in a 6 month, randomized, double-blind, placebo-controlled, parallel group design, study. The treatments included an energy restricted diet plus dietary fiber supplement of 7 g/day, or the diet plus placebo. The results showed that the fiber treated patients lost 5 significantly more weight relative to the placebo treated patients (5.5 ± 0.7 kg, vs. 3.0 ± 0.5 kg, $P = 0.005$). Hunger feelings, measured using visual analogue scales (VAS), were significantly reduced in the fiber-treated group, whereas a significant increase was seen in the placebo group ($P < 0.02$) (Rigaud 1990⁶³⁸).

In another study, ninety-seven mildly obese females participated in 52 week, 10 randomized, double-blind, placebo-controlled trial, study. The treatment consisted of a restricted diet providing 1,200 kcal/day and a dietary fiber supplement of 7 g/day for 11 weeks, (part I), followed by a diet providing 1,600 kcal/day and a dietary fiber supplement of 6 g/day for 16 weeks (part II). Finally placebo was withdrawn and all remaining 15 compliant subjects were given a dietary fiber supplement of 6 g/day and an ad libitum diet for the rest of the period (part III). Initial body weights were comparable in the fiber group and placebo group. The results showed that during part I, weight reduction in the fiber supplemented group was significantly higher compared to the placebo group (4.9 kg and 3.3 kg, respectively, $P = 0.05$). Accumulated weight reduction during part II remained 20 significantly higher in the fiber supplemented group compared to the placebo group (3.8 kg and 2.8 kg, respectively, $P < 0.05$). (Total weight loss in the fiber group after 52 weeks was 6.7 kg). The probability of adherence to the treatment regimen was significantly 25 higher in the fiber group from week 13 and onwards ($P < 0.01$). Initial blood pressures were comparable. A significant reduction of systolic blood pressure was observed in both groups. However, a significant reduction of diastolic blood pressure was observed in the fiber group only ($P < 0.05$) (Ryttig 1989⁶³⁹).

These studies show that dietary fiber consumption induces weight loss, reduces insulin resistance and attenuates hypertension.

(b) *atherosclerosis*

30 Soybean hull is a rich source of dietary fiber. Therefore, a diet enriched with soybean hull should attenuate atherosclerosis. Consider the following study.

Twenty five monkeys were divided into 5 groups, each subjected to a different diet. The T1 group received the basal diet; T2, the basal diet plus palm oil; T3, the basal diet plus palm oil and soybean hull; T4, the basal diet plus cholesterol, and T5, the basal diet plus cholesterol and soybean hull. The diets were given for a period of 8 months with water provided ad lib. At the end of the experiment thorax surgery was performed on the animals under general anesthesia. The aorta was removed for histopathological observation and stained with hematoxylin and eosine. Histopathological observation of the aorta showed that adding soybean hull to the basal diet + palm oil diet reduced formation of atherosclerotic lesions from 46.67 of the T1 group to 31.25% in the T3 group. Adding soybean hull to the basal diet + cholesterol reduced formation of lesion from 86.25 to 53.38% (Piliang 1996⁶⁴⁰). Based on these observations, Piliang, et al., concluded that "the soybean hull given in the diet has the ability to prevent the development of atherosclerosis in the aorta of the experimental animals."

15 (c) *Cancer*

Consumption of dietary fiber is associated with reduced risk of several types of cancer (Kim 2000⁶⁴¹, Madar 1999⁶⁴², Camire 1999⁶⁴³, Mohandas 1999⁶⁴⁴, Heaton 1999⁶⁴⁵, Cummings 1999⁶⁴⁶, Ravin 1999⁶⁴⁷, Reddy 1999A⁶⁴⁸, Reddy 1999B⁶⁴⁹, Earnest 1999⁶⁵⁰, Kritchevsky 1999⁶⁵¹, Cohen 1999⁶⁵²).

20 (b) *Acarbose*

25 Acarbose is a α -glucosidase inhibitor, a new class of drugs used in the treatment of diabetes mellitus. α -glucosidases are enzymes released from the brush border of the small intestine. The enzymes hydrolyze di- and oligosaccharides, derived from diet and luminal digestion of starch by pancreatic amylase, into monosaccharides. Since only monosaccharides are transported across intestinal cell membranes, α -glucosidase inhibition reduces carbohydrate absorption.

(1) *Effect on sodium butyrate*

Acarbose inhibits starch digestion in the human small intestine, and therefore, increases the amount of starch available for microbial fermentation to acetate, propionate, and butyrate in the colon. A study examined fermentations by fecal suspensions obtained

from subjects who participated in an acarbose-placebo crossover trial. The results showed that the concentrations of acetate, propionate, and butyrate were 57, 13, and 30% of the total final concentrations, respectively, for acarbose treated subjects and 57, 20, and 23% for untreated subjects (Wolin 1999⁶⁵³, Table 1, the statistical significance for the difference between acarbose and placebo was $P < 0.002$ for propionate, and $P < 0.02$ for butyrate). Based on these results, Wolin, *et al.*, concluded that "our results show that acarbose treatment results in decreases in the activities of colonic bacteria ... that form propionate and an increase in the activity of bacteria that produce butyrate."

To determine the effects of acarbose on colonic fermentation, another study gave subjects 50-200 mg acarbose, or placebo (cornstarch), three times per day, with meals in a double-blind crossover study. Fecal concentrations of starch and starch-fermenting bacteria were measured and fecal fermentation products were determined after incubation of fecal suspensions with and without added substrate for 6 and 24 h. Substrate additions were cornstarch, cornstarch plus acarbose and potato starch. Dietary starch consumption was similar during acarbose and placebo treatment periods. The results showed that butyrate in feces, measured either as concentration or percentage of total short-chain fatty acids, was significantly greater with acarbose treatment compared to placebo, while propionate was significantly smaller (Wolin 1999⁶⁵⁴, Table 1. $P < 0.0001$). Moreover, butyrate production was significantly greater in fermentations in samples collected during acarbose treatment, whereas production of acetate and propionate was significantly less. Based on their results, Wolin, *et al.*, concluded that "acarbose effectively augmented colonic butyrate production by several mechanisms; it reduced starch absorption, expanded concentrations of starch-fermenting and butyrate-producing bacteria and inhibited starch use by acetate- and propionate-producing bacteria."

25

(2) Effect on clinical symptoms

(a) Obesity

Acarbose or placebo was administered to non-insulin dependent diabetes (NIDDM) patients for 1 year in a randomized, double-blind, placebo-controlled, parallel design study. The effect of acarbose treatment on change in body weight is summarized in figure 48 (Wolever 1997⁶⁵⁵, Fig. 1).

After one year, the 130 subjects treated with acarbose each experienced an average weight loss of 0.46 ± 0.28 kg. In contrast, the 149 subject treated with placebo each experienced a 0.33 ± 0.25 kg weight gain ($P = 0.027$). Interestingly, acarbose had no effect on energy intakes, nutrient intakes, or dietary patterns.

5 c) *Vanadate*

An ERK phosphatase is an enzyme that inactivates ERK by dephosphorylation of either Thy, Tyr, or both residues (see above). The class of all ERK phosphatases includes, for instance, PP2A, a type 1/2 serine/threonine phosphatase, PTP1B, a protein tyrosine phosphatase, and MKP-1, a dual specificity phosphatase. Inhibition of an ERK phosphatase stimulates ERK phosphorylation. The increase in ERK phosphorylation increases transcription of GABP stimulated genes and decreases transcription of GABP suppressed genes (see above). Since, microcompetition has the opposite effect on these classes of genes, inhibition of an ERK phosphatase leads to slower progression of the microcompetition diseases. Consider vanadate as an example.

15 (1) Effect on PTP

Vanadate (VO_4^{3-}) and vanadate derivatives are general protein tyrosine phosphatase (PTP) inhibitors. Specifically, vanadate, and pervanadate (a general term for the variety of complexes formed between vanadate and hydrogen peroxide) were shown to inhibit the protein-tyrosine phosphatase PTP1B (Huyer 1997⁶⁵⁶).

20 (2) Effect on ERK

PTPs dephosphorylate and deactivate ERK (see above). As general PTP inhibitors, vanadate and vanadate derivatives are expected to activate ERK, an observation reported in several studies (Wang 2000⁶⁵⁷, Zhao 1996⁶⁵⁸, Pandey 1995⁶⁵⁹, D'Onofrio 1994⁶⁶⁰).

(3) Effect on GABP genes

25 (a) *F-type PFK-2/FBPase-2 is GABP stimulated gene*

The bifunctional enzyme 6-phosphofructo-2-kinase (EC 2.7.1.105, PFK-2)/fructose-2,6-bisphosphatase (EC 3.1.3.46 FBPase-2) catalyzes the synthesis and

degradation of fructose-2,6-bisphosphate. The rat PFK-2/FBPase-2 gene (gene A) codes for the fetal (F), muscle (M), and liver (L) mRNAs. Each of these mRNAs originates from a different promoter in the gene. The F-type promoter includes an enhancer in the (-1809-1615) region with three N-boxes at (-1747-1742), (-1716-1710) and (-1693-1688) (Darville 1992⁶⁶¹, Fig. 4). The enhancer stimulated transcription, especially in FTO2B hepatoma cells (Ibid, Table 1). DNase I protection experiments using the enhancer and extracts from FTO2B cell, from C2C12 myoblasts or myocytes, or from liver, but not from muscle, showed one specific footprint corresponding to the middle N-box (Ibid, Fig. 5). Gel retardation assays with extracts from FTO2B and HTC cells, L6 myoblasts and myocytes, and liver, but not muscle, showed a major complex (Ibid, Fig. 6A). When this enhancer fragment was methylated at single purines using dimethylsulfate and subsequently incubated with FTO2B extracts, three contact points were detected within the N-box (Ibid, Fig 4). The three points of methylation interference coincide with contact points identified by the same technique in the two N-boxes of the adenovirus E1A core enhancer which binds GABP. A subsequent study (Dupriez 1993⁶⁶²) showed that changing the GG, essential for ets DNA binding, to CC in both distal and proximal N-boxes decreased promoter activity by 15-20%. Changing GG to CC in the middle N-box decreased promoter activity by 75%. The study also showed that anti-GABP α and anti-GABP β antibodies inhibited formation of complexes on the middle N-box by FTO2B proteins (Ibid, Fig 4, lane 5 and 6). Transfection with recombinant GABP α and GABP β produced shifts that comigrated with these complexes and were inhibited by anti-GABP α antibodies (Ibid, Fig 4, lane 12-16). These observations suggest that the F-type PFK-2/FBPase-2 is a GABP stimulated gene.

GABP viruses microcompete with the F-type PFK-2/FBPase-2 enhancer for GABP. Therefore, viral infection of cells decreases F-type PFK-2/FBPase-2 expression. Moreover, the higher the concentration of viral DNA, the greater the decrease in F-type PFK-2/FBPase-2 expression.

(b) *Vanadate stimulates F-type PFK-2/FBPase-2 transcription*

ERK activation is expected to stimulate transcription of GABP stimulated genes. The rat F-type PFK-2/FBPase-2 gene is a GABP stimulated gene. Therefore, vanadate should stimulate transcription of F-type PFK-2/FBPase-2. Consider the following studies.

5 The effect of sodium orthovanadate by oral administration on liver PFK-2/FBPase-2 mRNA content was measured in rats with streptozotocin (STZ)-induced diabetes. The mRNA content was measured after 3, 5, 7 and 15 days of treatment. The results are presented in figure 49 (Miralpeix 1992⁶⁶³, Fig. 3).

10 Vanadate treatment of diabetic animals produced a progressive increase in liver PFK-2/FBPase-2 mRNA content, reaching a nearly normal level after 15 days. Similar results are reported by Inoue (1994⁶⁶⁴).

15 The F-type PFK-2/FBPase-2 is usually not expressed in liver cells. However, the F-type mRNA levels increase in proliferating cells. Dupreiz, et al., (1993⁶⁶⁵) measured tissue expression of the gene. F-type PFK-2/FBPase-2 mRNA was present in hepatoma, fibroblast, and myoblasts cell lines. The mRNA was found in fetal liver and muscle, the two fetal tissues examined. In adult tissues the mRNA was found in the lung and thymus. In the other adult tissues tested the mRNA was present at much lower concentrations or was undetectable. The highest concentration was in preterm placenta, with a decrease at term. The concentration decreased upon differentiation of L6 myoblasts into myocytes (Ibid, Fig. 2) and in Rat-1 fibroblasts made quiescent by lowering serum concentration in 20 culture from 10 to 0.1%. Moreover, F-type mRNA concentration increased in FTO2B cells upon dexamethasone treatment. Based on these observations, Dupreiz, et al., concluded that the "expression of the F-type mRNA appears to correlate with cell proliferation."

25 Usually, liver tissue shows limited cell proliferation. However, in the Miralpeix 1992 study (see above), vanadate was administered to male Sprague-Dawley rats one week after the animals were treated with a single intravenous injection of streptozotocin (STZ). As it turns out, STZ injection to Sprague-Dawley rats induces high levels of hepatocyte proliferation. Consider the following study.

Hepatocyte proliferation was measured in Sprague-Dawley rats made diabetic by iv injection of STZ. The results showed a 12% increase in the ratio of liver weight to body weight in diabetic rats 8 days after injection compare to normal rats, and a 44% increase at 30 days (Herrman 1999⁶⁶⁶). The results also showed an increase in hepatocyte mitosis to 5 300% of normal at 8 days, a return to normal at 30 days, and a decrease to 25% of normal at 90 days (Ibid, Fig. 1). Based on these results Herrman, *et al.*, concluded that "hepatomegaly observed in streptozotocin-induced experimental diabetes may be due primarily to early hyperplasia."

10 The Miralpeix 1992 study used a "1.4 kilobase rat liver PFK-2/FBPase-2 cDNA probe which corresponds to the mRNA for liver PFK-2/FBPase-2 devoid of the 5' end coding for amino acids 1-90." This probe does not distinguish between F-type and L-type PFK-2/FBPase-2 mRNA. Therefore, the reported increase in PFK-2/FBPase-2 mRNA is, most likely, a result of the increase in F-type PFK-2/FBPase-2 mRNA in hepatocytes induced to proliferate by a streptozotocin injection.

15

(4) Effect on clinical symptoms

(a) Obesity

20 Five week-old Zucker rats, an animal model of obesity and insulin resistance, were divided into three groups of 6 rats: lean (Fa/fa) control, obese (fa/fa) control and obese (fa/fa)-vanadate treated. The rats in the treated group received sodium orthovanadate through drinking water for four months. Obese rats had significantly higher body weight compared to lean controls. However, body weight of vanadate-treated obese decreased 43% to levels comparable to lean controls (Pugazhenthi 1995⁶⁶⁷, Table 1).

25 Similar results were reported by McNeill and Orvig (1996⁶⁶⁸). Wistar rats were divided into two groups, control (8 animals) and treated (11 animals). Treated animals received between 0.3 and 0.5 mmol/kg of bis(maltolato)oxovanadium/day in drinking water over a 77 day period. Beginning at day 56 the treated animals showed reduced weight gain compared to controls (Ibid, Fig. 1, group 2 vs. group 1). (See also Dai 1994⁶⁶⁹, and Bhanot 1994⁶⁷⁰.)

(b) Cancer

Cruz, *et al.*, (1995)⁶⁷¹ tested the antineoplastic effect of orthovanadate on a subcutaneous MDAY-D2 tumor mouse model. Ten week old DBA/2j female mice were injected subcutaneously in the posterior lateral side with 4×10^5 cells in 100 μ l of PBS. On day 5, the mice were divided into two groups. One group received subcutaneous 5 injections of 100 μ l of PBS and another group received 100 μ l of PBS containing 500 μ g of orthovanadate daily. The orthovanadate was administrated subcutaneously on the opposite, tumor-free, posterior lateral side. On day 14, the mice were sacrificed, weighed and tumors were resected and weighed. The results showed decreased tumor growth in treated mice compared to controls (*Ibid*, Fig. 6). In control mice, the tumor weights varied 10 from 0.86-1.74 g, whereas in orthovanadate treated mice, four mice showed no detectable tumors and 11 mice showed tumors varying from 0.08-0.47 g. Orthovanadate treatment reduced tumor growth by more than 85%, sometimes completely inhibiting tumor formation.

Another study tested the chemoprotective effect of vanadium against chemically 15 induced hepatocarcinogenesis in rats. Initiation was performed by a single intraperitoneal injection of diethylnitrosamine (DENa; 200 mg kg⁻¹) followed by promotion with phenobarbital (0.05%) in diet. Vanadium (0.5 ppm) was provided *ad libitum* throughout the experiment in drinking water. The results showed that after 20 weeks vanadium reduced the incidence ($P < 0.01$), total number and multiplicity ($P < 0.001$), and altered the 20 size distribution of visible persistent nodules (PNs) as compared with DENa controls (Bishayee and Chatterjee 1995⁶⁷²). Mean nodular volume ($P < 0.05$) and nodular volume as a percent of liver volume ($P < 0.01$) were also attenuated. Vanadium also caused a large decrease in number ($P < 0.001$) and surface area ($P < 0.01$) of gamma-glutamyltranspeptidase (GGT)-positive hepatocyte foci and in labeling index ($P < 0.001$) 25 of focal cells, coupled with increased ($P < 0.01$) remodeling. The activity of GGT, measured quantitatively, was found to be significantly less in PNs ($P < 0.001$) and non-nodular surrounding parenchyma ($P < 0.01$) of vanadium supplemented rats. Histopathological analysis of liver sections showed well-maintained hepatocellular 30 architecture compared to DENa control. Based on these results, Bishayee and Chatterjee (1995) concluded that "our results, thus, strongly suggest that vanadium may have a unique anti-tumor potential."

See also Liasko 1998⁶⁷³.

(c) Diabetes

5 Numerous *in vivo* studies demonstrated reduced blood glucose in insulin deficient diabetic animals, and improved glucose homeostasis in obese, insulin-resistant diabetic animals, following treatment with vanadate. In human studies, insulin sensitivity improved in NIDDM patients and in some IDDM patient after treatment with vanadate (see recent reviews Goldfine 1995⁶⁷⁴, Brichard 1995⁶⁷⁵)

10 As an example consider the study by Pugazhenthi, *et al.*, (1995, see above). This study also tested the effect of vanadate on diabetes. The obese Zucker rats showed elevated plasma levels of glucose and insulin. Vanadate treatment decreased plasma glucose and insulin levels by 36% and 80%, respectively (*Ibid*, Table 1).

d) PTP1B knockout

(1) Effect on PTP and ERK

15 Gene knockout is a special case of intervention. The results of a PTP1B gene knockout is PTP1B enzyme deficiency. Vanadate inhibits PTP1B (Huyer 1997⁶⁷⁶). Therefore, both PTP1B gene knockout and administration of vanadate result in reduced activity of the PTP1B enzyme. Considering the discussion above, the PTP1B gene knockout effect on clinical symptoms should be similar to the effects of vanadate treatment.

(2) Effect on clinical symptoms

20 (a) *Obesity*
A targeting vector was designed to delete a segment of the mouse homolog of the PTP1B gene. This segment included exon 5 and the tyrosine phosphatase active site in exon 6. The deleted segments were replaced with the neomycin resistance gene. Two separate embryonic stem cell clones that had undergone homologous recombination and possessed a single integration event were microinjected Balb/c blastocysts. Chimeric males were mated with wild-type Balb/c females, and heterozygotes from this cross were mated to product animals homozygous for the PTP1B mutation (Elchebly 1999⁶⁷⁷, Fig 1A). The PTP1B protein was absent in PTP1B null mice (PTP1B(-/-)), and heterozygotes

(PTP1B(+/-)) expressed about half the amount of PTP1B relative to wild type mice (Ibid, Fig. 1B). PTP1B null mice grew normally on regular diet, did not show any significant difference in weight gain compared to wild-type mice and lived longer than 1.5 years without any signs of abnormality and were fertile. To study the effect of PTP1B gene knockout on obesity, PTP1B(--), PTP1B(+/-) and wild type mice were fed a high-fat diet normally resulting in obesity. As expected, the wild-type mice rapidly gained weight. In contrast, the PTP1B(--), PTP1B(+/-) mice were protected from the diet induced weight gain (Ibid, Fig. 5). Based on these results, Elchebly, *et al.*, concluded that PTP1B deficiency results in obesity resistance.

10 Another study reported results of a PTP1B gene disruption. Klaman, *et al.*, (2000⁶⁷⁸) generated PTP1B-null mice by targeted disruption of the ATG coding exon (exon 1). The PTP1B-deficient mice showed low adiposity and protection from diet-induced obesity. The decreased adiposity resulted from reduced fat cell mass without a decrease in adipocyte number. Leanness in PTP1B-deficient mice was associated with 15 increased basal metabolic rate and total energy expenditure.

(b) *Diabetes*

Elchebly, *et al.*, (1999⁶⁷⁹) also tested the effect of PTP1B gene knockout on diabetes. In the fed state, PTP(--) mice given a regular diet showed a 13% reduction and PTP(+/-) a 8% reduction in blood glucose concentration relative to wild type mice (Ibid, Fig. 2A). Fed PTP1B(--), mice on regular diet had circulating insulin levels of about half of wild type fed animals (Ibid, Fig. 2B). The enhanced insulin sensitivity of the PTP1B(--), mice was also observed in glucose and insulin tolerance tests (Ibid, Fig. 3A and 3B). The PTP1B(--), PTP1B(+/-) and wild type mice were also fed a high-fat diet normally resulting in insulin resistant. As expected, the wild-type mice became insulin resistant. 20 In contrast, on a high-fat diet the PTP1B(--), mice showed glucose and insulin concentrations similar to animals on normal diet (Ibid, Table 1). PTP1B(--), mice also showed enhanced insulin sensitivity relative to wild type in both glucose and insulin tolerance tests (Ibid, Fig. 6A, 6B). On high-fat diet, the PTP1B(+/-), mice showed increased fasting concentrations of circulating insulin but similar fasting glucose 25 concentrations relative to animals on normal diet (Ibid, Table 1). Based on these results, Elchebly, *et al.*, concluded that PTP1B deficiency results in enhanced insulin sensitivity.

The PTP1B-deficient mice in Klaman, *et al.*, (2000⁶⁸⁰) showed similar enhanced insulin-stimulated whole-body glucose disposal.

As expected, both a PTP1B deficiency and vanadate treatment result in resistance to obesity and enhanced insulin sensitivity. We speculate that PTP1B gene knockout, in a 5 manner similar to vanadate treatment, also induces cancer resistance.

2. Antioxidants

Microcompetition and oxidative stress both decrease binding of GABP to the N-box. Therefore, microcompetition can be viewed as "excessive oxidative stress." Some 10 antioxidants reduce intracellular oxidative stress. These antioxidants stimulate the binding of GABP to the N-box thereby attenuating the effect of microcompetition on transcription, resulting in slower progression of the microcompetition diseases.

a) Garlic

(1) Effect on oxidative stress

Garlic is a scavenger of free radicals. A study investigated, using high pressure 15 liquid chromatography, the ability of unheated or heated garlic extract to scavenge hydroxyl radical (•OH) generated by photolysis of H₂O₂ (1.2-10 µmoles/ml) with ultraviolet (UV) light and trapped with salicylic acid (500 nmoles/ml). H₂O₂ produced •OH in a concentration-dependent manner as estimated by the •OH adduct products 2,3-dihydroxybenzoic acid (DHBA) and 2,5-DHBA. Garlic extract (5-100 µl/ml) inhibited 20 (30-100%) 2,3-DHBA and 2,5-DHBA production in a concentration-dependent manner (Prasad 1996⁶⁸¹, Fig. 3). Garlic activity was reduced by 10% approximately, when heated to 100 degrees C for 20, 40 or 60 min. Garlic extract also prevented the •OH-induced formation of malondialdehyde (MDA) in rabbit liver homogenate in a concentration-dependent manner (Ibid, Fig. 10). In the absence of •OH, garlic did not affect MDA 25 levels. Based on these results, Pasas, *et al.*, (1996) concluded that "garlic extract is a powerful scavenger of •OH."

Another study examined the antioxidant effects of garlic extract in a cellular system using bovine pulmonary artery endothelial cells (PAEC) and murine macrophages

(J774). The study used intracellular glutathione (GSH) depletion as an index of oxidative stress. Oxidized LDL (Ox-LDL) caused a depletion of GSH. Pretreatment with aged garlic extract inhibited Ox-LDL induced peroxides in PAEC and suppressed peroxides in macrophages in a dose-dependent manner (Ide 1999⁶⁸²). In a cell free system, the aged garlic extract was shown to scavenge H₂O₂ similarly. These results together show that aged garlic extract prevents the Ox-LDL-induced depletion of GSH in endothelial cells and macrophages.

5 (2) Effect on clinical symptoms

10 (a) Atherosclerosis

Garlic attenuates the formation of atherosclerotic plaque. A study involved the de-endothelialization of the right carotid artery of 24 rabbits by balloon catheterization in order to produce myointimal thickening. After 2 weeks the rabbits were randomly assigned to four groups: Group I received a standard diet (standard); Group II received standard diet supplemented with 800 µl/kg body weight/day of the aged garlic extract "Kyolic" (standard + Kyolic); Group III received a standard diet supplemented with 1% cholesterol (cholesterol-enriched); and Group IV received standard diet supplemented with 1% cholesterol and Kyolic (cholesterol-enriched + Kyolic). After 6 weeks, the cholesterol-enriched diet caused a 6-fold increase in serum cholesterol levels (Group III) compared to standard diet (Group I) ($P < 0.05$) (Efendy 1997⁶⁸³, Fig. 1). At 6 weeks, the cholesterol-enriched diet (Group III) showed fatty streak lesions covering approximately $70 \pm 8\%$ of the surface area of the thoracic aorta. The cholesterol-enriched + Kyolic group (Group IV) showed fatty lesions in only $25 \pm 3\%$ of the same surface area (Ibid, Fig. 2A and 2B), which represents a reduction of about 64%. No lesions were present in Groups I and II. The cholesterol-enriched diet also caused an increase in aortic arch cholesterol (2.1 ± 0.1 mg cholesterol/g tissue) which was significantly reduced by Kyolic (1.7 ± 0.2 mg cholesterol/g tissue) ($P < 0.05$). Kyolic significantly inhibited the development of thickened, lipid-filled lesions in the pre-formed neointimas produced by balloon-catheter injury of the right carotid artery in cholesterol-fed rabbits (intima as percent of artery wall, Group III $42.6 \pm 6.5\%$ versus Group IV $23.8 \pm 2.3\%$, $P < 0.01$). Kyolic had little effect in rabbits on a standard diet (Group II $18.4 \pm 5.0\%$ versus Group I $16.7 \pm 2.0\%$). *In vitro* studies showed that Kyolic inhibited smooth muscle proliferation (Ibid, Fig. 5). Based on

these results, Efendy, *et al.*, (1997) concluded that "Kyolic treatment reduces fatty streak development, vessel wall cholesterol accumulation and the development of fibro fatty plaques in neointimas of cholesterol-fed rabbits, thus providing protection against the onset of atherosclerosis."

5 Jain (1978⁶⁸⁴), Jain (1976⁶⁸⁵) and Bordia (1975⁶⁸⁶) reported similar observations. Jain (1978) and Jain (1976) used rabbits fed a 16 week standard or cholesterol-enriched diet supplemented with or without garlic extract. In both studies the results showed marked atherosclerotic lesions in animals fed a cholesterol-enriched diet relative to standard diet. The animals fed a cholesterol-enriched diet supplemented with garlic
10 extract showed attenuated lesion formation. Jain (1978) also reported reduced aorta cholesterol content in garlic treated animals. Bordia (1975) used rabbits fed for 3 months on similar diets. The results showed that garlic attenuated the formation of atherosclerotic plaque and the increase in lipid content of aorta.

15 Garlic treatment resulted in other favorable effects associated with attenuated atherosclerosis. A study measured the elastic properties of the aorta using pulse wave velocity (PWV) and pressure-standardized elastic vascular resistance (EVR) techniques. The subjects included healthy adults ($n = 101$; age 50 to 80 years) who were taking 300 mg/d or more of standardized garlic powder for at least 2 years and 101 age- and sex-matched controls. Blood pressure, heart rate, and plasma lipid levels were similar in the
20 two groups. The results showed that PWV (8.3 ± 1.46 versus 9.8 ± 2.45 m/s; $P < 0.0001$) and EVR (0.63 ± 0.21 versus 0.9 ± 0.44 $m^2 \cdot s^{-2} \cdot mm Hg^{-1}$; $P < 0.0001$) were lower in the garlic group than in the control group (Breithaupt-Grogler 1997⁶⁸⁷, Table 1, Fig. 1). PWV showed significant positive correlation with age (garlic group, $r = 0.44$; control group, $r = 0.52$, Fig. 3) and systolic blood pressure (SBP) (garlic group, $r = 0.48$; control group, $r = 0.54$, Fig. 4). With any degree of increase in age or SBP, PWV increased less in the garlic
25 group than in the control group ($P < 0.0001$, Fig. 3, Fig. 4). ANCOVA and multiple regression analyses demonstrated that age and SBP were the most important determinants of PWV and that the effect of garlic on PWV was independent of confounding factors. According to Breithaupt-Grogler, *et al.*, (1997), "The data suggested that the elastic
30 properties of the aorta were maintained better in the garlic group than in the control group." It is interesting that in experimental animals, changes of ratio of intimal (plaque)

area to medial area during progression and regression of atherosclerosis correlated with changes in indices of aortic elastic properties. Progression of atherosclerosis resulted in higher PWV, and vice versa (Farrar 1991⁶⁸⁸).

5 See also studies in the special supplement of the British Journal of Clinical Practice (1990, Supplement 69) dedicated to the clinical effects of garlic in ischemic heart disease.

10 Microcompetition increases the transcription of P-selectin in endothelial cells, increases the transcription of tissue factor (TF) and decreases the transcription of β_2 integrin and α_4 integrin in macrophages and decreases the transcription of retinoblastoma susceptibility gene (Rb) in smooth muscle cells (SMC). Garlic reduces oxidative stress in endothelial cells, macrophages and SMCs. The reduced oxidative stress stimulates the binding of GABP to these genes, decreasing the transcription of TF and P-selectin and increasing the transcription of β_2 integrin, α_4 integrin and Rb. Changes in the transcription levels of these genes attenuates the formation of atherosclerotic plaque and the thickening of the aortic intima.

15 (b) *Cancer*
The anticancer properties of garlic were recognized thousands of years ago. The ancient Egyptians used garlic externally for treatment of tumors. Hippocrates and physicians in ancient India are also reported to have used garlic externally for cancer treatment. Recent studies confirmed these properties. See, for instance, the section 20 "Garlic, Onions and Cancer," in the recent review by Ali, *et al.*, (2000⁶⁸⁹), the meta-analysis of the epidemiologic literature on garlic consumption and the risk of stomach and colon cancer (Fleischauer 2000⁶⁹⁰), and specific animals studies demonstrating garlic suppression of chemically induced tumors (Singh 1998⁶⁹¹, Singh 1996⁶⁹²).

3. Viral N-box agents

25 A viral N-box agent reduces the number of active viral N-boxes in the host cell. The reduction can be accomplished by an overall reduction in the copy number of viral genomes present, or by inhibition of viral N-boxes (for instance by antisense), etc. The

reduced number of active viral N-boxes eases microcompetition and consequently slows progression of the microcompetition diseases.

a) Direct antiviral agents

(1) *Ganciclovir*

5 (a) *Effect on viral DNA elongation*

Ganciclovir (Cytovene, DHPG) is a guanosine analogue. The prodrug is phosphorylated by thymidine kinase to the active triphosphate form after uptake into the infected cell. The triphosphate form inhibits viral DNA polymerase by competing with cellular deoxyguanosine triphosphate for incorporation into viral DNA causing chain 10 termination. Ganciclovir is effective against herpes simplex virus 1 and 2 (HSV-1, HSV-2), cytomegalovirus (CMV), Epstein- Barr virus (EBV) and varicella-zoster virus (Spector 1999⁶⁹³).

15 Aciclovir (acyclovir) and its oral form valacyclovir, and penciclovir and its oral form famciclovir are guanosine analogues similar to ganciclovir. These drugs are also effective against HSV-1, HSV-2 and CMV. See, for instance, a recent meta-analysis of 30 aciclovir clinical trials in HSV infections (Leflore 2000⁶⁹⁴), a review on aciclovir recommended treatments in HSV infections (Kesson 1998⁶⁹⁵), reviews on valaciclovir effectiveness in HSV and CMV infections (Ormrod 2000⁶⁹⁶, Bell 1999⁶⁹⁷) and a review of famciclovir and penciclovir (Sacks 1999⁶⁹⁸).

20 (b) *Effect on latent viral DNA load*

The load of viral DNA during latent infection is directly correlated with the extent of viral replication during the preceding productive infection (Reddehase 1994⁶⁹⁹, Collins 1993⁷⁰⁰). Therefore, reduction of viral replication should reduce the load of viral DNA during a subsequent latent infection. Consider the following studies.

25 Bone marrow transplantation (BMT) was performed as a syngeneic BMT with female BALB/c (H-2^d) mice used at the age of 8 weeks as both bone marrow donors and recipients. Two hours after BMT, the mice were infected subcutaneously in the left hind footpad with murine CMV. The mice were then divided into four groups. Three groups

received therapy with increasing doses of CD8 T cells. The forth groups served as controls. The results showed that increasing doses of CD8 T cells significantly reduced the extent and duration of virus replication in vital organs, such as lungs and adrenal glands (Steffens 1998⁷⁰¹, Fig 2). Moreover, 12 months after BMT, the viral DNA load was measured. The results showed that the amount of DNA was smaller in the groups given CD8 T cell therapy. The viral DNA load in the lungs of mice given no immunotherapy was 5,000 viral genomes per 10^6 lung cells. The load following treatment with 10^5 and 10^6 CD8 T cells was 3,000 and 1,000 per 10^6 lung cells, respectively. Since there were no infectious virus present, the study shows that attenuated viral replication during the acute phase of infection reduces the load of viral DNA during the subsequent latent phase of infection.

The study also measured the recurrence of viral infection following therapy. Five latently infected mice with no therapy and five mice treated with 10^7 CD8 T cells were subjected to immunoablative γ -ray treatment of 6.5 Gy. Recurrence of viral infectivity was measured 14 days later in separate lobes of the lungs. The group receiving no therapy showed a high latent DNA load and recurrence of infectivity in all five mice in all five lobes of the lungs (with some variance). In contrast, the group receiving CD8T cells showed low viral load and recurrence of infectivity in only two mice and only in a single lobe in each mouse (Steffens 1998, Fig 7). These results show that a reduction in viral replication reduces latent viral DNA load and the probability viral disease.

Thackary and Field, in a series of studies, also tested the effect of preemptive therapy against viral infection. However, instead of CD8 T cells, the studies administered famciclovir (FCV), valaciclovir (VACV), or human immunoglobulin (IgG) to mice infected via the ear pinna or the left side of the neck with either HSV-1 or HSV-2 (Thackray 2000A⁷⁰², Thackray 2000B⁷⁰³, Thackray 2000C⁷⁰⁴, Field 2000⁷⁰⁵, Thackray 1998⁷⁰⁶). The results showed that 9-10 days of FCV treatment early in infection was effective in limiting the establishment of viral latency several months after treatment. Based on their results, Field and Thackary conclude that "Thus, the implication of our results is that even intensive antiviral therapy starting within a few hour of exposure is unlikely to completely abrogate latency. However, our results also show a significant

reduction in the number of foci that are established and imply that there may also be a quantitative reduction in the latent genomes." (Field 2000).

Another study compared the effect of aciclovir (ACV) and immunoglobulin (IgG) preemptive therapy on mice infected via scarified corneas with HSV-1. Both therapies 5 were administered for 7 days commencing on the first day post infection. The results showed that ACV treatment resulted in a reduced copy number of latent HSV-1 genome on day 44 post infection relative to IgG (LeBlanc 1999⁷⁰⁷, Fig 5). Since no untreated mice survived the infection, the study could not compare ACV treatment to no treatment. However, if we assume that IgG treatment either reduced or did not change the copy 10 number of latent viral genomes, we can conclude that the ACV preemptive treatment resulted in a reduced load of latent viral DNA.

Ganciclovir is similar to aciclovir and penciclovir. Therefore, a reasonable conclusion from these studies is that preemptive treatment with ganciclovir will also reduce the load of viral DNA.

15

(c) *Effect on clinical symptoms*

(i) *Atherosclerosis*

Accelerated coronary atherosclerosis can be observed in the donor heart following heart transplantation (TxCAD). Transplanting a heart from a CMV seropositive donor to a seronegative recipient increases the probability of a primary infection in the recipient 20 (Bowden 1991⁷⁰⁸, Chou 1988⁷⁰⁹, Chou 1987⁷¹⁰, Chou 1986⁷¹¹, Grundy 1988⁷¹², Grundy 1987⁷¹³, Grundy 1986⁷¹⁴). The Thackary and LeBlanc studies demonstrated that administration of aciclovir or penciclovir prophylaxis early in primary infection reduces the load of the subsequent latent viral DNA in the infected animals (see above). Since 25 microcompetition between viral and cellular DNA results in atherosclerosis, prophylactic administration of ganciclovir, a drug similar to aciclovir and penciclovir, early after heart transplantation, should reduce atherosclerosis. Consider the following study.

One hundred and forty-nine consecutive patients (131 men and 18 women, aged 48 ± 13 years) randomly received either ganciclovir or placebo. The study drug was commenced on the first postoperative day and was administered for 28 days. In 22% of

patients drug administration was delayed by up to 6 days due to acute-care problems. Immunosuppression consisted of muromonab-CD3 (OKT-3) prophylaxis and maintenance with cyclosporine, prednisone, and azathioprine. Coronary angiography was performed annually after heart transplantation. Mean follow-up time was 4.7 ± 1.3 years. TxCAD was defined as the presence of any angiographic disease irrespective of severity because of the recognized underestimation of TxCAD by angiography. The actuarial incidence of TxCAD was determined from these annual angiograms and from autopsy data. CMV infection was determined in recipient and donor. The results showed that actuarial incidence of TxCAD at follow-up was $43 \pm 8\%$ in patients treated with ganciclovir compared with $60 \pm 11\%$ in placebo group ($P < 0.1$). Moreover, the protective effect of ganciclovir was even more evident when the population of CMV seronegative recipients was considered exclusively. Of the 14 CMV seronegative recipients randomized to prophylactic ganciclovir, 4 (28%), developed TxCAD compared with 9 (69%) of the seronegative patients randomized to placebo (Valentine 1999⁷¹⁵). The effect of ganciclovir is less evident in the population as a whole since among seropositive recipients there was no difference between ganciclovir and placebo. TxCAD developed in 22 (47%) of 48 patients randomized to ganciclovir compared with 21 (47%) of 46 in the placebo group. Based on these results, Valentine, et al., concluded that "prophylactic treatment with ganciclovir initiated immediately after heart transplantation reduces the incidence of TxCAD."

It is interesting to note that in a multivariate analysis, the study found that the variable "CMV illness" was not an independent predictor of TxCAD when "lack of ganciclovir" and "donor age" were included in the analysis. We suspect that high correlation (multicollinearity) between "lack of ganciclovir" and "CMV illness" produced this result. Such a correlation was demonstrated in numerous studies. See, for instance, table 5 in Sia (2000⁷¹⁶), which lists 10 clinical studies showing that early administration of ganciclovir prophylaxis in solid-organ transplantation resulted in reduced CMV disease compared to no treatment, administration of placebo, treatment with immunoglobulin or treatment with acyclovir. From this correlation we deduce that Valentine (1999) also measured reduced CMV disease (the study is mute on this statistic). The key parameter that determines the overall and organ-specific risks of CMV disease is the copy number of

latent viral genomes in various tissues (Reddehase 1994⁷¹⁷). Therefore, the reduced CMV disease indicates a reduction in the copy number of latent viral genome, which, again, explains the reduction in observed atherosclerosis.

5 (2) Zidovudine (AZT), didanosine (ddI), zalcitabine (ddC)

(a) *Effect on viral DNA elongation*

Didanosine (2',3'-dideoxyinosine, ddI) is a synthetic purine nucleoside analogue used against HIV infection. After passive diffusion into the cell, the drug undergoes phosphorylation by cellular (rather than viral, see above) enzymes to dideoxyadenosine-5'-triphosphate (ddATP), the active moiety. ddATP competes with the natural substrate for HIV-1 reverse transcriptase (deoxyadenosine 5'-triphosphate) and cellular DNA polymerase. Because ddATP lacks the 3'-hydroxyl group present in the naturally occurring nucleoside, incorporation into viral DNA leads to termination of DNA chain elongation and inhibition of viral DNA growth (see a recent review of ddI in Perry 1999⁷¹⁸).

Zidovudine (retrovir, ZDV, AZT) and zalcitabine (ddC) are nucleosides similar to ddI.

(b) *Effect on latent viral DNA load*

20 A study measured the change in HIV-1 DNA and RNA load relative to baseline in 42 antiretroviral naive HIV-1 infected persons treated with either AZT monotherapy, a combination of AZT + ddC or a combination of AZT + ddI over a period of 80 weeks. Figure 50 presents the results (Breisten 1998⁷¹⁹, Fig 1A).

25 At week 80, AZT treatment alone was associated with an increase, ddC + AZT with a small decrease and ddI + AZT with a larger decrease in viral DNA. To compare the results statistically, the mean log change from baseline over all time points was compared between ddI + AZT and ddC + AZT. The mean change was -0.3375 and -0.20458 for ddI + AZT and ddC + AZT, respectively ($P = 0.02$). It is interesting that, although not significant statistically ($P = 0.29$), rank order of the ddI + AZT and ddC + AZT effect on RNA is reversed, that is, the mean effect of ddC + AZT on viral RNA was larger than ddI

+ AZT. Since the combination therapy of AZT and ddC is additive (Magnani 1997⁷²⁰), the ddC monotherapy effect on viral DNA was calculated as the ddC + AZT effect minus the AZT monotherapy effect. The calculated effect of ddC monotherapy on viral DNA was compared to the effect of AZT monotherapy. The mean log change from baseline over all 5 time points was -0.15458 and -0.05 for ddC and AZT, respectively (P = 0.09). The statistical analysis suggests that the ranking of ddI > ddC > AZT in terms of their effect on viral DNA, is significant. Moreover, the results suggest that at later time points, AZT tend to be associated with increased levels of viral DNA.

10 This statistical analysis is different from the analysis reported by Bruisten, *et al* (1986). To test whether an "early" response occurred, Bruisten, *et al.*, averaged the values of weeks 4, 8, and 12 and for a "late" response the values of weeks 32, 40, and 48. The test showed that only the ddI + AZT treatment decreased the HIV-1 viral DNA "early" and "late." The P value of "early" compared to baseline is 0.002, the p value of "late" compare to baseline is 0.052. The same values for ddC + AZT are 0.191 and 0.08. These 15 values also indicate that ddI is more effective than ddC in reducing viral DNA.

20 Another study (Pauza 1994⁷²¹) measured the total viral DNA by polymerase chain reaction (PCR) assays for viral LTR sequences in 51 HIV infected patients. This assay detects linear, circular, and integrated HIV-1 DNA and also includes preintegration complexes that completed the first translocation step. Twenty patients were treated with AZT, 4 patients with ddI and 7 patients with ddC. After Southern blotting and hybridization, fragments were excised from the membrane and bound radioactivity was determined by scintillation counting. The measured LTR DNA levels were expressed on a scale of 1 to 5 (1 is lowest). Negative samples were labeled zero. The average ranking of viral DNA load for patients treated with ddI, ddC and AZT, was 2.25, 2.71 and 2.74, 25 respectively. The difference between ddC and AZT is small. However, the average CD4/ μ l count for ddC and AZT treated patients was 82 and 191.55, respectively (p < 0.03 for the difference). Hence, the viral DNA load of the AZT group is most likely biased downward. Overall, this ranking of treatment effectiveness measured in terms of reduced viral DNA load is identical to the ranking in Breisten 1998 above.

A third study (Chun 1997⁷²²) measured total HIV-1 DNA in 9 patients. Eight patients were on triple therapy including two nucleosides and one protease inhibitor. One patient received two nucleosides and two protease inhibitors. Six patients had undetectable plasma HIV RNA. The other three patients had 814, 2,800 and 6,518 copies/ml. The study also reports the year of seroconversion. A regression analysis with viral DNA level as dependent variable and number of years since seroconversion as independent variable produces the results shown in figure 51:

$$\text{Viral DNA load} = 9,909 + 142 \times \text{Years since seroconversion}$$

The viral DNA load is measured in copies of HIV-1 DNA per 10^6 resting CD4+ T cells. The p values for the intercept and coefficient are 1.31E-05 and 0.131481, respectively. Since the sample size is small, the p value for the coefficient is considered as borderline significant, which means that even with triple and quadruple therapies, and in patients with mostly undetectable plasma HIV RNA, viral DNA load increases with an increase in the number of years since seroconversion.

The difference between the expected and the observed number of viral DNA copies was calculated for each patient. The therapy of two patients included ddI and the average difference for these patients was -828 copies. The therapy of five patients included AZT and the average difference for these patients was +317 copies. These results suggest that ddI is associated with a decrease and AZT with an increase in the number of viral DNA copies in this group of patients.

Under different conditions, with monotherapy, triple and quadruple therapy with a protease inhibitor and with detectable and undetectable RNA, the results are consistent. ddI is associated with a larger reduction in viral DNA load compared to ddC, and AZT is associated with an increase in viral DNA load.

25

(c) *Effect on clinical symptoms*

(i) *Obesity*

A study observed 306 six HIV-infected women between December 1997 and February 1998 (Gervasoni 1999⁷²³). The women were treated with two or more antiretroviral drugs. One hundred and sixty two patients were treated with two

nucleosides (double therapy) and 144 with three or more drugs including at least one protease inhibitor (PI) (triple therapy). Fat redistribution (FR) was confirmed by means of a physical examination and dual-energy X-ray absorptiometry (DEXA). FR was observed in 32 women (10.5%) (12 on double therapy, 20 on triple therapy). The body changes 5 were reported to gradually emerge over a period of 12-72 weeks. A statistical analysis showed that a combination treatment which included ddI was significantly associated with the absence of FR ($P = 0.019$). A combination treatment which included ddC was also significantly associated with the absence of FR ($P = 0.049$). The p values indicate that a ddI-including combination was more effective than a ddC-including therapy in preventing 10 FR. Contrary to ddI and ddC, a combination therapy which included AZT was associated with a low risk of developing FR (OR 0.3).

The association between ddI-, ddC- and AZT-including therapeutic combinations with fat redistribution is consistent with their effect on reducing or increasing viral DNA load.

15 Another interesting observation in this study was that the longer median total duration of antiretroviral drug treatment in women with FR compared to those without FR (1,187 versus 395 days). Only one of the 32 women with FR received antiretroviral drug therapy for less than 1,000 days. The risk of FR for women under antiretroviral drug 20 therapy for more than 1,000 days was 10 times greater than in those who received shorter drug therapy (OR 10.8, $P = 0.0207$).

A statistical analysis of the results in Chun 1997 (see above) showed that viral DNA load increases with an increase in the number of years since seroconversion. Since the duration of antiretroviral drug treatment most often increases with the number of years since seroconversion, longer duration correlates with higher viral DNA load. Higher viral 25 DNA load results in more intense microcompetition, and therefore, fat redistribution.

(3) Garlic

(a) *Effect on viral infectivity*

Garlic has antiviral activity. See for instance Guo, *et al.*, (1993⁷²⁴) and Weber, *et al.*, (1992⁷²⁵).

(b) *Effect on clinical symptoms*

See above.

b) *Immune stimulating agents*

5 The balance between two forces, the virus drive to replicate, and the capacity of the immune system to control or clear the infection, determines the copy number of viral genome present in infected cells. A stable equilibrium between these two forces determines the copy number in a persistent and latent infections. A major determinant of the immune system capacity to clear or control an infection is the efficiency of the Th1 response. An increase in this efficiency reduces the viral copy number.

10

(1) Infection with non-GABP viruses

15 Data obtained in animals indicate that neonatal immune responses are biased toward Th2. Consider the effects of a productive infection with a GABP virus during early life. The extent of viral replication during productive infection determines the load of viral DNA during the subsequent latent infection (see discussion above). The lower the Th1 efficiency during the productive infection, the higher the copy number of viral genome in the subsequent latent period. Infection with some viruses, such as measles, hepatitis A, and *Mycobacterium tuberculosis* induce a strong polarized Th1-type response in early life. These infections reduce GABP virus replication and subsequent genome copy number during latent infection. The reduced copy number attenuates 20 microcompetition, therefore, reducing the probability and severity of microcompetition diseases, such as, atopy, asthma, diabetes, cancer, atherosclerosis, osteoarthritis, obesity, etc. Consider the following studies.

25

BCG is a freeze-dried preparation made from a living culture of the Calmette-Guerin strain of *mycobacterium Bovis*. It was first developed as a vaccine against tuberculosis in 1921 but also has been used as an immunotherapeutic treatment for carcinoma. Vaccination with BCG induces a Th1-type immune response in human newborn and adults human (Marchant 1999⁷²⁶). Moreover, BCG immunization prior to challenge with herpes simplex virus increased survival rate of newborn mice (Starr 1976⁷²⁷). To investigate whether the prevalence of atopy is lower in children who have 30 been vaccinated with BCG in infancy than in children who have not been vaccinated, a

study measured skin test reactivity to three allergens (*Dermatophagoides pteronyssinus*, *D. farinae* and cockroach) in 400 children, aged 3-14 years, in an urban area of Bissau, the capital of Guinea-Bissau in west Africa. The results showed that 57 (21%) of the 5 vaccinated children were atopic (any reaction > or = 2 mm), compared with 21 (40%) of the unvaccinated children [odds ratio, after controlling for potential confounding factors, 0.19 (95% CI 0.06-0.59)]. When atopy was defined using the 3-mm criterion, the reduction in atopy associated with BCG was greater the earlier the age at vaccination, and the largest reduction was seen in children vaccinated in the first week of life (Aaby 2000⁷²⁸). Based on these results, Aaby, et al., concluded that "BCG vaccination given 10 early in infancy may prevent the development of atopy in African children."

Results of numerous studies suggest that measles, hepatitis A, and *Mycobacterium tuberculosis* infection in early life may prevent subsequent development of atopic diseases. In humans, immunomodulation during the first two years of life is most successful in 15 producing long-lasting prevention effects (von Hertzen 2000⁷²⁹). See also von Mutisu 2000⁷³⁰, von Hertzen 1999⁷³¹. As a result of this observed effect, there are currently attempts to use BCG as a vaccine for asthma (see review Scanga 2000⁷³²).

A study evaluated the protective effect of repeated BCG vaccinations on 20 preventing diabetes in NOD mice. The results showed that 17/32 (53%) of the control group, 8/31 (26%) of the single vaccine-treated (at age 35 days) mice, and 7/23 (30%) of the single vaccine-treated (at age 90 days) mice developed diabetes, and none of the 25 repeated BCG vaccination (at age 35 & 90 days, n = 14) animals developed the disease, up to 250 days of age (p < 0.05, compared with controls and each of the single-vaccination groups). The repeated BCG vaccination reduced the severity of insulitis at age 120 days as compared with controls and single BCG-vaccination groups (Shehadeh 1997⁷³³). On the relation between BCG immunization and type 1 diabetes, see also Qin 1997⁷³⁴, Harada 1990⁷³⁵ and a recent review Hiltunen 1999⁷³⁶.

Another study showed that an infection of NOD mice with *Mycobacterium avium*, before the mice show overt diabetes, results in permanent protection of the animals from 30 diabetes. This protective effect was associated with increased numbers of CD4+ T cells and B220+ B cells (Martins 1999⁷³⁷). The study also showed that the protection was

associated with changes in the expression of Fas (CD95) and FasL by immune cells, and alterations in cytotoxic activity, IFN γ and IL-4 production and activation of T cells of infected animals. Based on these results, Martins and Aguas concluded that the "data indicate that protection of NOD mice from diabetes is a Th1-type response that is 5 mediated by up-regulation of the Fas-FasL pathway and involves an increase in the cytotoxicity of T cells." See also Bras 1996⁷³⁸.

(2) Breast feeding

Breast feeding increases the efficiency of the Th1 immune response. Consider the following studies.

10 A study measured the blast transformation and cytokine production by lymphocytes, and T cell changes of 59 formula-fed and 64 breast fed 12-month-old children blast, before and after measles-mumps-rubella vaccination (MMR). The results showed that before vaccination, lymphocytes of breast fed children had lower levels of blast transformation without antigen ($p < 0.001$), with tetanus toxoid ($p < 0.02$) or Candida ($p < 0.04$), and lower IFN γ production ($p < 0.03$). Fourteen days after live viral 15 vaccination, only breast fed children had increased production of IFN γ ($p < 0.02$) and increased percentages of CD56+ ($p < 0.022$) and CD8+ cells ($p < 0.004$) (Pabst 1997⁷³⁹). Based on these results, Pabst, *et al.*, concluded that "these findings are consistent with a Th1 type response by breast fed children, not evident in formula-fed children. Feeding 20 mode has an important long-term immunomodulating effect on infants beyond weaning." See also the review Pabst 1997⁷⁴⁰.

Another study showed immunophenotypic differences between breast-fed and formula-fed infants consistent with accelerated development of immune system in breast-fed infants (Hawkes 1999⁷⁴¹).

25 Since breast feeding increases the efficiency of the Th1 immune response, it should reduce the probability and severity of microcompetition diseases (see above for detail). Consider the following studies.

A study examined the association between breast feeding and type II diabetes (also called non-insulin-dependent diabetes, or NIDDM) in Pima Indians, a population with a

high prevalence of this disorder. Data were available for 720 Pima Indians aged between 10 and 39 years. 325 people who were exclusively bottle fed had significantly higher age-adjusted and sex-adjusted mean relative weights (146%) than 144 people who were exclusively breast fed (140%) or 251 people who had some breast feeding (139%) (p = 0.019). The results showed that people who were exclusively breast fed had significantly lower rates of NIDDM than those who were exclusively bottle fed in all age-groups. The odds ratio for NIDDM in exclusively breast fed people, compared with exclusively bottle fed, was 0.41 (95% CI 0.18-0.93) adjusted for age, sex, birth date, parental diabetes, and birth weight (Pettitt 1997⁷⁴²). Based on these results Pettitt, *et al.*, concluded that "exclusive breast feeding for the first 2 months of life is associated with a significantly lower rate of NIDDM in Pima Indians."

Another study measured the impact of breast-feeding on overweight and obesity in children at school entry was assessed in a cross sectional study in Bavaria in 1997. The school entry health examination enrolled 134,577 children. Data on early feeding were collected in two rural districts (eligible population n=13,345). The analyses were confined to 5 or 6 year old children with German nationality. The study measured overweight (BMI>90th percentile for all German children seen at the 1997 school entry health examination in Bavaria) and obesity (BMI>97th percentile). Information on breast-feeding was available for 9,206 children of whom 56% had been breast-fed for any length of time. The results showed that in non breast-fed children the upper tail of the BMI distribution was enlarged as compared to the breast-fed children whereas the median was almost identical (von Kries 2000⁷⁴³). The prevalence of obesity in children who had never been breast-fed was 4.5% as compared to 2.8% in ever breast-fed children. A clear dose response effect for the duration of breast-feeding on the prevalence of obesity was found: 3.8%, 2.3%, 1.7% and 0.8% for exclusive breast-feeding for up to 2, 3 to 5, 6 to 12 and more than 12 months, respectively. The results for overweight were very similar. The protective effect of breast feeding on overweight and obesity could not be explained by differences in social class or lifestyle. The adjusted odds ratios of breast-feeding for any length of time was 0.71 (95% CI 0.56-0.90) for obesity and 0.77 (95%CI 0.66-0.88) for overweight. This data set did not allow to adjust for maternal weight, an important risk factor for obesity in children. Maternal overweight, however, could not explain the effect of breast feeding on overweight and obesity in a similar study. The reduction in the risk

for overweight and obesity is therefore more likely to be related to the properties of human milk than to factors associated with breast-feeding. See also von Kries 1999⁷⁴⁴.

Table of Cited References

- ¹ Scholer H, Haslinger A, Heguy A, Holtgreve H, Karin M. In Vivo Competition Between a Metallothionein Regulatory Element and the SV40 Enhancer. *Science* 1986;232: 76-80.
- ² Adam GI, Miller SJ, Ulleras E, Franklin GC. Cell-type-specific modulation of PDGF-B regulatory elements via viral enhancer competition: a caveat for the use of reference plasmids in transient transfection assays. *Gene*. 1996 Oct 31;178(1-2):25-9.
- ³ Allebach ES, Boettiger D, Pacifici M, Adams SL. Control of types I and II collagen and fibronectin gene expression in chondrocytes delineated by viral transformation. *Mol Cell Biol*. 1985 May;5(5):1002-8.
- ⁴ Parker IM, Smith AA, Gevers W. Absence of α 2(1) Procollagen Synthesis in a Clone of SV40-transformed WI-38 Human Fibroblasts. *The Journal of Biological Chemistry*, 1989, 264(13): 7147-7152.
- ⁵ Moro L, Smith BD. Identification of collagen alpha1(I) trimer and normal type I collagen in a polyoma virus-induced mouse tumor. *Arch Biochem Biophys* 1977 Jul;182(1):33-41.
- ⁶ Parker IM, Smith AA, Mundell K, Collins M, Boast S, Ramirez F. The abolition of collagen gene expression in SV40-transformed fibroblasts is associated with trans-acting factor switching. *Nucleic Acids Research*, 1992, 20(21): 5825-5830.
- ⁷ Le Naour R, Lussiez C, Raoul H, Mabondzo A, Dormont D. Expression of cell adhesion molecules at the surface of *in vitro* human immunodeficiency virus type 1-infected human monocytes: relationships with tumor necrosis factor alpha, interleukin 1beta, and interleukin 6 syntheses. *AIDS Res Hum Retroviruses* 1997 Jul 1;13(10):841-55.
- ⁸ Tanaka Y, Fukudome K, Hayashi M, Takagi S, Yoshie O. Induction of ICAM-1 and LFA-3 by Tax1 of human T-cell leukemia virus type 1 and mechanism of down-regulation of ICAM-1 or LFA-1 in adult-T-cell-leukemia cell lines. *Int J Cancer* 1995 Feb 8;60(4):554-61.
- ⁹ Patarroyo M, Prieto J, Ernberg I, Gahmberg CG. Absence, or low expression, of leukocyte adhesion molecules CD11 and CD18 on Burkitt lymphoma cells. *Int J Cancer* 1988 Jun 15;41(6):901-7.
- ¹⁰ Nuclear Respiratory Factor 2 should not be confused with NF-E2 Related Factor 2 which is also abbreviated NRF2 or NRF-2.
- ¹¹ Watanabe H, Imai T, Sharp PA, Handa H. Identification of two transcription factors that bind to specific elements in the promoter of the adenovirus early-region 4. *Mol Cell Biol* 1988 8(3):1290-300. The transcription factor binds to the promoter of the adenovirus early-region 4 (E4). Hence the name E4 transcription factor 1.
- ¹² Enhancer Factor 1A should not be confused with Elongation Factor 1A which is also abbreviated EF-1A.
- ¹³ Rosmarin AG, Luo M, Caprio DG, Shang J, Simkovich CP. Sp1 Cooperates with the ets Transcription Factor, GABP, to Activate the CD18 (β_2 Leukocyte Integrin) Promoter. *Journal of Biological Chemistry* 1998 273(21): 13097-13103.
- ¹⁴ Bannert R, Avots A, Baier M, Serfling E, Kurth R. GA-binding protein factors, in concert with the coactivator CREB binding protein/p300, control the induction of the interleukin 16 promoter in T lymphocytes. *Proc. Natl. Acad. Sci. USA* 1999 96:1541-1546.
- ¹⁵ Avots A, Hoffmeyer A, Flory E, Cimanis A, Rapp UR, Serfling E. GABP factors bind to a distal interleukin 2 (IL-2) enhancer and contribute to c-Raf-mediated increase in IL-2 induction. *Molecular and Cellular Biology* 1997 17(8):4381-4389.
- ¹⁶ Lin JX, Bhat NK, John S, Queale WS, Leonard WJ. Characterization of the human interleukin-2 receptor beta-chain gene promoter: regulation of promoter activity by ets gene products. *Mol Cell Biol*. 1993 Oct;13(10):6201-10.
- ¹⁷ Markiewicz S, Bosselut R, Le Deist F, de Villartay JP, Hivroz C, Ghysdael J, Fischer A, de Saint Basile G. Tissue-specific activity of the gammac chain gene promoter depends upon an Ets binding site and is regulated by GA-binding protein. *J Biol Chem*. 1996 Jun 21;271(25):14849-55.
- ¹⁸ Smith MF Jr, Carl VS, Lodie T, Fenton MJ. Secretory interleukin-1 receptor antagonist gene expression requires both a PU.1 and a novel composite NF-kappaB/PU.1/ GA-binding protein binding site. *J Biol Chem*. 1998 Sep 11;273(37):24272-9.
- ¹⁹ Sowa Y, Shiio Y, Fujita T, Matsumoto T, Okuyama Y, Kato D, Inoue J, Sawada J, Goto M, Watanabe H, Handa H, Sakai T. Retinoblastoma binding factor 1 site in the core promoter region of the human RB gene is activated by hGABP/E4TF1. *Cancer Res*. 1997 Aug 1;57(15):3145-8.

²⁰ Kamura T, Handa H, Hamasaki N, Kitajima S. Characterization of the human thrombopoietin gene promoter. A possible role of an Ets transcription factor, E4TF1/GABP. *J Biol Chem*. 1997 Apr 25;272(17):11361-8.

²¹ Wang K, Bohren KM, Gabbay KH. Characterization of the human aldose reductase gene promoter. *J Biol Chem*. 1993 Jul 25;268(21):16052-8.

²² Nuchprayoon I, Shang J, Simkovich CP, Luo M, Rosmarin AG, Friedman AD. An enhancer located between the neutrophil elastase and proteinase 3 promoters is activated by Sp1 and an Ets factor. *J Biol Chem*. 1999 Jan 8;274(2):1085-91.

²³ Nuchprayoon I, Simkovich CP, Luo M, Friedman AD, Rosmarin AG. GABP cooperates with c-Myb and C/EBP to activate the neutrophil elastase promoter. *Blood*. 1997 Jun 15;89(12):4546-54.

²⁴ Sadasivan E, Cedeno MM, Rothenberg SP. Characterization of the gene encoding a folate-binding protein expressed in human placenta. Identification of promoter activity in a G-rich SP1 site linked with the tandemly repeated GGAAG motif for the ets encoded GA-binding protein. *J Biol Chem*. 1994 Feb 18;269(7):4725-35.

²⁵ Basu A, Park K, Atchison ML, Carter RS, Avadhani NG. Identification of a transcriptional initiator element in the cytochrome c oxidase subunit Vb promoter which binds to transcription factors NF-E1 (YY-1, delta) and Sp1. *J Biol Chem*. 1993 Feb 25;268(6):4188-96.

²⁶ Sucharov C, Basu A, Carter RS, Avadhani NG. A novel transcriptional initiator activity of the GABP factor binding ets sequence repeat from the murine cytochrome c oxidase Vb gene. *Gene Expr*. 1995;5(2):93-111.

²⁷ Carter RS, Avadhani NG. Cooperative binding of GA-binding protein transcription factors to duplicated transcription initiation region repeats of the cytochrome c oxidase subunit IV gene. *J Biol Chem*. 1994 Feb 11;269(6):4381-7.

²⁸ Carter RS, Bhat NK, Basu A, Avadhani NG. The basal promoter elements of murine cytochrome c oxidase subunit IV gene consist of tandemly duplicated ets motifs that bind to GABP-related transcription factors. *J Biol Chem*. 1992 Nov 15;267(32):23418-26.

²⁹ Virbasius JV, Scarpulla RC. Activation of the human mitochondrial transcription factor A gene by nuclear respiratory factors: a potential regulatory link between nuclear and mitochondrial gene expression in organelle biogenesis. *Proc Natl Acad Sci U S A*. 1994 Feb 15;91(4):1309-13.

³⁰ Villena JA, Vinas O, Mampel T, Iglesias R, Giralt M, Villarroya F. Regulation of mitochondrial biogenesis in brown adipose tissue: nuclear respiratory factor-2/GA-binding protein is responsible for the transcriptional regulation of the gene for the mitochondrial ATP synthase beta subunit. *Biochem J*. 1998 Apr 1;331 (Pt 1):121-7.

³¹ Ouyang L, Jacob KK, Stanley FM. GABP mediates insulin-increased prolactin gene transcription. *J Biol Chem*. 1996 May 3;271(18):10425-8.

³² Hoare S, Copland JA, Wood TG, Jeng YJ, Izban MG, Soloff MS. Identification of a GABP alpha/beta binding site involved in the induction of oxytocin receptor gene expression in human breast cells, potentiation by c-Fos/c-Jun. *Endocrinology*. 1999 May;140(5):2268-79.

³³ Suzuki F, Goto M, Sawa C, Ito S, Watanabe H, Sawada J, Handa H. Functional interactions of transcription factor human GA-binding protein subunits. *J Biol Chem*. 1998 Nov 6;273(45):29302-8.

³⁴ Bannert N, Avots A, Baier M, Serfling E, Kurth R. GA-binding protein factors, in concert with the coactivator CREB binding protein/p300, control the induction of the interleukin 16 promoter in T lymphocytes. *Proc, Natl, Acad, Sci, USA* 1999 96:1541-1546.

³⁵ Kamei Y, Xu L, Heinzel T, Torchia J, Kurokawa R, Gloss B, Lin SC, Heyman RA, Rose DW, Glass CK, Rosenfeld MG. A CBP integrator complex mediates transcriptional activation and AP-1 inhibition by nuclear receptors. *Cell*. 1996 May 3;85(3):403-14.

³⁶ Horvai AB, Xu L, Korzus E, Brard G, Kalafus D, Mullen TM, Rose DW, Rosenfeld MG, Glass CK. Nuclear integration of JAK/STAT and Ras/AP-1 signaling by CBP and p300. *Proc Natl Acad Sci U S A*. 1997 Feb 18;94(4):1074-9.

³⁷ Hottiger MO, Felzien LK, Nabel GJ. Modulation of cytokine-induced HIV gene expression by competitive binding of transcription factors to the coactivator p300. *EMBO J*. 1998 Jun 1;17(11):3124-34.

³⁸ Asano M, Murakami Y, Furukawa K, Yamaguchi-Iwai Y, Stake M, Ito Y. A Polayomavirus Enhancers Binding Protein, PEBP5, Responsive to 12-O-Tetradecanoylphorbol-13-Acetate but Distinct From AP-1. *Journal of Virology* 1990 64(12):5927-5938.

³⁹ Higashino F, Yoshida K, Fujinaga Y, Kamio K, Fujinaga K. Isolation fo a cDNA Encoding the Adenovirus E1A Enhancer Binding Protein: A New Human Member of the ets Oncogene Family. *Nucleic Acids Research* 1993 21(3):547-553.

⁴⁰ Laimins LA, Tsichlis P, Khoury G. Multiple Enhancer Domains in the 3' Terminus of the Prague Strain of Rous Sarcoma Virus. *Nucleic Acids Research* 1984 12(16):6427-6442.

⁴¹ LaMarco KL, McKnight SL. Purification of a set of cellular polypeptides that bind to the purine-rich cis-regulatory element of herpes simplex virus immediate early genes. *Genes Dev* 1989 3(9):1372-83.

⁴² Douville P, Hagmann M, Georgiev O, Schaffner W. Positive and negative regulation at the herpes simplex virus ICP4 and ICP0 TAATGARAT motifs. *Virology*. 1995 Feb 20;207(1):107-16.

⁴³ Boshart M, Weber F, Jahn G, Dorsch-Hasler K, Fleckenstein B, Schaffner W. A very strong enhancer is located upstream of an immediate early gene of human cytomegalovirus. *Cell* 1985 Jun;41(2):521-30.

⁴⁴ Gunther CV, Graves BJ. Identification of ETS domain proteins in murine T lymphocytes that interact with the Moloney murine leukemia virus enhancer. *Mol Cell Biol* 1994 14(11): 7569-80

⁴⁵ Flory E, Hoffmeyer A, Smola U, Rapp UR, Bruder JT. Raf-1 kinase targets GA-binding protein in transcriptional regulation of the human immunodeficiency virus type 1 promoter. *J Virol* 1996 Apr;70(4):2260-8.

⁴⁶ Rawlins DR, Milman G, Hayward SD, Hayward GS. Sequence-specific DNA binding of the Epstein-Barr virus nuclear antigen (EBNA-1) to clustered sites in the plasmid maintenance region. *Cell* 1985 Oct;42(3):859-68.

⁴⁷ Mauclere P, Mahieux R, Garcia-Calleja JM, Salla R, Tekaia F, Millan J, De The G, Gessain A. A new HTLV-II subtype A isolate in an HIV-1 infected prostitute from Cameroon, Central Africa. *AIDS Res Hum Retroviruses*. 1995 Aug;11(8):989-93.

⁴⁸ Kornfeld H, Riedel N, Viglianti GA, Hirsch V, Mullins JL. Cloning of HTLV-4 and its relation to simian and human immunodeficiency viruses. *Nature* 1987 326(6113);610-613.

⁴⁹ Bannert N, Avots A, Baier M, Serfling E, Kurth R. GA-binding protein factors, in concert with the coactivator CREB binding protein/p300, control the induction of the interleukin 16 promoter in T lymphocytes. *Proc, Natl, Acad, Sci, USA* 1999 96:1541-1546.

⁵⁰ Flory E, Hoffmeyer A, Smola U, Rapp UR, Bruder JT. Raf-1 kinase targets GA-binding protein in transcriptional regulation of the human immunodeficiency virus type 1 promoter. *J Virol* 1996 Apr;70(4):2260-8.

⁵¹ Douville P, Hagmann M, Georgiev O, Schaffner W. Positive and negative regulation at the herpes simplex virus ICP4 and ICP0 TAATGARAT motifs. *Virology*. 1995 Feb 20;207(1):107-16.

⁵² Bruder JT, Hearing P. Cooperative binding of EF-1A to the E1A enhancer region mediates synergistic effects on E1A transcription during adenovirus infection. *J Virol*. 1991 Sep;65(9):5084-7.

⁵³ Bruder JT, Hearing P. Nuclear factor EF-1A binds to the adenovirus E1A core enhancer element and to other transcriptional control regions. *Mol Cell Biol*. 1989 Nov;9(11):5143-53.

⁵⁴ Ostapchuk P, Difley JF, Bruder JT, Stillman B, Levine AJ, Hearing P. Interaction of a nuclear factor with the polyomavirus enhancer region. *Proc Natl Acad Sci U S A*. 1986 Nov;83(22):8550-4.

⁵⁵ Gunther CV, Graves BJ. Identification of ETS domain proteins in murine T lymphocytes that interact with the Moloney murine leukemia virus enhancer. *Mol Cell Biol* 1994 14(11): 7569-80

⁵⁶ Scholer HR, Gruss P. Specific interaction between enhancer-containing molecules and cellular components. *Cell*. 1984 Feb;36(2):403-11.

⁵⁷ Bannert N, Avots A, Baier M, Serfling E, Kurth R. GA-binding protein factors, in concert with the coactivator CREB binding protein/p300, control the induction of the interleukin 16 promoter in T lymphocytes. *Proc, Natl, Acad, Sci, USA* 1999 96:1541-1546.

⁵⁸ Hipskind RA, Bilbe G. MAP kinase signaling cascades and gene expression in osteoblasts. *Front Biosci*. 1998 Aug 1;3:D804-16.

⁵⁹ Camps M, Nichols A, Arkinstall S. Dual specificity phosphatases: a gene family for control of MAP kinase function. *FASEB J*. 2000 Jan;14(1):6-16.

⁶⁰ Saxena M, Mustelin T. Extracellular signals and scores of phosphatases: all roads lead to MAP kinase. *Semin Immunol*. 2000 Aug;12(4):387-96.

⁶¹ Keyse SM. Protein phosphatases and the regulation of MAP kinase activity. *Semin Cell Dev Biol*. 1998 Apr;9(2):143-52.

⁶² Espinosa E, Le Van Thai A, Pomies C, Weber MJ. Cooperation between phosphorylation and acetylation processes in transcriptional control. *Mol Cell Biol* 1999 May;19(5):3474-84.

⁶³ Schaeffer L, Duclert N, Huchet-Dymanus M, Changeux JP. Implication of a multisubunit Ets-related transcription factor in synaptic expression of the nicotinic acetylcholine receptor. *EMBO J.* 1993 Jun 1;17(11):3078-90.

⁶⁴ Shiraishi M, Hirasawa N, Kobayashi Y, Oikawa S, Murakami A, Ohuchi K. Participation of mitogen-activated protein kinase in thapsigargin- and TPA-induced histamine production in murine macrophage RAW 264.7 cells. *Br J Pharmacol* 2000 Feb;129(3):515-24.

⁶⁵ Herrera R, Hubbell S, Decker S, Petruzzelli L. A role for the MEK/MAPK pathway in PMA-induced cell cycle arrest: modulation of megakaryocytic differentiation of K562 cells. *Exp Cell Res* 1998 Feb 1;238(2):407-14.

⁶⁶ Stadheim TA, Kucera GL. Extracellular signal-regulated kinase (ERK) activity is required for TPA-mediated inhibition of drug-induced apoptosis. *Biochem Biophys Res Commun* 1998 Apr 7;245(1):266-71.

⁶⁷ Yen A, Roberson MS, Varvayanis S. Retinoic acid selectively activates the ERK2 but not JNK/SAPK or p38 MAP kinases when inducing myeloid differentiation. *In Vitro Cell Dev Biol Anim.* 1999 Oct;35(9):527-32.

⁶⁸ Liu MK, Brownsey RW, Reiner NE. Γ interferon induces rapid and coordinate activation of mitogen-activated protein kinase (extracellular signal-regulated kinase) and calcium-independent protein kinase C in human monocytes. *Infect Immun*, Jul 1994, 2722-2731, Vol 62, No. 7.

⁶⁹ Nishiya T, Uehara T, Edamatsu H, Kaziro Y, Itoh H, Nomura Y. Activation of Stat1 and subsequent transcription of inducible nitric oxide synthase gene in C6 glioma cells is independent of interferon- γ -induced MAPK activation that is mediated by p21ras. *FEBS Lett* 1997 May 12;408(1):33-8.

⁷⁰ Lessor T, Yoo JY, Davis M, Hamburger AW. Regulation of heregulin beta1-induced differentiation in a human breast carcinoma cell line by the extracellular-regulated kinase (ERK) pathway. *J Cell Biochem* 1998 Sep 15;70(4):587-95.

⁷¹ Marte BM, Graus-Porta D, Jeschke M, Fabbro D, Hynes NE, Taverna D. NDF/hereregulin activates MAP kinase and p70/p85 S6 kinase during proliferation or differentiation of mammary epithelial cells. *Oncogene* 1995 Jan 5;10(1):167-75.

⁷² Sepp-Lorenzino L, Eberhard I, Ma Z, Cho C, Serve H, Liu F, Rosen N, Lupu R. Signal transduction pathways induced by heregulin in MDA-MB-453 breast cancer cells. *Oncogene* 1996 Apr 18;12(8):1679-87.

⁷³ Fiddes RJ, James PW, Sivertsen SP, Sutherland RL, Musgrove EA, Daly RJ. Inhibition of the MAP kinase cascade blocks heregulin-induced cell cycle progression in T-47D human breast cancer cells. *Oncogene* 1998 May 28;16(21):2803-13.

⁷⁴ Park JA, Koh JY. Induction of an immediate early gene egr-1 by zinc through extracellular signal-regulated kinase activation in cortical culture: its role in zinc-induced neuronal death. *J Neurochem*. 1999 Aug;73(2):450-6.

⁷⁵ Kiss Z, Crilly KS, Tomono M. Bombesin and zinc enhance the synergistic mitogenic effects of insulin and phosphocholine by a MAP kinase-dependent mechanism in Swiss 3T3 cells. *FEBS Lett*. 1997 Sep 22;415(1):71-4.

⁷⁶ Wu W, Graves LM, Jaspers I, Devlin RB, Reed W, Samet JM. Activation of the EGF receptor signaling pathway in human airway epithelial cells exposed to metals. *Am J Physiol*. 1999 Nov;277(5 Pt 1):L924-31.

⁷⁷ Samet JM, Graves LM, Quay J, Dailey LA, Devlin RB, Ghio AJ, Wu W, Bromberg PA, Reed W. Activation of MAPKs in human bronchial epithelial cells exposed to metals. *Am J Physiol*. 1998 Sep;275(3 Pt 1):L551-8.

⁷⁸ Migliaccio A, Di Domenico M, Castoria G, de Falco A, Bontempo P, Nola E, Auricchio F. Tyrosine kinase/p21ras/MAP-kinase pathway activation by estradiol-receptor complex in MCF-7 cells. *EMBO J.* 1996 Mar 15;15(6):1292-300.

⁷⁹ Ruzicka AL. Effects of 17 beta-estradiol and progesterone on mitogen-activated protein kinase expression and activity in rat uterine smooth muscle. *Eur J Pharmacol*. 1996 Apr 11;300(3):247-54.

⁸⁰ Nuedling S, Kahlert S, Loebbert K, Meyer R, Vetter H, Grohe C. Differential effects of 17beta-estradiol on mitogen-activated protein kinase pathways in rat cardiomyocytes. *FEBS Lett*. 1999 Jul 9;454(3):271-6.

⁸¹ Laporte JD, Moore PE, Abraham JH, Maksym GN, Fabry B, Panettieri RA Jr, Shore SA. Role of ERK MAP kinases in responses of cultured human airway smooth muscle cells to IL-1beta. *Am J Physiol* 1999 Nov;277(5 Pt 1):L943-51.

⁸² Kumar A, Middleton A, Chambers TC, Mehta KD. Differential roles of extracellular signal-regulated kinase-1/2 and p38(MAPK) in interleukin-1beta- and tumor necrosis factor-alpha-induced low density lipoprotein receptor expression in HepG2 cells. *J Biol Chem*. 1998 Jun 19;273(25):15742-8.

⁸³ Larsen CM, Wadt KA, Juhl LF, Andersen HU, Karlsen AE, Su MS, Seedorf K, Shapiro L, Dinarello CA, Mandrup-Poulsen T. Interleukin-1beta-induced rat pancreatic islet nitric oxide synthesis requires both the p38 and extracellular signal-regulated kinase 1/2 mitogen-activated protein kinases. *J Biol Chem*. 1998 Jun 12;273(24):15294-300.

⁸⁴ Daeipour M, Kumar G, Amaral MC, Nel AE. Recombinant IL-6 activates p42 and p44 mitogen-activated protein kinases in the IL-6 responsive B cell line, AF-10. *J Immunol*. 1993 Jun 1;150(11):4743-53.

⁸⁵ Leonard M, Ryan MP, Watson AJ, Schramek H, Healy E. Role of MAP kinase pathways in mediating IL-6 production in human primary mesangial and proximal tubular cells. *Kidney Int*. 1999 Oct;56(4):1366-77.

⁸⁶ Hartsough MT, Mulder KM. Transforming growth factor beta activation of p44mapk in proliferating cultures of epithelial cells. *J Biol Chem*. 1995 Mar 31;270(13):7117-24.

⁸⁷ Yonekura A, Osaki M, Hirota Y, Tsukazaki T, Miyazaki Y, Matsumoto T, Ohtsuru A, Namba H, Shindo H, Yamashita S. Transforming growth factor-beta stimulates articular chondrocyte cell growth through p44/42 MAP kinase (ERK) activation. *Endocr J*. 1999 Aug;46(4):545-53.

⁸⁸ Strakova Z, Copland JA, Lolait SJ, Soloff MS. ERK2 mediates oxytocin-stimulated PGE2 synthesis. *Am J Physiol*. 1998 Apr;274(4 Pt 1):E634-41.

⁸⁹ Copland JA, Jeng YJ, Strakova Z, Ives KL, Hellmich MR, Soloff MS. Demonstration of functional oxytocin receptors in human breast Hs578T cells and their up-regulation through a protein kinase C-dependent pathway. *Endocrinology*. 1999 May;140(5):2258-67.

⁹⁰ Hoare S, Copland JA, Wood TG, Jeng YJ, Izban MG, Soloff MS. Identification of a GABP alpha/beta binding site involved in the induction of oxytocin receptor gene expression in human breast cells, potentiation by c-Fos/c-Jun. *Endocrinology*. 1999 May;140(5):2268-79.

⁹¹ Flory E, Hoffmeyer A, Smola U, Rapp UR, Bruder JT. Raf-1 kinase targets GA-binding protein in transcriptional regulation of the human immunodeficiency virus type 1 promoter. *J Virol* 1996 Apr;70(4):2260-8.

⁹² Avots A, Hoffmeyer A, Flory E, Cimamis A, Rapp UR, Serfling E. GABP factors bind to a distal interleukin 2 (IL-2) enhancer and contribute to c-Raf-mediated increase in IL-2 induction. *Molecular and Cellular Biology* 1997 17(8):4381-4389.

⁹³ Hoffmeyer A, Avots A, Flory E, Weber CK, Serfling E, Rapp UR. The GABP-responsive element of the interleukin-2 enhancer is regulated by JNK/SAPK-activating pathways in T lymphocytes. *J Biol Chem*. 1998 Apr 24;273(17):10112-9.

⁹⁴ Tomaras GD, Foster DA, Burre CM, Taffet SM. ETS transcription factors regulate an enhancer activity in the third intron of TNF-alpha. *J Leukoc Biol* 1999 Jul;66(1):183-93.

⁹⁵ Zhong H, Voll RE, Ghosh S. Phosphorylation of NF-kappa B p65 by PKA stimulates transcriptional activity by promoting a novel bivalent interaction with the coactivator CBP/p300. *Mol Cell*. 1998 Apr;1(5):661-71.

⁹⁶ Bevilacqua MA, Faniello MC, Cimino F, Costanzo F. Okadaic acid stimulates H ferritin transcription in HeLa cells by increasing the interaction between the p300 CO-activator molecule and the transcription factor Bbf. *Biochem Biophys Res Commun*. 1997 Nov 7;240(1):179-82.

⁹⁷ Kuo MH, Allis CD. Roles of histone acetyltransferases and deacetylases in gene regulation. *BioEssays* 1998 20:615-626.

⁹⁸ Hebbes TR, Clayton AL, Thorne AW, Crane-Robinson C. Core histone hyperacetylation co-maps with generalized DNase I sensitivity in the chicken beta-globin chromosomal domain. *EMBO J*. 1994 Apr 15;13(8):1823-30.

⁹⁹ Kuhnert P, Peterhans E, Pauli U. Chromatin structure and DNase I hypersensitivity in the transcriptionally active and inactive porcine tumor necrosis factor gene locus. *Nucleic Acids Res*. 1992 Apr 25;20(8):1943-8.

¹⁰⁰ Tomaras GD, Foster DA, Burre CM, Taffet SM. ETS transcription factors regulate an enhancer activity in the third intron of TNF-alpha. *J Leukoc Biol* 1999 Jul;66(1):183-93.

¹⁰¹ Espinos E, Le Van Thai A, Pomies C, Weber MJ. Cooperation between phosphorylation and acetylation processes in transcriptional control. *Mol Cell Biol* 1999 May;19(5):3474-84.

¹⁰² Herschlag D., Johnson F. B., 1993. Synergism in transcriptional activation: a kinetic view. *Genes and Development*, 7:173-179.

¹⁰³ Espinos E, Le Van Thai A, Pomies C, Weber MJ. Cooperation between phosphorylation and acetylation processes in transcriptional control. *Mol Cell Biol* 1999 May;19(5):3474-84.

¹⁰⁴ Bannert N, Avots A, Baier M, Serfling E, Kurth R. GA-binding protein factors, in concert with the coactivator CREB binding protein/p300, control the induction of the interleukin 16 promoter in T lymphocytes. *Proc, Natl, Acad, Sci, USA* 1999 96:1541-1546.

¹⁰⁵ Eckner R, Ewen MB, Newsome D, Gerdes M, DeCaprio JA, Lawrence JB, Livingston DM. Molecular cloning and functional analysis of the adenovirus B1A-associated 300-kD protein (p300) reveals a protein with properties of a transcriptional adaptor. *Genes Dev.* 1994 Apr 15;8(8):869-84.

¹⁰⁶ Flory E, Hoffmeyer A, Smola U, Rapp UR, Bruder JT. Raf-1 kinase targets GA-binding protein in transcriptional regulation of the human immunodeficiency virus type 1 promoter. *J Virol* 1996 Apr;70(4):2260-8.

¹⁰⁷ Avots A, Hoffmeyer A, Flory E, Cimanis A, Rapp UR, Serfling E. GABP factors bind to a distal interleukin 2 (IL-2) enhancer and contribute to c-Raf-mediated increase in IL-2 induction. *Molecular and Cellular Biology* 17(8):4381-4389.

¹⁰⁸ Hoffmeyer A, Avots A, Flory E, Weber CK, Serfling E, Rapp UR. The GABP-responsive element of the interleukin-2 enhancer is regulated by JNK/SAPK-activating pathways in T lymphocytes. *J Biol Chem.* 1998 Apr 24;273(17):10112-9.

¹⁰⁹ Martin ME, Chinenov Y, Yu M, Schmidt TK, Yang XY. Redox regulation of GA-binding protein-alpha DNA binding activity. *J Biol Chem.* 1996 Oct 11;271(41):25617-23.

¹¹⁰ Hoare S, Copland JA, Wood TG, Jeng YJ, Izban MG, Soloff MS. Identification of a GABP alpha/beta binding site involved in the induction of oxytocin receptor gene expression in human breast cells, potentiation by c-Fos/c-Jun. *Endocrinology*. 1999 May;140(5):2268-79.

¹¹¹ Rosmarin AG, Luo M, Caprio DG, Shang J, Simkovich CP. Sp1 cooperates with the ets transcription factor, GABP, to activate the CD18 (beta2 leukocyte integrin) promoter. *J Biol Chem* 1998 May 22;273(21):13097-103.

¹¹² Lin JX, Bhat NK, John S, Queale WS, Leonard WJ. Characterization of the human interleukin-2 receptor beta-chain gene promoter: regulation of promoter activity by ets gene products. *Mol Cell Biol.* 1993 Oct;13(10):6201-10.

¹¹³ Markiewicz S, Bosselut R, Le Deist F, de Villartay JP, Hivroz C, Ghysdael J, Fischer A, de Saint Basile G. Tissue-specific activity of the gammac chain gene promoter depends upon an Ets binding site and is regulated by GA-binding protein. *J Biol Chem.* 1996 Jun 21;271(25):14849-55.

¹¹⁴ Suzuki F, Goto M, Sawa C, Ito S, Watanabe H, Sawada J, Handa H. Functional interactions of transcription factor human GA-binding protein subunits. *J Biol Chem.* 1998 Nov 6;273(45):29302-8.

¹¹⁵ Tomaras GD, Foster DA, Burrer CM, Taffet SM. ETS transcription factors regulate an enhancer activity in the third intron of TNF-alpha. *J Leukoc Biol* 1999 Jul;66(1):183-93.

¹¹⁶ Bottinger EP, Shelley CS, Farokhzad OC, Arnaout MA. The human beta 2 integrin CD18 promoter consists of two inverted Ets cis elements. *Mol Cell Biol.* 1994 Apr;14(4):2604-15.

¹¹⁷ Sowa Y, Shiio Y, Fujita T, Matsumoto T, Okuyama Y, Kato D, Inoue J, Sawada J, Goto M, Watanabe H, Handa H, Sakai T. Retinoblastoma binding factor 1 site in the core promoter region of the human RB gene is activated by hGABP/E4TF1. *Cancer Res.* 1997 Aug 1;57(15):3145-8.

¹¹⁸ Atlas E, Stramwasser M, Whiskin K, Mueller CR. GA-binding protein alpha/beta is a critical regulator of the BRCA1 promoter. *Oncogene* 2000 Apr 6;19(15):1933-40.

¹¹⁹ Li XR, Chong AS, Wu J, Roebuck KA, Kumar A, Parrillo JE, Rapp UR, Kimberly RP, Williams JW, Xu X. Transcriptional regulation of Fas gene expression by GA-binding protein and AP-1 in T cell antigen receptor/CD3 complex-stimulated T cells. *J Biol Chem.* 1999 Dec 3;274(49):35203-10.

¹²⁰ Donovan-Peluso M, George LD, Hassett AC. Lipopolysaccharide induction of tissue factor expression in THP-1 monocytic cells. Protein-DNA interactions with the promoter. *J Biol Chem.* 1994 Jan 14;269(2):1361-9.

¹²¹ Group ER, Donovan-Peluso M. Lipopolysaccharide induction of THP-1 cells activates binding of c-Jun, Ets, and Egr-1 to the tissue factor promoter. *J Biol Chem.* 1996 May 24;271(21):12423-30.

¹²² Hall AJ, Vos HL, Bertina RM. Lipopolysaccharide induction of tissue factor in THP-1 cells involves Jun protein phosphorylation and nuclear factor kappaB nuclear translocation. *J Biol Chem*. 1999 Jan 1;274(1):376-83.

¹²³ Holzmüller H, Moll T, Hofer-Warbinek R, Mechtcheriakova D, Binder BR, Hofer E. A transcriptional repressor of the tissue factor gene in endothelial cells. *Arterioscler Thromb Vasc Biol*. 1999 Jul;19(7):1804-11.

¹²⁴ Donovan-Peluso M, George LD, Hassett AC. Lipopolysaccharide induction of tissue factor expression in THP-1 monocytic cells. Protein-DNA interactions with the promoter. *J Biol Chem*. 1994 Jan 14;269(2):1361-9.

¹²⁵ Holzmüller H, Moll T, Hofer-Warbinek R, Mechtcheriakova D, Binder BR, Hofer E. A transcriptional repressor of the tissue factor gene in endothelial cells. *Arterioscler Thromb Vasc Biol*. 1999 Jul;19(7):1804-11.

¹²⁶ Moll T, Czyz M, Holzmüller H, Hofer-Warbinek R, Wagner B, Winkler H, Bach FH, Hofer E. Regulation of the tissue factor promoter in endothelial cells. Binding of NF kappa B-, AP-1-, and Sp1-like transcription factors. *J Biol Chem*. 1995 Feb 24;270(8):3849-57.

¹²⁷ Nathwani AC, Gale KM, Pemberton KD, Crossman DC, Tuddenham EG, McVey JH. Efficient gene transfer into human umbilical vein endothelial cells allows functional analysis of the human tissue factor gene promoter. *Br J Haematol*. 1994 Sep;88(1):122-8.

¹²⁸ Mackman N, Fowler BJ, Edgington TS, Morrissey JH. Functional analysis of the human tissue factor promoter and induction by serum. *Proc Natl Acad Sci U S A*. 1990 Mar;87(6):2254-8.

¹²⁹ Key NS, Bach RR, Vercellotti GM, Moldow CF. Herpes simplex virus type I does not require productive infection to induce tissue factor in human umbilical vein endothelial cells. *Lab Invest*. 1993 Jun;68(6):645-51.

¹³⁰ Oeth P, Yao J, Fan ST, Mackman N. Retinoic acid selectively inhibits lipopolysaccharide induction of tissue factor gene expression in human monocytes. *Blood*. 1998 Apr 15;91(8):2857-65.

¹³¹ Pendurthi UR, Williams JT, Rao LV. Resveratrol, a polyphenolic compound found in wine, inhibits tissue factor expression in vascular cells : A possible mechanism for the cardiovascular benefits associated with moderate consumption of wine. *Arterioscler Thromb Vasc Biol*. 1999 Feb;19(2):419-26.

¹³² Bach RR, Moldow CF. Mechanism of tissue factor activation on HL-60 cells. *Blood*. 1997 May 1;89(9):3270-6.

¹³³ Nemerson Y, Giesen PL. Some thoughts about localization and expression of tissue factor. *Blood Coagul Fibrinolysis*. 1998 Mar;9 Suppl 1:S45-7.

¹³⁴ Wolberg AS, Kon RH, Monroe DM, Ezban M, Roberts HR, Hoffman M. Decryption of Cellular Tissue Factor Is Independent of Its Cytoplasmic Domain. *Biochem Biophys Res Commun*. 2000 Jun 7;272(2):332-336.

¹³⁵ Schechter AD, Giesen PL, Taby O, Rosenfield CL, Rossikhina M, Fyfe BS, Kohtz DS, Fallon JT, Nemerson Y, Taubman MB. Tissue factor expression in human arterial smooth muscle cells. TF is present in three cellular pools after growth factor stimulation. *J Clin Invest*. 1997 Nov 1;100(9):2276-85.

¹³⁶ Schechter AD, Giesen PL, Taby O, Rosenfield CL, Rossikhina M, Fyfe BS, Kohtz DS, Fallon JT, Nemerson Y, Taubman MB. Tissue factor expression in human arterial smooth muscle cells. TF is present in three cellular pools after growth factor stimulation. *J Clin Invest*. 1997 Nov 1;100(9):2276-85.

¹³⁷ Schechter AD, Giesen PL, Taby O, Rosenfield CL, Rossikhina M, Fyfe BS, Kohtz DS, Fallon JT, Nemerson Y, Taubman MB. Tissue factor expression in human arterial smooth muscle cells. TF is present in three cellular pools after growth factor stimulation. *J Clin Invest*. 1997 Nov 1;100(9):2276-85.

¹³⁸ Pan J, Xia L, McEver RP. Comparison of promoters for the murine and human P-selectin genes suggests species-specific and conserved mechanisms for transcriptional regulation in endothelial cells. *J Biol Chem*. 1998 Apr 17;273(16):10058-67.

¹³⁹ Rosmarin AG, Caprio DG, Kirsch DG, Handa H, Simkovich CP. GABP and PU.1 compete for binding, yet cooperate to increase CD18 (beta 2 leukocyte integrin) transcription. *J Biol Chem*. 1995 Oct 6;270(40):23627-33.

¹⁴⁰ Rosmarin AG, Luo M, Caprio DG, Shang J, Simkevich CP. Sp1 cooperates with the ets transcription factor, GABP, to activate the CD18 (beta2 leukocyte integrin) promoter. *J Biol Chem* 1998 May 22;273(21):13097-103.

¹⁴¹ Le Naour R, Lussiez C, Raoul H, Mabondzo A, Dormont D. Expression of cell adhesion molecules at the surface of *in vitro* human immunodeficiency virus type 1-infected human monocytes: relationships with tumor necrosis factor alpha, interleukin 1beta, and interleukin 6 syntheses. *AIDS Res Hum Retroviruses* 1997 Jul 1;13(10):841-55.

¹⁴² Tanaka Y, Fukudome K, Hayashi M, Takagi S, Yoshie O. Induction of ICAM-1 and LFA-3 by Tax1 of human T-cell leukemia virus type 1 and mechanism of down-regulation of ICAM-1 or LFA-1 in adult-T-cell-leukemia cell lines. *Int J Cancer* 1995 Feb 8;60(4):554-61.

¹⁴³ Patarroyo M, Prieto J, Ernberg I, Gahmberg CG. Absence, or low expression, of leukocyte adhesion molecules CD11 and CD18 on Burkitt lymphoma cells. *Int J Cancer* 1988 Jun 15;41(6):901-7.

¹⁴⁴ Rosen GD, Barks JL, Iademarco MF, Fisher RJ, Dean DC. An intricate arrangement of binding sites for the Ets family of transcription factors regulates activity of the alpha 4 integrin gene promoter. *J Biol Chem* 1994 Jun 3;269(22):15652-60.

¹⁴⁵ Talmud PJ, Palmen J, Walker M. Identification of genetic variation in the human hormone-sensitive lipase gene and 5' sequences: homology of 5' sequences with mouse promoter and identification of potential regulatory elements. *Biochem Biophys Res Commun* 1998 Nov 27;252(3):661-8.

¹⁴⁶ Grober J, Laurell H, Blaise R, Fabry B, Schaak S, Holm C, Langin D. Characterization of the promoter of human adipocyte hormone-sensitive lipase. *Biochem J* 1997 Dec 1;328 (Pt 2):453-61.

¹⁴⁷ Yu M, Yang XY, Schmidt T, Chinenov Y, Wang R, Martin ME. GA-binding protein-dependent transcription initiator elements. Effect of helical spacing between polyomavirus enhancer a factor 3(PEA3)/Ets-binding sites on initiator activity. *J Biol Chem* 1997 Nov 14;272(46):29060-7.

¹⁴⁸ Blaise R, Grober J, Rouet P, Tavernier G, Daegelen D, Langin D. Testis expression of hormone-sensitive lipase is conferred by a specific promoter that contains four regions binding testicular nuclear proteins. *J Biol Chem* 1999 Apr 2;274(14):9327-34.

¹⁴⁹ Talmud PJ, Palmen J, Walker M. Identification of genetic variation in the human hormone-sensitive lipase gene and 5' sequences: homology of 5' sequences with mouse promoter and identification of potential regulatory elements. *Biochem Biophys Res Commun* 1998 Nov 27;252(3):661-8.

¹⁵⁰ Kawamura M, Jensen DF, Wancewicz EV, Joy LL, Khoo JC, Steinberg D. Hormone-sensitive lipase in differentiated 3T3-L1 cells and its activation by cyclic AMP-dependent protein kinase. *Proc Natl Acad Sci U S A* 1981 Feb;78(2):732-6.

¹⁵¹ Gordeladze JO, Hovik KE, Merendino JJ, Hermouet S, Gutkind S, Accili D. Effect of activating and inactivating mutations of Gs- and G12-alpha protein subunits on growth and differentiation of 3T3-L1 preadipocytes. *J Cell Biochem* 1997 Feb;64(2):242-57.

¹⁵² Awazu S, Nakata K, Hida D, Sakamoto T, Nagata K, Ishii N, Kanematsu T. Stable transfection of retinoblastoma gene promotes contact inhibition of cell growth and hepatocyte nuclear factor-1-mediated transcription in human hepatoma cells. *Biochem Biophys Res Commun* 1998 Nov 9;252(1):269-73.

¹⁵³ Armelin HA, Armelin MC, Kelly K, Stewart T, Leder P, Cochran BH, Stiles CD. Functional role for c-myc in mitogenic response to platelet-derived growth factor. *Nature* 1984 Aug 23-29;310(5979):655-60.

¹⁵⁴ Cepko CL, Roberts BE, Mulligan RC. Construction and applications of a highly transmissible murine retrovirus shuttle vector. *Cell* 1984 Jul;37(3):1053-62.

¹⁵⁵ Higgins C, Chatterjee S, Cherington V. The block of adipocyte differentiation by a C-terminally truncated, but not by full-length, simian virus 40 large tumor antigen is dependent on an intact retinoblastoma susceptibility protein family binding domain. *J Virol* 1996 Feb;70(2):745-52.

¹⁵⁶ Higgins C, Chatterjee S, Cherington V. The block of adipocyte differentiation by a C-terminally truncated, but not by full-length, simian virus 40 large tumor antigen is dependent on an intact retinoblastoma susceptibility protein family binding domain. *J Virol* 1996 Feb;70(2):745-52.

¹⁵⁷ Cherington V, Brown M, Paucha E, St Louis J, Spiegelman BM, Roberts TM. Separation of simian virus 40 large-T-antigen-transforming and origin-binding functions from the ability to block differentiation. *Mol Cell Biol* 1988 Mar;8(3):1380-4.

¹⁵⁸ Sellers WR, Kaelin WG Jr. Role of the retinoblastoma protein in the pathogenesis of human cancer. *J Clin Oncol* 1997 Nov;15(11):3301-12.

¹⁵⁹ Dou QP, An B. RB and apoptotic cell death. *Front Biosci*. 1998 Apr 6;3:d419-30.

¹⁶⁰ Coppola JA, Lewis BA, Cole MD. Increased retinoblastoma gene expression is associated with late stages of differentiation in many different cell types. *Oncogene* 1990 Nov;5(11):1731-3.

¹⁶¹ Levine RA, Hopman T, Guo L, Chang MJ, Johnson N. Induction of retinoblastoma gene expression during terminal growth arrest of a conditionally immortalized fetal rat lung epithelial cell line and during fetal lung maturation. *Exp Cell Res*. 1998 Mar 15;239(2):264-76.

¹⁶² Slack RS, Hamel PA, Bladon TS, Gill RM, McBurney MW. Regulated expression of the retinoblastoma gene in differentiating embryonal carcinoma cells. *Oncogene*. 1993 Jun;8(6):1585-91.

¹⁶³ Richon VM, Rifkind RA, Marks PA. Expression and phosphorylation of the retinoblastoma protein during induced differentiation of murine erythroleukemia cells. *Cell Growth Differ*. 1992 Jul;3(7):413-20.

¹⁶⁴ Schwartz B, Avivi-Green C, Polak-Charcon S. Sodium butyrate induces retinoblastoma protein dephosphorylation, p16 expression and growth arrest of colon cancer cells. *Mol Cell Biochem*. 1998 Nov;188(1-2):21-30.

¹⁶⁵ Thompson ME, Jensen RA, Obermiller PS, Page DL, Holt JT. Decreased expression of BRCA1 accelerates growth and is often present during sporadic breast cancer progression. *Nat Genet* 1995 Apr;9(4):444-50.

¹⁶⁶ Rao VN, Shao N, Ahmad M, Reddy ES. Antisense RNA to the putative tumor suppressor gene BRCA1 transforms mouse fibroblasts. *Oncogene*. 1996 Feb 1;12(3):523-8.

¹⁶⁷ Holt JT, Thompson ME, Szabo C, Robinson-Benion C, Arteaga CL, King MC, Jensen RA. Growth retardation and tumour inhibition by BRCA1. *Nat Genet*. 1996 Mar;12(3):298-302.

¹⁶⁸ Tait DL, Obermiller PS, Redlin-Frazier S, Jensen RA, Welcsh P, Darn J, King MC, Johnson DH, Holt JT. A phase I trial of retroviral BRCA1sv gene therapy in ovarian cancer. *Clin Cancer Res*. 1997 Nov;3(11):1959-68.

¹⁶⁹ Russell PA, Pharoah PD, De Foy K, Ramus SJ, Symmonds I, Wilson A, Scott I, Ponder BA, Gayther SA. Frequent loss of BRCA1 mRNA and protein expression in sporadic ovarian cancers. *Int J Cancer*. 2000 Aug;87(3):317-321.

¹⁷⁰ Rio PG, Maurizis JC, Peffault de Latour M, Bignon YJ, Bernard-Gallon DJ. Quantification of BRCA1 protein in sporadic breast carcinoma with or without loss of heterozygosity of the BRCA1 gene. *Int J Cancer* 1999 Mar 15;80(6):823-6.

¹⁷¹ Rice JC, Massey-Brown KS, Futscher BW. Aberrant methylation of the BRCA1 CpG island promoter is associated with decreased BRCA1 mRNA in sporadic breast cancer cells. *Oncogene*. 1998 Oct 8;17(14):1807-12.

¹⁷² Magdinier F, Ribieras S, Lenoir GM, Frappart L, Danté R. Down-regulation of BRCA1 in human sporadic breast cancer: analysis of DNA methylation patterns of the putative promoter region. *Oncogene*. 1998 Dec 17;17(24):3169-76.

¹⁷³ Ozcelik H, To MD, Couture J, Bull SB, Andrulis IL. Preferential allelic expression can lead to reduced expression of BRCA1 in sporadic breast cancers. *Int J Cancer*. 1998 Jul 3;77(1):1-6.

¹⁷⁴ Thompson ME, Jensen RA, Obermiller PS, Page DL, Holt JT. Decreased expression of BRCA1 accelerates growth and is often present during sporadic breast cancer progression. *Nat Genet* 1995 Apr;9(4):444-50.

¹⁷⁵ Russell PA, Pharoah PD, De Foy K, Ramus SJ, Symmonds I, Wilson A, Scott I, Ponder BA, Gayther SA. Frequent loss of BRCA1 mRNA and protein expression in sporadic ovarian cancers. *Int J Cancer*. 2000 Aug;87(3):317-321.

¹⁷⁶ Rio PG, Maurizis JC, Peffault de Latour M, Bignon YJ, Bernard-Gallon DJ. Quantification of BRCA1 protein in sporadic breast carcinoma with or without loss of heterozygosity of the BRCA1 gene. *Int J Cancer* 1999 Mar 15;80(6):823-6.

¹⁷⁷ Futscher BW, Liu Q, Shattuck-Bidens D, Cochran C, Harshman K, Tavtigian S, Bennett LM, Haugen-Strano A, Swensen J, Miki Y, et al. BRCA1 mutations in primary breast and ovarian carcinomas. *Science* 1994 Oct 7;266(5182):120-2.

¹⁷⁸ Merajver SD, Pham TM, Caduff RF, Chen M, Poy EL, Cooney KA, Weber BL, Collins FS, Johnston C, Frank TS. Somatic mutations in the BRCA1 gene in sporadic ovarian tumours. *Nat Genet*. 1995 Apr;9(4):439-43.

¹⁷⁹ Catteau A, Harris WH, Xu CF, Solomon E. Methylation of the BRCA1 promoter region in sporadic breast and ovarian cancer: correlation with disease characteristics. *Oncogene*. 1999 Mar 18;18(11):1957-65.

¹⁸⁰ Magdimer F, Ribieras S, Lenoir GM, Frappart L, Dante R. Down-regulation of BRCA1 in human sporadic breast cancer; analysis of DNA methylation patterns of the putative promoter region. *Oncogene*. 1998 Dec 17;17(24):3169-76.

¹⁸¹ Rice JC, Massey-Brown KS, Futscher BW. Aberrant methylation of the BRCA1 CpG island promoter is associated with decreased BRCA1 mRNA in sporadic breast cancer cells. *Oncogene*. 1998 Oct 8;17(14):1807-12.

¹⁸² Dobrovic A, Simpfendorfer D. Methylation of the BRCA1 gene in sporadic breast cancer. *Cancer Res.* 1997 Aug 15;57(16):3347-50.

¹⁸³ Davidson WF, Giese T, Fredrickson TN. Spontaneous development of plasmacytoid tumors in mice with defective Fas-Fas ligand interactions. *J Exp Med.* 1998 Jun 1;187(11):1825-38.

¹⁸⁴ Drappa J, Vaishnav AK, Sullivan KE, Chu JL, Elkon KB. Fas gene mutations in the Canale-Smith syndrome, an inherited lymphoproliferative disorder associated with autoimmunity. *N Engl J Med.* 1996 Nov 28;335(22):1643-9.

¹⁸⁵ Keane MM, Ettenberg SA, Lowrey GA, Russell EK, Lipkowitz S. Fas expression and function in normal and malignant breast cell lines. *Cancer Res.* 1996 Oct 15;56(20):4791-8.

¹⁸⁶ Gratas C, Tohma Y, Barnas C, Taniere P, Hainaut P, Ohgaki H. Up-regulation of Fas (APO-1/CD95) ligand and down-regulation of Fas expression in human esophageal cancer. *Cancer Res.* 1998 May 15;58(10):2057-62.

¹⁸⁷ Strand S, Hofmann WJ, Hug H, Muller M, Otto G, Strand D, Mariami SM, Stremmel W, Krammer PH, Galle PR. Lymphocyte apoptosis induced by CD95 (APO-1/Fas) ligand-expressing tumor cells—a mechanism of immune evasion? *Nat Med.* 1996 Dec;2(12):1361-6.

¹⁸⁸ Moller P, Koretz K, Leithauser F, Bruderlein S, Henne C, Quentmeier A, Krammer PH. Expression of APO-1 (CD95), a member of the NGF/TNP receptor superfamily, in normal and neoplastic colon epithelium. *Int J Cancer.* 1994 May 1;57(3):371-7.

¹⁸⁹ Leithauser F, Dhein J, Mechtersheimer G, Koretz K, Bruderlein S, Henne C, Schmidt A, Debatin KM, Krammer PH, Moller P. Constitutive and induced expression of APO-1, a new member of the nerve growth factor/tumor necrosis factor receptor superfamily, in normal and neoplastic cells. *Lab Invest.* 1993 Oct;69(4):415-29.

¹⁹⁰ Das H, Koizumi T, Sugimoto T, Chakraborty S, Ichimura T, Hasegawa K, Nishimura R. Quantitation of Fas and Fas ligand gene expression in human ovarian, cervical and endometrial carcinomas using real-time quantitative RT-PCR. *Br J Cancer.* 2000 May;82(10):1682-8.

¹⁹¹ Butler LM, Hewett PJ, Butler WJ, Cowled PA. Down-regulation of Fas gene expression in colon cancer is not a result of allelic loss or gene rearrangement. *Br J Cancer.* 1998 May;77(9):1454-9.

¹⁹² Keane MM, Ettenberg SA, Lowrey GA, Russell EK, Lipkowitz S. Fas expression and function in normal and malignant breast cell lines. *Cancer Res.* 1996 Oct 15;56(20):4791-8.

¹⁹³ Bertoni F, Conconi A, Carobbio S, Realini C, Codegoni AM, Zucca E, Cavalli F. Analysis of Fas/CD95 gene somatic mutations in ovarian cancer cell lines. *Int J Cancer.* 2000 May 1;86(3):450.

¹⁹⁴ Lee SH, Shin MS, Park WS, Kim SY, Kim HS, Han JY, Park GS, Dong SM, Pi JH, Kim CS, Kim SH, Lee JY, Yoo NJ. Alterations of Fas (Apo-1/CD95) gene in non-small cell lung cancer. *Oncogene.* 1999 Jun 24;18(25):3754-60.

¹⁹⁵ Lee SH, Shin MS, Park WS, Kim SY, Dong SM, Pi JH, Lee HK, Kim HS, Jang JJ, Kim CS, Kim SH, Lee JY, Yoo NJ. Alterations of Fas (APO-1/CD95) gene in transitional cell carcinomas of urinary bladder. *Cancer Res.* 1999 Jul 1;59(13):3068-72.

¹⁹⁶ Shin MS, Park WS, Kim SY, Kim HS, Kang SJ, Song KY, Park JY, Dong SM, Pi JH, Oh RR, Lee JY, Yoo NJ, Lee SH. Alterations of Fas (Apo-1/CD95) gene in cutaneous malignant melanoma. *Am J Pathol.* 1999 Jun;154(6):1785-91.

¹⁹⁷ Butler LM, Hewett PJ, Butler WJ, Cowled PA. Down-regulation of Fas gene expression in colon cancer is not a result of allelic loss or gene rearrangement. *Br J Cancer.* 1998 May;77(9):1454-9.

¹⁹⁸ Butler LM, Dobrovic A, Bianco T, Cowled PA. Promoter region methylation does not account for the frequent loss of expression of the Fas gene in colorectal carcinoma. *Br J Cancer.* 2000 Jan;82(1):131-5.

¹⁹⁹ Lessor T, Yoo JY, Davis M, Hamburger AW. Regulation of heregulin beta1-induced differentiation in a human breast carcinoma cell line by the extracellular-regulated kinase (ERK) pathway. *J Cell Biochem* 1998 Sep 15;70(4):587-95.

²⁰⁰ Lessor T, Yoo JY, Davis M, Hamburger AW. Regulation of heregulin beta1-induced differentiation in a human breast carcinoma cell line by the extracellular-regulated kinase (ERK) pathway. *J Cell Biochem* 1998 Sep 15;70(4):587-95.

²⁰¹ He H, Wang X, Gorospe M, Holbrook NJ, Trush MA. Phorbol ester-induced mononuclear cell differentiation is blocked by the mitogen-activated protein kinase kinase (MEK) inhibitor PD98059. *Cell Growth Differ* 1999 May;10(5):307-15.

²⁰² Levine RA, Hopman T, Guo L, Chang MJ, Johnson N. Induction of retinoblastoma gene expression during terminal growth arrest of a conditionally immortalized fetal rat lung epithelial cell line and during fetal lung maturation. *Exp Cell Res*. 1998 Mar 15;239(2):264-76.

²⁰³ Vossen RC, Persoons MC, Slobbe-van Drunen ME, Bruggeman CA, van Dam-Mieras

MC. Intracellular thiol redox status affects rat cytomegalovirus infection of vascular cells. *Virus Res*. 1997 May;48(2):173-83.

²⁰⁴ Scholz M, Cinatl J, Gross V, Vogel JU, Blaheta RA, Freisleben HJ, Markus BH, Doerr HW. Impact of oxidative stress on human cytomegalovirus replication and on cytokine-mediated stimulation of endothelial cells. *Transplantation*. 1996 Jun 27;61(12):1763-70.

²⁰⁵ Ranjan D, Siquijor A, Johnston TD, Wu G, Nagabhuskahn M. The effect of curcumin on human B-cell immortalization by Epstein-Barr virus. *Am Surg*. 1998 Jan;64(1):47-51; discussion 51-2.

²⁰⁶ Nakamura Y, Kawamoto N, Ohto Y, Torikai K, Murakami A, Ohigashi H. A diacetylenic spiroketal enol ether epoxide, AL-1, from Artemisia lactiflora inhibits 12-O-tetradecanoylphorbol-13-acetate-induced tumor promotion possibly by suppression of oxidative stress. *Cancer Lett*. 1999 Jun 1;140(1-2):37-45.

²⁰⁷ Allard JP, Aghdassi E, Chau J, Salit I, Walmsley S. Oxidative stress and plasma antioxidant micronutrients in humans with HIV infection. *Am J Clin Nutr* 1998 Jan;67(1):143-7.

²⁰⁸ Allard JP, Aghdassi E, Chau J, Tam C, Kovacs CM, Salit IE, Walmsley SL. Effects of vitamin E and C supplementation on oxidative stress and viral load in HIV-infected subjects. *AIDS*. 1998 Sep 10;12(13):1653-9.

²⁰⁹ Helen A, Krishnakumar K, Vijayammal PL, Augusti KT. Antioxidant effect of onion oil (*Allium cepa* Linn) on the damages induced by nicotine in rats as compared to alpha-tocopherol. *Toxicol Lett*. 2000 Jul 27;116(1-2):61-8.

²¹⁰ Yildiz D, Liu YS, Ercal N, Armstrong DW. Comparison of pure nicotine- and smokeless tobacco extract-induced toxicities and oxidative stress. *Arch Environ Contam Toxicol*. 1999 Nov;37(4):434-9.

²¹¹ Yildiz D, Ercal N, Armstrong DW. Nicotine enantiomers and oxidative stress. *Toxicology* 1998 Sep 15;130(2-3):155-65.

²¹² Afiaq F, Abidi P, Rahman Q. N-acetyl L-cysteine attenuates oxidant-mediated toxicity induced by chrysotile fibers. *Toxicol Lett*. 2000 Sep 30;117(1-2):53-60.

²¹³ Abidi P, Afiaq F, Arif JM, Lohani M, Rahman Q. Chrysotile-mediated imbalance in the glutathione redox system in the development of pulmonary injury. *Toxicol Lett* 1999 May 20;106(1):31-9.

²¹⁴ Liu W, Ernst JD, Courtney Broaddus V. Phagocytosis of crocidolite asbestos induces oxidative stress, DNA damage, and apoptosis in mesothelial cells. *Am J Respir Cell Mol Biol*. 2000 Sep;23(3):371-8.

²¹⁵ Marczyński B, Kraus T, Rozynek P, Raithel HJ, Baur X. Association between 8-hydroxy-2'-deoxyguanosine levels in DNA of workers highly exposed to asbestos and their clinical data, occupational and non-occupational confounding factors, and cancer. *Mutat Res*. 2000 Jul 10;468(2):203-12.

²¹⁶ Marczyński B, Rozynek P, Kraus T, Schlosser S, Raithel HJ, Baur X. Levels of 8-hydroxy-2'-deoxyguanosine in DNA of white blood cells from workers highly exposed to asbestos in Germany. *Mutat Res*. 2000 Jul 10;468(2):195-202.

²¹⁷ Fisher CB, Rossi AG, Shaw J, Beswick PH, Donaldson K. Release of TNFalpha in response to SiC fibres: differential effects in rodent and human primary macrophages, and in macrophage-like cell lines. *Toxicol In Vitro*. 2000 Feb;14(1):25-31.

²¹⁸ Brown DM, Beswick PH, Bell KS, Donaldson K. Depletion of glutathione and ascorbate in lung lining fluid by respirable fibres. *Ann Occup Hyg.* 2000 Mar;44(2):101-8.

²¹⁹ Butel JS. Viral carcinogenesis: revelation of molecular mechanisms and etiology of human disease. *Carcinogenesis.* 2000 Mar;21(3):405-26.

²²⁰ zur Hausen H. Viruses in human cancers. *Eur J Cancer.* 1999 Aug;35(8):1174-81.

²²¹ Hoppe-Seyler F, Butz K. Human tumor viruses. *Anticancer Res.* 1999 Nov-Dec;19(6A):4747-58.

²²² Bonnet M, Guinebretiere JM, Kremmer B, Grunewald V, Benhamou E, Contesso G, Joab I. Detection of Epstein-Barr virus in invasive breast cancers. *J Natl Cancer Inst.* 1999 Aug 18;91(16):1376-81.

²²³ Labrecque LG, Barnes DM, Fentiman IS, Griffin BE. Epstein-Barr virus in epithelial cell tumors: a breast cancer study. *Cancer Res.* 1995 Jan 1;55(1):39-45.

²²⁴ Magrath I, Bhatia K. Breast cancer: a new Epstein-Barr virus-associated disease? *J Natl Cancer Inst.* 1999 Aug 18;91(16):1349-50.

²²⁵ Rakowicz-Szulcynska EM, Jackson B, Szulcynska AM, Smith M. Human immunodeficiency virus type 1-like DNA sequences and immunoreactive viral particles with unique association with breast cancer. *Clin Diagn Lab Immunol.* 1998 Sep;5(5):645-53.

²²⁶ Sanserson CM, Smith GL. Cell motility and cell morphology: how some viruses take control. 4 May 1999, <http://www-ermm.cbcu.cam.ac.uk/99000629h.htm>

²²⁷ Dore M, Korthuis RJ, Granger DN, Entman ML, Smith CW. P-selectin mediates spontaneous leukocyte rolling in vivo. *Blood* 1993 Aug 15;82(4):1308-16.

²²⁸ Shang XZ, Issekutz AC. Contribution of CD11a/CD18, CD11b/CD18, ICAM-1 (CD54) and -2 (CD102) to human monocyte migration through endothelium and connective tissue fibroblast barriers. *Eur J Immunol.* 1998 Jun;28(6):1970-9.

²²⁹ Shang XZ, Lang BJ, Issekutz AC. Adhesion molecule mechanisms mediating monocyte migration through synovial fibroblast and endothelium barriers: role for CD11/CD18, very late antigen-4 (CD49d/CD29), very late antigen-5 (CD49e/CD29), and vascular cell adhesion molecule-1 (CD106). *J Immunol.* 1998 Jan 1;160(1):467-74.

²³⁰ Meerschaert J, Furie MB. The adhesion molecules used by monocytes for migration across endothelium include CD11a/CD18, CD11b/CD18, and VLA-4 on monocytes and ICAM-1, VCAM-1, and other ligands on endothelium. *J Immunol.* 1995 Apr 15;154(8):4099-112.

²³¹ Meerschaert J, Furie MB. Monocytes use either CD11/CD18 or VLA-4 to migrate across human endothelium in vitro. *J Immunol.* 1994 Feb 15;152(4):1915-26.

²³² Chuluyan HE, Issekutz AC. VLA-4 integrin can mediate CD11/CD18-independent transendothelial migration of human monocytes. *J Clin Invest.* 1993 Dec;92(6):2768-77.

²³³ Kavanaugh AF, Lightfoot E, Lipsky PE, Oppenheimer-Marks N. Role of CD11/CD18 in adhesion and transendothelial migration of T cells. Analysis utilizing CD18-deficient T cell clones. *J Immunol.* 1991 Jun 15;146(12):4149-56.

²³⁴ Wu C, Fields AJ, Kapteijn BA, McDonald JA. The role of alpha 4 beta 1 integrin in cell motility and fibronectin matrix assembly. *J Cell Sci.* 1995 Feb;108 (Pt 2):821-9.

²³⁵ Saltzman WM, Livingston TL, Parkhurst MR. Antibodies to CD18 influence neutrophil migration through extracellular matrix. *J Leukoc Biol.* 1999 Mar;65(3):356-63.

²³⁶ Fernandez-Segura E, Garcia JM, Campos A. Topographic distribution of CD18 integrin on human neutrophils as related to shape changes and movement induced by chemotactic peptide and phorbol esters. *Cell Immunol.* 1996 Jul 10;171(1):120-5.

²³⁷ Weir J, Xie X, Hedqvist P, Ruoslahti E, Lindblom L. beta1 integrins are critically involved in neutrophil locomotion in extravascular tissue In vivo. *J Exp Med.* 1998 Jun 15;187(12):2091-6.

²³⁸ Wu C, Fields AJ, Kapteijn BA, McDonald JA. The role of alpha 4 beta 1 integrin in cell motility and fibronectin matrix assembly. *J Cell Sci.* 1995 Feb;108 (Pt 2):821-9.

²³⁹ Saltzman WM, Livingston TL, Parkhurst MR. Antibodies to CD18 influence neutrophil migration through extracellular matrix. *J Leukoc Biol.* 1999 Mar;65(3):356-63.

²⁴⁰ Muller M, Albrecht S, Golfert F, Hofer A, Funk RH, Magdolen V, Flossel C, Luther T. Localization of tissue factor in actin-filament-rich membrane areas of epithelial cells. *Exp Cell Res.* 1999 Apr 10;248(1):136-47.

²⁴¹ Ott I, Fischer EG, Miyagi Y, Mueller BM, Ruf W. A role for tissue factor in cell adhesion and migration mediated by interaction with actin-binding protein 280. *J Cell Biol.* 1998 Mar 9;140(5):1241-53.

²⁴² Muller M, Albrecht S, Golfer F, Hofer A, Funk RH, Magdolen V, Flossel C, Luther T. Localization of tissue factor in actin-filament-rich membrane areas of epithelial cells. *Exp Cell Res.* 1999 Apr 10;248(1):136-47.

²⁴³ Cunningham CC, Gorlin JB, Kwiatkowski DJ, Hartwig JH, Janmey PA, Byers HR, Stossel TP. Actin-binding protein requirement for cortical stability and efficient locomotion. *Science.* 1992 Jan 17;255(5042):325-7.

²⁴⁴ Ott I, Fischer EG, Miyagi Y, Mueller BM, Ruf W. A role for tissue factor in cell adhesion and migration mediated by interaction with actin-binding protein 280. *J Cell Biol.* 1998 Mar 9;140(5):1241-53.

²⁴⁵ Randolph GJ, Luther T, Albrecht S, Magdolen V, Muller WA. Role of tissue factor in adhesion of mononuclear phagocytes to and trafficking through endothelium in vitro. *Blood.* 1998 Dec 1;92(11):4167-77.

²⁴⁶ Randolph GJ, Luther T, Albrecht S, Magdolen V, Muller WA. Role of tissue factor in adhesion of mononuclear phagocytes to and trafficking through endothelium in vitro. *Blood.* 1998 Dec 1;92(11):4167-77.

²⁴⁷ Ott I, Fischer EG, Miyagi Y, Mueller BM, Ruf W. A role for tissue factor in cell adhesion and migration mediated by interaction with actin-binding protein 280. *J Cell Biol.* 1998 Mar 9;140(5):1241-53.

²⁴⁸ Ott I, Fischer EG, Miyagi Y, Mueller BM, Ruf W. A role for tissue factor in cell adhesion and migration mediated by interaction with actin-binding protein 280. *J Cell Biol.* 1998 Mar 9;140(5):1241-53.

²⁴⁹ Chang LC, Wang JP. Examination of the signal transduction pathways leading to activation of extracellular signal-regulated kinase by formyl-methionyl-leucyl-phenylalanine in rat neutrophils. *FEBS Lett.* 1999 Jul 2;454(1-2):165-8.

²⁵⁰ Yagisawa M, Saeki K, Okuma E, Kitamura T, Kitagawa S, Hirai H, Yazaki Y, Takaku F, Yuo A. Signal transduction pathways in normal human monocytes stimulated by cytokines and mediators: comparative study with normal human neutrophils or transformed cells and the putative roles in functionality and cell biology. *Exp Hematol.* 1999 Jun;27(6):1063-76.

²⁵¹ Coffer PJ, Geijssen N, M'rabet L, Schweizer RC, Maikoc T, Raaijmakers JA, Lammers JW, Koenderman L. Comparison of the roles of mitogen-activated protein kinase kinase and phosphatidylinositol 3-kinase signal transduction in neutrophil effector function. *Biochem J* 1998 Jan 1;329 (Pt 1):121-30.

²⁵² Yamada T, Fan J, Shimokama T, Tokunaga O, Watanabe T. Induction of fatty streak-like lesions in vitro using a culture model system simulating arterial intima. *Am J Pathol.* 1992 Dec;141(6):1435-44.

²⁵³ Kusuhsara M, Chait A, Cader A, Berk BC. Oxidized LDL stimulates mitogen-activated protein kinases in smooth muscle cells and macrophages. *Arterioscler Thromb Vasc Biol.* 1997 Jan;17(1):141-8.

²⁵⁴ Deigner HP, Claus R. Stimulation of mitogen activated protein kinase by LDL and oxLDL in human U-937 macrophage-like cells. *FEBS Lett.* 1996 May 6;385(3):149-53.

²⁵⁵ Balagopalakrishna C, Bhunia AK, Rifkind JM, Chatterjee S. Minimally modified low density lipoproteins induce aortic smooth muscle cell proliferation via the activation of mitogen activated protein kinase. *Mol Cell Biochem.* 1997 May;170(1-2):85-9.

²⁵⁶ Kamanna VS, Bassa BV, Vaziri ND, Roh DD. Atherogenic lipoproteins and tyrosine kinase mitogenic signaling in mesangial cells. *Kidney Int Suppl* 1999 Jul;71:S70-5.

²⁵⁷ Bassa BV, Roh DD, Kirschenbaum MA, Kamanna VS. Atherogenic lipoproteins stimulate mesangial cell p42 mitogen-activated protein kinase. *J Am Soc Nephrol.* 1998 Mar;9(3):488-96.

²⁵⁸ Quinn MT, Parthasarathy S, Fong LG, Steinberg D. Oxidatively modified low density lipoproteins: a potential role in recruitment and retention of monocyte/macrophages during atherosclerosis. *Proc Natl Acad Sci U S A.* 1987 May;84(9):2995-8.

²⁵⁹ Martin ME, Chinenov Y, Yu M, Schmidt TK, Yang XY. Redox regulation of GA-binding protein-alpha DNA binding activity. *J Biol Chem.* 1996 Oct 11;271(41):25617-23.

²⁶⁰ Crutchley DJ, Que BG. Copper-induced tissue factor expression in human monocytic THP-1 cells and its inhibition by antioxidants. *Circulation.* 1995 Jul 15;92(2):238-43.

²⁶¹ Caspar-Bauguil S, Tkaczuk J, Haure MJ, Durand M, Alcouffe J, Thomsen M, Salvayre R, Benoit H. Mildly oxidized low-density lipoproteins decrease early production of interleukin 2 and nuclear factor kappaB binding to DNA in activated T-lymphocytes. *Biochem J.* 1999 Jan 15;337 (Pt 2):269-74.

²⁶² Matsumura T, Sakai M, Matsuda K, Furukawa N, Kaneko K, Shichiri M. Cis-acting DNA elements of mouse granulocyte/macrophage colony-stimulating factor gene responsive to oxidized low density lipoprotein. *J Biol Chem.* 1999 Dec 31;274(53):37665-72.

²⁶³ Hamilton TA, Major JA, Armstrong D, Tebo JM. Oxidized LDL modulates activation of NF kappa B in mononuclear phagocytes by altering the degradation of IkappaBs. *J Leukoc Biol.* 1998 Nov;64(5):667-74.

²⁶⁴ Schackelford RE, Misra UK, Florine-Casteel K, Thai SF, Pizzo SV, Adams DO. Oxidized low density lipoprotein suppresses activation of NF kappa B in macrophages via a pertussis toxin-sensitive signaling mechanism. *J Biol Chem.* 1995 Feb 24;270(8):3475-8.

²⁶⁵ Ohlsson BG, Englund MC, Karlsson AL, Knutson E, Erixon C, Skribeck H, Liu Y,

Bondjers G, Wiklund O. Oxidized low density lipoprotein inhibits lipopolysaccharide-induced binding of nuclear factor-kappaB to DNA and the subsequent expression of tumor necrosis factor-alpha and interleukin-1beta in macrophages. *J Clin Invest* 1996 Jul 1;98(1):78-89.

²⁶⁶ Yan SD, Schmidt AM, Anderson GM, Zhang J, Brett J, Zou YS, Pinsky D, Stern D. Enhanced cellular oxidant stress by the interaction of advanced glycation end products with their receptors/binding proteins. *J Biol Chem.* 1994 Apr 1;269(13):9889-97.

²⁶⁷ Khechou F, Ollivier V, Brudey F, Amar M, Hakim J, de Prost D. Effect of advanced glycation end product-modified albumin on tissue factor expression by monocytes. Role of oxidant stress and protein tyrosine kinase activation. *Arterioscler Thromb Vasc Biol.* 1997 Nov;17(11):2885-90.

²⁶⁸ Crutchley DJ, Que BG. Copper-induced tissue factor expression in human monocytic THP-1 cells and its inhibition by antioxidants. *Circulation.* 1995 Jul 15;92(2):238-43.

²⁶⁹ Brisseau GF, Dackiw AP, Cheung PY, Christie N, Rotstein OD. Posttranscriptional regulation of macrophage tissue factor expression by antioxidants. *Blood* 1995 Feb 15;85(4):1025-35.

²⁷⁰ Ichikawa K, Yoshinari M, Iwase M, Wakisaka M, Doi Y, Iino K, Yamamoto M, Fujishima M. Advanced glycosylation end products induced tissue factor expression in human monocyte-like U937 cells and increased tissue factor expression in monocytes from diabetic patients. *Atherosclerosis.* 1998 Feb;136(2):281-7.

²⁷¹ Carson SD, Pirruccello SJ. Immunofluorescent studies of tissue factor on U87MG cells: evidence for non-uniform distribution. *Blood Coagul Fibrinolysis.* 1993 Dec;4(6):911-20.

²⁷² Lewis JC, Bennett-Cain AL, DeMars CS, Doellgast GJ, Grant KW, Jones NL, Gupta M. Procoagulant activity after exposure of monocyte-derived macrophages to minimally oxidized low density lipoprotein. Co-localization of tissue factor antigen and nascent fibrin fibers at the cell surface. *Am J Pathol.* 1995 Oct;147(4):1029-40.

²⁷³ Lewis JC, Bennett-Cain AL, DeMars CS, Doellgast GJ, Grant KW, Jones NL, Gupta M. Procoagulant activity after exposure of monocyte-derived macrophages to minimally oxidized low density lipoprotein. Co-localization of tissue factor antigen and nascent fibrin fibers at the cell surface. *Am J Pathol.* 1995 Oct;147(4):1029-40.

²⁷⁴ Cui MZ, Penn MS, Chisolm GM. Native and oxidized low density lipoprotein induction of tissue factor gene expression in smooth muscle cells is mediated by both Egr-1 and Sp1. *J Biol Chem.* 1999 Nov 12;274(46):32795-802.

²⁷⁵ Fei H, Berliner JA, Parhami F, Drake TA. Regulation of endothelial cell tissue factor expression by minimally oxidized LDL and lipopolysaccharide. *Arterioscler Thromb.* 1993 Nov;13(11):1711-7.

²⁷⁶ Li D, Mehta JL. Upregulation of endothelial receptor for oxidized LDL (LOX-1) by oxidized LDL and implications in apoptosis of human coronary artery endothelial cells: evidence from use of antisense LOX-1 mRNA and chemical inhibitors. *Arterioscler Thromb Vasc Biol.* 2000 Apr;20(4):1116-22.

²⁷⁷ Maziere C, Auclair M, Djavaheri-Mergny M, Packer L, Maziere JC. Oxidized low density lipoprotein induces activation of the transcription factor NF kappa B in fibroblasts, endothelial and smooth muscle cells. *Biochem Mol Biol Int.* 1996 Aug;39(6):1201-7.

²⁷⁸ Montoya MC, Luscinskas FW, del Pozo MA, Aragones J, de Landazuri MO. Reduced intracellular oxidative metabolism promotes firm adhesion of human polymorphonuclear leukocytes to vascular endothelium under flow conditions. *Eur J Immunol.* 1997 Aug;27(8):1942-51.

²⁷⁹ Martin ME, Chinenov Y, Yu M, Schmidt TK, Yang XY. Redox regulation of GA-binding protein-alpha DNA binding activity. *J Biol Chem.* 1996 Oct 11;271(41):25617-23.

²⁸⁰ Rosmarin AG, Luo M, Caprio DG, Shang J, Simkevich CP. Sp1 cooperates with the ets transcription factor, GABP, to activate the CD18 (beta2 leukocyte integrin) promoter. *J Biol Chem* 1998 May 22;273(21):13097-103.

²⁸¹ Therond P, Abella A, Laurent D, Couturier M, Chalas J, Legrand A, Lindenbaum A. In vitro study of the cytotoxicity of isolated oxidized lipid low-density lipoproteins fractions in human endothelial cells: relationship with the glutathione status and cell morphology. *Free Radic Biol Med* 2000 Feb 15;28(4):585-96.

²⁸² Lizard G, Gueldry S, Sordet O, Monier S, Athias A, Miguet C, Bessede G, Lemaire S, Solary E, Gambert P. Glutathione is implied in the control of 7-ketcholesterol-induced apoptosis, which is associated with radical oxygen species production. *FASEB J* 1998 Dec;12(15):1651-63.

²⁸³ Gray JL, Shankar R. Down regulation of CD11b and CD18 expression in atherosclerotic lesion-derived macrophages. *Am Surg* 1995 Aug;61(8):674-9; discussion 679-80.

²⁸⁴ Trach CC, Wulfroth PM, Severs NJ, Robenek H. Influence of native and modified lipoproteins on migration of mouse peritoneal macrophages and the effect of the antioxidants vitamin E and Probucol. *Eur J Cell Biol* 1996 Oct;71(2):199-205.

²⁸⁵ Pataki M, Lusztig G, Robenek H. Endocytosis of oxidized LDL and reversibility of migration inhibition in macrophage-derived foam cells in vitro. A mechanism for atherosclerosis regression? *Arterioscler Thromb* 1992 Aug;12(8):936-44.

²⁸⁶ Quinn MT, Parthasarathy S, Steinberg D. Endothelial cell-derived chemotactic activity for mouse peritoneal macrophages and the effects of modified forms of low density lipoprotein. *Proc Natl Acad Sci U S A* 1985 Sep;82(17):5949-53.

²⁸⁷ Yamada T, Fan J, Shimokama T, Tokunaga O, Watanabe T. Induction of fatty streak-like lesions in vitro using a culture model system simulating arterial intima. *Am J Pathol* 1992 Dec;141(6):1435-44.

²⁸⁸ Virmani R, Kolodgie FD, Burke AP, Farb A, Schwartz SM. Lessons from sudden coronary death: a comprehensive morphological classification scheme for atherosclerotic lesions. *Arterioscler Thromb Vasc Biol* 2000 May;20(5):1262-75.

²⁸⁹ Pentikainen MO, Oorni K, Ala-Korpela M, Kovanen PT. Modified LDL - trigger of atherosclerosis and inflammation in the arterial intima. *J Intern Med* 2000 Mar;247(3):359-70.

²⁹⁰ Nordestgaard BG, Hjelms E, Stender S, Kjeldsen K. Different efflux pathways for high and low density lipoproteins from porcine aortic intima. *Arteriosclerosis* 1990 May-Jun;10(3):477-85.

²⁹¹ Boren J, Olin K, Lee I, Chait A, Wight TN, Imerarity TL. Identification of the principal proteoglycan-binding site in LDL. A single-point mutation in apo-B100 severely affects proteoglycan interaction without affecting LDL receptor binding. *J Clin Invest* 1998 Jun 15;101(12):2658-64.

²⁹² Pentikainen MO, Oorni K, Ala-Korpela M, Kovanen PT. Modified LDL - trigger of atherosclerosis and inflammation in the arterial intima. *J Intern Med* 2000 Mar;247(3):359-70.

²⁹³ Nordestgaard BG, Tybjaerg-Hansen A, Lewis B. Influx in vivo of low density, intermediate density, and very low density lipoproteins into aortic intimas of genetically hyperlipidemic rabbits. Roles of plasma concentrations, extent of aortic lesion, and lipoprotein particle size as determinants. *Arterioscler Thromb* 1992 Jan;12(1):6-18.

²⁹⁴ Schwenke DC. Comparison of aorta and pulmonary artery: II. LDL transport and metabolism correlate with susceptibility to atherosclerosis. *Circ Res* 1997 Sep;81(3):346-54.

²⁹⁵ Kao CH, Chen JK, Yang VC. Ultrastructure and permeability of endothelial cells in branched regions of rat arteries. *Atherosclerosis* 1994 Jan;105(1):97-114.

²⁹⁶ Kao CH, Chen JK, Kuo JS, Yang VC. Visualization of the transport pathways of low density lipoproteins across the endothelial cells in the branched regions of rat arteries. *Atherosclerosis* 1995 Jul;116(1):27-41.

²⁹⁷ Nordestgaard BG, Wootton R, Lewis B. Selective retention of VLDL, IDL, and LDL in the arterial intima of genetically hyperlipidemic rabbits in vivo. Molecular size as a determinant of fractional loss from the intima-inner media. *Arterioscler Thromb Vasc Biol* 1995 Apr;15(4):534-42.

²⁹⁸ Gerrity RG. The role of the monocyte in atherogenesis: II. Migration of foam cells from atherosclerotic lesions. *Am J Pathol* 1981 May;103(2):191-200.

²⁹⁹ Faggiotto A, Ross R, Harker L. Studies of hypercholesterolemia in the nonhuman primate. I. Changes that lead to fatty streak formation. *Arteriosclerosis* 1984 Jul-Aug;4(4):323-40.

³⁰⁰ Faggiotto A, Ross R. Studies of hypercholesterolemia in the nonhuman primate. II. Fatty streak conversion to fibrous plaque. *Arteriosclerosis* 1984 Jul-Aug;4(4):341-56.

³⁰¹ Kling D, Holzschuh T, Betz E. Recruitment and dynamics of leukocytes in the formation of arterial intimal thickening—a comparative study with normo- and hypercholesterolemic rabbits. *Atherosclerosis*. 1993 Jun;101(1):79-96.

³⁰² Landers SC, Gupta M, Lewis JC. Ultrastructural localization of tissue factor on monocyte-derived macrophages and macrophage foam cells associated with atherosclerotic lesions. *Virchows Arch*. 1994;425(1):49-54.

³⁰³ Faggiotto A, Ross R, Harker L. Studies of hypercholesterolemia in the nonhuman primate. I. Changes that lead to fatty streak formation. *Arteriosclerosis*. 1984 Jul-Aug;4(4):323-40.

³⁰⁴ Malek AM, Alper SL, Izumo S. Hemodynamic shear stress and its role in atherosclerosis. *JAMA*. 1999 Dec 1;282(21):2035-42.

³⁰⁵ Trach CC, Wulfroth PM, Severs NJ, Robenek H. Influence of native and modified lipoproteins on migration of mouse peritoneal macrophages and the effect of the antioxidants vitamin E and Probucol. *Eur J Cell Biol*. 1996 Oct;71(2):199-205.

³⁰⁶ Pataki M, Luszting G, Robenek H. Endocytosis of oxidized LDL and reversibility of migration inhibition in macrophage-derived foam cells in vitro. A mechanism for atherosclerosis regression? *Arterioscler Thromb*. 1992 Aug;12(8):936-44.

³⁰⁷ Wissler RW, Vesselimovich D. Can atherosclerotic plaques regress? Anatomic and biochemical evidence from nonhuman animal models. *Am J Cardiol*. 1990 Mar 20;65(12):33F-40F.

³⁰⁸ Dudrick SJ. Regression of atherosclerosis by the intravenous infusion of specific biochemical nutrient substrates in animals and humans. *Ann Surg*. 1987 Sep;206(3):296-315.

³⁰⁹ Tucker CF, Catsulis C, Strong JP, Eggen DA. Regression of early cholesterol-induced aortic lesions in rhesus monkeys. *Am J Pathol*. 1971 Dec;65(3):493-514.

³¹⁰ Collins RG, Velji R, Guevara NV, Hicks MJ, Chan L, Beaudet AL. P-Selectin or intercellular adhesion molecule (ICAM)-1 deficiency substantially protects against atherosclerosis in apolipoprotein E-deficient mice. *J Exp Med*. 2000 Jan 3;191(1):189-94.

³¹¹ Dong ZM, Chapman SM, Brown AA, Frenette PS, Hynes RO, Wagner DD. The combined role of P- and E-selectins in atherosclerosis. *J Clin Invest*. 1998 Jul 1;102(1):145-52.

³¹² Patel SS, Thiagarajan R, Willerson JT, Yeh ET. Inhibition of alpha4 integrin and ICAM-1 markedly attenuate macrophage homing to atherosclerotic plaques in ApoE-deficient mice. *Circulation*. 1998 Jan 6-13;97(1):75-81.

³¹³ Pentikainen MO, Oorni K, Ala-Korpela M, Kovanen PT. Modified LDL - trigger of atherosclerosis and inflammation in the arterial intima. *J Intern Med*. 2000 Mar;247(3):359-70.

³¹⁴ Stary HC, Chandler AB, Glagov S, Guyton JR, Insull Jr W, Rosenfeld ME, Schaffer SA, Schwartz CJ, Wagner WD, Wissler RW. A Definition of Initial, Fatty Streak, and Intermediate Lesions of Atherosclerosis. A Report From the Committee on Vascular Lesions of the Council on Arteriosclerosis, American Heart Association. AHA Medical/Scientific Statement. 1994. <http://www.americanheart.org/Scientific/statements/1994/059401.html>

³¹⁵ Taylor-Wiedeman J, Sissons P, Sinclair J. Induction of endogenous human cytomegalovirus gene expression after differentiation of onocytes from healthy carriers. *J Virol*. 1994 Mar;68(3):1597-604.

³¹⁶ Guetta E, Guetta V, Shibutani T, Epstein SE. Monocytes harboring cytomegalovirus: interactions with endothelial cells, smooth muscle cells, and oxidized low-density lipoprotein. Possible mechanisms for activating virus delivered by monocytes to sites of vascular injury. *Circ Res* 1997 Jul;81(1):8-16.

³¹⁷ Ikuta K, Luftig RB. Inhibition of cleavage of Moloney murine leukemia virus gag and env coded precursor polyproteins by cerulenin. *Virology*. 1986 Oct 15;154(1):195-206.

³¹⁸ Katoh I, Yoshinaka Y, Luftig RB. The effect of cerulenin on Moloney murine leukemia virus morphogenesis. *Virus Res*. 1986 Aug;5(2-3):265-76.

³¹⁹ Goldfine H, Harley JB, Wyke JA. Effects of inhibitors of lipid synthesis on the replication of Rous sarcoma virus. A specific effect of cerulenin on the processing of major non-glycosylated viral structural proteins. *Biochim Biophys Acta* 1978 Sep 22;512(2):229-40.

³²⁰ Taylor-Wiedeman J, Sissons P, Sinclair J. Induction of endogenous human cytomegalovirus gene expression after differentiation of onocytes from healthy carriers. *J Virol*. 1994 Mar;68(3):1597-604.

³²¹ Ibanez CE, Schrier R, Ghazal P, Wiley C, Nelson JA. Human cytomegalovirus productively infects primary differentiated macrophages. *J Virol*. 1991 Dec;65(12):6581-8.

³²² Lathey JL, Spector SA. Unrestricted replication of human cytomegalovirus in hydrocortisone-treated macrophages. *J Virol*. 1991 Nov;65(11):6371-5.

³²³ Weinshenker BG, Wilton S, Rice GP. Phorbol ester-induced differentiation permits productive human cytomegalovirus infection in a monocytic cell line. *J Immunol*. 1988 Mar 1;140(5):1625-31.

³²⁴ Gonczol E, Andrews PW, Plotkin SA. Cytomegalovirus replicates in differentiated but not in undifferentiated human embryonal carcinoma cells. *Science*. 1984 Apr 13;224(4645):159-61.

³²⁵ Guyton JR. The role of lipoproteins in atherogenesis. *Adv Exp Med Biol*. 1995;369:29-38.

³²⁶ Stary HC, Chandler AB, Dinsmore RE, Fuster V, Glagov S, Insull W Jr, Rosenfeld ME, Schwartz CJ, Wagner WD, Wissler RW. A Definition of Advanced Types of Atherosclerotic Lesions and a Histological Classification of Atherosclerosis: A Report From the Committee on Vascular Lesions of the Council on Arteriosclerosis, American Heart Association. *AHA Medical/Scientific Statement*. 1995. <http://www.americanheart.org/Scientific/statements/1995/17950005.html>

³²⁷ Randolph GJ, Furie MB. Mononuclear phagocytes egress from an in vitro model of the vascular wall by migrating across endothelium in the basal to apical direction: role of intercellular adhesion molecule 1 and the CD11/CD18 integrins. *J Exp Med*. 1996 Feb 1;183(2):451-62.

³²⁸ Randolph GJ, Luther T, Albrecht S, Magdolen V, Muller WA. Role of tissue factor in adhesion of mononuclear phagocytes to and trafficking through endothelium in vitro. *Blood*. 1998 Dec 1;92(11):4167-77.

³²⁹ Key NS, Bach RR, Vercellotti GM, Moldow CF. Herpes simplex virus type I does not require productive infection to induce tissue factor in human umbilical vein endothelial cells. *Lab Invest*. 1993 Jun;68(6):645-51.

³³⁰ Schechter AD, Giesen PI, Taby O, Rosenfield CL, Rossikhina M, Fyfe BS, Koitz DS, Fallon JT, Nemerson Y, Taubman MB. Tissue factor expression in human arterial smooth muscle cells. TF is present in three cellular pools after growth factor stimulation. *J Clin Invest*. 1997 Nov 1;100(9):2276-85.

³³¹ Lewis JC, Bennett-Cain AL, DeMars CS, Doellgast GJ, Grant KW, Jones NL, Gupta M. Procoagulant activity after exposure of monocyte-derived macrophages to minimally oxidized low density lipoprotein. Co-localization of tissue factor antigen and nascent fibrin fibers at the cell surface. *Am J Pathol*. 1995 Oct;147(4):1029-40.

³³² Randolph GJ, Furie MB. Mononuclear phagocytes egress from an in vitro model of the vascular wall by migrating across endothelium in the basal to apical direction: role of intercellular adhesion molecule 1 and the CD11/CD18 integrins. *J Exp Med*. 1996 Feb 1;183(2):451-62.

³³³ Virmani R, Kolodgie FD, Burke AP, Farb A, Schwartz SM. Lessons from sudden coronary death: a comprehensive morphological classification scheme for atherosclerotic lesions. *Arterioscler Thromb Vasc Biol*. 2000 May;20(5):1262-75.

³³⁴ Zhou YF, Guetta E, Yu ZX, Finkel T, Epstein SE. Human cytomegalovirus increases modified low density lipoprotein uptake and scavenger receptor mRNA expression in vascular smooth muscle cells. *J Clin Invest*. 1996 Nov 1;98(9):2129-38.

³³⁵ Benditt EP, Barrett T, McDougall JK. Viruses in the etiology of atherosclerosis. *Proc Natl Acad Sci U S A* 1983 Oct;80(20):6386-9.

³³⁶ Wang H, Liu B, Fu M, Zeng C. [Transcriptional expression of oncogenes and Rb antioncogene in experimental atherosclerotic lesions]. *Hua Hsi I Ko Ta Hsueh Hsueh Pao*. 1996 Jun;27(2):117-21. Chinese.

³³⁷ Claudio PP, Fratta L, Farina F, Howard CM, Stassi G, Numata S, Pacilio C, Davis A, Lavitrano M, Volpe M, Wilson JM, Trimarco B, Giordano A, Condorelli G. Adenoviral RB2/p130 gene transfer inhibits smooth muscle cell proliferation and prevents restenosis after angioplasty. *Circ Res*. 1999 Nov 26;85(11):1032-9.

³³⁸ Schwartz LB, Moawad J, Svensson EC, Tufts RL, Meyerson SL, Baunoch D, Leiden JM. Adenoviral-mediated gene transfer of a constitutively active form of the retinoblastoma gene product attenuates neointimal thickening in experimental vein grafts. *J Vasc Surg*. 1999 May;29(5):874-81; discussion 882-3.

³³⁹ Smith RC, Wills KN, Antelman D, Perlman H, Truong LN, Krasinski K, Walsh K. Adenoviral constructs encoding phosphorylation-competent full-length and truncated forms of the human retinoblastoma protein inhibit myocyte proliferation and neointima formation. *Circulation*. 1997 Sep 16;96(6):1899-905.

³⁴⁰ Gallo R, Padurean A, Jayaraman T, Marx S, Roque M, Adelman S, Chesebro J, Fallon J, Fuster V, Marks A, Badimon JJ. Inhibition of intimal thickening after balloon angioplasty in porcine coronary arteries by targeting regulators of the cell cycle. *Circulation*. 1999 Apr 27;99(16):2164-70.

³⁴¹ Chiu B. Multiple infections in carotid atherosclerotic plaques. *Am Heart J*. 1999 Nov;138(5 Pt 2):534-536.

³⁴² Nieto FJ. Viruses and atherosclerosis: A critical review of the epidemiologic evidence. *Am Heart J* 1999 Nov;138(5 Pt 2):453-460.

³⁴³ Adam E, Melnick JL, Probsfield JL, Petrie BL, Burek J, Bailey KR, McCollum CH, DeBakey MB. High levels of cytomegalovirus antibody in patients requiring vascular surgery for atherosclerosis. *Lancet*. 1987 Aug 8;2(8554):291-3.

³⁴⁴ Li B, Xu C, Wang Q. The detection of the antibodies of human cytomegalovirus in the sera of patients with coronary heart disease. *Chung Hua Nei Ko Tsa Chih*. 1996 Nov;35(11):741-3. (in Chinese).

³⁴⁵ Liuzzo G, Caligiuri G, Grillo RL, et al. Helicobacter pylori and cytomegalovirus infections are strongly associated with atherosclerosis, but are not responsible for the instability of angina [abstract]. *J Am Coll Cardiol* 1997;29(suppl A):217A.

³⁴⁶ Blum A, Giladi M, Weinberg M, Kaplan G, Pasternack H, Laniado S, Miller H. High anti-cytomegalovirus (CMV) IgG antibody titer is associated with coronary artery disease and may predict post-coronary balloon angioplasty restenosis. *Am J Cardiol*. 1998 Apr 1;81(7):866-8.

³⁴⁷ Nieto FJ. Viruses and atherosclerosis: A critical review of the epidemiologic evidence. *Am Heart J* 1999 Nov;138(5 Pt 2):453-460.

³⁴⁸ Sorlie PD, Nieto FJ, Adam E, Folsom AR, Shahar E, Massing M. A prospective study of cytomegalovirus, herpes simplex virus 1, and coronary heart disease: the atherosclerosis risk in communities (ARIC) study. *Arch Intern Med*. 2000 Jul 10;160(13):2027-32.

³⁴⁹ Fabricant CG, Fabricant J. Atherosclerosis induced by infection with Marek's disease herpesvirus in chickens. *Am Heart J* 1999 Nov;138(5 Pt 2):S465-8.

³⁵⁰ Dodet B, Plotkin SA. Infection and atherosclerosis. *Am Heart J* 1999 Nov;138(5 Pt 2):417-418.

³⁵¹ Fong IW. Emerging relations between infectious diseases and coronary artery disease and atherosclerosis. *CMAJ*. 2000 Jul 11;163(1):49-56.

³⁵² zur Hausen H. Viruses in human cancers. *Eur J Cancer*. 1999 Dec;35(14):1878-85.

³⁵³ Crawford L. Criteria for establishing that a virus is oncogenic. *Ciba Found Symp*. 1986;120:104-16.

³⁵⁴ Butel JS. Viral carcinogenesis: revelation of molecular mechanisms and etiology of human disease. *Carcinogenesis*. 2000 Mar;21(3):405-26.

³⁵⁵ Sawada M, Miyake S, Ohshima S, Matsubara O, Masuda S, Yakumaru K, Yoshizawa Y. Expression of tissue factor in non-small-cell lung cancers and its relationship to metastasis. *Br J Cancer*. 1999 Feb;79(3-4):472-7.

³⁵⁶ Shigemori C, Wada H, Matsumoto K, Shiku H, Nakamura S, Suzuki H. Tissue factor expression and metastatic potential of colorectal cancer. *Thromb Haemost*. 1998 Dec;80(6):894-8.

³⁵⁷ Mueller BM, Reisfeld RA, Edgington TS, Ruf W. Expression of tissue factor by melanoma cells promotes efficient hematogenous metastasis. *Proc Natl Acad Sci U S A*. 1992 Dec 15;89(24):11832-6.

³⁵⁸ Adamson AS, Francis JL, Witherow RO, Snell ME. Urinary tissue factor levels in prostatic carcinoma: a potential marker of metastatic spread? *Br J Urol*. 1993 May;71(5):587-92.

³⁵⁹ Kataoka H, Uchino H, Asada Y, Hatakeyama K, Nabeshima K, Sumiyoshi A, Koono M. Analysis of tissue factor and tissue factor pathway inhibitor expression in human colorectal carcinoma cell lines and metastatic sublines to the liver. *Int J Cancer*. 1997 Sep 4;72(5):878-84.

³⁶⁰ Sturm U, Luther T, Albrecht S, Flossel C, Grossmann H, Muller M. Immunohistological detection of tissue factor in normal and abnormal human mammary glands using monoclonal antibodies. *Virchows Arch A Pathol Anat Histopathol*. 1992;421(2):79-86.

³⁶¹ Hu T, Bach RR, Horton R, Konigsberg WH, Todd MB. Procoagulant activity in cancer cells is dependent on tissue factor expression. *Oncol Res*. 1994;6(7):321-7.

³⁶² Ruf W, Fischer EG, Huang HY, Miyagi Y, Ott I, Riewald M, Mueller BM. Diverse functions of protease receptor tissue factor in inflammation and metastasis. *Immunol Res*. 2000;21(2-3):289-92.

³⁶³ Schwartz JD, Simantov R. Thrombosis and malignancy: pathogenesis and prevention. *In Vivo*. 1998 Nov-Dec;12(6):619-24.

³⁶⁴ Bromberg ME, Konigsberg WH, Madison JF, Pawashe A, Garen A. Tissue factor promotes melanoma metastasis by a pathway independent of blood coagulation. *Proc Natl Acad Sci U S A*. 1995 Aug 29;92(18):8205-9.

³⁶⁵ Gebken J, Luders B, Notbohm H, Klein HH, Brinckmann J, Muller PK, Batge B. Hypergravity stimulates collagen synthesis in human osteoblast-like cells: evidence for the involvement of p44/42 MAP-kinases (ERK 1/2). *J Biochem (Tokyo)*. 1999 Oct;126(4):676-82.

³⁶⁶ Byers PH, Duvic M, Atkinson M, Robinow M, Smith LT, Krane SM, Greally MT, Ludman M, Matalon R, Pauker S, Quanbeck D, Schwarze U. Ehlers-Danlos syndrome type VIIA and VIIB result from splice-junction mutations or genomic deletions that involve exon 6 in the COL1A1 and COL1A2 genes of type I collagen. *Am J Med Genet* 1997 Oct 3;72(1):94-105.

³⁶⁷ Giunta C, Superti-Furga A, Spranger S, Cole WG, Steinmann B. Ehlers-Danlos syndrome type VII: clinical features and molecular defects. *J Bone Joint Surg Am* 1999 Feb;81(2):225-38.

³⁶⁸ Grahame R. Joint hypermobility and genetic collagen disorders: are they related? *Arch Dis Child*, 1999, 80: 188-191.

³⁶⁹ Batti'e MC, Bigos SJ, Sheehy A, Wortley MD. Spinal flexibility and individual factors that influence it. *Physical Therapy* 1987 67(5):653-658.

³⁷⁰ Grahame R. How often, when and how does joint hypermobility lead to osteoarthritis? *Br J Rheumatol* 1989 Aug;28(4):320.

³⁷¹ Scott D, Bird H, Wright V. Joint laxity leading to osteoarthritis. *Rheumatol Rehabil*. 1979 Aug;18(3):167-9.

³⁷² Sharma L, Lou C, Felson DT, Dunlop DD, Kirwan-Mellis G, Hayes KW, Weinrach D, Buchanan TS. Laxity in healthy and osteoarthritic knees. *Arthritis Rheum*. 1999 May;42(5):861-70.

³⁷³ Jonsson H, Valtysdottir ST, Kjartansson O, Brekkan A. Hypermobility associated with osteoarthritis of the thumb base: a clinical and radiological subset of hand osteoarthritis. *Ann Rheum Dis* 1996 Aug;55(8):540-3.

³⁷⁴ Cicuttini FM, Baker JR, Spector TD. The Association of Obesity with Osteoarthritis of the Hand and Knee in Women: A Twin Study. *The Journal of Rheumatology*, 1996, 23:7, 1221-1226.

³⁷⁵ Carman WJ, Sowers M, Hawthorne VM, Weissfeld LA. Obesity as a risk factor for osteoarthritis of the hand and wrist: a prospective study. *Am J Epidemiol* 1994 Jan 15;139(2):119-29.

³⁷⁶ Van Saase JLCM, Vandenbroucke MP, van Romunde LKJ, Valkenburg HA. Osteoarthritis and Obesity in the General Population. A Relationship Calling for and Explanation. *The Journal of Rheumatology*, 1988, 15(7): 1152-1158.

³⁷⁷ Ferguson KA, Love LL, Ryan CF. Effect of mandibular and tongue protrusion on upper airway size during wakefulness. *Am J Respir Crit Care Med* 1997 May;155(5):1748-54.

³⁷⁸ Miyamoto K, Ozbek MM, Lowe AA, Sjoholm TT, Love LL, Fleetham JA, Ryan CF. Mandibular posture during sleep in patients with obstructive sleep apnoea. *Arch Oral Biol* 1999 Aug;44(8):657-64.

³⁷⁹ Ferguson KA, Love LL, Ryan CF. Effect of mandibular and tongue protrusion on upper airway size during wakefulness. *Am J Respir Crit Care Med* 1997 May;155(5):1748-54.

³⁸⁰ Mokdad AH, Serdula MK, Dietz WH, Bowman BA, Marks JS, Koplan JP. The spread of the obesity epidemic in the United States, 1991-1998. *JAMA*. 1999 Oct 27;282(16):1519-22.

³⁸¹ Weinsier RL, Hunter GR, Heini AF, Goran MI, Sell SM. The etiology of obesity: relative contribution of metabolic factors, diet, and physical activity. *Am J Med*. 1998 Aug;105(2):145-50.

³⁸² Heini AF, Weinsier RL. Divergent trends in obesity and fat intake patterns: the American paradox. *Am J Med*. 1997 Mar;102(3):259-64.

³⁸³ Hebebrand J, Wulffange H, Goerg T, Ziegler A, Hinney A, Barth N, Mayer H, Remschmidt H. Epidemic obesity: are genetic factors involved via increased rates of assortative mating? *Int J Obes Relat Metab Disord*. 2000 Mar;24(3):345-53.

³⁸⁴ Hill JO, Peters JC. Environmental contributions to the obesity epidemic. *Science*. 1998 May 29;280(5368):1371-4.

³⁸⁵ Koplan JP, Dietz WH. Caloric imbalance and public health policy. *JAMA*. 1999 Oct 27;282(16):1579-81.

³⁸⁶ Beattie JH, Wood AM, Newman AM, Bremner I, Choo KHA, Michalska AE, Duncan JS, Trayhurn P. Obesity and hyperleptinemia in metallothionein (-I and-II) null mice. *Proc. Natl. Acad. Sci. USA* 1998 95(1): 358-363.

³⁸⁷ Rosmarin AG, Caprio DG, Kirsch DG, Handa H, Simkovich CP. GABP and PU.1 compete for binding, yet cooperate to increase CD18 (beta 2 leukocyte integrin) transcription. *J Biol Chem* 1995 Oct 6;270(40):23627-33.

³⁸⁸ Rosmarin AG, Luo M, Caprio DG, Shang J, Simkovich CP. Sp1 cooperates with the ets transcription factor, GABP, to activate the CD18 (beta2 leukocyte integrin) promoter. *J Biol Chem* 1998 May 22;273(21):13097-103.

³⁸⁹ Le Naour R, Lussiez C, Raoul H, Mabondzo A, Dormont D. Expression of cell adhesion molecules at the surface of *in vitro* human immunodeficiency virus type 1-infected human monocytes: relationships with tumor necrosis factor alpha, interleukin 1beta, and interleukin 6 syntheses. *AIDS Res Hum. Retroviruses* 1997 Jul 1;13(10):841-55.

³⁹⁰ Tanaka Y, Fukudome K, Hayashi M, Takagi S, Yoshie O. Induction of ICAM-1 and LFA-3 by Tax1 of human T-cell leukemia virus type 1 and mechanism of down-regulation of ICAM-1 or LFA-1 in adult-T-cell-leukemia cell lines. *Int J Cancer* 1995 Feb 8;60(4):554-61.

³⁹¹ Patarroyo M, Prieto J, Ernberg I, Gahmberg CG. Absence, or low expression, of leukocyte adhesion molecules CD11 and CD18 on Burkitt lymphoma cells. *Int J Cancer* 1988 Jun 15;41(6):901-7.

³⁹² Dong ZM, Gutierrez-Ramos JC, Coxon A, Mayadas TN, Wagner DD. A new class of obesity genes encodes leukocyte adhesion receptors. *Proc. Natl. Acad. Sci. USA* 1997 (94):7526-7530.

³⁹³ Large V, Reynisdottir S, Langin D, Fredby K, Klannemark M, Holm C, Arner P. Decreased expression and function of adipocyte hormone-sensitive lipase in subcutaneous fat cells of obese subjects. *J Lipid Res.* 1999 Nov;40(11):2059-66.

³⁹⁴ Elizalde M, Ryden M, van Harmelen V, Eneroth P, Gyllenhammar H, Holm C, Ramel S, Ohlund A, Arner P, Andersson K. Expression of nitric oxide synthases in subcutaneous adipose tissue of nonobese and obese humans. *J Lipid Res.* 2000 Aug;41(8):1244-51.

³⁹⁵ Maudsley S, Pierce KL, Zamah AM, Miller WE, Ahn S, Daaka Y, Lefkowitz RJ, Luttrell LM. The beta(2)-adrenergic receptor mediates extracellular signal-regulated kinase activation via assembly of a multi-receptor complex with the epidermal growth factor receptor. *J Biol Chem.* 2000 Mar 31;275(13):9572-80.

³⁹⁶ Pierce KL, Maudsley S, Daaka Y, Luttrell LM, Lefkowitz RJ. Role of endocytosis in the activation of the extracellular signal-regulated kinase cascade by sequestering and nonsequestering G protein-coupled receptors. *Proc Natl Acad Sci U S A.* 2000 Feb 15;97(4):1489-94.

³⁹⁷ Elorza A, Sarnago S, Mayor F Jr. Agonist-dependent modulation of G protein-coupled receptor kinase 2 by mitogen-activated protein kinases. *Mol Pharmacol.* 2000 Apr;57(4):778-83.

³⁹⁸ Luttrell LM, Ferguson SS, Daaka Y, Miller WE, Maudsley S, Della Rocca GJ, Lin F, Kawakatsu H, Owada K, Luttrell DK, Caron MG, Lefkowitz RJ. Beta-arrestin-dependent formation of beta2 adrenergic receptor-Src protein kinase complexes. *Science.* 1999 Jan 29;283(5402):655-61.

³⁹⁹ Daaka Y, Luttrell LM, Ahn S, Della Rocca GJ, Ferguson SS, Caron MG, Lefkowitz RJ. Essential role for G protein-coupled receptor endocytosis in the activation of mitogen-activated protein kinase. *J Biol Chem.* 1998 Jan 9;273(2):685-8.

⁴⁰⁰ Cao W, Luttrell LM, Medvedev AV, Pierce KL, Daniel KW, Dixon TM, Lefkowitz RJ, Collins S. Direct Binding of Activated c-Src to the Beta3-Adrenergic Receptor is Required for MAP Kinase Activation. *J Biol Chem.* 2000 Sep 29.

⁴⁰¹ Gerhardt CC, Gros J, Strosberg AD, Issad T. Stimulation of the extracellular signal-regulated kinase 1/2 pathway by human beta-3 adrenergic receptor: new pharmacological profile and mechanism of activation. *Mol Pharmacol.* 1999 Feb;55(2):255-62.

⁴⁰² Soeder KJ, Snedden SK, Cao W, Della Rocca GJ, Daniel KW, Luttrell LM, Collins S. The beta3-adrenergic receptor activates mitogen-activated protein kinase in adipocytes through a Gi-dependent mechanism. *J Biol Chem.* 1999 Apr 23;274(17):12017-22.

⁴⁰³ Hellstrom L, Langin D, Reynisdottir S, Dauzats M, Arner P. Adipocyte lipolysis in normal weight subjects with obesity among first-degree relatives. *Diabetologia.* 1996 Aug;39(8):921-8.

⁴⁰⁴ Shimizu Y, Tamishita T, Minokoshi Y, Shimazu T. Activation of mitogen-activated protein kinase by norepinephrine in brown adipocytes from rats. *Endocrinology.* 1997 Jan;138(1):248-53.

⁴⁰⁵ Yarwood SJ, Kilgour E, Anderson NG. Cyclic AMP stimulates the phosphorylation and activation of p42 and p44 mitogen-activated protein kinases in 3T3-F442A preadipocytes. *Biochem Biophys Res Commun.* 1996 Jul 25;224(3):734-9.

⁴⁰⁶ Gerhardt CC, Gros J, Strosberg AD, Issad T. Stimulation of the extracellular signal-regulated kinase 1/2 pathway by human beta-3 adrenergic receptor: new pharmacological profile and mechanism of activation. *Mol Pharmacol.* 1999 Feb;55(2):255-62.

⁴⁰⁷ Large V, Reynisdottir S, Langin D, Fredby K, Klannemark M, Holm C, Arner P. Decreased expression and function of adipocyte hormone-sensitive lipase in subcutaneous fat cells of obese subjects. *J Lipid Res.* 1999 Nov;40(11):2059-66.

⁴⁰⁸ Hellstrom L, Reynisdottir S. Influence of heredity for obesity on adipocyte lipolysis in lean and obese subjects. *Int J Obes Relat Metab Disord.* 2000 Mar;24(3):340-4.

⁴⁰⁹ Bougnères P, Stunff CL, Pecqueur C, Pinglier E, Adnot P, Ricquier D. In vivo resistance of lipolysis to epinephrine. A new feature of childhood onset obesity. *J Clin Invest.* 1997 Jun 1;99(11):2568-73.

⁴¹⁰ Horowitz JF, Klein S. Whole body and abdominal lipolytic sensitivity to epinephrine is suppressed in upper body obese women. *Am J Physiol Endocrinol Metab.* 2000 Jun;278(6):E1144-52.

⁴¹¹ Osuga J, Ishibashi S, Oka T, Yagyu H, Tozawa R, Fujimoto A, Shionoiri F, Yahagi N, Kraemer FB, Tsutsumi O, Yamada N. Targeted disruption of hormone-sensitive lipase results in male sterility and adipocyte hypertrophy, but not in obesity. *Proc Natl Acad Sci U S A.* 2000 Jan 18;97(2):787-92.

⁴¹² Classon M, Kennedy BK, Mulloy R, Harlow E. Opposing roles of pRB and p107 in adipocyte differentiation. *Proc Natl Acad Sci U S A.* 2000 Sep 26;97(20):10826-31.

⁴¹³ Puigserver P, Ribot J, Serra F, Gianotti M, Bonet ML, Nadal-Ginard B, Palou A. Involvement of the retinoblastoma protein in brown and white adipocyte cell differentiation: functional and physical association with the adipogenic transcription factor C/EBPalpha. *Eur J Cell Biol.* 1998 Oct;77(2):117-23.

⁴¹⁴ Richon VM, Rifkind RA, Marks PA. Expression and phosphorylation of the retinoblastoma protein during induced differentiation of murine erythroleukemia cells. *Cell Growth Differ.* 1992 Jul;3(7):413-20.

⁴¹⁵ Roncari DA, Kindler S, Hollenberg CH. Excessive proliferation in culture of reverted adipocytes from massively obese persons. *Metabolism.* 1986 Jan;35(1):1-4.

⁴¹⁶ Roncari DA, Lau DC, Kindler S. Exaggerated replication in culture of adipocyte precursors from massively obese persons. *Metabolism.* 1981 May;30(5):425-7.

⁴¹⁷ Stock S, Granstrom L, Backman L, Mathiesen AS, Uvnas-Moberg K. Elevated plasma levels of oxytocin in obese subjects before and after gastric banding. *Int J Obes.* 1989;13(2):213-22.

⁴¹⁸ Johnson SR, Kolberg BH, Varner MW, Railsback LD. Maternal obesity and pregnancy. *Surg Gynecol Obstet.* 1987 May;164(5):431-7.

⁴¹⁹ Yakinci C, Pac A, Kucukbay FZ, Tayfun M, Gul A. Serum zinc, copper, and magnesium levels in obese children. *Acta Paediatr Jpn.* 1997 Jun;39(3):339-41.

⁴²⁰ D'Ocon C, Alonso de Armino V, Frasquet I. Levels of Zn and Cu in the serum of a diabetic population. *Rev Esp Fisiol.* 1987 Sep;43(3):335-8. Spanish.

⁴²¹ Taneja SK, Mahajan M, Arya P. Excess bioavailability of zinc may cause obesity in humans. *Experientia.* 1996 Jan 16;52(1):31-3.

⁴²² Ludvik B, Nolan JJ, Baloga J, Sacks D, Olefsky J. Effect of obesity on insulin resistance in normal subjects and patients with NIDDM. *Diabetes.* 1995 Sep;44(9):1121-5.

⁴²³ Prager R, Wallace P, Olefsky JM. Hyperinsulinemia does not compensate for peripheral insulin resistance in obesity. *Diabetes.* 1987 Mar;36(3):327-34.

⁴²⁴ Tasaka Y, Yanagisawa K, Iwamoto Y. Human plasma leptin in obese subjects and diabetics. *Endocr J.* 1997 Oct;44(5):671-6.

⁴²⁵ Bjorbaek C, El-Haschimi K, Frantz JD, Flier JS. The role of SOCS-3 in leptin signaling and leptin resistance. *J Biol Chem.* 1999 Oct 15;274(42):30059-65.

⁴²⁶ de Waard F, Poortman J, de Pedro-Alvarez Ferrero M, Baanders-van Halewijn EA. Weight reduction and oestrogen excretion in obese post-menopausal women. *Maturitas.* 1982 Aug;4(2):155-62.

⁴²⁷ Cauley JA, Gutai JP, Kuller LH, LeDonne D, Powell JG. The epidemiology of serum sex hormones in postmenopausal women. *Am J Epidemiol.* 1989 Jun;129(6):1120-31.

⁴²⁸ Cauley JA, Gutai JP, Kuller LH, Scott J, Nevitt MC. Black-white differences in serum sex hormones and bone mineral density. *Am J Epidemiol.* 1994 May 15;139(10):1035-46.

⁴²⁹ Galea J, Armstrong J, Gadsdon P, Holden H, Francis SE, Holt CM. Interleukin-1 beta in coronary arteries of patients with ischemic heart disease. *Arterioscler Thromb Vasc Biol*. 1996 Aug;16(8):1000-6.

⁴³⁰ Hasdai D, Scheinowitz M, Leibovitz B, Sclarovsky S, Eldar M, Barak V. Increased serum concentrations of interleukin-1 beta in patients with coronary artery disease. *Heart*. 1996 Jul;76(1):24-8.

⁴³¹ Pickup JC, Mattock MB, Chusney GD, Burt D. NIDDM as a disease of the innate immune system: association of acute-phase reactants and interleukin-6 with metabolic syndrome X. *Diabetologia*. 1997 Nov;40(11):1286-92.

⁴³² Pickup JC, Crook MA. Is type II diabetes mellitus a disease of the innate immune system? *Diabetologia*. 1998 Oct;41(10):1241-8.

⁴³³ Hrnciar J, Gabor D, Hrnciarova M, Okapcova J, Szentivanyi M, Kuray P. [Relation between cytokines (TNF-alpha, IL-1 and 6) and homocysteine in android obesity and the phenomenon of insulin resistance syndromes]. *Vnitr Lek*. 1999 Jan;45(1):11-6. Slovak.

⁴³⁴ Avots A, Hoffmeyer A, Flory E, Cimanis A, Rapp UR, Serfling E. GABP factors bind to a distal interleukin 2 (IL-2) enhancer and contribute to c-Raf-mediated increase in IL-2 induction. *Molecular and Cellular Biology* 1997 17(8):4381-4389.

⁴³⁵ Klein JB, Rane MJ, Scherzer JA, Coxon PY, Kettritz R, Mathiesen JM, Buridi A, McLeish KR. Granulocyte-macrophage colony-stimulating factor delays neutrophil constitutive apoptosis through phosphoinositide 3-kinase and extracellular signal-regulated kinase pathways. *J Immunol* 2000 Apr 15;164(8):4286-91.

⁴³⁶ Valledor AF, Comalada M, Xaus J, Celada A. The differential time-course of extracellular-regulated kinase activity correlates with the macrophage response toward proliferation or activation. *J Biol Chem* 2000 Mar 10;275(10):7403-9.

⁴³⁷ Thomas RS, Tymms MJ, McKinlay LH, Shannon MF, Seth A, Kola I. ETS1, NFkappaB and AP1 synergistically transactivate the human GM-CSF promoter. *Oncogene*. 1997 Jun 12;14(23):2845-55.

⁴³⁸ Dhurandhar NV, Israel BA, Kolesar JM, Mayhew GF, Cook ME, Atkinson RL. Increased adiposity in animals due to a human virus. *Int J Obes Relat Metab Disord*. 2000 Aug;24(8):989-96.

⁴³⁹ Behrens GM, Stoll M, Schmidt RE. Lipodystrophy syndrome in HIV infection: what is it, what causes it and how can it be managed? *Drug Saf*. 2000 Jul;23(1):57-76.

⁴⁴⁰ Engelson ES, Kotler DP, Tan Y, Agin D, Wang J, Pierson RN Jr, Heymsfield SB. Fat distribution in HIV-infected patients reporting truncal enlargement quantified by whole-body magnetic resonance imaging. *Am J Clin Nutr*. 1999 Jun;69(6):1162-9.

⁴⁴¹ Clement K, Vaisse C, Lahlou N, Cabrol S, Pelloix V, Cassuto D, Gourmelen M, Dina C, Chambaz J, Lacorte JM, Basdevant A, Bougnères P, Lebouc Y, Froguel P, Guy-Grand B. A mutation in the human leptin receptor gene causes obesity and pituitary dysfunction. *Nature*. 1998 Mar 26;392(6674):398-401.

⁴⁴² Chen H, Charlat O, Tartaglia LA, Woolf EA, Weng X, Ellis SJ, Lakey ND, Culpepper J, Moore KJ, Breitbart RE, Duyk GM, Tepper RI, Morgenstern JP. Evidence that the diabetes gene encodes the leptin receptor: identification of a mutation in the leptin receptor gene in db/db mice. *Cell* 1996 Feb 9;84(3):491-5.

⁴⁴³ da Silva BA, Bjorbaek C, Uotani S, Flier JS. Functional properties of leptin receptor isoforms containing the gln->pro extracellular domain mutation of the fatty rat. *Endocrinology*. 1998 Sep;139(9):3681-90.

⁴⁴⁴ Yamashita T, Murakami T, Otani S, Kuwajima M, Shima K. Leptin receptor signal transduction: OBR α and OBR β of fa type. *Biochem Biophys Res Commun*. 1998 May 29;246(3):752-9.

⁴⁴⁵ del Rey A, Besedovsky H. Antidiabetic effects of interleukin 1. *Proc Natl Acad Sci U S A* 1989 Aug;86(15):5943-7.

⁴⁴⁶ Ilyin SE, Plata-Salamon CR. Molecular regulation of the brain interleukin-1 beta system in obese (fa/fa) and lean (Fa/Fa) Zucker rats. *Brain Res Mol Brain Res*. 1996 Dec 31;43(1-2):209-18.

⁴⁴⁷ Luheshi GN, Gardner JD, Rushforth DA, Loudon AS, Rothwell NJ. Leptin actions on food intake and body temperature are mediated by IL-1. *Proc Natl Acad Sci U S A* 1999 Jun 8;96(12):7047-52.

⁴⁴⁸ Plata-Salamon CR, Vasselli JR, Sonti G. Differential responsiveness of obese (fa/fa) and lean (Fa/Fa) Zucker rats to cytokine-induced anorexia. *Obes Res* 1997 Jan;5(1):36-42.

⁴⁴⁹ Faggioni R, Fuller J, Moser A, Feingold KR, Grunfeld C. LPS-induced anorexia in leptin-deficient (ob/ob) and leptin receptor-deficient (db/db) mice. *Am J Physiol*. 1997 Jul;273(1 Pt 2):R181-6.

⁴⁵⁰ Baroni MG, D'Andrea MP, Montali A, Pannitteri G, Barilla F, Campagna F, Mazzci E, Lovari S, Seccareccia F, Campa PP, Ricci G, Pozzilli P, Urbinati G, Arca M. A common mutation of the insulin receptor substrate-1 gene is a risk factor for coronary artery disease. *Arterioscler Thromb Vasc Biol*. 1999 Dec;19(12):2975-80.

⁴⁵¹ Park K, Kim SJ, Bang YJ, Park JG, Kim NK, Roberts AB, Sporn MB. Genetic changes in the transforming growth factor beta (TGF-beta) type II receptor gene in human gastric cancer cells: correlation with sensitivity to growth inhibition by TGF-beta. *Proc Natl Acad Sci U S A*. 1994 Sep 13;91(19):8772-6.

⁴⁵² Myeroff LL, Parsons R, Kim SJ, Hedrick L, Cho KR, Orth K, Mathis M, Kinzler KW, Lutterbaugh J, Park K, et al. A transforming growth factor beta receptor type II gene mutation common in colon and gastric but rare in endometrial cancers with microsatellite instability. *Cancer Res*. 1995 Dec 1;55(23):5545-7.

⁴⁵³ McCaffrey TA, Du B, Consigli S, Szabo P, Bray PJ, Hartner L, Weksler BB, Sanborn TA, Bergman G, Bush HL Jr. Genomic instability in the type II TGF-beta1 receptor gene in atherosclerotic and restenotic vascular cells. *J Clin Invest*. 1997 Nov 1;100(9):2182-8.

⁴⁵⁴ Serra R, Johnson M, Filvaroff EH, LaBorde J, Sheehan DM, Deryck R, Moses HL. Expression of a truncated, kinase-defective TGF-beta type II receptor in mouse skeletal tissue promotes terminal chondrocyte differentiation and osteoarthritis. *J Cell Biol*. 1997 Oct 20;139(2):541-52.

⁴⁵⁵ Caruso A, Fortini A, Fulghesu AM, Pistilli E, Cucinelli F, Lanzone A, Mancuso S. Ovarian sensitivity to follicle-stimulating hormone during the follicular phase of the human menstrual cycle and in patients with polycystic ovarian syndrome. *Fertil Steril*. 1993 Jan;59(1):115-20.

⁴⁵⁶ Wronski TJ, Schenck PA, Cintron M, Walsh CC. Effect of body weight on osteopenia in ovariectomized rats. *Calcif Tissue Int*. 1987 Mar;40(3):155-9.

⁴⁵⁷ Singh RB, Niaz MA, Rastogi SS, Bajaj S, Gaoli Z, Shoumin Z. Current zinc intake and risk of diabetes and coronary artery disease and factors associated with insulin resistance in rural and urban populations of North India. *J Am Coll Nutr*. 1998 Dec;17(6):564-70.

⁴⁵⁸ Beattie JH, Wood AM, Newman AM, Bremner I, Choo KH, Michalska AE, Duncan JS, Trayhurn P. Obesity and hyperleptinemia in metallothionein (-I and -II) null mice. *Proc Natl Acad Sci U S A*. 1998 Jan 6;95(1):358-63.

⁴⁵⁹ Flaherty SF, Golenbock DT, Milham FH, Ingalls RR. CD11/CD18 leukocyte integrins: new signaling receptors for bacterial endotoxin. *J Surg Res*. 1997 Nov;73(1):85-9.

⁴⁶⁰ Ingalls RR, Golenbock DT. CD11c/CD18, a transmembrane signaling receptor for lipopolysaccharide. *J Exp Med*. 1995 Apr 1;181(4):1473-9.

⁴⁶¹ Ingalls RR, Arnaout MA, Golenbock DT. Outside-in signaling by lipopolysaccharide through a tailless integrin. *J Immunol*. 1997 Jul 1;159(1):433-8.

⁴⁶² Dong ZM, Gutierrez-Ramos JC, Coxon A, Mayadas TN, Wagner DD. A new class of obesity genes encodes leukocyte adhesion receptors. *Proc. Natl. Acad. Sci. USA* 1997 (94):7526-7530.

⁴⁶³ Lammie GA, Sandercock PA, Dennis MS. Recently occluded intracranial and extracranial carotid arteries. Relevance of the unstable atherosclerotic plaque. *Stroke*. 1999 Jul;30(7):1319-25.

⁴⁶⁴ Chambliss LE, Folsom AR, Clegg LX, Sharrett AR, Shahar E, Nieto FJ, Rosamond WD, Evans G. Carotid wall thickness is predictive of incident clinical stroke: the Atherosclerosis Risk in Communities (ARIC) study. *Am J Epidemiol* 2000 Mar 1;151(5):478-87.

⁴⁶⁵ O'Leary DH, Polak JF, Krommal RA, Manolio TA, Burke GL, Wolfson SK. Carotid-artery intima and media thickness as a risk factor for myocardial infarction and stroke in older adults. *Cardiovascular Health Study Collaborative Research Group*. *N Engl J Med*. 1999 Jan 7;340(1):14-22.

⁴⁶⁶ Hart DN. Dendritic cells: unique leukocyte populations which control the primary immune response. *Blood*. 1997 Nov 1;90(9):3245-87.

⁴⁶⁷ Zhuravskaya T, Maciejewski JP, Netski DM, Bruening E, Mackintosh FR, St Jeor S. Spread of human cytomegalovirus (HCMV) after infection of human hematopoietic progenitor cells: model of HCMV latency. *Blood* 1997 Sep 15;90(6):2482-91.

⁴⁶⁸ Maciejewski JP, St Jeor SC. Human cytomegalovirus infection of human hematopoietic progenitor cells. *Leuk Lymphoma* 1999 Mar;33(1-2):1-13.

⁴⁶⁹ Sindre H, Tjoonnfjord GE, Rollag H, Ranneberg-Nilsen T, Veiby OP, Beck S, Degre M, Hestdal K. Human cytomegalovirus suppression of and latency in early hematopoietic progenitor cells. *Blood* 1996 Dec 15;88(12):4526-33.

⁴⁷⁰ Kappelmayer J, Berecki D, Misz M, Olah L, Fekete I, Csiba L, Blasko G. Monocytes express tissue factor in young patients with cerebral ischemia. *Cerebrovasc Dis.* 1998 Jul-Aug;8(4):235-9.

⁴⁷¹ Constant SL, Bottomly K. Induction of Th1 and Th2 CD4+ T cell responses: the alternative approaches. *Annu Rev Immunol.* 1997;15:297-322.

⁴⁷² Rogers PR, Croft M. Peptide dose, affinity, and time of differentiation can contribute to the Th1/Th2 cytokine balance. *J Immunol.* 1999 Aug 1;163(3):1205-13.

⁴⁷³ Rogers PR, Croft M. Peptide dose, affinity, and time of differentiation can contribute to the Th1/Th2 cytokine balance. *J Immunol.* 1999 Aug 1;163(3):1205-13.

⁴⁷⁴ Rovere P, Fazzini F, Sabbadini MG, Manfredi AA. Apoptosis and systemic autoimmunity: the dendritic cell connection. *Eur J Histochem.* 2000;44(3):229-36.

⁴⁷⁵ Rovere P, Vallinoto C, Bondanza A, Crosti MC, Rescigno M, Ricciardi-Castagnoli P, Rugarli C, Manfredi AA. Bystander apoptosis triggers dendritic cell maturation and antigen-presenting function. *J Immunol.* 1998 Nov 1;161(9):4467-71.

⁴⁷⁶ Heath WR, Kurnts C, Miller JF, Carbone FR. Cross-tolerance: a pathway for inducing tolerance to peripheral tissue antigens. *J Exp Med.* 1998 May 18;187(10):1549-53.

⁴⁷⁷ Sallusto F, Lanzavecchia A. Mobilizing dendritic cells for tolerance, priming, and chronic inflammation. *J Exp Med.* 1999 Feb 15;189(4):611-4.

⁴⁷⁸ O'Brien BA, Harmon BV, Cameron DP, Allan DJ. Beta-cell apoptosis is responsible for the development of IDDM in the multiple low-dose streptozotocin model. *J Pathol.* 1996 Feb;178(2):176-81.

⁴⁷⁹ Lenzen S, Dringern J, Tiedge M. Low antioxidant enzyme gene expression in pancreatic islets compared with various other mouse tissues. *Free Radic Biol Med.* 1996;20(3):463-6.

⁴⁸⁰ Tiedge M, Lortz S, Dringern J, Lenzen S. Relation between antioxidant enzyme gene expression and antioxidative defense status of insulin-producing cells. *Diabetes.* 1997 Nov;46(11):1733-42.

⁴⁸¹ Harman AW, McKenna M, Adamson GM. Postnatal development of enzyme activities associated with protection against oxidative stress in the mouse. *Biol Neonate.* 1990;57(3-4):187-93.

⁴⁸² O'Brien BA, Harmon BV, Cameron DP, Allan DJ. Nicotinamide prevents the development of diabetes in the cyclophosphamide-induced NOD mouse model by reducing beta-cell apoptosis. *J Pathol.* 2000 May;191(1):86-92.

⁴⁸³ Hotta M, Tashiro F, Ikegami H, Niwa H, Ogiwara T, Yodoi J, Miyazaki J. Pancreatic beta cell-specific expression of thioredoxin, an antioxidative and antiapoptotic protein, prevents autoimmune and streptozotocin-induced diabetes. *J Exp Med.* 1998 Oct 19;188(8):1445-51.

⁴⁸⁴ Kubisch HM, Wang J, Bray TM, Phillips JP. Targeted overexpression of Cu/Zn superoxide dismutase protects pancreatic beta-cells against oxidative stress. *Diabetes.* 1997 Oct;46(10):1563-6.

⁴⁸⁵ Kim JY, Chi JK, Kim EJ, Park SY, Kim YW, Lee SK. Inhibition of diabetes in non-obese diabetic mice by nicotinamide treatment for 5 weeks at the early age. *J Korean Med Sci.* 1997 Aug;12(4):293-7.

⁴⁸⁶ Reddy S, Bibby NJ, Elliott RB. Early nicotinamide treatment in the NOD mouse: effects on diabetes and insulitis suppression and autoantibody levels. *Diabetes Res.* 1990 Oct;15(2):95-102.

⁴⁸⁷ Faust A, Burkart V, Ulrich H, Weischer CH, Kolb H. Effect of lipoic acid on cyclophosphamide-induced diabetes and insulitis in non-obese diabetic mice. *Int J Immunopharmacol.* 1994 Jan;16(1):61-6.

⁴⁸⁸ Rabinovitch A, Suarez WL, Power RF. Lazaroid antioxidant reduces incidence of diabetes and insulitis in nonobese diabetic mice. *J Lab Clin Med.* 1993 Apr;121(4):603-7.

⁴⁸⁹ Mori Y, Suko M, Okudaira H, Matsuba I, Tsuruoka A, Sasaki A, Yokoyama H, Tanase T, Shida T, Nishimura M, et al. Preventive effects of cyclosporin on diabetes in NOD mice. *Diabetologia.* 1986 Apr;29(4):244-7.

⁴⁹⁰ Laupacis A, Stiller CR, Gardell C, Keown P, Dupre J, Wallace AC, Thibert P. Cyclosporin prevents diabetes in BB Wistar rats. *Lancet.* 1983 Jan 1;1(8314-5):10-2.

⁴⁹¹ Sevilla N, Kunz S, Holz A, Lewicki H, Homann D, Yamada H, Campbell KP, de La Torre JC, Oldstone MB. Immunosuppression and resultant viral persistence by specific viral targeting of dendritic cells. *J Exp Med.* 2000 Nov 6;192(9):1249-60.

⁴⁹² Roman LM, Simons LF, Hammer RR, Sambrook JF, Gething MJ. The expression of influenza virus hemagglutinin in the pancreatic beta cells of transgenic mice results in autoimmune diabetes. *Cell.* 1990 May 4;61(3):383-96.

⁴⁹³ Sarvetnick N, Shizuru J, Liggett D, Martin L, McIntyre B, Gregory A, Parslow T, Stewart T. Loss of pancreatic islet tolerance induced by beta-cell expression of interferon-gamma. *Nature.* 1990 Aug 30;346(6287):844-7.

⁴⁹⁴ Yamaoka T, Yano M, Idehara C, Yamada T, Tomonari S, Moritani M, Ii S, Yoshimoto K, Hata J, Itakura M. Apoptosis and remodelling of beta cells by paracrine interferon-gamma without insulitis in transgenic mice. *Diabetologia*. 1999 May;42(5):566-73.

⁴⁹⁵ Ohashi PS, Oehen S, Buerki K, Pircher H, Ohashi CT, Odermatt B, Malissen B, Zinkernagel RM, Hengartner H. Ablation of "tolerance" and induction of diabetes by virus infection in viral antigen transgenic mice. *Cell*. 1991 Apr 19;65(2):305-17.

⁴⁹⁶ Oldstone MB, Nerenberg M, Southern P, Price J, Lewicki H. Virus infection triggers insulin-dependent diabetes mellitus in a transgenic model: role of anti-self (virus) immune response. *Cell*. 1991 Apr 19;65(2):319-31.

⁴⁹⁷ von Herrath M, Holz A. Pathological changes in the islet milieu precede infiltration of islets and destruction of beta-cells by autoreactive lymphocytes in a transgenic model of virus-induced IDDM. *J Autoimmun*. 1997 Jun;10(3):231-8.

⁴⁹⁸ Garza KM, Chan SM, Suri R, Nguyen LT, Odermatt B, Schoenberger SP, Ohashi PS. Role of antigen-presenting cells in mediating tolerance and autoimmunity. *J Exp Med*. 2000 Jun 5;191(11):2021-7.

⁴⁹⁹ Pradier O, Willems F, Abramowicz D, Schandene L, de Boer M, Thielemans K, Capel P, Goldman M. CD40 engagement induces monocyte procoagulant activity through an interleukin-10 resistant pathway. *Eur J Immunol*. 1996 Dec;26(12):3048-54.

⁵⁰⁰ Mach F, Schonbeck U, Bonnefoy JY, Pober JS, Libby P. Activation of monocyte/macrophage functions related to acute atheroma complication by ligation of CD40: induction of collagenase, stromelysin, and tissue factor. *Circulation*. 1997 Jul 15;96(2):396-9.

⁵⁰¹ Schonbeck U, Mach F, Sukhova GK, Herman M, Gruber P, Kehry MR, Libby P. CD40 ligation induces tissue factor expression in human vascular smooth muscle cells. *Am J Pathol*. 2000 Jan;156(1):7-14.

⁵⁰² Moodycliffe AM, Shreedhar V, Ullrich SE, Walterscheid J, Bucana C, Kripke ML, Flores-Romo L. CD40-CD40 ligand interactions in vivo regulate migration of antigen-bearing dendritic cells from the skin to draining lymph nodes. *J Exp Med*. 2000 Jun 5;191(11):2011-20.

⁵⁰³ Ehl S, Hombach J, Aichele P, Rulicke T, Odermatt B, Hengartner H, Zinkernagel R, Pircher H. Viral and bacterial infections interfere with peripheral tolerance induction and activate CD8+ T cells to cause immunopathology. *J Exp Med*. 1998 Mar 2;187(5):763-74.

⁵⁰⁴ Hart DN. Dendritic cells: unique leukocyte populations which control the primary immune response. *Blood*. 1997 Nov 1;90(9):3245-87.

⁵⁰⁵ Zhuravskaya T, Maciejewski JP, Netski DM, Bruening E, Mackintosh FR, St Jeor S. Spread of human cytomegalovirus (HCMV) after infection of human hematopoietic progenitor cells: model of HCMV latency. *Blood* 1997 Sep 15;90(6):2482-91.

⁵⁰⁶ Maciejewski JP, St Jeor SC. Human cytomegalovirus infection of human hematopoietic progenitor cells. *Leuk Lymphoma* 1999 Mar;33(1-2):1-13.

⁵⁰⁷ Sindre H, Tjoornfjord GE, Rollag H, Ranneberg-Nilsen T, Veiby OP, Beck S, Degre M, Hestdal K. Human cytomegalovirus suppression of and latency in early hematopoietic progenitor cells. *Blood* 1996 Dec 15;88(12):4526-33.

⁵⁰⁸ Ilowite NT. Premature atherosclerosis in systemic lupus erythematosus. *J Rheumatol*. 2000 Apr;27 Suppl 58:15-9.

⁵⁰⁹ Urowitz M, Gladman D, Bruce I. Atherosclerosis and Systemic Lupus Erythematosus. *Curr Rheumatol Rep* 2000 Feb;2(1):19-23

⁵¹⁰ Dobado-Berrios PM, Lopez-Pedrera C, Velasco F, Aguirre MA, Torres A, Cuadrado MJ. Increased levels of tissue factor mRNA in mononuclear blood cells of patients with primary antiphospholipid syndrome. *Thromb Haemost* 1999 Dec;82(6):1578-82.

⁵¹¹ Ludewig B, Odermatt B, Landmann S, Hengartner H, Zinkernagel RM. Dendritic cells induce autoimmune diabetes and maintain disease via de novo formation of local lymphoid tissue. *J Exp Med*. 1998 Oct 19;188(8):1493-501.

⁵¹² Fearnley DB, Whyte LF, Carnoutsos SA, Cook AH, Hart DN. Monitoring human blood dendritic cell numbers in normal individuals and in stem cell transplantation. *Blood*. 1999 Jan 15;93(2):728-36.

⁵¹³ Barraitt-Boyce SM, Zimmer MI, Harshyne LA, Meyer EM, Watkins SC,

Capuano S,

Murphey-Corb M, Falo LD, Donnenberg AD. Maturation and trafficking of monocyte-derived dendritic cells in monkeys: implications for dendritic cell-based vaccines. *J Immunol*. 2000 Mar 1;164(5):2487-95.

⁵¹⁴ Hermans IF, Ritchie DS, Yang J, Roberts JM, Ronchese F. CD8+ T cell-dependent elimination of dendritic cells in vivo limits the induction of antitumor immunity. *J Immunol*. 2000 Mar 15;164(6):3095-101.

⁵¹⁵ Ludewig B, Ochsenbein AF, Odermatt B, Paulin D, Hengartner H, Zinkernagel RM. Immunotherapy with dendritic cells directed against tumor antigens shared with normal host cells results in severe autoimmune disease. *J Exp Med*. 2000 Mar 6;191(5):795-804.

⁵¹⁶ Roskrow MA, Dilloo D, Suzuki N, Zhong W, Rooney CM, Brenner MK. Autoimmune disease induced by dendritic cell immunization against leukemia. *Leuk Res* 1999 Jun;23(6):549-57.

⁵¹⁷ Lipton HL, Pritchard AE, Calenoff MA. Attenuation of neurovirulence of Theiler's murine encephalomyelitis virus strain GDVII is not sufficient to establish persistence in the central nervous system. *J Gen Virol*. 1998 May;79 (Pt 5):1001-4.

⁵¹⁸ Tsunoda I, Kurtz CI, Fujinami RS. Apoptosis in acute and chronic central nervous system disease induced by Theiler's murine encephalomyelitis virus. *Virology*. 1997 Feb 17;228(2):388-93.

⁵¹⁹ Ha-Lee YM, Dillon K, Kosaras B, Sidman R, Revell P, Fujinami R, Chow M. Mode of spread to and within the central nervous system after oral infection of neonatal mice with the DA strain of Theiler's murine encephalomyelitis virus. *J Virol*. 1995 Nov;69(11):7354-61.

⁵²⁰ Lipton HL, Twaddle G, Jelachich ML. The predominant virus antigen burden is present in macrophages in Theiler's murine encephalomyelitis virus-induced demyelinating disease. *J Virol*. 1995 Apr;69(4):2525-33.

⁵²¹ Miller SD, Vanderlugt CL, Begolka WS, Pao W, Yauch RL, Neville KL, Katz-Levy Y, Carrizosa A, Kim BS. Persistent infection with Theiler's virus leads to CNS autoimmunity via epitope spreading. *Nat Med*. 1997 Oct;3(10):1133-6.

⁵²² Signore A, Chiarelli M, Parisella MG, Capriotti G, Giacalone P, Di Leve G, Barone R. In vivo imaging of insulitis in autoimmune diabetes. *J Endocrinol Invest*. 1999 Feb;22(2):151-8.

⁵²³ Foulis AK, McGill M, Farquharson MA. Insulitis in type 1 (insulin-dependent) diabetes mellitus in man-macrophages, lymphocytes, and interferon-gamma containing cells. *J Pathol*. 1991 Oct;165(2):97-103.

⁵²⁴ Foulis AK, Stewart JA. The pancreas in recent-onset type 1 (insulin-dependent) diabetes mellitus: insulin content of islets, insulitis and associated changes in the exocrine acinar tissue. *Diabetologia*. 1984 Jun;26(6):456-61.

⁵²⁵ Roivainen M, Rasilainen S, Ylipaasto P, Nissinen R, Ustinov J, Bouwens L, Eizirik DL, Hovi T, Otonkoski T. Mechanisms of coxsackievirus-induced damage to human pancreatic beta-cells. *J Clin Endocrinol Metab* 2000 Jan;85(1):432-40.

⁵²⁶ Andreoletti L, Hober D, Hober-Vandenbergh C, Fajard I, Belaich S, Lambert V, Vantyghem MC, Lefebvre J, Wattre P. Coxsackie B virus infection and beta cell autoantibodies in newly diagnosed IDDM adult patients. *Clin Diagn Virol*. 1998 Apr;9(2-3):125-33.

⁵²⁷ Andreoletti L, Hober D, Hober-Vandenbergh C, Belaich S, Vantyghem MC, Lefebvre J, Wattre P. Detection of coxsackie B virus RNA sequences in whole blood samples from adult patients at the onset of type I diabetes mellitus. *J Med Virol*. 1997 Jun;52(2):121-7.

⁵²⁸ Frisk G, Diderholm H. Antibody responses to different strains of coxsackie B4 virus in patients with newly diagnosed type I diabetes mellitus or aseptic meningitis. *J Infect*. 1997 May;34(3):205-10.

⁵²⁹ Clements GB, Galbraith DN, Taylor KW. Coxsackie B virus infection and onset of childhood diabetes. *Lancet*. 1995 Jul 22;346(8969):221-3.

⁵³⁰ De Simone R, Giampaolo A, Giometto B, Gallo P, Levi G, Peschle C, Aloisi F. The costimulatory molecule B7 is expressed on human microglia in culture and in multiple sclerosis acute lesions. *J Neuropathol Exp Neurol*. 1995 Mar;54(2):175-87.

⁵³¹ Windhagen A, Newcombe J, Dangond F, Strand C, Woodroffe MN, Cuzner ML, Hafler DA. Expression of costimulatory molecules B7-1 (CD80), B7-2 (CD86), and interleukin 12 cytokine in multiple sclerosis lesions. *J Exp Med*. 1995 Dec 1;182(6):1985-96.

⁵³² Boven LA, Montagne L, Nottet HS, De Groot CJ. Macrophage inflammatory protein-1alpha (MIP-1alpha), MIP-1beta, and RANTES mRNA semiquantification and protein expression in active demyelinating multiple sclerosis (MS) lesions. *Clin Exp Immunol*. 2000 Nov;122(2):257-63.

⁵³³ Khanna KV, Markham RB. A perspective on cellular immunity in the elderly. *Clin Infect Dis* 1999 Apr;28(4):710-3.

⁵³⁴ Ginaldi L, De Martinis M, D'Ostilio A, Marini L, Loreto MF, Martorelli V, Quaglino D. The immune system in the elderly: II. Specific cellular immunity. *Immunol Res* 1999;20(2):109-15.

⁵³⁵ Liedtke W, Opalka B, Zimmermann CW, Lignitz E. Age distribution of latent herpes simplex virus 1 and varicella-zoster virus genome in human nervous tissue. *J Neurol Sci*. 1993 May;116(1):6-11.

⁵³⁶ Beer WE, Smith AE, Kassab JY, Smith PH, Rowland Payne CM. Concomitance of psoriasis and atopic dermatitis. *Dermatology*. 1992;184(4):265-70.

⁵³⁷ Abrams JR, Kelley SL, Hayes E, Kikuchi T, Brown MJ, Kang S, Lebwohl MG, Guzzo CA, Jegesothy BV, Linsley PS, Krueger JG. Blockade of T lymphocyte costimulation with cytotoxic T lymphocyte-associated antigen 4-immunoglobulin (CTLA4Ig) reverses the cellular pathology of psoriatic plaques, including the activation of keratinocytes, dendritic cells, and endothelial cells. *J Exp Med*. 2000 Sep 4;192(5):681-94.

⁵³⁸ Ohki O, Yokozeki H, Katayama I, Umeda T, Azuma M, Okumura K, Nishioka K. Functional CD86 (B7-2/B70) is predominantly expressed on Langerhans cells in atopic dermatitis. *Br J Dermatol* 1997 Jun;136(6):838-45.

⁵³⁹ Asadullah K, Prosch S, Audring H, Buttnerova I, Volk HD, Sterry W, Docke WD. A high prevalence of cytomegalovirus antigenaemia in patients with moderate to severe chronic plaque psoriasis: an association with systemic tumour necrosis factor alpha overexpression. *Br J Dermatol*. 1999 Jul;141(1):94-102.

⁵⁴⁰ Steigleder GK, Rasokat H, Wemmer U. [Psoriasis in HTLV-III-induced immunologic defect--status of cellular immunity and immunohistologic findings]. *Z Hautkr* 1986 Dec 1;61(23):1671-8. [Article in German]

⁵⁴¹ Montazeri A, Kanitakis J, Bazex J. Psoriasis and HIV infection. *Int J Dermatol*. 1996 Jul;35(7):475-9.

⁵⁴² Fischer T, Schworer H, Vente C, Reich K, Ramadori G. Clinical improvement of HIV-associated psoriasis parallels a reduction of HIV viral load induced by effective antiretroviral therapy. *AIDS*. 1999 Apr 1;13(5):628-9.

⁵⁴³ Vermaelen KY, Carro-Muino I, Lambrecht BN, Pauwels RA. Specific Migratory Dendritic Cells Rapidly Transport Antigen from the Airways to the Thoracic Lymph Nodes. *J Exp Med* 2001 Jan 1;193(1):51-60.

⁵⁴⁴ Lambrecht BN, Pauwels RA, Fazekas De St Groth B. Induction of rapid T cell activation, division, and recirculation by intratracheal injection of dendritic cells in a TCR transgenic model. *J Immunol*. 2000 Mar 15;164(6):2937-46.

⁵⁴⁵ Lambrecht BN, De Veerman M, Coyle AJ, Gutierrez-Ramos JC, Thielemans K, Pauwels RA. Myeloid dendritic cells induce Th2 responses to inhaled antigen, leading to eosinophilic airway inflammation. *J Clin Invest*. 2000 Aug;106(4):551-9.

⁵⁴⁶ Lambrecht BN, Salomon B, Klatzmann D, Pauwels RA. Dendritic cells are required for the development of chronic eosinophilic airway inflammation in response to inhaled antigen in sensitized mice. *J Immunol*. 1998 Apr 15;160(8):4090-7.

⁵⁴⁷ Mathur M, Herrmann K, Qin Y, Gulmen F, Li X, Krimins R, Weinstock J, Elliott D, Bluestone JA, Padrid P. CD28 interactions with either CD80 or CD86 are sufficient to induce allergic airway inflammation in mice. *Am J Respir Cell Mol Biol*. 1999 Oct;21(4):498-509.

⁵⁴⁸ Haczku A, Takeda K, Redai I, Hamelmann E, Cieslewicz G, Joetham A, Loader J, Lee JJ, Irvin C, Gelfand EW. Anti-CD86 (B7.2) treatment abolishes allergic airway hyperresponsiveness in mice. *Am J Respir Crit Care Med*. 1999 May;159(5 Pt 1):1638-43.

⁵⁴⁹ Padrid PA, Mathur M, Li X, Herrmann K, Qin Y, Cattamanchi A, Weinstock J, Elliott D, Sperling AI, Bluestone JA. CTLA4Ig inhibits airway eosinophilia and hyperresponsiveness by regulating the development of Th1/Th2 subsets in a murine model of asthma. *Am J Respir Cell Mol Biol*. 1998 Apr;18(4):453-62.

⁵⁵⁰ Keane-Myers AM, Gause WC, Finkelman FD, Xhou XD, Wills-Karp M. Development of murine allergic asthma is dependent upon B7-2 costimulation. *J Immunol*. 1998 Jan 15;160(2):1036-43.

⁵⁵¹ Balsa A, Dixey J, Sansom DM, Maddison PJ, Hall ND. Differential expression of the costimulatory molecules B7.1 (CD80) and B7.2 (CD86) in rheumatoid synovial tissue. *Br J Rheumatol* 1996 Jan;35(1):33-7.

⁵⁵² Liu MF, Kohsaka H, Sakurai H, Azuma M, Okumura K, Saito I, Miyasaka N. The presence of costimulatory molecules CD86 and CD28 in rheumatoid arthritis synovium. *Arthritis Rheum* 1996 Jan;39(1):110-4.

⁵⁵³ Watanabe H, Inaba M, Adachi Y, Sugiura K, Hisha H, Iguchi T, Ito T, Yasumizu R, Inaba K, Yamashita T, Ichihara S. Experimental autoimmune thyroiditis induced by thyroglobulin-pulsed dendritic cells. *Autoimmunity* 1999;31(4):273-82.

⁵⁵⁴ Tandon N, Metcalfe RA, Barnett D, Weetman AP. Expression of the costimulatory molecule B7/BB1 in autoimmune thyroid disease. *Q J Med*. 1994 Apr;87(4):231-6.

⁵⁵⁵ Muthalif MM, Benter IF, Karzoun N, Fatima S, Harper J, Uddin MR, Malik KU. 20-Hydroxyeicosatetraenoic acid mediates calcium/calmodulin-dependent protein kinase II-induced mitogen-activated protein kinase activation in vascular smooth muscle cells. *Proc Natl Acad Sci U S A*. 1998 Oct 13;95(21):12701-6.

⁵⁵⁶ Wen Y, Nadler JL, Gonzales N, Scott S, Clouser E, Natarajan R. Mechanisms of ANG II-induced mitogenic responses: role of 12-lipoxygenase and biphasic MAP kinase. *Am J Physiol*. 1996 Oct;271(4 Pt 1):C1212-20.

⁵⁵⁷ Rao GN, Baas AS, Glasgow WC, Eling TE, Runge MS, Alexander RW. Activation of mitogen-activated protein kinases by arachidonic acid and its metabolites in vascular smooth muscle cells. *J Biol Chem*. 1994 Dec 23;269(51):32586-91.

⁵⁵⁸ Chen JK, Wang DW, Falck JR, Capdevila J, Harris RC. Transfection of an active cytochrome P450 arachidonic acid epoxygenase indicates that 14,15-epoxyeicosatrienoic acid functions as an intracellular second messenger in response to epidermal growth factor. *J Biol Chem*. 1999 Feb 19;274(8):4764-9.

⁵⁵⁹ Bylund J, Ericsson J, Oliw EH. Analysis of cytochrome P450 metabolites of arachidonic and linoleic acids by liquid chromatography-mass spectrometry with ion trap MS. *Anal Biochem*. 1998 Dec 1;265(1):55-68.

⁵⁶⁰ Imaoka S, Wedlund PJ, Ogawa H, Kimura S, Gonzalez FJ, Kim HY. Identification of CYP2C23 expressed in rat kidney as an arachidonic acid epoxygenase. *J Pharmacol Exp Ther*. 1993 Nov;267(2):1012-6.

⁵⁶¹ Zeldin DC, Plitman JD, Kobayashi J, Miller RF, Snapper JR, Falck JR, Szarek JL, Philpot RM, Capdevila JH. The rabbit pulmonary cytochrome P450 arachidonic acid metabolic pathway: characterization and significance. *J Clin Invest*. 1995 May;95(5):2150-60.

⁵⁶² Rifkind AB, Lee C, Chang TK, Waxman DJ. Arachidonic acid metabolism by human cytochrome P450s 2C8, 2C9, 2E1, and 1A2: regioselective oxygenation and evidence for a role for CYP2C enzymes in arachidonic acid epoxidation in human liver microsomes. *Arch Biochem Biophys*. 1995 Jul 10;320(2):380-9.

⁵⁶³ Luo G, Zeldin DC, Blaisdell JA, Hodgson E, Goldstein JA. Cloning and expression of murine CYP2Cs and their ability to metabolize arachidonic acid. *Arch Biochem Biophys*. 1998 Sep 1;357(1):45-57.

⁵⁶⁴ Keeney DS, Skinner C, Travers JB, Capdevila JH, Namay LB, King LB Jr, Waterman MR. Differentiating keratinocytes express a novel cytochrome P450 enzyme, CYP2B19, having arachidonate monooxygenase activity. *J Biol Chem*. 1998 Nov 27;273(48):32071-9.

⁵⁶⁵ Kidd RS, Straughn AB, Meyer MC, Blaisdell J, Goldstein JA, Dalton JT. Pharmacokinetics of chlorpheniramine, phenytoin, glipizide and nifedipine in an individual homozygous for the CYP2C9*3 allele. *Pharmacogenetics*. 1999 Feb;9(1):71-80.

⁵⁶⁶ Ring BJ, Binkley SN, Vandenbranden M, Wrighton SA. *In vitro* interaction of the antipsychotic agent olanzapine with human cytochromes P450 CYP2C9, CYP2C19, CYP2D6 and CYP3A. *Br J Clin Pharmacol*. 1996 Mar;41(3):181-6.

⁵⁶⁷ Miners JO, Birkett DJ. Cytochrome P4502C9: an enzyme of major importance in human drug metabolism. *Br J Clin Pharmacol*. 1998 Jun;45(6):525-38. Review.

⁵⁶⁸ Egger J, Brett EM. Effects of sodium valproate in 100 children with special reference to weight. *Br Med J (Clin Res Ed)*. 1981 Aug 29;283(6291):577-81.

⁵⁶⁹ Kidd RS, Straughn AB, Meyer MC, Blaisdell J, Goldstein JA, Dalton JT. Pharmacokinetics of chlorpheniramine, phenytoin, glipizide and nifedipine in an individual homozygous for the CYP2C9*3 allele. *Pharmacogenetics*. 1999 Feb;9(1):71-80.

⁵⁷⁰ Campbell IW, Menzies DG, Chalmers J, McBain AM, Brown IR. One year comparative trial of metformin and glipizide in type 2 diabetes mellitus. *Diabete Metab* 1994 Jul-Aug;20(4):394-400.

⁵⁷¹ Petersen KU. Review article: omeprazole and the cytochrome P450 system. *Aliment Pharmacol Ther* 1995 Feb;9(1):1-9.

⁵⁷² Meyer UA. Interaction of proton pump inhibitors with cytochromes P450: consequences for drug interactions. *Yale J Biol Med* 1996 May-Jun;69(3):203-9.

⁵⁷³ Hogan RE, Bertrand ME, Deaton RL, Sommerville KW. Total percentage body weight changes during add-on therapy with tiagabine, carbamazepine and phenytoin. *Epilepsy Res*. 2000 Aug;41(1):23-8.

⁵⁷⁴ Mattson RH, Cramer JA, Collins JF. A comparison of valproate with carbamazepine for the treatment of complex partial seizures and secondarily generalized tonic-clonic seizures in adults. The Department of Veterans Affairs Epilepsy Cooperative Study No. 264 Group. *N Engl J Med*. 1992 Sep 10;327(11):765-71.

⁵⁷⁵ Sadeque AJM, Fisher MB, Korzekwa KR, Gonzalez FJ, Rettie AE. Human CYP2C9 and CYP2A6 mediate formation of the hepatotoxin 4-ene-valproic acid. *J Pharmacol Exp Ther*. 1997 Nov;283(2):698-703.

⁵⁷⁶ Bruni J, Wilder BJ. Valproic acid. Review of a new antiepileptic drug. *Arch Neurol* 1979 Jul;36(7):393-8.

⁵⁷⁷ Egger J, Brett EM. Effects of sodium valproate in 100 children with special reference to weight. *Br Med J (Clin Res Ed)*. 1981 Aug 29;283(6291):577-81.

⁵⁷⁸ Zaccara G, Campostrini R, Paganini M, Messori A, Valenza T, Arnetoli G, Zappoli R. Long-term treatment with sodium valproate: monitoring of venous ammonia concentrations and adverse effects. *Ther Drug Monit*. 1987;9(1):34-40.

⁵⁷⁹ Mattson RH, Cramer JA, Collins JF. A comparison of valproate with carbamazepine for the treatment of complex partial seizures and secondarily generalized tonic-clonic seizures in adults. The Department of Veterans Affairs Epilepsy Cooperative Study No. 264 Group. *N Engl J Med*. 1992 Sep 10;327(11):765-71.

⁵⁸⁰ Sharpe C, Buchanan N. Juvenile myoclonic epilepsy: diagnosis, management and outcome. *Med J Aust*. 1995 Feb 6;162(3):133-4.

⁵⁸¹ Song JC, White CM. Pharmacologic, pharmacokinetic, and therapeutic differences among angiotensin II receptor antagonists. *Pharmacotherapy*. 2000 Feb;20(2):130-9. Review

⁵⁸² Meadowcroft AM, Williamson KM, Patterson JH, Hinderliter AL, Pieper

JA. The effects of fluvastatin, a CYP2C9 inhibitor, on losartan pharmacokinetics in healthy volunteers. *J Clin Pharmacol*. 1999 Apr;39(4):418-24.

⁵⁸³ Miners JO, Birkett DJ. Cytochrome P4502C9: an enzyme of major importance in human drug metabolism. *Br J Clin Pharmacol*. 1998 Jun;45(6):525-38. Review.

⁵⁸⁴ Camargo MJ, von Lutterotti N, Pecker MS, James GD, Timmermans PB,

Laragh JH. DuP 753 increases survival in spontaneously hypertensive stroke-prone rats fed a high sodium diet. *Am J Hypertens*. 1991 Apr;4(4 Pt 2):341S-345S.

⁵⁸⁵ Transon C, Leemann T, Dayer P. *In vitro* comparative inhibition profiles of major human drug metabolising cytochrome P450 isozymes (CYP2C9, CYP2D6 and CYP3A4) by HMG-CoA reductase inhibitors. *Eur J Clin Pharmacol*. 1996;50(3):209-15.

⁵⁸⁶ Matthews PG, Wahlqvist ML, Marks SJ, Myers KA, Hodgson JM. Improvement in arterial stiffness during hypolipidaemic therapy is offset by weight gain. *Int J Obes Relat Metab Disord*. 1993 Oct;17(10):579-83.

⁵⁸⁷ Ring BJ, Binkley SN, Vandenbranden M, Wrighton SA. *In vitro* interaction of the antipsychotic agent olanzapine with human cytochromes P450 CYP2C9, CYP2C19, CYP2D6 and CYP3A. *Br J Clin Pharmacol*. 1996 Mar;41(3):181-6.

⁵⁸⁸ Osser DN, Najarian DM, Dufresne RL. Olanzapine increases weight and serum triglyceride levels. *J Clin Psychiatry*. 1999 Nov;60(11):767-70.

⁵⁸⁹ Koran LM, Ringold AL, Elliott MA. Olanzapine augmentation for treatment-resistant obsessive-compulsive disorder. *J Clin Psychiatry*. 2000 Jul;61(7):514-7.

⁵⁹⁰ Ring BJ, Binkley SN, Vandenbranden M, Wrighton SA. *In vitro* interaction of the antipsychotic agent olanzapine with human cytochromes P450 CYP2C9, CYP2C19, CYP2D6 and CYP3A. *Br J Clin Pharmacol*. 1996 Mar;41(3):181-6.

⁵⁹¹ Fang J, Coutts RT, McKenna KF, Baker GB. Elucidation of individual cytochrome P450 enzymes involved in the metabolism of clozapine. *Naunyn Schmiedebergs Arch Pharmacol*. 1998 Nov;358(5):592-9.

⁵⁹² Prior TI, Chue PS, Tibbo P, Baker GB. Drug metabolism and atypical antipsychotics. *Eur Neuropsychopharmacol*. 1999 Jun;9(4):301-9. Review.

⁵⁹³ Osser DN, Najarian DM, Dufresne RL. Olanzapine increases weight and serum triglyceride levels. *J Clin Psychiatry*. 1999 Nov;60(11):767-70.

⁵⁹⁴ Olesen OV, Limet K. Fluvoxamine-Clozapine drug interaction: inhibition *in vitro* of five cytochrome P450 isoforms involved in clozapine metabolism. *J Clin Psychopharmacol*. 2000 Feb;20(1):35-42.

⁵⁹⁵ Miners JO, Birkett DJ. Cytochrome P4502C9: an enzyme of major importance in human drug metabolism. *Br J Clin Pharmacol*. 1998 Jun;45(6):525-38. Review.

⁵⁹⁶ Schmidler J, Greenblatt DJ, von Moltke LL, Karsov D, Shader RI. Inhibition of CYP2C9 by selective serotonin reuptake inhibitors *in vitro*: studies of phenytoin p-hydroxylation. *Br J Clin Pharmacol*. 1997 Nov;44(5):495-8.

⁵⁹⁷ Harvey BH, Bouwer CD. Neuropharmacology of paradoxical weight gain with selective serotonin reuptake inhibitors. *Clin Neuropharmacol*. 2000 Mar-Apr;23(2):90-7. Review.

⁵⁹⁸ Sansone RA, Wiederman MW, Shrader JA. Naturalistic study of the weight effects of amitriptyline, fluoxetine, and sertraline in an outpatient medical setting. *J Clin Psychopharmacol*. 2000 Apr;20(2):272-4.

⁵⁹⁹ Michelson D, Amsterdam JD, Quitkin FM, Reimherr FW, Rosenbaum JF,

Zajecka J, Sundell KL, Kim Y, Beasley CM Jr. Changes in weight during a 1-year trial of fluoxetine. *Am J Psychiatry*. 1999 Aug;156(8):1170-6.

⁶⁰⁰ Darga LL, Carroll-Michals L, Botsford SJ, Lucas CP. Fluoxetine's effect on weight loss in obese subjects. *Am J Clin Nutr*. 1991 Aug;54(2):321-5.

⁶⁰¹ Ring BJ, Binkley SN, Vandenbranden M, Wrighton SA. *In vitro* interaction of the antipsychotic agent olanzapine with human cytochromes P450 CYP2C9, CYP2C19, CYP2D6 and CYP3A. *Br J Clin Pharmacol*. 1996 Mar;41(3):181-6.

⁶⁰² Miners JO, Birkett DJ. Cytochrome P4502C9: an enzyme of major importance in human drug metabolism. *Br J Clin Pharmacol*. 1998 Jun;45(6):525-38. Review.

⁶⁰³ Lasker JM, Wester MR, Aramsombatdee B, Raucy JL. Characterization of CYP2C19 and CYP2C9 from human liver: respective roles in microsomal tolbutamide, S-mephenytoin, and omeprazole hydroxylations. *Arch Biochem Biophys*. 1998 May 1;353(1):16-28.

⁶⁰⁴ Wissler RW, Borensztajn J, Rubenstein A, Getz G, Vesselinovitch D. The effects of tolbutamide on the development of atherosclerosis in rhesus monkeys fed an average American table-prepared diet. *Adv Exp Med Biol*. 1975;63:379-80.

⁶⁰⁵ Ballagi-Pordany G, Koltai MZ, Aranyi Z, Pogatsa G. Direct effect of hypoglycemic sulphonylureas on the cardiovascular system of dogs. *Diabetes Res Clin Pract*. 1991 Jan;11(1):47-52.

⁶⁰⁶ Grimm SW, Dyroff MC. Inhibition of human drug metabolizing cytochromes P450 by anastrozole, a potent and selective inhibitor of aromatase. *Drug Metab Dispos*. 1997 May;25(5):598-602.

⁶⁰⁷ Wiseman LR, Adkins JC. Anastrozole. A review of its use in the management of postmenopausal women with advanced breast cancer. *Drugs Aging*. 1998 Oct;13(4):321-32. Review.

⁶⁰⁸ Lonning PE. Aromatase inhibitors and their future role in post-menopausal women with early breast cancer. *Br J Cancer*. 1998 Sep;78 Suppl 4:12-5.

⁶⁰⁹ Buzdar AU. Anastrozole: a new addition to the armamentarium against advanced breast cancer. *Am J Clin Oncol*. 1998 Apr;21(2):161-6. Review.

⁶¹⁰ Jonat W. Clinical overview of anastrozole--a new selective oral aromatase inhibitor. *Oncology*. 1997;54 Suppl 2:15-8. Review.

⁶¹¹ Buzdar AU, Jonat W, Howell A, Plourde PV. ARIMIDEX: a potent and selective aromatase inhibitor for the treatment of advanced breast cancer. *J Steroid Biochem Mol Biol*. 1997 Apr;61(3-6):145-9. Review.

⁶¹² Hammarford M. Role of new selective aromatase inhibitor in therapy for metastatic breast cancer in postmenopausal women. *Nurse Pract*. 1997 Mar;22(3):195-6, 201-2.

⁶¹³ Buzdar AU, Jones SE, Vogel CL, Wolter J, Plourde P, Webster A. A phase III trial comparing anastrozole (1 and 10 milligrams), a potent and selective aromatase inhibitor, with megestrol acetate in postmenopausal women with advanced breast carcinoma. Arimidex Study Group. *Cancer*. 1997 Feb 15;79(4):730-9.

⁶¹⁴ Buzdar A, Jonat W, Howell A, Jones SE, Blomqvist C, Vogel CL, Eiermann W, Wolter JM, Azab M, Webster A, Plourde PV. Anastrozole, a potent and selective aromatase inhibitor, versus megestrol acetate in postmenopausal women with advanced breast cancer: results of overview analysis of two phase III trials. Arimidex Study Group. *J Clin Oncol*. 1996 Jul;14(7):2000-11.

⁶¹⁵ Jonat W, Howell A, Blomqvist C, Eiermann W, Winblad G, Tyrell C, Mauriac L, Roche H, Lundgren S, Hellmud R, Azab M. A randomised trial comparing two doses of the new selective aromatase inhibitor anastrozole (Arimidex) with megestrol acetate in postmenopausal patients with advanced breast cancer. *Eur J Cancer*. 1996 Mar;32A(3):404-12.

⁶¹⁶ Khaliq Y, Gallicano K, Seguin I, Fyke K, Carignan G, Bulman D, Badley

A, Cameron DW. Single and multiple dose pharmacokinetics of nelfinavir and CYP2C19 activity in human immunodeficiency virus-infected patients with chronic liver disease. *Br J Clin Pharmacol*. 2000 Aug;50(2):108-15.

⁶¹⁷ Lillibridge JH, Liang BH, Kerr BM, Webber S, Quart B, Shetty BV, Lee CA. Characterization of the selectivity and mechanism of human cytochrome P450 inhibition by the human immunodeficiency virus-protease inhibitor nelfinavir mesylate. *Drug Metab Dispos*. 1998 Jul;26(7):609-16.

⁶¹⁸ Muirhead GJ, Wulff MB, Fielding A, Kleinermans D, Buss N. Pharmacokinetic interactions between sildenafil and saquinavir/ritonavir. *Br J Clin Pharmacol*. 2000 Aug;50(2):99-107.

⁶¹⁹ Kumar GN, Dykstra J, Roberts EM, Jayanti VK, Hickman D, Uchic J, Yao Y, Surber B, Thomas S, Gramman GR. Potent inhibition of the cytochrome P-450 3A-mediated human liver microsomal metabolism of a novel HIV protease inhibitor by ritonavir: A positive drug-drug interaction. *Drug Metab Dispos*. 1999 Aug;27(8):902-8.

⁶²⁰ Kumar GN, Rodrigues AD, Buko AM, Denissen JF. Cytochrome P450-mediated metabolism of the HIV-1 protease inhibitor ritonavir (ABT-538) in human liver microsomes. *J Pharmacol Exp Ther*. 1996 Apr;277(1):423-31.

⁶²¹ Eagling VA, Back DJ, Barry MG. Differential inhibition of cytochrome P450 isoforms by the protease inhibitors, ritonavir, saquinavir and indinavir. *Br J Clin Pharmacol*. 1997 Aug;44(2):190-4.

⁶²² Fung HB, Kirschenbaum HL, Hameed R. Amprenavir: a new human immunodeficiency virus type 1 protease inhibitor. *Clin Ther*. 2000 May;22(5):549-72. Review.

⁶²³ Eagling VA, Back DJ, Barry MG. Differential inhibition of cytochrome P450 isoforms by the protease inhibitors, ritonavir, saquinavir and indinavir. *Br J Clin Pharmacol*. 1997 Aug;44(2):190-4.

⁶²⁴ Fisslthaler B, Hinsch N, Chataigneau T, Popp R, Kiss L, Busse R, Fleming I. Nifedipine increases cytochrome P4502C expression and endothelium-derived hyperpolarizing factor-mediated responses in coronary arteries. *Hypertension*. 2000 Aug;36(2):270-5.

⁶²⁵ Krakoff L. Effectiveness of nifedipine gastrointestinal therapeutic system for treatment of hypertension: results of the MATH Trial. *J Cardiovasc Pharmacol*. 1993;21 Suppl 2:S14-7.

⁶²⁶ Maccario M, Oleandri SE, Avogadro E, Rossetto R, Grottoli S, Procopio M, Camanni F, Ghigo E. Effects of 3-month nifedipine treatment on endocrine-metabolic parameters in patients with abdominal obesity and mild hypertension. *J Endocrinol Invest*. 1998 Jan;21(1):56-63.

⁶²⁷ Andronico G, Piazza G, Mangano MT, Mule G, Carone MB, Cerasola G. Nifedipine vs. enalapril in treatment of hypertensive patients with glucose intolerance. *J Cardiovasc Pharmacol*. 1991;18 Suppl 10:S52-4.

⁶²⁸ Barreiro P, Soriano V, Blanco F, Casimiro C, de la Cruz JJ, Gonzalez-Lahoz J. Risks and benefits of replacing protease inhibitors by nevirapine in HIV-infected subjects under long-term successful triple combination therapy. *AIDS*. 2000 May 5;14(7):807-12.

⁶²⁹ Mulligan K, Grunfeld C, Tai VW, Algren H, Pang M, Chernoff DN, Lo JC, Schambelan M. Hyperlipidemia and insulin resistance are induced by protease inhibitors independent of changes in body composition in patients with HIV infection. *J Acquir Immune Defic Syndr*. 2000 Jan 1;23(1):35-43.

⁶³⁰ Gervasoni C, Ridolfo AL, Trifiro G, Santambrogio S, Norbiato G, Musicco M, Clerici M, Galli M, Moroni M. Redistribution of body fat in HIV-infected women undergoing combined antiretroviral therapy. *AIDS*. 1999 Mar 11;13(4):465-71.

⁶³¹ Carr A, Copper DA. A randomized, multicenter study of protease inhibitor (PI) substitution in aviremic patients with antiretroviral (ARV) lipodystrophy syndrome. 7th Conference on Retroviruses and Opportunistic Infections. 2000 (Abstract).

⁶³² Martinez E, Blanco JL, Garcia MA, Buira E, Bianchi L, Conget I, Casamitjana R, Gatell JM. Impact of switching from HIV-1 protease Inhibitors (PI) to efavirenz (EFV) in patients with lipodystrophy. 7th Conference on Retroviruses and Opportunistic Infections. 2000 (Abstract).

⁶³³ Passalaris JD, Sepkowitz KA, Glesby MJ. Coronary artery disease and human immunodeficiency virus infection. *Clin Infect Dis*. 2000 Sep;31(3):787-97.

⁶³⁴ Andrews GK, Adamson ED. Butyrate selectively activates the metallothionein gene in teratocarcinoma cells and induces hypersensitivity to metal induction. *Nucleic Acids Research*. 1987 15(13): 5461-5475.

⁶³⁵ Thomas DJ, Angle CR, Swanson SA, Caffrey TC. Effect of sodium butyrate on metallothionein induction and cadmium cytotoxicity in ROS 17/2.8 cells. *Toxicology* 1991 Feb 11;66(1):35-46.

⁶³⁶ Liu J, McKim JM Jr, Liu YP, Klaassen CD. Effects of butyrate homologues on metallothionein induction in rat primary hepatocyte cultures. *In Vitro Cell Dev Biol* 1992 May;28A(5):320-6.

⁶³⁷ Ludwig DS, Pereira MA, Kroenke CH, Hilner JE, Van Horn L, Slattery ML, Jacobs DR Jr. Dietary fiber, weight gain, and cardiovascular disease risk factors in young adults. *JAMA*. 1999 Oct 27;282(16):1539-46.

⁶³⁸ Rigaud D, Ryttig KR, Angel LA, Apfelbaum M. Overweight treated with energy restriction and a dietary fibre supplement: a 6-month randomized, double-blind, placebo-controlled trial. *Int J Obes*. 1990 Sep;14(9):763-9.

⁶³⁹ Ryttig KR, Tellnes G, Haegh L, Boe E, Fagerthun H. A dietary fibre supplement and weight maintenance after weight reduction: a randomized, double-blind, placebo-controlled long-term trial. *Int J Obes*. 1989;13(2):165-71.

⁶⁴⁰ Piliang WG, Djojosoebagio S, Suprayogi A. Soybean hull and its effect on atherosclerosis in non-human primates (Macaca fascicularis). *Biomed Environ Sci* 1996 Sep;9(2-3):137-43.

⁶⁴¹ Kim YI. AGA technical review: impact of dietary fiber on colon cancer occurrence. *Gastroenterology*. 2000 Jun;118(6):1235-57.

⁶⁴² Madar Z, Stark A. Dietary fiber and colorectal cancer. *N Engl J Med*. 1999 Jun 17;340(24):1925-6; discussion 1926.

⁶⁴³ Camire ME. Dietary fiber and colorectal cancer. *N Engl J Med*. 1999 Jun 17;340(24):1926.

⁶⁴⁴ Mohandas KM. Dietary fiber and colorectal cancer. *N Engl J Med*. 1999 Jun 17;340(24):1925; discussion 1926.

⁶⁴⁵ Heaton KW, Lewis SJ. Dietary fiber and colorectal cancer. *N Engl J Med*. 1999 Jun 17;340(24):1925; discussion 1926.

⁶⁴⁶ Cummings JH, Southgate DA. Dietary fiber and colorectal cancer. *N Engl J Med*. 1999 Jun 17;340(24):1925; discussion 1926.

⁶⁴⁷ Ravin ND. Dietary fiber and colorectal cancer. *N Engl J Med*. 1999 Jun 17;340(24):1924-5; discussion 1926.

⁶⁴⁸ Reddy BS. Role of dietary fiber in colon cancer: an overview. *Am J Med*. 1999 Jan 25;106(1A):16S-19S; discussion 50S-51S.

⁶⁴⁹ Reddy BS. Prevention of colon carcinogenesis by components of dietary fiber. *Anticancer Res*. 1999 Sep-Oct;19(5A):3681-3.

⁶⁵⁰ Ernest DL, Einspahr JG, Alberts DS. Protective role of wheat bran fiber: data from marker trials. *Am J Med*. 1999 Jan 25;106(1A):32S-37S.

⁶⁵¹ Kritchevsky D. Protective role of wheat bran fiber: preclinical data. *Am J Med*. 1999 Jan 25;106(1A):28S-31S.

⁶⁵² Cohen LA. Dietary fiber and breast cancer. *Anticancer Res*. 1999 Sep-Oct;19(5A):3685-8.

⁶⁵³ Wolin MJ, Miller TL, Yerry S, Zhang Y, Bank S, Weaver GA. Changes of fermentation pathways of fecal microbial communities associated with a drug treatment that increases dietary starch in the human colon. *Appl Environ Microbiol* 1999 Jul;65(7):2807-12.

⁶⁵⁴ Wolin MJ, Miller TL, Yerry S, Zhang Y, Bank S, Weaver GA. Changes of fermentation pathways of fecal microbial communities associated with a drug treatment that increases dietary starch in the human colon. *Appl Environ Microbiol* 1999 Jul;65(7):2807-12.

⁶⁵⁵ Wolever TM, Chiasson JL, Josse RG, Hunt JA, Palmason C, Rodger NW, Ross SA, Ryan EA, Tan MH. Small weight loss on long-term acarbose therapy with no change in dietary pattern or nutrient intake of individuals with non-insulin-dependent diabetes. *Int J Obes Relat Metab Disord*. 1997 Sep;21(9):756-63.

⁶⁵⁶ Huyer G, Liu S, Kelly J, Moffat J, Payette P, Kennedy B, Tsaprailis G, Gresser MJ, Ramachandran C. Mechanism of inhibition of protein-tyrosine phosphatases by vanadate and pervanadate. *J Biol Chem* 1997 Jan 10;272(2):843-51.

⁶⁵⁷ Wang YZ, Bonner JC. Mechanism of extracellular signal-regulated kinase (ERK)-1 and ERK-2 activation by vanadium pentoxide in rat pulmonary myofibroblasts. *Am J Respir Cell Mol Biol*. 2000 May;22(5):590-6.

⁶⁵⁸ Zhao Z, Tan Z, Diltz CD, You M, Fischer EH. Activation of mitogen-activated protein (MAP) kinase pathway by pervanadate, a potent inhibitor of tyrosine phosphatases. *J Biol Chem*. 1996 Sep 6;271(36):22251-5.

⁶⁵⁹ Pandey SK, Chiasson JL, Srivastava AK. Vanadium salts stimulate mitogen-activated protein (MAP) kinases and ribosomal S6 kinases. *Mol Cell Biochem*. 1995 Dec 6-20;153(1-2):69-78.

⁶⁶⁰ D'Onofrio F, Le MQ, Chiasson JL, Srivastava AK. Activation of mitogen activated protein (MAP) kinases by vanadate is independent of insulin receptor autophosphorylation. *FEBS Lett*. 1994 Mar 7;340(3):269-75.

⁶⁶¹ Darville MI, Antoine IV, Rousseau GG. Characterization of an enhancer upstream from the muscle-type promoter of a gene encoding 6-phosphofructo-2-kinase/fructose-2,6-bisphosphatase. *Nucleic Acids Res*. 1992 Jul 25;20(14):3575-83.

⁶⁶² Dupriez VJ, Darville MI, Antoine IV, Gegonne A, Ghysdael J, Rousseau GG. Characterization of a hepatoma mRNA transcribed from a third promoter of a 6-phosphofructo-2-kinase/fructose-2,6-bisphosphatase-encoding gene and controlled by ets oncogene-related products. *Proc Natl Acad Sci U S A*. 1993 Sep 1;90(17):8224-8.

⁶⁶³ Miralpeix M, Carballo E, Bartrons R, Crepin K, Hue L, Rousseau GG. Oral administration of vanadate to diabetic rats restores liver 6-phosphofructo-2-kinase content and mRNA. *Diabetologia*. 1992 Mar;35(3):243-8.

⁶⁶⁴ Inoue H, Kaku K, Matsutani A, Tao T, Ayame H, Kaneko T. Insulin-like effects of vanadate on rat liver 6-phosphofructo-2-kinase/fructose-2,6-bisphosphatase mRNA and protein inductions in diabetic rats. *Endocr J*. 1994 Feb;41(1):75-82.

⁶⁶⁵ Dupriez VJ, Darville MI, Antoine IV, Gegonne A, Ghysdael J, Rousseau GG. Characterization of a hepatoma mRNA transcribed from a third promoter of a 6-phosphofructo-2-kinase/fructose-2,6-bisphosphatase-encoding gene and controlled by ets oncogene-related products. *Proc Natl Acad Sci U S A*. 1993 Sep 1;90(17):8224-8.

⁶⁶⁶ Herrman CE, Sanders RA, Klaunig JE, Schwarz LR, Watkins JB 3rd. Decreased apoptosis as a mechanism for hepatomegaly in streptozotocin-induced diabetic rats. *Toxicol Sci* 1999 Jul;50(1):146-51.

⁶⁶⁷ Pugazhenthi S, Tanha F, Dahl B, Khandelwal RL. Decrease in protein tyrosine phosphatase activities in vanadate-treated obese Zucker (fa/fa) rat liver. *Mol Cell Biochem*. 1995 Dec 6-20;153(1-2):125-9.

⁶⁶⁸ McNeill JH, Orvig C. Bis(maltolato)oxovanadium compositions for the treatment of elevated blood sugar. US Pat No 5,527,790, June 18, 1996.

⁶⁶⁹ Dai S, Thompson KH, McNeill JH. One-year treatment of streptozotocin-induced diabetic rats with vanadyl sulphate. *Pharmacol Toxicol* 1994 Feb;74(2):101-9.

⁶⁷⁰ Bhanot S, McNeill JH. Vanadyl sulfate lowers plasma insulin and blood pressure in spontaneously hypertensive rats. *Hypertension*. 1994 Nov;24(5):625-32.

⁶⁷¹ Cruz TF, Morgan A, Min W. In vitro and in vivo antineoplastic effects of orthovanadate. *Mol Cell Biochem*. 1995 Dec 6-20;153(1-2):161-6.

⁶⁷² Bishayee A, Chatterjee M. Inhibitory effect of vanadium on rat liver carcinogenesis initiated with diethylnitrosamine and promoted by phenobarbital. *Br J Cancer*. 1995 Jun;71(6):1214-20.

⁶⁷³ Liasko R, Kabanos TA, Karkabounas S, Malamas M, Tasiopoulos AJ, Stefanou D, Collery P, Evangelou A. Beneficial effects of a vanadium complex with cysteine, administered at low doses on benzo(alpha)pyrene-induced leiomyosarcomas in Wistar rats. *Anticancer Res*. 1998 Sep-Oct;18(5A):3609-13.

⁶⁷⁴ Goldfine AB, Simonson DC, Folli F, Patti ME, Kahn CR. In vivo and in vitro studies of vanadate in human and rodent diabetes mellitus. *Mol Cell Biochem*. 1995 Dec 6-20;153(1-2):217-31.

⁶⁷⁵ Brichard SM, Henquin JC. The role of vanadium in the management of diabetes. *Trends Pharmacol Sci*. 1995 Aug;16(8):265-70.

⁶⁷⁶ Huyer G, Liu S, Kelly J, Moffat J, Payette P, Kennedy B, Tsaprailis G, Gresser MJ, Ramachandran C. Mechanism of inhibition of protein-tyrosine phosphatases by vanadate and pervanadate. *J Biol Chem* 1997 Jan 10;272(2):843-51.

⁶⁷⁷ Elchebly M, Payette P, Michaliszyn E, Cromlish W, Collins S, Loy AL, Normandin D, Cheng A, Himms-Hagen J, Chan CC, Ramachandran C, Gresser MJ, Tremblay ML, Kennedy BP. Increased insulin sensitivity and obesity resistance in mice lacking the protein tyrosine phosphatase-1B gene. *Science*. 1999 Mar 5;283(5407):1544-8.

⁶⁷⁸ Klaman LD, Boss O, Peroni OD, Kim JK, Martino JL, Zabolotny JM, Moghal N, Lubkin M, Kim YB, Sharpe AH, Stricker-Krongrad A, Shulman GI, Neel BG, Kahn BB. Increased energy expenditure, decreased adiposity, and tissue-specific insulin sensitivity in protein-tyrosine phosphatase 1B-deficient mice. *Mol Cell Biol*. 2000 Aug;20(15):5479-89.

⁶⁷⁹ Elchebly M, Payette P, Michaliszyn E, Cromlish W, Collins S, Loy AL, Normandin D, Cheng A, Himms-Hagen J, Chan CC, Ramachandran C, Gresser MJ, Tremblay ML, Kennedy BP. Increased insulin sensitivity and obesity resistance in mice lacking the protein tyrosine phosphatase-1B gene. *Science*. 1999 Mar 5;283(5407):1544-8.

⁶⁸⁰ Klaman LD, Boss O, Peroni OD, Kim JK, Martino JL, Zabolotny JM, Moghal N, Lubkin M, Kim YB, Sharpe AH, Stricker-Krongrad A, Shulman GI, Neel BG, Kahn BB. Increased energy expenditure, decreased adiposity, and tissue-specific insulin sensitivity in protein-tyrosine phosphatase 1B-deficient mice. *Mol Cell Biol*. 2000 Aug;20(15):5479-89.

⁶⁸¹ Prasad K, Laxdal VA, Yu M, Raney BL. Evaluation of hydroxyl radical-scavenging property of garlic. *Mol Cell Biochem*. 1996 Jan 12;154(1):55-63.

⁶⁸² Ide N, Lau BH. Aged garlic extract attenuates intracellular oxidative stress. *Phytomedicine* 1999 May;6(2):125-31.

⁶⁸³ Efendi JL, Simmons DL, Campbell GR, Campbell JH. The effect of the aged garlic extract, 'Kyolic', on the development of experimental atherosclerosis. *Atherosclerosis*. 1997 Jul 11;132(1):37-42.

⁶⁸⁴ Jain RC, Konar DB. Effect of garlic oil in experimental cholesterol atherosclerosis. *Atherosclerosis*. 1978 Feb;29(2):125-9.

⁶⁸⁵ Jain RC. Onion and garlic in experimental cholesterol induced atherosclerosis. *Indian J Med Res*. 1976 Oct;64(10):1509-15.

⁶⁸⁶ Bordia A, Arora SK, Kothari LK, Jain KC, Rathore BS, Rathore AS, Dube MK, Bhu N. The protective action of essential oils of onion and garlic in cholesterol-fed rabbits. *Atherosclerosis*. 1975 Jul-Aug;22(1):103-9.

⁶⁸⁷ Breithaupt-Grogler K, Ling M, Boudoulas H, Belz GG. Protective effect of chronic garlic intake on elastic properties of aorta in the elderly. *Circulation*. 1997 Oct 21;96(8):2649-55.

⁶⁸⁸ Farrar DJ, Bond MG, Riley WA, Sawyer JK. Anatomic correlates of aortic pulse wave velocity and carotid artery elasticity during atherosclerosis progression and regression in monkeys. *Circulation*. 1991 May;83(5):1754-63.

⁶⁸⁹ Ali M, Thomson M, Afzal M. Garlic and onions: their effect on eicosanoid metabolism and its clinical relevance. *Prostaglandins Leukot Essent Fatty Acids*. 2000 Feb;62(2):55-73.

⁶⁹⁰ Fleischauer AT, Poole C, Arab L. Garlic consumption and cancer prevention: meta-analyses of colorectal and stomach cancers. *Am J Clin Nutr*. 2000 Oct;72(4):1047-52.

⁶⁹¹ Singh A, Shukla Y. Antitumour activity of diallyl sulfide on polycyclic aromatic hydrocarbon-induced mouse skin carcinogenesis. *Cancer Lett*. 1998 Sep 25;131(2):209-14.

⁶⁹² Singh SV, Mohan RR, Agarwal R, Benson PJ, Hu X, Rudy MA, Xia H, Katoh A, Srivastava SK, Mukhtar H, Gupta V, Zaren HA. Novel anti-carcinogenic activity of an organosulfide from garlic: inhibition of H-RAS oncogene transformed tumor growth in vivo by diallyl disulfide is associated with inhibition of p21^{H-ras} processing. *Biochem Biophys Res Commun.* 1996 Aug 14;225(2):660-5.

⁶⁹³ Spector SA. Oral ganciclovir. *Adv Exp Med Biol.* 1999;458:121-7.

⁶⁹⁴ Leflore S, Anderson PL, Fletcher CV. A risk-benefit evaluation of aciclovir for the treatment and prophylaxis of herpes simplex virus infections. *Drug Saf.* 2000 Aug;23(2):131-42.

⁶⁹⁵ Kesson AM. Use of aciclovir in herpes simplex virus infections. *J Paediatr Child Health.* 1998 Feb;34(1):9-13.

⁶⁹⁶ Ormrod D, Scott LJ, Perry CM. Valaciclovir: a review of its long term utility in the management of genital herpes simplex virus and cytomegalovirus infections. *Drugs.* 2000 Apr;59(4):839-63.

⁶⁹⁷ Bell AR. Valaciclovir update. *Adv Exp Med Biol.* 1999;458:149-57.

⁶⁹⁸ Sacks SL, Wilson B. Famciclovir/penciclovir. *Adv Exp Med Biol.* 1999;458:135-47.

⁶⁹⁹ Reddehase MJ, Balthesen M, Rapp M, Jonjic S, Pavic I, Koszinowski UH. The conditions of primary infection define the load of latent viral genome in organs and the risk of recurrent cytomegalovirus disease. *J Exp Med.* 1994 Jan 1;179(1):185-93.

⁷⁰⁰ Collins T, Pomeroy C, Jordan MC. Detection of latent cytomegalovirus DNA in diverse organs of mice. *J Infect Dis.* 1993 Sep;168(3):725-9.

⁷⁰¹ Steffens HP, Kurz S, Holtappels R, Reddehase MJ. Preemptive CD8 T-cell immunotherapy of acute cytomegalovirus infection prevents lethal disease, limits the burden of latent viral genomes, and reduces the risk of virus recurrence. *J Virol.* 1998 Mar;72(3):1797-804.

⁷⁰² Thackray AM, Field HJ. The effects of antiviral therapy on the distribution of herpes simplex virus type 1 to ganglionic neurons and its consequences during, immediately following and several months after treatment. *J Gen Virol.* 2000 Oct;81 Pt 10:2385-96.

⁷⁰³ Thackray AM, Field HJ. Further evidence from a murine infection model that famciclovir interferes with the establishment of HSV-1 latent infections. *J Antimicrob Chemother.* 2000 Jun;45(6):825-33.

⁷⁰⁴ Thackray AM, Field HJ. Effects of famciclovir and valacyclovir on herpes simplex virus type 1 infection, latency, and reactivation in mice: how dissimilar are study results? *J Infect Dis.* 2000 Apr;181(4):1517-8.

⁷⁰⁵ Field HJ, Thackray AM. Early therapy with valaciclovir or famciclovir reduces but does not abrogate herpes simplex virus neuronal latency. *Nucleosides Nucleotides Nucleic Acids.* 2000 Jan-Feb;19(1-2):461-70.

⁷⁰⁶ Thackray AM, Field HJ. Famciclovir and valaciclovir differ in the prevention of herpes simplex virus type 1 latency in mice: a quantitative study. *Antimicrob Agents Chemother.* 1998 Jul;42(7):1555-62.

⁷⁰⁷ LeBlanc RA, Pesnicak L, Godleski M, Straus SE. Treatment of HSV-1 infection with immunoglobulin or acyclovir: comparison of their effects on viral spread, latency, and reactivation. *Virology.* 1999 Sep 15;262(1):230-6.

⁷⁰⁸ Bowden RA. Cytomegalovirus infections in transplant patients: methods of prevention of primary cytomegalovirus. *Transplant Proc.* 1991 Jun;23(3 Suppl 3):136-8, discussion 138.

⁷⁰⁹ Chou SW, Norman DJ. The influence of donor factors other than serologic status on transmission of cytomegalovirus to transplant recipients. *Transplantation.* 1988 Jul;46(1):89-93.

⁷¹⁰ Chou SW. Cytomegalovirus infection and reinfection transmitted by heart transplantation. *J Infect Dis.* 1987 May;155(5):1054-6.

⁷¹¹ Chou SW. Acquisition of donor strains of cytomegalovirus by renal-transplant recipients. *N Engl J Med.* 1986 May 29;314(22):1418-23.

⁷¹² Grundy JE, Lui SF, Super M, Berry NJ, Sweny P, Fernando ON, Moorhead J, Griffiths PD. Symptomatic cytomegalovirus infection in seropositive kidney recipients: reinfection with donor virus rather than reactivation of recipient virus. *Lancet.* 1988 Jul 16;2(8603):132-5.

⁷¹³ Grundy JE, Super M, Lui S, Sweny P, Griffiths PD. The source of cytomegalovirus infection in seropositive renal allograft recipients is frequently the donor kidney. *Transplant Proc.* 1987 Feb;19(1 Pt 3):2126-8.

⁷¹⁴ Grundy JE, Super M, Lui SF, Griffiths PD. Donor strains of cytomegalovirus in renal-transplant recipients. *N Engl J Med.* 1986 Nov 6;315(19):1229.

⁷¹⁵ Valantine HA, Gao SZ, Memon SG, Renlund DG, Hunt SA, Oyer P, Stinson EB, Brown BW Jr, Merigan TC, Schroeder JS. Impact of prophylactic immediate posttransplant ganciclovir on development of

transplant atherosclerosis: a post hoc analysis of a randomized, placebo-controlled study. *Circulation*. 1999 Jul 6;100(1):61-6.

⁷¹⁶ Sia IG, Patel R. New strategies for prevention and therapy of cytomegalovirus infection and disease in solid-organ transplant recipients. *Clin Microbiol Rev*. 2000 Jan;13(1):83-121.

⁷¹⁷ Reddehase MJ, Balthesen M, Rapp M, Jonjic S, Pavic I, Koszinowski UH. The conditions of primary infection define the load of latent viral genome in organs and the risk of recurrent cytomegalovirus disease. *J Exp Med* 1994 Jan 1;179(1):185-93.

⁷¹⁸ Perry CM, Noble S. Didanosine: an updated review of its use in HIV infection. *Drugs*. 1999 Dec;58(6):1099-135.

⁷¹⁹ Bruisten SM, Reiss P, Loeliger AE, van Swieten P, Schuurman R, Boucher CA, Weverling GJ, Huisman JG. Cellular proviral HIV type 1 DNA load persists after long-term RT-inhibitor therapy in HIV type 1 infected persons. *AIDS Res Hum Retroviruses*. 1998 Aug 10;14(12):1053-8.

⁷²⁰ Magnani M, Rossi L, Fraternali A, Casabianca A, Brandi G, Benatti U, De Flora A. Targeting antiviral nucleotide analogues to macrophages. *J Leukoc Biol* 1997 Jul;62(1):133-7.

⁷²¹ Pauza CD, Trivedi P, McKechnie TS, Richman DD, Graziano FM. 2-LTR circular viral DNA as a marker for human immunodeficiency virus type 1 infection in vivo. *Virology*. 1994 Dec;205(2):470-8.

⁷²² Chun TW, Stuyver L, Mizell SB, Ehler LA, Mican JA, Baseler M, Lloyd AL, Nowak MA, Fauci AS. Presence of an inducible HIV-1 latent reservoir during highly active antiretroviral therapy. *Proc Natl Acad Sci U S A*. 1997 Nov 25;94(24):13193-7.

⁷²³ Gervasoni C, Ridolfo AL, Trifiro G, Santambrogio S, Norbiato G, Musicco M, Clerici M, Galli M, Moroni M. Redistribution of body fat in HIV-infected women undergoing combined antiretroviral therapy. *AIDS*. 1999 Mar 11;13(4):465-71.

⁷²⁴ Guo NL, Lu DP, Woods GL, Reed E, Zhou GZ, Zhang LB, Waldman RH. Demonstration of the anti-viral activity of garlic extract against human cytomegalovirus in vitro. *Chin Med J (Engl)* 1993 Feb;106(2):93-6.

⁷²⁵ Weber ND, Andersen DO, North JA, Murray BK, Lawson LD, Hughes BG. In vitro virucidal effects of Allium sativum (garlic) extract and compounds. *Planta Med*. 1992 Oct;58(5):417-23.

⁷²⁶ Marchant A, Goetghebuer T, Ota MO, Wolfe I, Ceesay SJ, De Groote D, Corrah T, Bennett S, Wheeler J, Huygen K, Aaby P, McAdam KP, Newport MJ. Newborns develop a Th1-type immune response to *Mycobacterium bovis* bacillus Calmette-Guerin vaccination. *J Immunol*. 1999 Aug 15;163(4):2249-55.

⁷²⁷ Starr SE, Visintine AM, Tomeh MO, Nahmias AJ. Effects of immunostimulants on resistance of newborn mice to herpes simplex type 2 infection. *Proc Soc Exp Biol Med*. 1976 May;152(1):57-60.

⁷²⁸ Aaby P, Shaheen SO, Heyes CB, Goudiaby A, Hall AJ, Shiell AW, Jensen H, Marchant A. Early BCG vaccination and reduction in atopy in Guinea-Bissau. *Clin Exp Allergy* 2000 May;30(5):644-50.

⁷²⁹ von Hertzen LC. Puzzling associations between childhood infections and the later occurrence of asthma and atopy. *Ann Med* 2000 Sep;32(6):397-400.

⁷³⁰ von Mutius E, Pearce N, Beasley R, Cheng S, von Ehrenstein O, Bjorksten B, Weiland S. International patterns of tuberculosis and the prevalence of symptoms of asthma, rhinitis, and eczema. *Thorax* 2000 Jun;55(6):449-53.

⁷³¹ von Hertzen L, Klaakka T, Mattila H, Haahtela T. *Mycobacterium tuberculosis* infection and the subsequent development of asthma and allergic conditions. *J Allergy Clin Immunol*. 1999 Dec;104(6):1211-4.

⁷³² Scanga CB, Le Gros G. Development of an asthma vaccine: research into BCG. *Drugs*. 2000 Jun;59(6):1217-21.

⁷³³ Shehadeh N, Etzioni A, Cahana A, Tenenbaum G, Gorodetsky B, Barzilai D, Karnieli E. Repeated BCG vaccination is more effective than a single dose in preventing diabetes in non-obese diabetic (NOD) mice. *Isr J Med Sci*. 1997 Nov;33(11):711-5.

⁷³⁴ Qin HY, Singh B. BCG vaccination prevents insulin-dependent diabetes mellitus (IDDM) in NOD mice after disease acceleration with cyclophosphamide. *J Autoimmun*. 1997 Jun;10(3):271-8.

⁷³⁵ Harada M, Kishimoto Y, Makino S. Prevention of overt diabetes and insulitis in NOD mice by a single BCG vaccination. *Diabetes Res Clin Pract*. 1990 Jan;8(2):85-9.

⁷³⁶ Hiltunen M, Lonnrot M, Hyoty H. Immunisation and type 1 diabetes mellitus: is there a link? *Drug Saf*. 1999 Mar;20(3):207-12.

⁷³⁷ Martins TC, Aguas AP. Mechanisms of *Mycobacterium avium*-induced resistance against insulin-dependent diabetes mellitus (IDDM) in non-obese diabetic (NOD) mice: role of Fas and Th1 cells. *Clin Exp Immunol* 1999 Feb;115(2):248-54.

⁷³⁸ Bras A, Aguas AP. Diabetes-prone NOD mice are resistant to *Mycobacterium avium* and the infection prevents autoimmune disease. *Immunology*. 1996 Sep;89(1):20-5.

⁷³⁹ Pabst HF, Spady DW, Pilarski LM, Carson MM, Beeler JA, Krezolek MP. Differential modulation of the immune response by breast- or formula-feeding of infants. *Acta Paediatr*. 1997 Dec;86(12):1291-7.

⁷⁴⁰ Pabst HF. Immunomodulation by breast-feeding. *Pediatr Infect Dis J*. 1997 Oct;16(10):991-5.

⁷⁴¹ Hawkes JS, Neumann MA, Gibson RA. The effect of breast feeding on lymphocyte subpopulations in healthy term infants at 6 months of age. *Pediatr Res* 1999 May;45(5 Pt 1):648-51.

⁷⁴² Pettitt DJ, Forman MR, Hanson RL, Knowler WC, Bennett PH. Breastfeeding and incidence of non-insulin-dependent diabetes mellitus in Pima Indians. *Lancet*. 1997 Jul 19;350(9072):166-8.

⁷⁴³ von Kries R, Koletzko B, Sauerwald T, von Mutius E. Does breast-feeding protect against childhood obesity? *Adv Exp Med Biol*. 2000;478:29-39.

⁷⁴⁴ von Kries R, Koletzko B, Sauerwald T, von Mutius E, Barnert D, Grunert V, von Voss H. Breast feeding and obesity: cross sectional study. *BMJ*. 1999 Jul 17;319(7203):147-50.

Accordingly, it is to be understood that the embodiments of the invention herein described are merely illustrative of the application of the principles of the invention. Reference herein to details of the illustrated embodiments is not intended to limit the scope of the claims, which themselves recite those features regarded as essential to the invention.

What is claimed is:

1. A method of treating adverse affects associated with a disruption of GABP's metabolic pathway, comprising administering to a patient an effective amount of an agent selected from a group consisting of:
 - 4 a) an agent that increases concentration of a GABP stimulator;
 - 5 b) an agent that decreases concentration of a GABP suppressor;
 - 6 c) an agent that increases effectiveness of a GABP stimulator; and
 - 7 d) an agent that decreases effectiveness of a GABP suppressor.
- 1 2. The method of claim 1 wherein said adverse affect associated with microcompetition is
2 cancer and said patient is being treated for cancer.
- 1 3. The method of claim 1 wherein said adverse affect associated with microcompetition is
2 atherosclerosis and said patient is being treated for atherosclerosis.
- 1 4. The method of claim 1 wherein said adverse affect associated with microcompetition is
2 osteoarthritis and said patient is being treated for osteoarthritis.
- 1 5. The method of claim 1 wherein said adverse affect associated with microcompetition is
2 obesity and said patient is being treated for obesity.
- 1 6. A method of treating adverse affects associated with a disruption of GABP's metabolic
2 pathway, comprising administering an effective amount of an agent selected from a
3 group consisting of:
 - 4 a) an agent that increases concentration of GABP α ;
 - 5 b) an agent that increases concentration of GABP β ;
 - 6 c) an agent that decreases concentration of GABP γ ;
 - 7 d) an agent that increases phosphorylation of GABP;
 - 8 e) an agent that increases affinity between GABP and p300/CBP;
 - 9 f) an agent that stimulates binding of GABP to DNA; and
 - 10 g) an agent that increases concentration of p300/CBP.
- 1 7. The method of claim 6 wherein said adverse affect associated with microcompetition is
2 cancer and said patient is being treated for cancer.

- 1 8. The method of claim 6 wherein said adverse affect associated with microcompetition is
2 atherosclerosis and said patient is being treated for atherosclerosis.
- 1 9. The method of claim 6 wherein said adverse affect associated with microcompetition is
2 osteoarthritis and said patient is being treated for osteoarthritis.
- 1 10. The method of claim 6 wherein said adverse affect associated with microcompetition
2 is obesity and said patient is being treated for obesity.
- 1 11. A method of treating adverse affects associated with a disruption of GABP's
2 metabolic pathway, comprising administering an effective amount of an agent
3 selected from a group consisting of:
 - 4 a) an agent that increases concentration of a GABP kinase;
 - 5 b) an agent that stimulates phosphorylation of a GABP kinase;
 - 6 c) an agent that increases affinity between GABP and GABP kinase;
 - 7 d) an agent that decreases oxidative effects on GABP; and
 - 8 e) an agent that decreases foreign DNA N-boxes in cells.
- 1 12. The method of claim 11 wherein said adverse affect associated with microcompetition
2 is cancer and said patient is being treated for cancer.
- 1 13. The method of claim 11 wherein said adverse affect associated with microcompetition
2 is atherosclerosis and said patient is being treated for atherosclerosis.
- 1 14. The method of claim 11 wherein said adverse affect associated with microcompetition
2 is osteoarthritis and said patient is being treated for osteoarthritis.
- 1 15. The method of claim 11 wherein said adverse affect associated with microcompetition
2 is obesity and said patient is being treated for obesity.
- 1 16. A method of treating adverse affects associated with a disruption of GABP's
2 metabolic pathway, comprising administering an effective amount of an agent that
3 decreases oxidative effects on GABP.

- 1 17. The method of claim 16 wherein said adverse affect associated with microcompetition
2 is cancer and said patient is being treated for cancer.
- 1 18. The method of claim 16 wherein said adverse affect associated with microcompetition
2 is atherosclerosis and said patient is being treated for atherosclerosis.
- 1 19. The method of claim 16 wherein said adverse affect associated with microcompetition
2 is osteoarthritis and said patient is being treated for osteoarthritis.
- 1 20. The method of claim 16 wherein said adverse affect associated with microcompetition
2 is obesity and said patient is being treated for obesity.
- 1 21. A method of treating adverse affects associated with a disruption of GABP's
2 metabolic pathway, comprising administering an effective amount of an agent that
3 decreases foreign DNA N-boxes in cells.
- 1 22. The method of claim 20 wherein said adverse affect associated with microcompetition
2 is cancer and said patient is being treated for cancer.
- 1 23. The method of claim 20 wherein said adverse affect associated with microcompetition
2 is atherosclerosis and said patient is being treated for atherosclerosis.
- 1 24. The method of claim 20 wherein said adverse affect associated with microcompetition
2 is osteoarthritis and said patient is being treated for osteoarthritis.
- 1 25. The method of claim 20 wherein said adverse affect associated with microcompetition
2 is obesity and said patient is being treated for obesity.
- 1 26. A method of identifying compounds to be tested for treating adverse affects associated
2 with a disruption of GABP's metabolic pathway, comprising:
3 a) providing an assay capable of determining compounds that perform a function
4 selected from a group consisting of:
5 i) increases concentration of a GABP stimulator,
6 ii) decreases concentration of a GABP suppressor,
7 iii) increases effectiveness of a GABP stimulator, and

34. The method of claim 31 wherein said adverse affect associated with microcompetition is osteoarthritis and said patient is being treated for osteoarthritis.
35. The method of claim 31 wherein said adverse affect associated with microcompetition is obesity and said patient is being treated for obesity.
36. A method of identifying compounds to be tested for treating adverse affects associated with a disruption of GABP's metabolic pathway, comprising:
 - a) providing an assay capable of determining compounds that perform a function selected from a group consisting of:
 - i) increases concentration of a GABP kinase,
 - ii) stimulates phosphorylation of a GABP kinase, and
 - iii) increases affinity between GABP and GABP kinase; and
 - b) running sample compounds through said assay and identifying any compound that performs one of said functions as a compound to be tested.
37. The method of claim 36 wherein said adverse affect associated with microcompetition is cancer and said patient is being treated for cancer.
38. The method of claim 36 wherein said adverse affect associated with microcompetition is atherosclerosis and said patient is being treated for atherosclerosis.
39. The method of claim 36 wherein said adverse affect associated with microcompetition is osteoarthritis and said patient is being treated for osteoarthritis.
40. The method of claim 36 wherein said adverse affect associated with microcompetition is obesity and said patient is being treated for obesity.
41. A method of identifying compounds to be tested for treating adverse affects associated with a disruption of GABP's metabolic pathway, comprising:
 - a) providing an assay capable of determining compounds that decrease oxidative effect on GABP; and
 - b) running sample compounds through said assay and identifying any compound that performs one of said functions as a compound to be tested.

- 1 42. The method of claim 41 wherein said adverse affect associated with microcompetition
2 is cancer and said patient is being treated for cancer.
- 1 43. The method of claim 41 wherein said adverse affect associated with microcompetition
2 is atherosclerosis and said patient is being treated for atherosclerosis.
- 1 44. The method of claim 41 wherein said adverse affect associated with microcompetition
2 is osteoarthritis and said patient is being treated for osteoarthritis.
- 1 45. The method of claim 41 wherein said adverse affect associated with microcompetition
2 is obesity and said patient is being treated for obesity.
- 1 46. A method of identifying compounds to be tested for treating adverse affects associated
2 with a disruption of GABP's metabolic pathway, comprising:
3 a) providing an assay capable of determining compounds decreases foreign
4 DNA N-boxes in cells; and
5 b) running sample compounds through said assay and identifying any compound
6 that performs one of said functions as a compound to be tested.
- 1 47. The method of claim 46 wherein said adverse affect associated with microcompetition
2 is cancer and said patient is being treated for cancer.
- 1 48. The method of claim 46 wherein said adverse affect associated with microcompetition
2 is atherosclerosis and said patient is being treated for atherosclerosis.
- 1 49. The method of claim 46 wherein said adverse affect associated with microcompetition
2 is osteoarthritis and said patient is being treated for osteoarthritis.
- 1 50. The method of claim 46 wherein said adverse affect associated with microcompetition
2 is obesity and said patient is being treated for obesity.

1/27

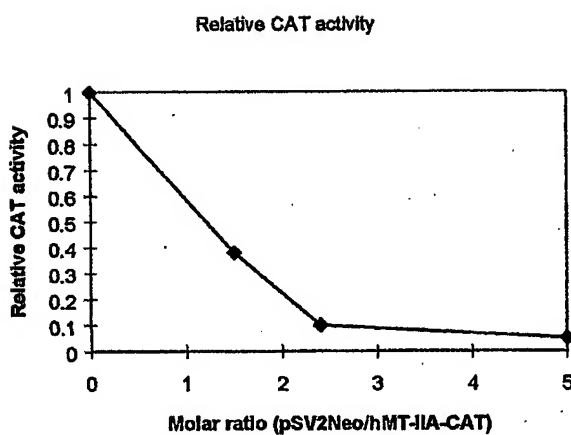


Figure 1

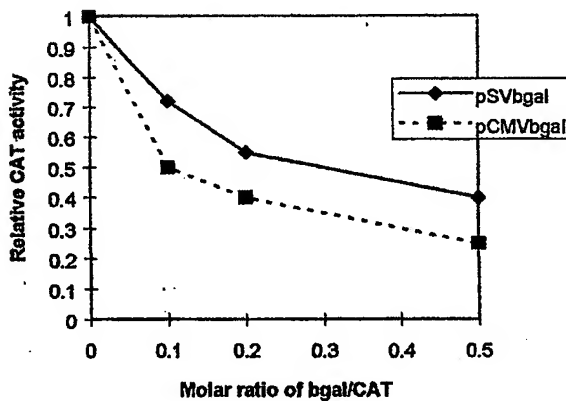


Figure 2

2/27

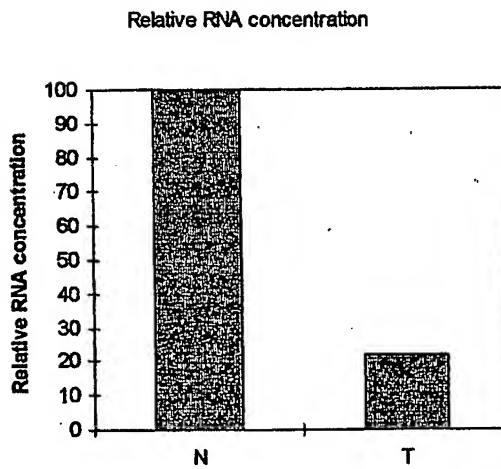


Figure 3

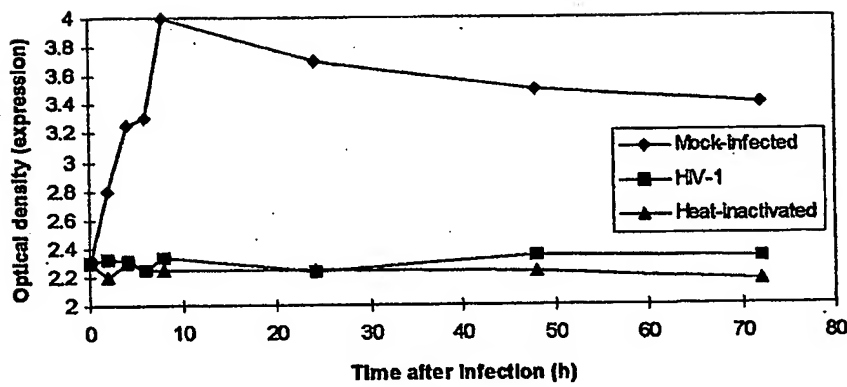


Figure 4

3/27

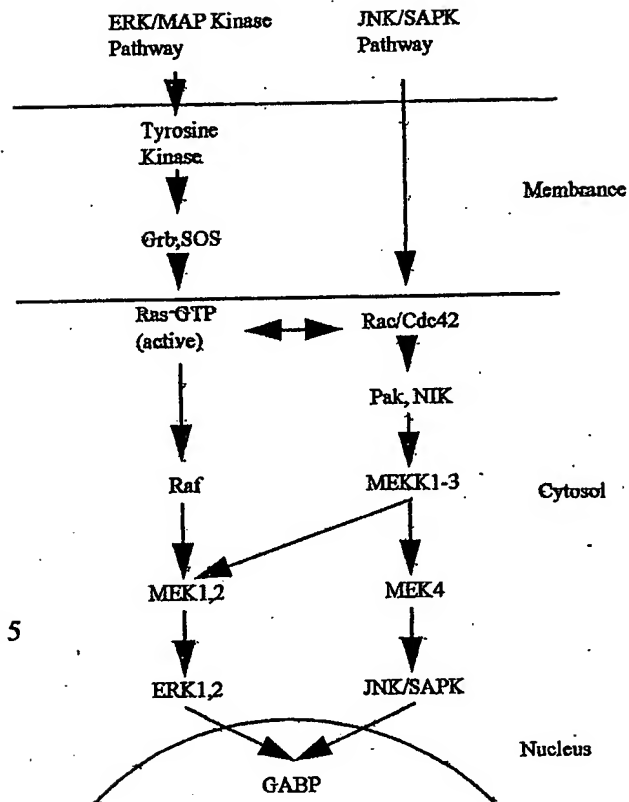


Figure 5

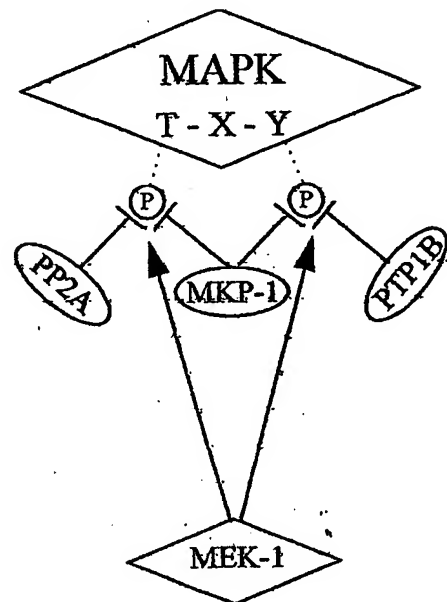


Figure 6

4/27

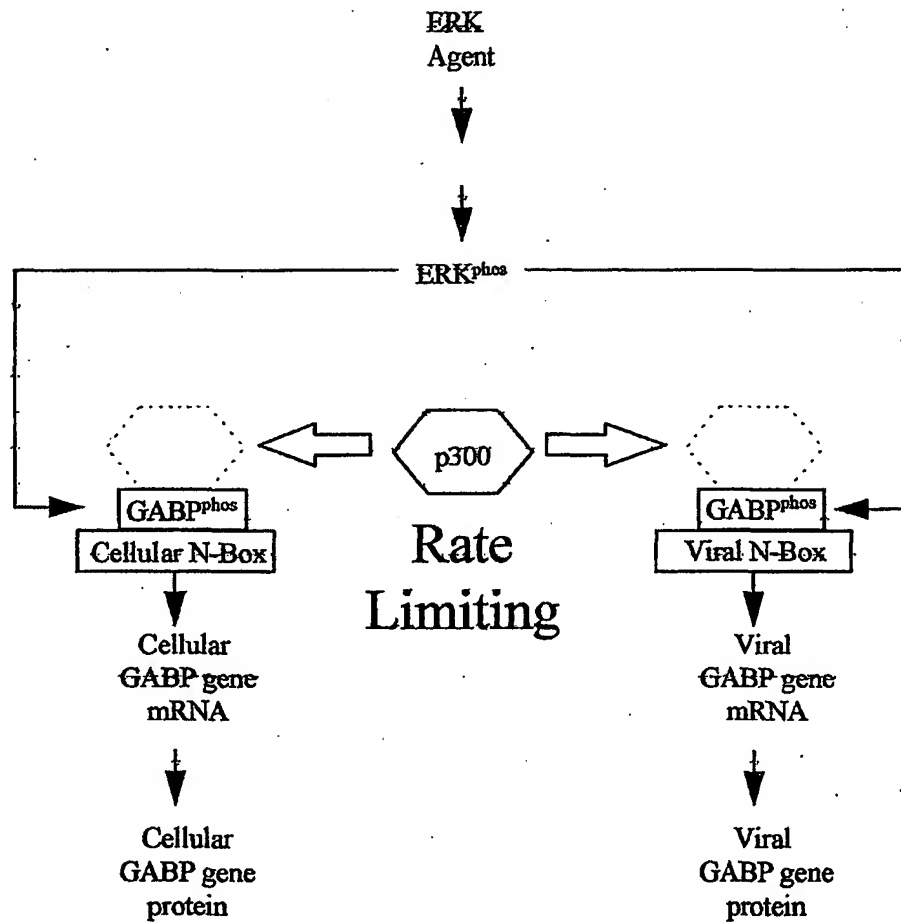


Figure 7

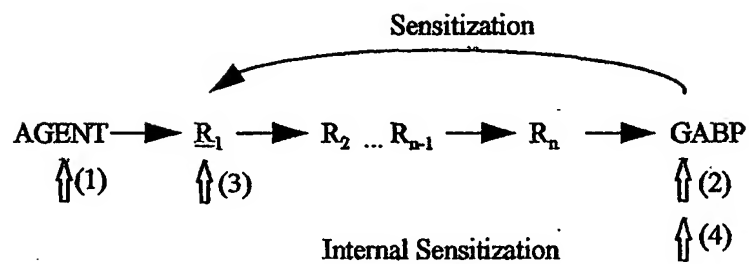


Figure 8

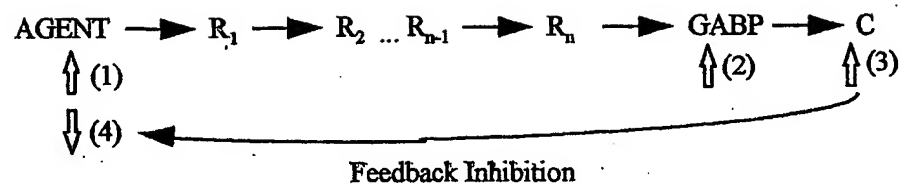
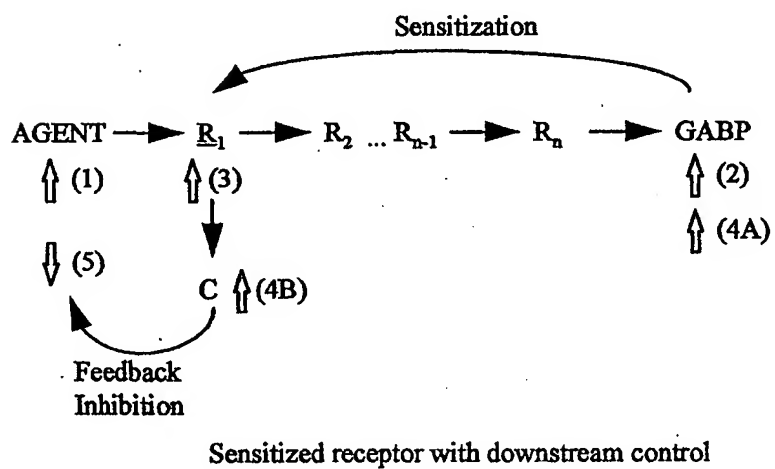


Figure 9



Sensitized receptor with downstream control

Figure 10

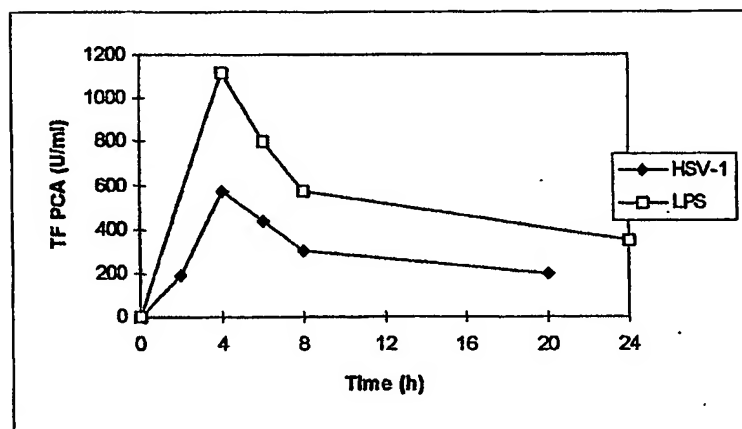


Figure 11

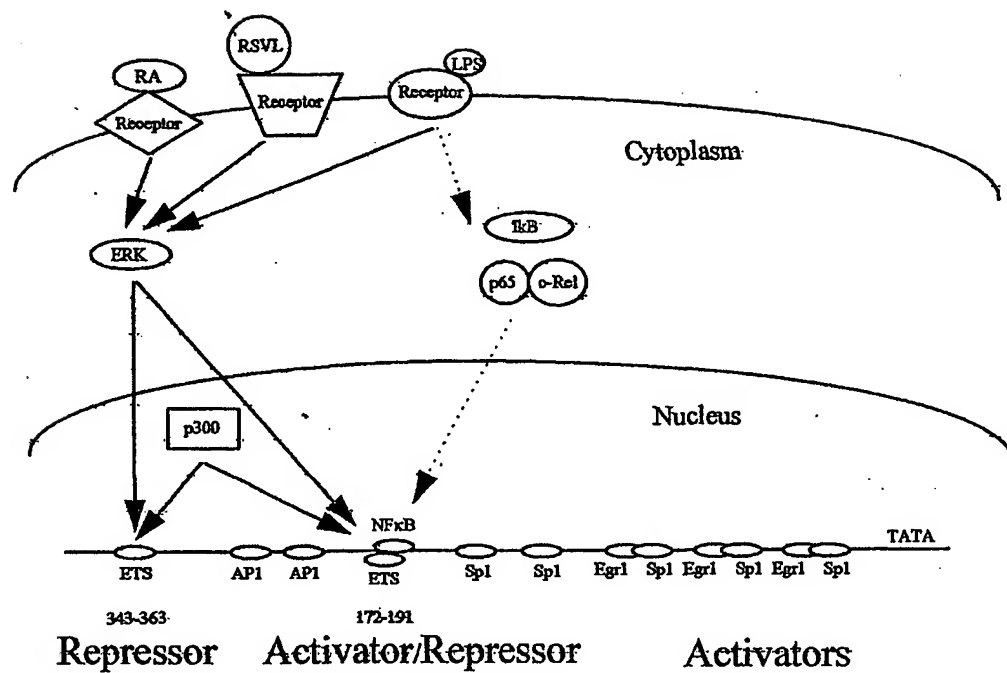


Figure 12

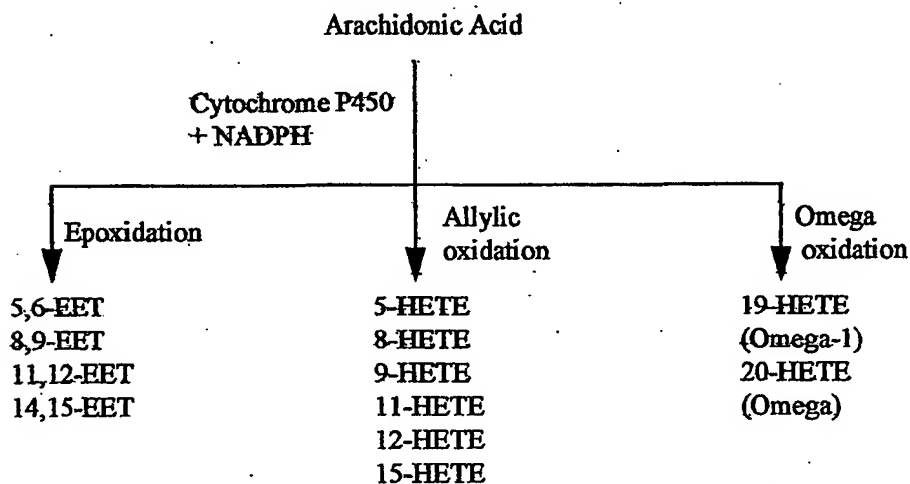


Figure 13

7/27

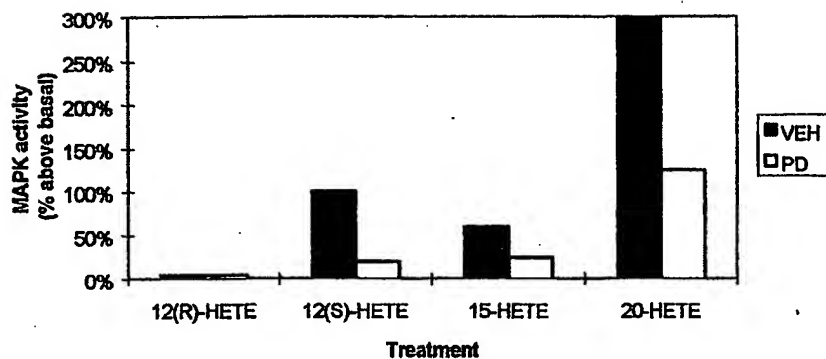


Figure 14

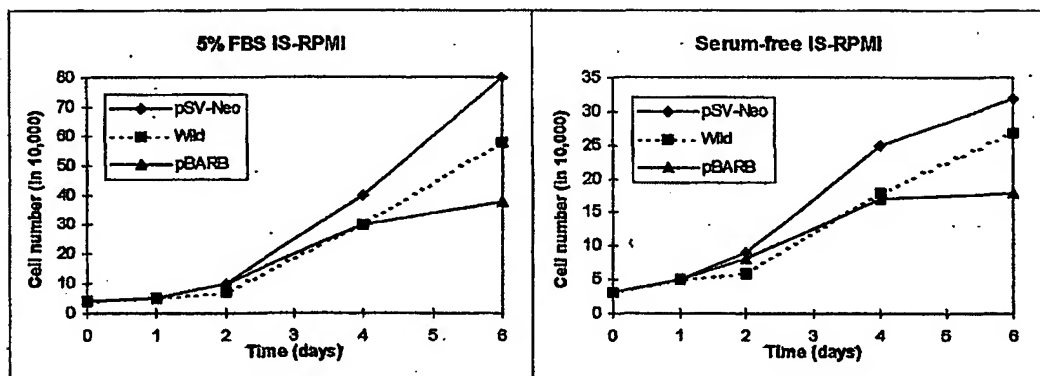


Figure 15

8/27

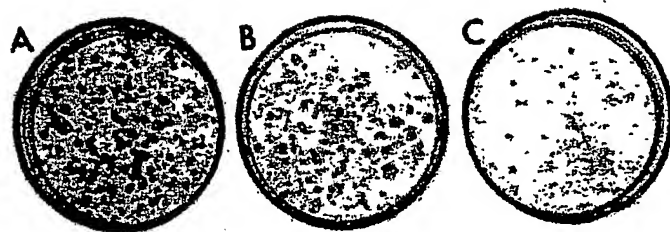


Figure 16

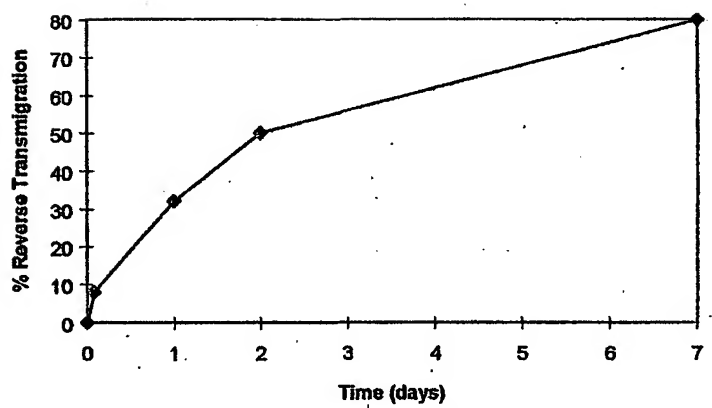


Figure 17

9/27

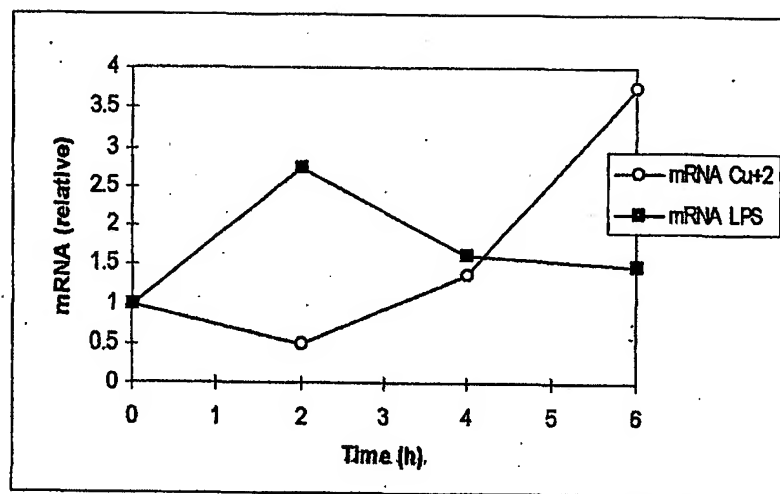


Figure 18

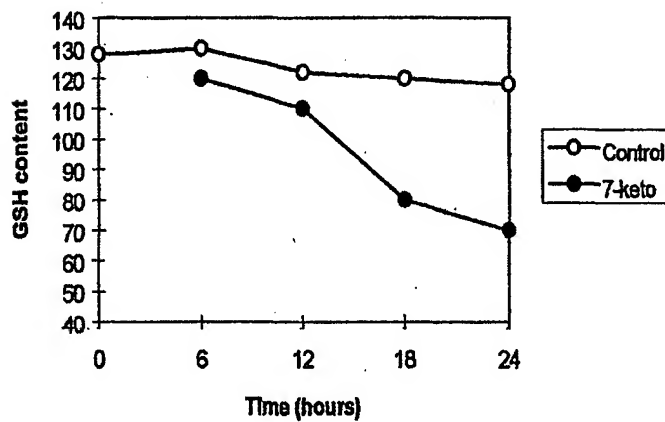


Figure 19

10/27

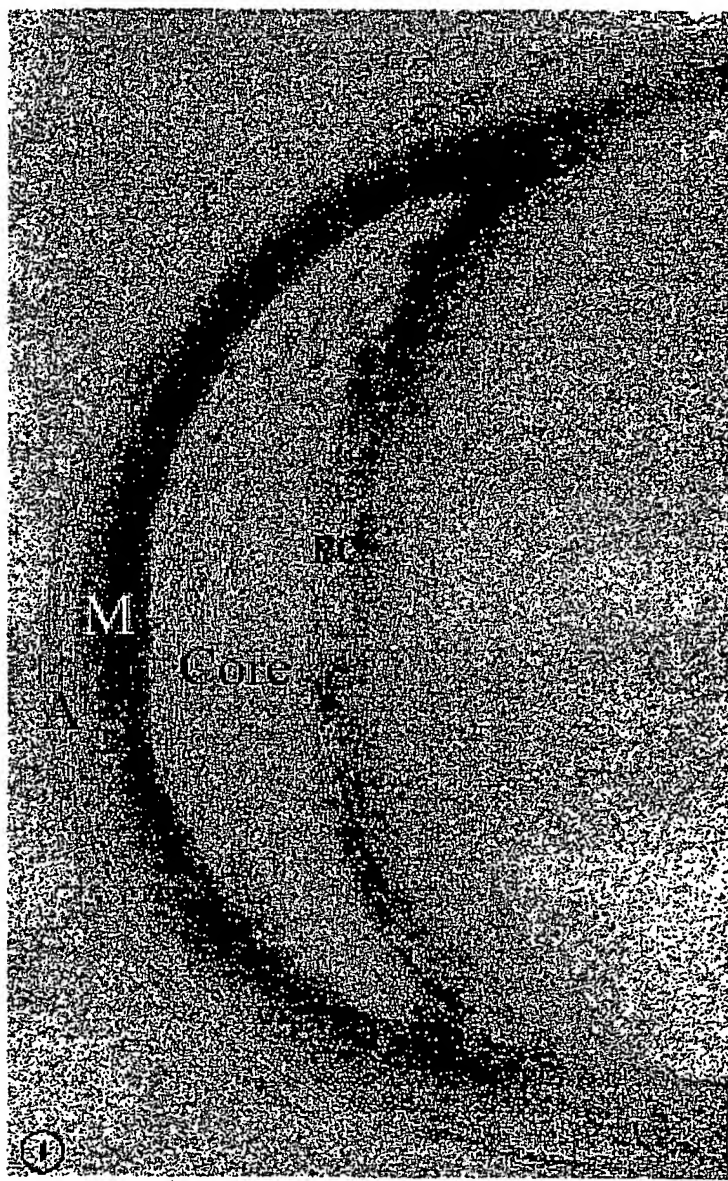


Figure 20

11/27



Figure 21

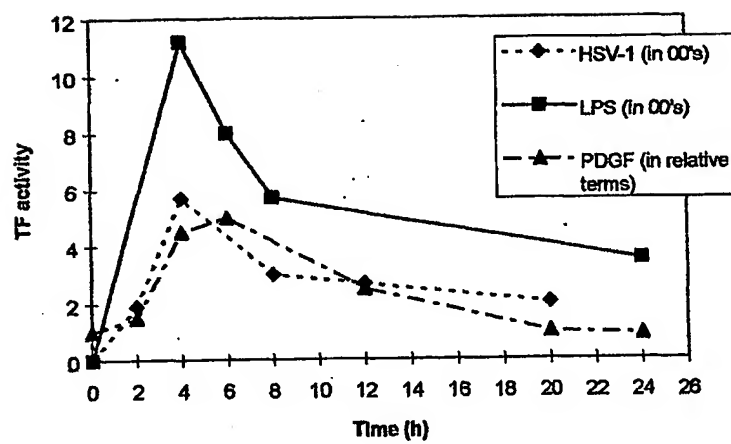


Figure 22

12/27

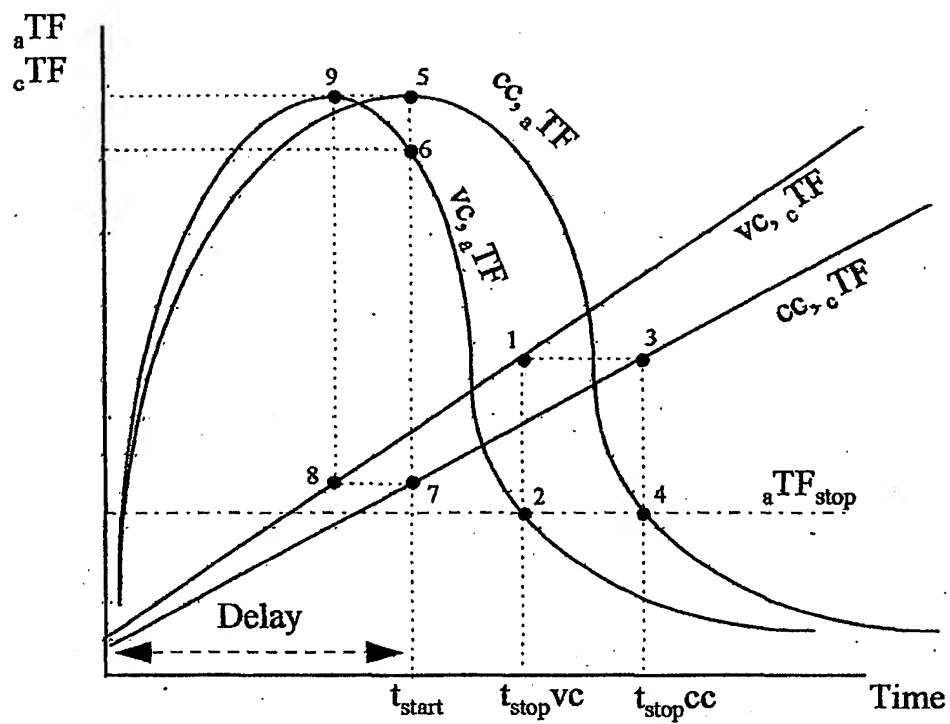


Figure 23

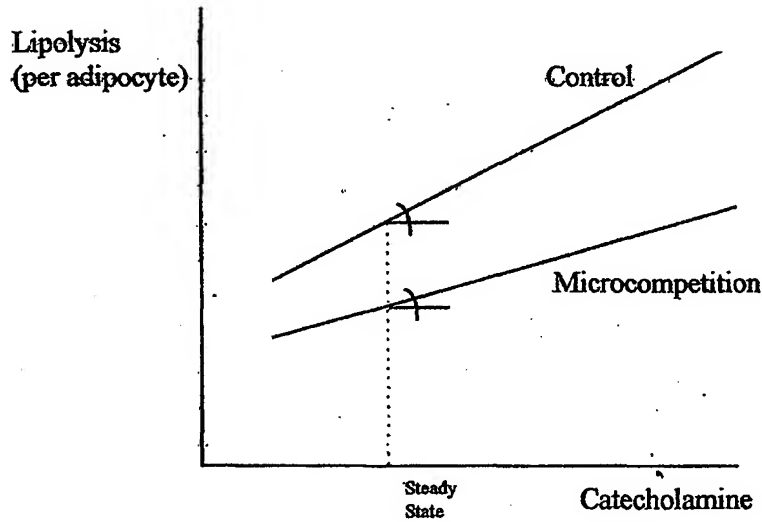


Figure 24

13/27

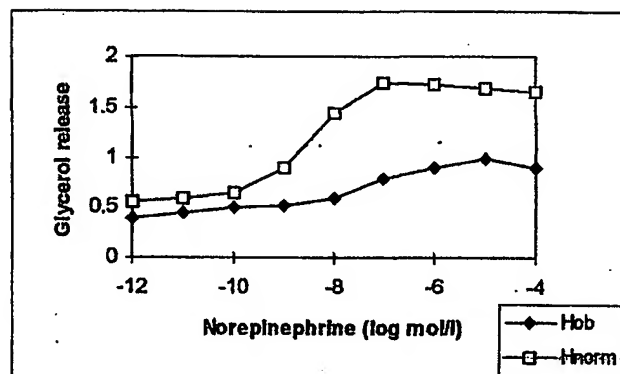


Figure 25

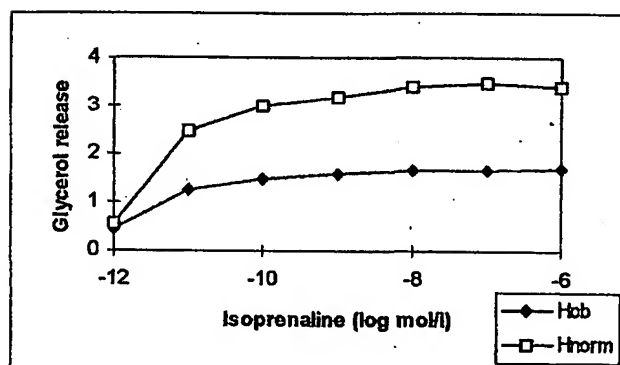


Figure 26

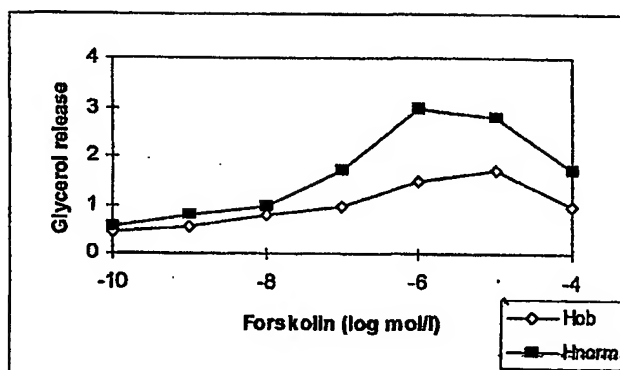


Figure 27

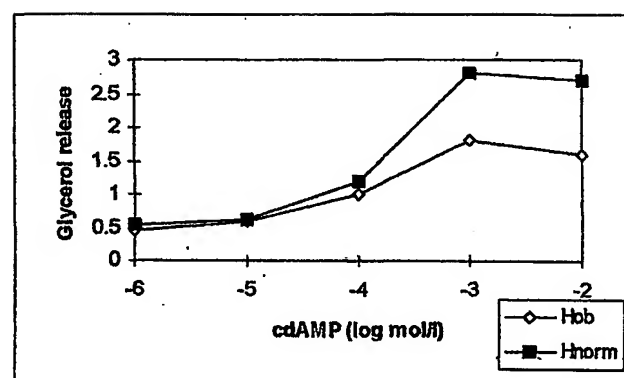


Figure 28

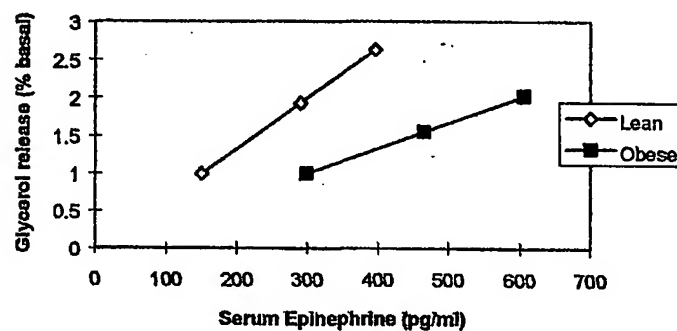


Figure 29

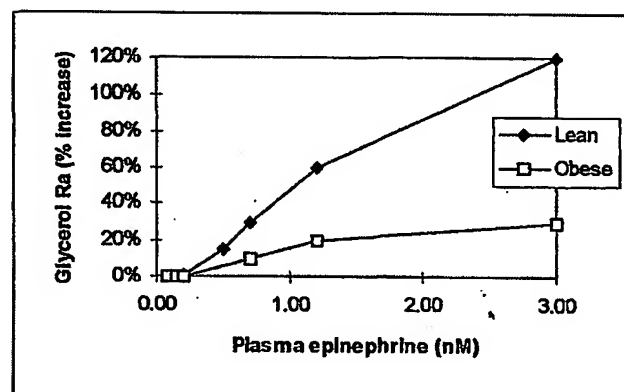


Figure 30

15/27

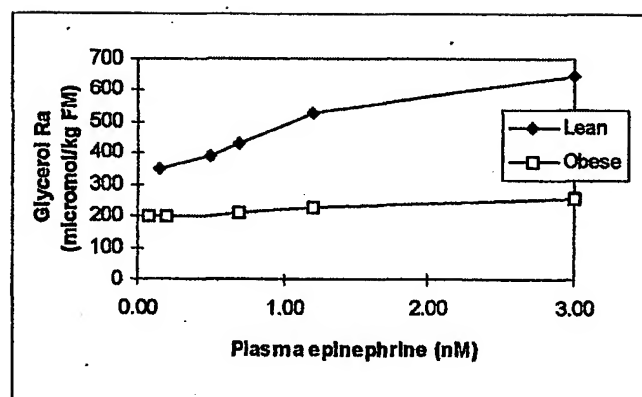


Figure 31

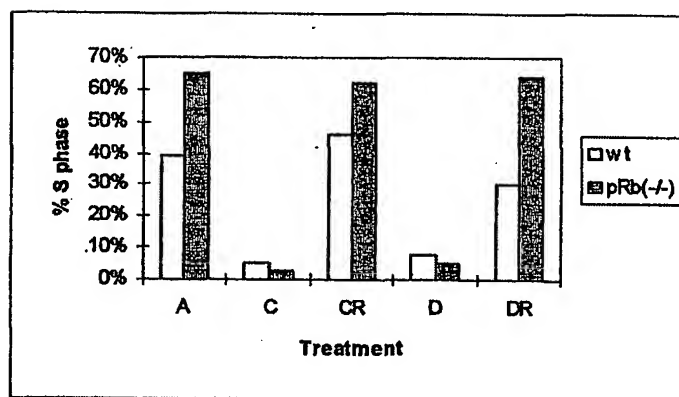


Figure 32

16/27

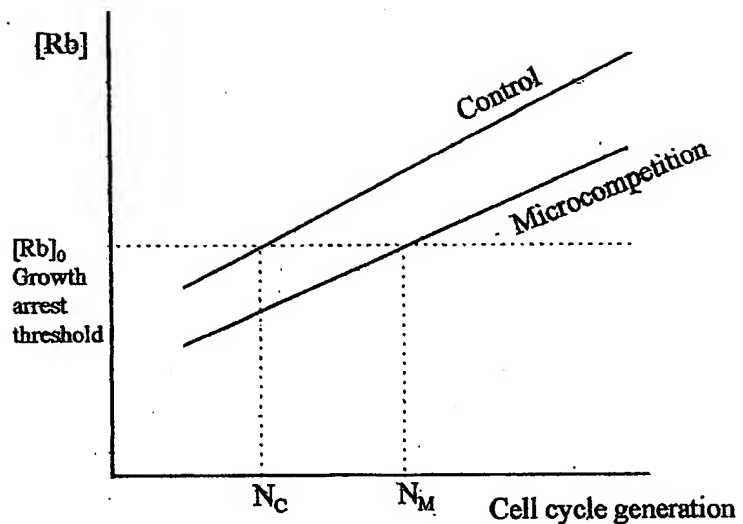


Figure 33

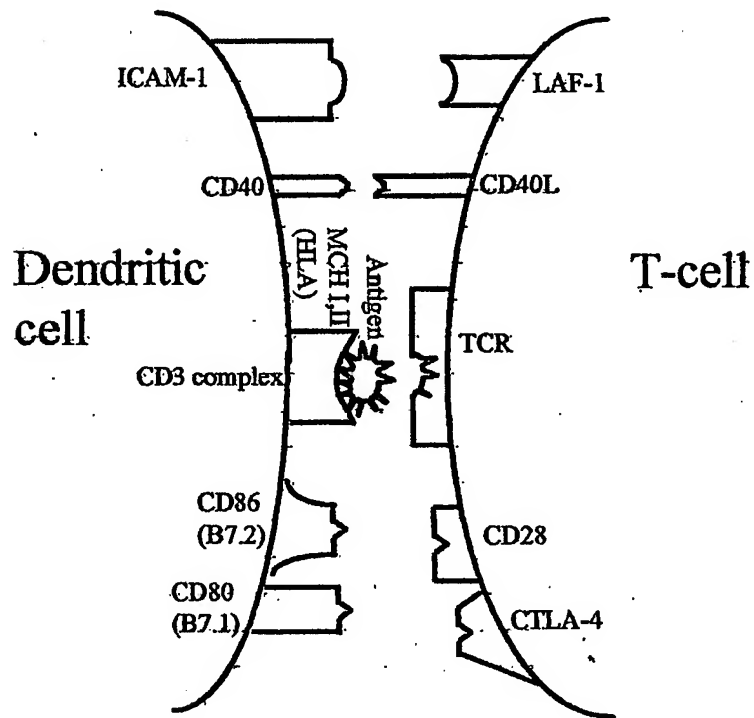


Figure 34

17/27

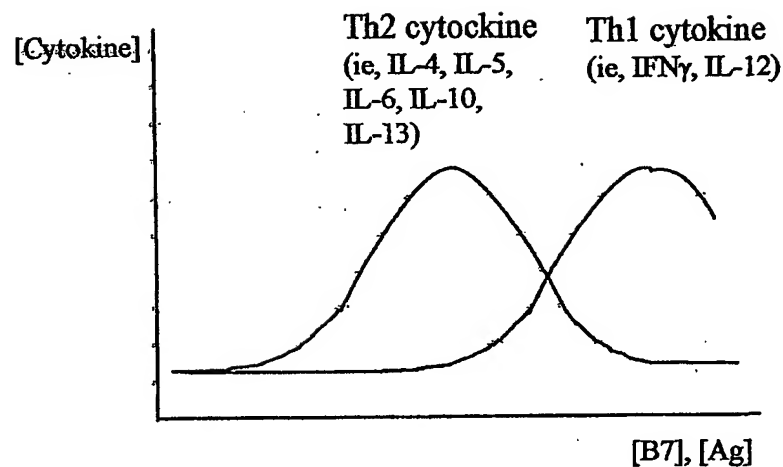


Figure 35

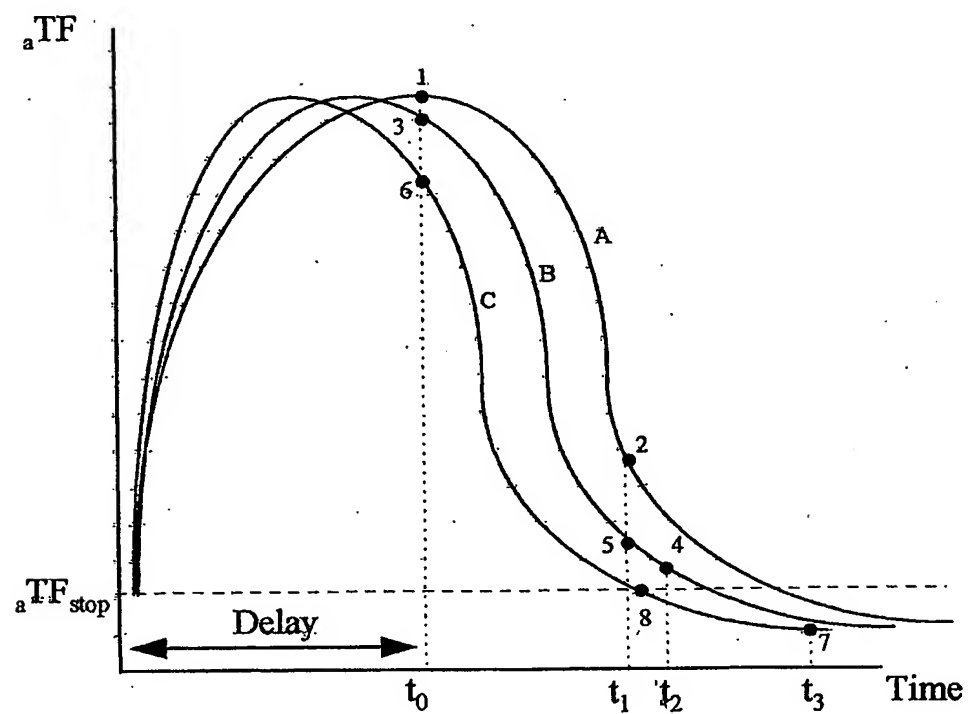


Figure 36

18/27

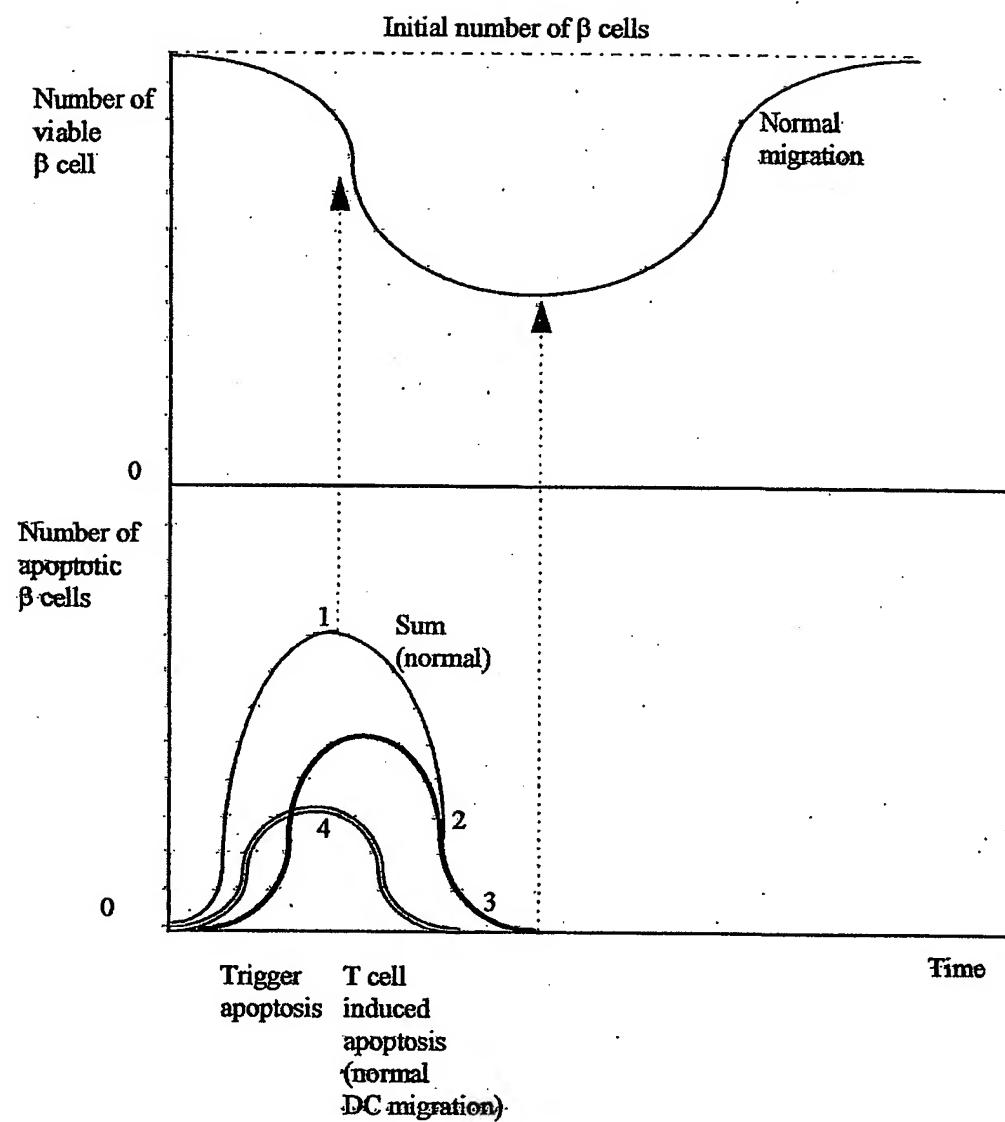


Figure 37

19/27

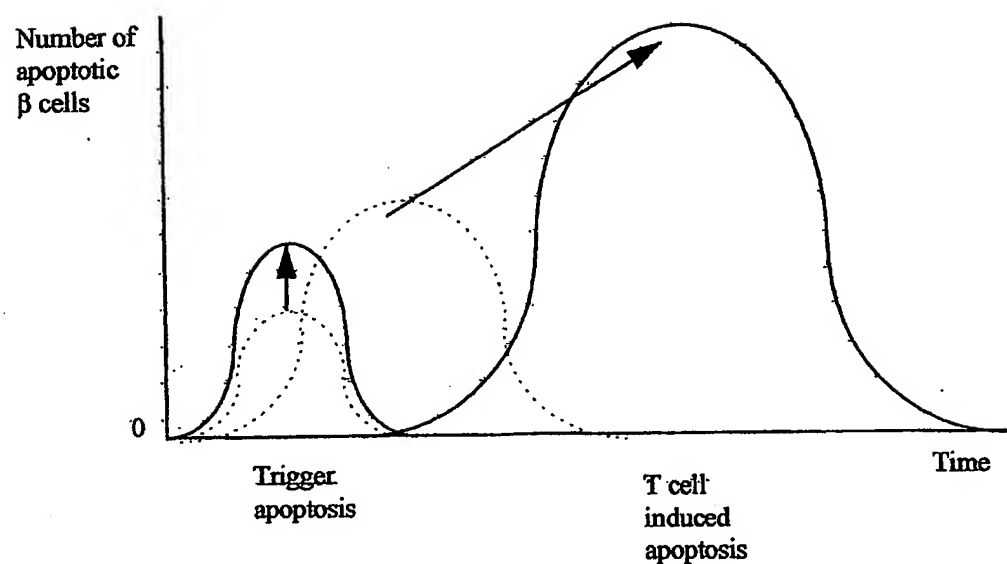


Figure 38

20/27

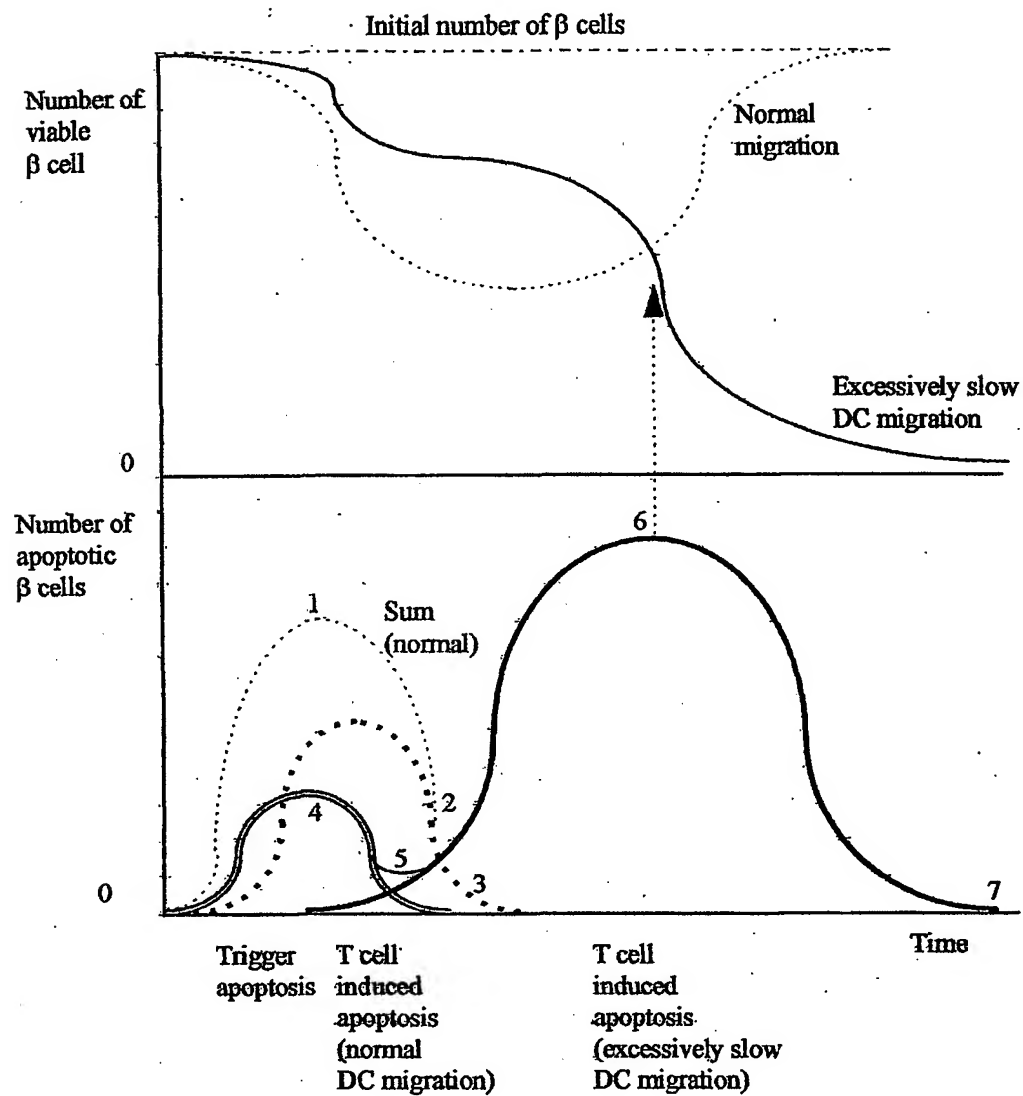


Figure 39

21/27

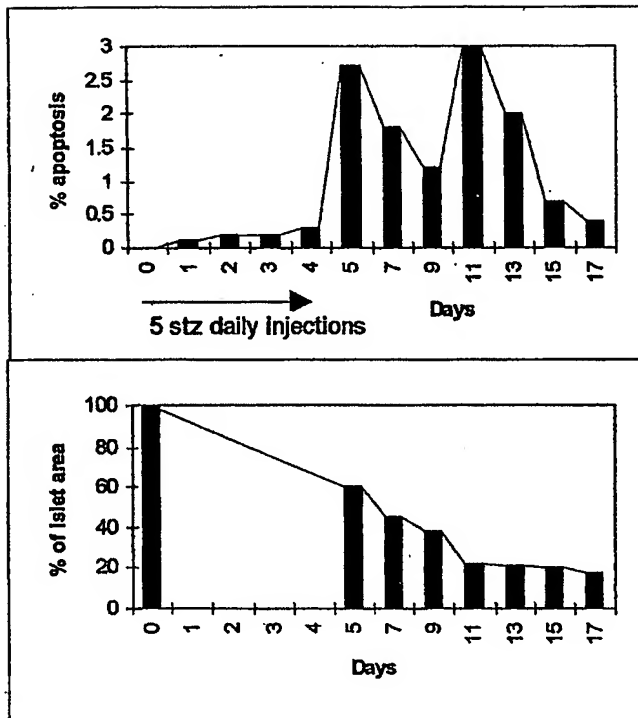


Figure 40

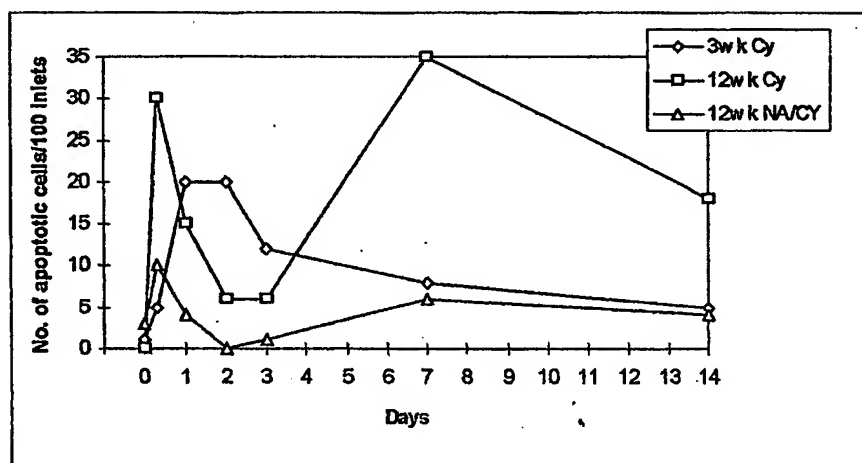


Figure 41

22/27

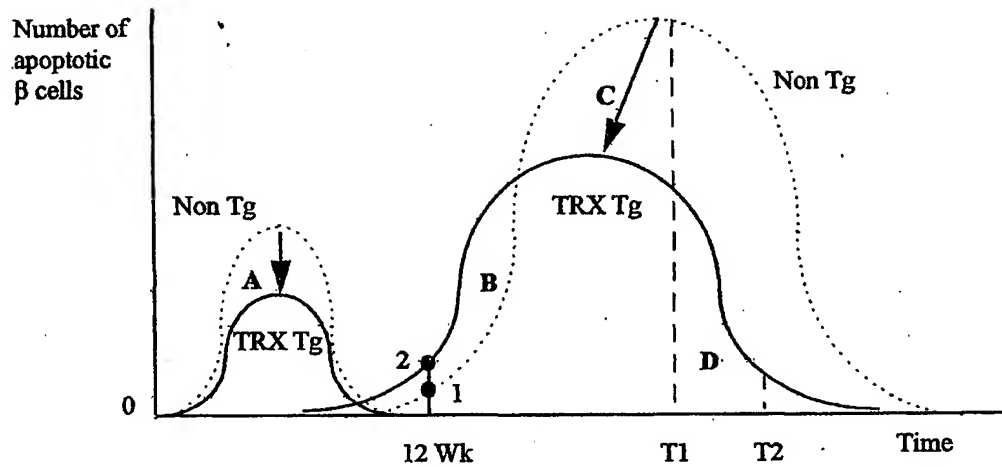


Figure 42

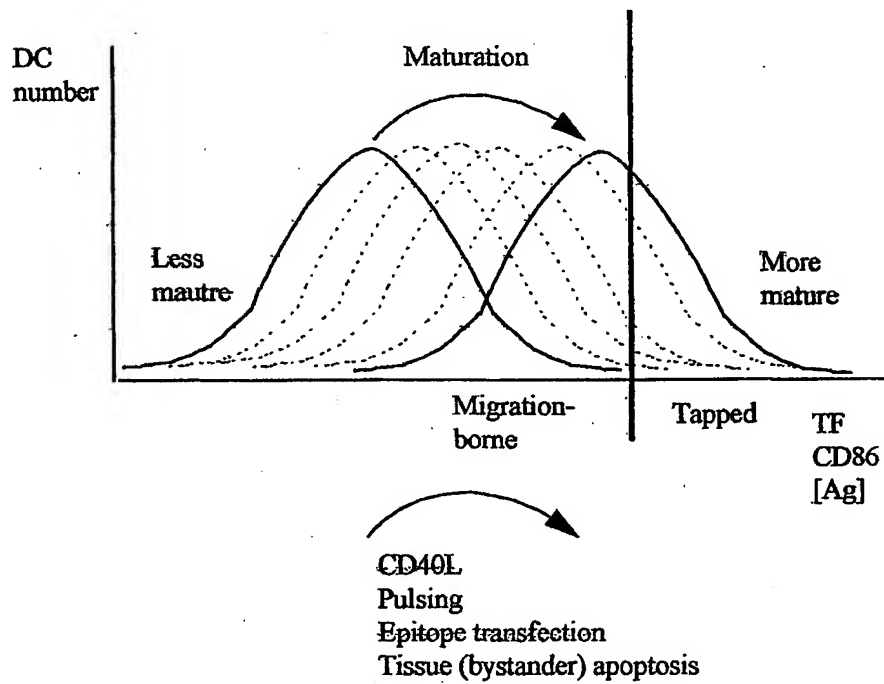


Figure 43

23/27

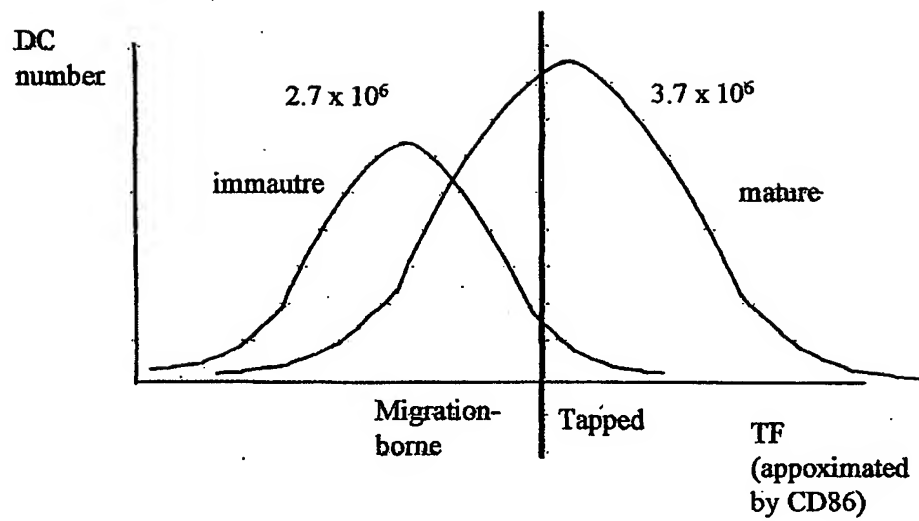


Figure 44

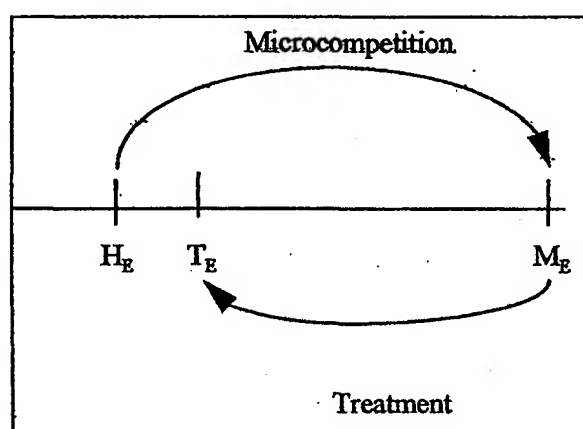


Figure 45

24/27

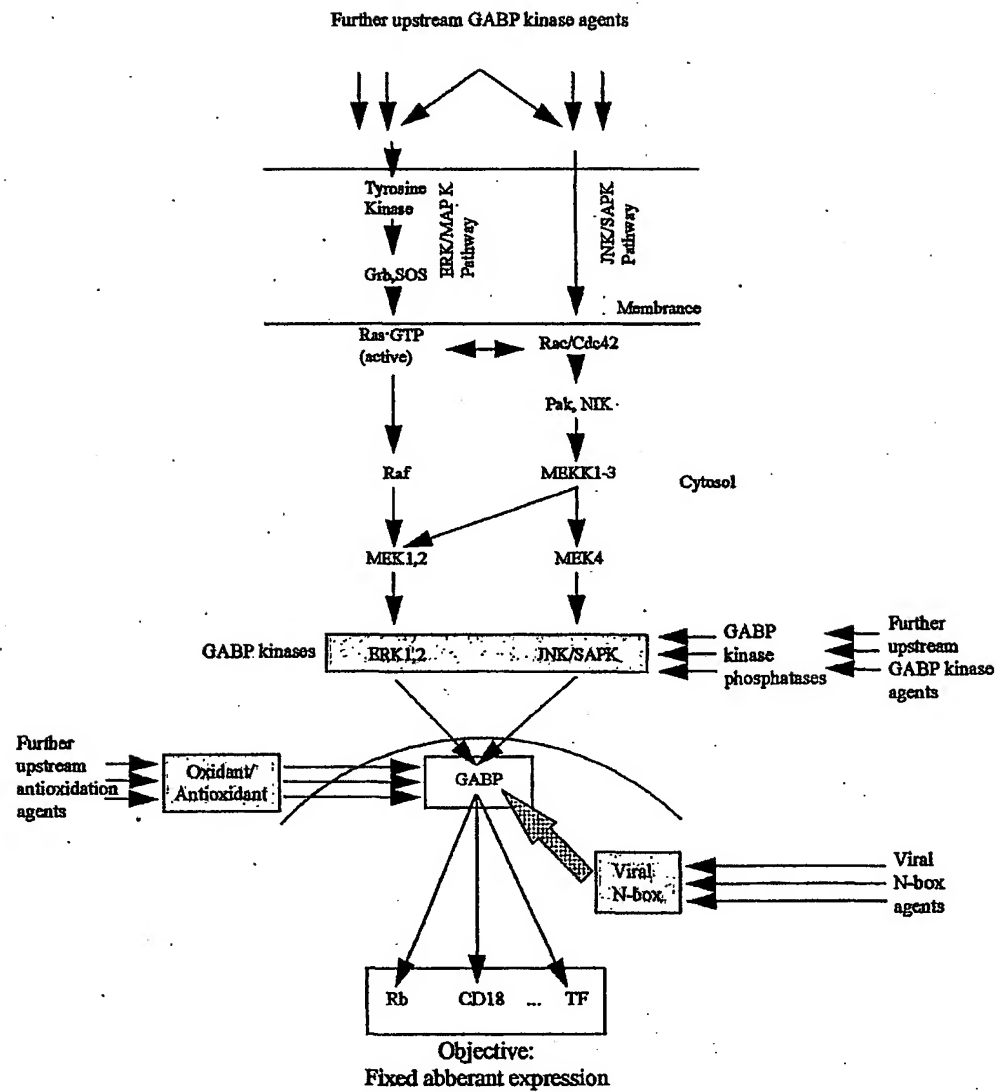


Figure 46

25/27

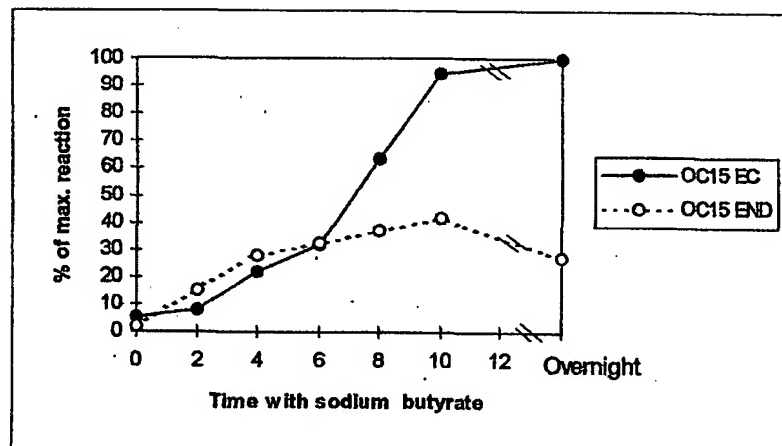


Figure 47

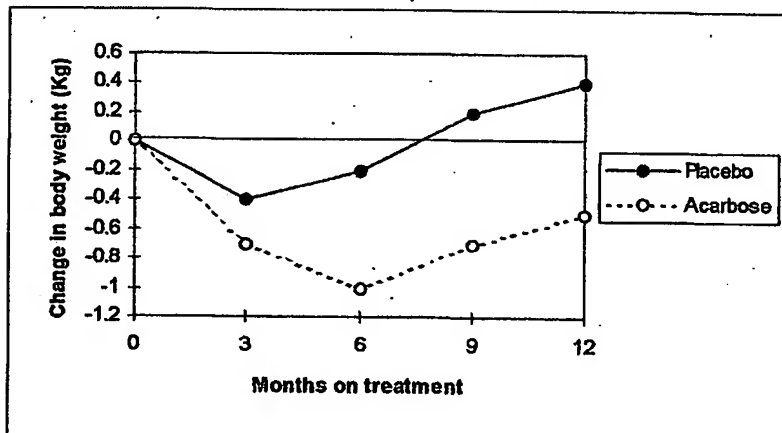


Figure 48

26/27

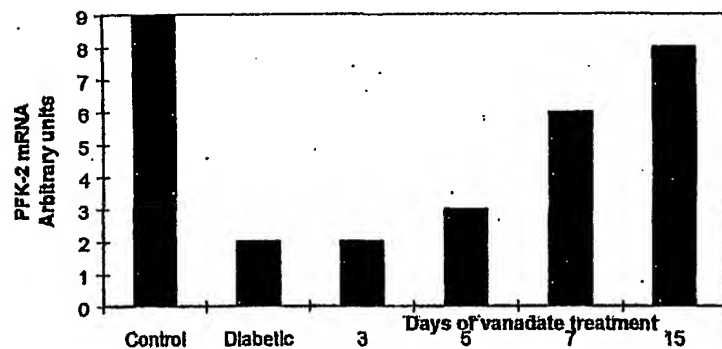


Figure 49

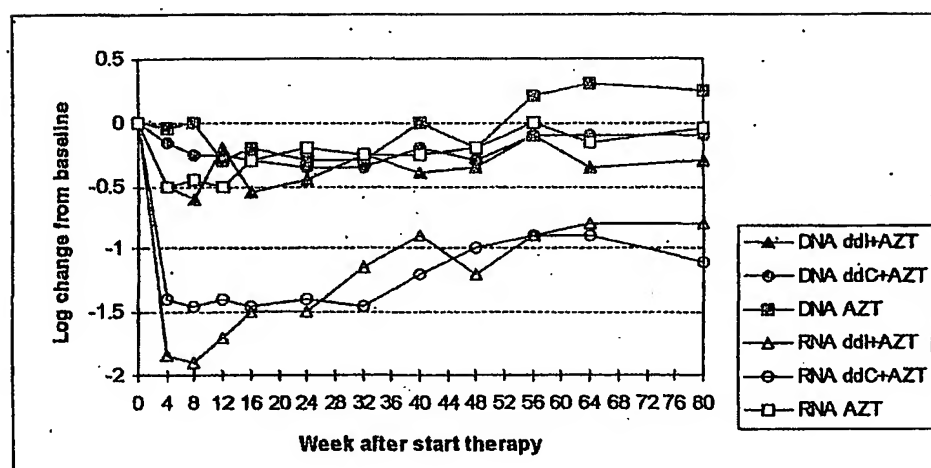


Figure 50

27/27

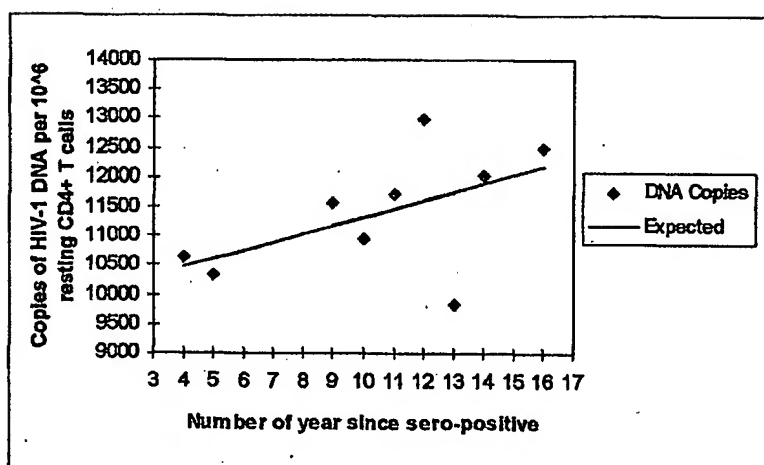


Figure 51